

**MODELING OF POST FLAME OXIDATION PROCESS OF UNBURNED
HYDROCARBONS IN SPARK IGNITION ENGINES**

by

Kuo-Chun Wu

**Bachelor of Science in Mechanical Engineering
National Taiwan University
(1990)**

**Master of Science in Mechanical Engineering
Massachusetts Institute of Technology
(1994)**

Submitted to the Department of Mechanical Engineering
in partial fulfillment of the requirements for the Degree of

DOCTOR OF PHILOSOPHY

at the

MASSACHUSETTS INSTITUTE OF TECHNOLOGY

September, 1997

© 1997 Massachusetts Institute of Technology
All rights reserved


Signature of Author _____
Department of Mechanical Engineering
June 30, 1997

Certified by _____
Simone Hochgreb
Associate Professor, Department of Mechanical Engineering
Thesis Supervisor

Accepted by _____
Ain A. Sonin
Chairman, Department Graduate Committee

JAN 06 1998

LIBRARIES

A handwritten signature or scribble consisting of several overlapping loops and lines, rendered in black ink on a white background.

MODELING OF POST FLAME OXIDATION PROCESS OF UNBURNED HYDROCARBONS IN SPARK IGNITION ENGINES

by

Kuo-Chun Wu

Submitted to the Department of Mechanical Engineering in partial fulfillment of the requirements for the Degree of Doctor of Philosophy in Mechanical Engineering

ABSTRACT

A fraction of the hydrocarbons escaping combustion during flame passage in spark ignition engines oxidize later in the post flame environment. The level of oxidation is highly dependent on the fuel type and operating conditions. A one-dimensional numerical model incorporating detailed chemistry has been formulated to simulate the post flame oxidation process of unburned hydrocarbons, to investigate the role of oxidation chemistry and transport on the oxidation processes taking place between a thin layer of unburned hydrocarbons adjacent to the walls and the surrounding hot burned gas.

Simulations show that the unburned fuel is transported towards the hot burned gases, where intermediate species are quickly generated. The cold region near the walls acts as a reservoir that preserves the intermediate species from quick oxidation. Radicals are generated close to the burned gas during the oxidation process, at much higher concentrations than the original burned gas radical concentrations, indicating that the radicals in the burned gas do not have a significant effect on the oxidation level. Flux analysis indicates that the convective term can be neglected in comparison with diffusive and reactive terms. The production and consumption of the intermediate species keep their concentrations approximately constant throughout the reactions.

The extent of oxidation of unburned hydrocarbons is very sensitive to the burned gas temperature. Simulation results show that the in cylinder process is largely controlled by diffusion rates for temperatures above 1500 K burned gas temperatures. Large differences in oxidation rates are found for different fuels for the same initial conditions of burned gas temperatures and stoichiometries. The differences can be attributed to the lengths of the reaction chain, the diffusion of intermediate products towards the walls, which lead to differences in the generation of hydrogen atoms in the reacting zone.

Approximations were made to represent the oxidation of crevice hydrocarbons by the one-dimensional model, and integration of the one-dimensional results was conducted to calculate the hydrocarbon emissions. Calculations indicate that for propane, over 90% of the crevice outflow of hydrocarbons is completely oxidized before leaving the cylinder, while about 80% for iso-octane. Moreover, in comparison with experimental data, the correlation works reasonably well in spite of the approximations.

Thesis Supervisor: Professor Simone Hochgreb
Associate Professor of Mechanical Engineering

ACKNOWLEDGEMENTS

It is with great and sincere gratitude that I acknowledge my advisor Professor Simone Hochgreb for his assistance and guidance in making this thesis reality. I am grateful for our discussions, which always forced me to delve deeper into my results and to look at my research from a different perspective. I would also like to thank Professors Heywood, Cheng, and Keck for setting examples of academic excellence and for complementing the instruction of Professor Hochgreb. Sincere thanks to Professors Ghoniem, Hart, and Howard as well for their supports and suggestions.

This work was sponsored by the MIT Engine-Fuels Interaction Consortium (Chevron Res. Co., Exxon Res. Eng. Co., Nippon Oil Co. and Shell Research Ltd.) and EPA center on Airborne Organics at MIT. It was initiated through a summer internship at Shell Research Ltd. at Thornton, England. The invaluable help of Drs. Rob Lee, Chris Morley and Laurence Scales at Thornton is gratefully acknowledged.

My time at the Sloan Automotive Laboratory has been incalculably enriched by the many graduate students and visiting scholars that I have met and had the opportunity to work with. I would like to thank Drs. Kuo-Chiang Chen, Tung-Ching Tseng, Wolf Bauer, Hiroyuki Nagaki, and Josmar Pagliuso for their friendships and scientific assistance. I am also grateful to Nancy Cook, Cynthia Chuang, Chuang-Chia Lin, and Joey Wong, for their timely care, support and friendship. They have made the lonely research at MIT much easier and memorable.

Most importantly, I want to thank my family for the support, understanding and love they have provided throughout my life. This thesis is dedicated to them.

Kuo-Chun Wu
30 June 1997

Table of Contents

ABSTRACT	3
ACKNOWLEDGEMENTS	5
TABLE OF CONTENTS.....	6
LIST OF TABLES	8
LIST OF FIGURES	9
NOMENCLATURE.....	13
CHAPTER 1 INTRODUCTION.....	14
1.1 BACKGROUND.....	14
1.2 HYDROCARBON EMISSIONS MECHANISMS	14
1.2.1 Sources of unburned hydrocarbons.....	15
1.2.2 Post flame oxidation.....	16
1.3 OBJECTIVES.....	18
CHAPTER 2 METHODOLOGY.....	19
2.1 EXPERIMENTAL OBSERVATIONS OF THE POST-FLAME OXIDATION PROCESS	19
2.2 ONE-DIMENSIONAL MODEL FORMULATION.....	20
2.2.1 Numerical model.....	20
2.2.2 Initial and boundary conditions.....	23
2.3 SUB-MODELS	24
2.3.1 Physical properties	24
2.3.2 Turbulence model.....	25
2.3.3 Chemical kinetic models	27
CHAPTER 3 THE REACTIVE/DIFFUSIVE PROCESS.....	31
3.1 REFERENCE MODEL : PROPANE	31
3.1.1 Features of the evolution of diffusive-reactive processes.....	31
3.1.2 Flux analysis.....	33
3.1.3 Spatially integrated species concentrations.....	34
3.1.4 Effect of the initial specification of the transition zone.....	35

3.1.5 Effect of initial burned gas temperature	36
3.2 EFFECT OF DIFFUSION	37
3.3 EFFECTS OF REACTANT CHEMISTRY	38
3.3.1 Ethane versus ethylene	39
3.3.2 Isooctane	40
CHAPTER 4 HYDROCARBON EMISSION ANALYSIS	61
4.1 CREVICE MASS INTEGRATED EMISSIONS	61
4.2 EFFECT OF REACTANT FUEL TYPE ON OVERALL OXIDATION.....	64
4.3 EFFECT OF THE WIDTH OF THE HYDROCARBON LAYER	65
4.4 EFFECT OF WALL TEMPERATURE ON OVERALL OXIDATION	66
4.5 EFFECT OF EQUIVALENCE RATIO	67
CHAPTER 5 REACTION PATH ANALYSIS	78
5.1 REACTION PATH ANALYSIS FOR OXIDATION OF HYDROCARBON SPECIES.....	78
5.1.1 Propane	78
5.1.2 Isooctane	79
5.2 FLUX ANALYSIS FOR RADICAL POOL GENERATION	80
CHAPTER 6 SUMMARY AND CONCLUSIONS	89
REFERENCES	92
APPENDIX 1 COORDINATE TRANSFORM	97
APPENDIX 2 CHEMICAL KINETIC REACTION MECHANISMS	99
APPENDIX 3 ONE DIMENSIONAL PROGRAM	121

List of Tables

TABLE 2-1 INITIAL CONDITIONS FOR SIMULATIONS.....	29
---	----

List of Figures

<i>Number</i>	<i>Page</i>
FIGURE 2-1 SCHEMATIC LAYOUT FOR THE SIMULATION.....	29
FIGURE 2-2 MESH DISTRIBUTION FOR THE SIMULATION.....	30
FIGURE 2-3 SPATIAL MOLECULAR DIFFUSIVITY AND TURBULENT DIFFUSIVITY PROFILES AT THE START OF REACTION (SOLID LINE), AND 25 CRANK ANGLE DEGREES AFTER START OF REACTION (DASHED LINE) (FUEL : PROPANE, INITIAL CORE TEMPERATURE : 1500 K).....	30
FIGURE 3-1 PREDICTED TEMPERATURE AND PRESSURE HISTORIES DURING EXPANSION PROCESS FOR THE BASELINE OPERATING CONDITION.....	41
FIGURE 3-2 SPATIAL TEMPERATURE PROFILES. (FUEL : PROPANE, INITIAL CORE TEMPERATURE : 1500 K)....	41
FIGURE 3-3 TIME-EVOLVING SPATIAL DISTRIBUTION OF PROPANE. (FUEL : PROPANE, INITIAL CORE TEMPERATURE : 1500 K).....	42
FIGURE 3-4 TIME-EVOLVING SPATIAL DISTRIBUTION OF ETHYLENE. (FUEL : PROPANE, INITIAL CORE TEMPERATURE : 1500 K).....	42
FIGURE 3-5 TIME-EVOLVING SPATIAL DISTRIBUTION OF CARBON MONOXIDE. (FUEL : PROPANE, INITIAL CORE TEMPERATURE : 1500 K).....	43
FIGURE 3-6 TIME-EVOLVING SPATIAL DISTRIBUTION OF HYDROXYL. (FUEL : PROPANE, INITIAL CORE TEMPERATURE : 1500 K).....	43
FIGURE 3-7 COMPARISON OF THE TIME-EVOLVING SPATIAL DISTRIBUTION OF HYDROXYL BETWEEN THE ORIGINAL CASE (SOLID LINE) AND THE CASE OF EQUILIBRIUM COMPOSITION AT 1500 K SET ON THE BURNED GAS SIDE (DASHED LINE). (FUEL : PROPANE, INITIAL CORE TEMPERATURE : 1500 K).....	44
FIGURE 3-8 SPATIAL DISTRIBUTION OF MAJOR SPECIES MOLAR FRACTIONS AT 25 CRANK ANGLE DEGREES AFTER START OF REACTION. (FUEL : PROPANE, INITIAL CORE TEMPERATURE : 1500 K).....	44
FIGURE 3-9 CONTRIBUTION OF REACTION AND TRANSPORT TO THE RATE OF CHANGE OF PROPANE AT 25 CRANK ANGLE DEGREES AFTER START OF REACTION. (FUEL : PROPANE, INITIAL CORE TEMPERATURE : 1500 K).....	45
FIGURE 3-10 CONTRIBUTION OF REACTION AND TRANSPORT TO THE RATE OF CHANGE OF ETHYLENE AT 25 CRANK ANGLE DEGREES AFTER START OF REACTION. (FUEL : PROPANE, INITIAL CORE TEMPERATURE : 1500 K).....	45
FIGURE 3-11 CONTRIBUTION OF REACTION AND TRANSPORT TO THE RATE OF CHANGE OF CARBON MONOXIDE AT 25 CRANK ANGLE DEGREES AFTER START OF REACTION. (FUEL : PROPANE, INITIAL CORE TEMPERATURE : 1500 K).....	46
FIGURE 3-12 CONTRIBUTION OF REACTION AND TRANSPORT TO THE RATE OF CHANGE OF HYDROXYL AT 25 CRANK ANGLE DEGREES AFTER START OF REACTION. (FUEL : PROPANE, INITIAL CORE TEMPERATURE : 1500 K).....	46
FIGURE 3-13 EVOLUTION OF FRACTIONAL CONTRIBUTIONS TO SPATIALLY INTEGRATED TOTAL HYDROCARBONS FOR FUEL, NON-FUEL AND CARBON MONOXIDE. CONCENTRATIONS ARE NORMALIZED BY THE ORIGINAL TOTAL HYDROCARBONS (IN PPM _{C1}) (FUEL : PROPANE, INITIAL CORE TEMPERATURE : 1500 K).....	47
FIGURE 3-14 COMPARISON OF THE SURVIVING FRACTION OF TOTAL HYDROCARBONS AND FUEL/NON-FUEL DISTRIBUTION AT TOP DEAD CENTER OF THE EXHAUST PROCESS BETWEEN THE CASES OF THE DIFFERENT WIDTH OF TRANSITION ZONE AND OF DIFFERENT TEMPERATURE PROFILES IN THE TRANSITION ZONE FOR TWO DIFFERENT INITIAL BURNED GAS TEMPERATURES. ((A) : LINEAR TEMPERATURE PROFILE, (B) : TEMPERATURE PROFILE DEFINED IN EQUATION (3-5)). (FUEL : PROPANE).....	47
FIGURE 3-15 EVOLUTION OF THE FRACTION OF SURVIVING TOTAL HYDROCARBONS (F_{HC}) FOR VARIOUS INITIAL PHASES. (FUEL : PROPANE).....	48
FIGURE 3-16 SPATIAL TEMPERATURE PROFILES. (FUEL : PROPANE, INITIAL CORE TEMPERATURE : 1800 K)....	48
FIGURE 3-17 TIME-EVOLVING SPATIAL DISTRIBUTION OF PROPANE. (FUEL : PROPANE, INITIAL CORE TEMPERATURE : 1800 K).....	49
FIGURE 3-18 TIME-EVOLVING SPATIAL DISTRIBUTION OF ETHYLENE. (FUEL : PROPANE, INITIAL CORE TEMPERATURE : 1800 K).....	49

FIGURE 3-19 TIME-EVOLVING SPATIAL DISTRIBUTION OF CARBON MONOXIDE. (FUEL : PROPANE, INITIAL CORE TEMPERATURE : 1800 K).....	50
FIGURE 3-20 TIME-EVOLVING SPATIAL DISTRIBUTION OF HYDROXYL. (FUEL : PROPANE, INITIAL CORE TEMPERATURE : 1800 K).....	50
FIGURE 3-21 SPATIAL TEMPERATURE PROFILES. (FUEL : PROPANE, INITIAL CORE TEMPERATURE : 1300 K)...	51
FIGURE 3-22 TIME-EVOLVING SPATIAL DISTRIBUTION OF PROPANE. (FUEL : PROPANE, INITIAL CORE TEMPERATURE : 1300 K).....	51
FIGURE 3-23 TIME-EVOLVING SPATIAL DISTRIBUTION OF ETHYLENE. (FUEL : PROPANE, INITIAL CORE TEMPERATURE : 1300 K).....	52
FIGURE 3-24 TIME-EVOLVING SPATIAL DISTRIBUTION OF CARBON MONOXIDE. (FUEL : PROPANE, INITIAL CORE TEMPERATURE : 1300 K).....	52
FIGURE 3-25 TIME-EVOLVING SPATIAL DISTRIBUTION OF HYDROXYL. (FUEL : PROPANE, INITIAL CORE TEMPERATURE : 1300 K).....	53
FIGURE 3-26 COMPARISONS OF SURVIVING FRACTION OF HYDROCARBONS AND FUEL/NON-FUEL DISTRIBUTION BETWEEN THE CASES OF NON-EQUILIBRIUM AND EQUILIBRIUM BURNED GAS COMPOSITION FOR INITIAL CORE TEMPERATURES OF 1300 K AND 1500 K.....	53
FIGURE 3-27 EFFECT OF INITIAL CORE TEMPERATURE ON THE SURVIVING FRACTION OF HYDROCARBONS AND FUEL/NON-FUEL DISTRIBUTION AT TOP DEAD CENTER OF THE EXHAUST PROCESS. (FUEL : PROPANE)	54
FIGURE 3-28 COMPARISON OF SPATIAL DISTRIBUTION OF SPECIES CONCENTRATIONS BETWEEN THE ORIGINAL CASE (SOLID LINE) AND HIGH TURBULENT DIFFUSIVITY ($2U'$) (DASHED LINE) (FUEL : PROPANE, INITIAL CORE TEMPERATURE : 1400 K)	54
FIGURE 3-29 COMPARISON OF THE EVOLUTION OF THE FRACTION OF SURVIVING TOTAL HYDROCARBONS (F_{HC}) BETWEEN THE ORIGINAL CASE (SOLID LINE) AND HIGH TURBULENT DIFFUSIVITY ($2U'$) (DASHED LINE). (FUEL : PROPANE).....	55
FIGURE 3-30 COMPARISON OF THE SURVIVING FRACTION OF TOTAL HYDROCARBONS AND FUEL/NON-FUEL DISTRIBUTION AT TOP DEAD CENTER OF THE EXHAUST PROCESS BETWEEN THE ORIGINAL CASE (A) AND (B) HIGH TURBULENT DIFFUSIVITY ($2U'$). RESULTS ARE NORMALIZED IN PPM _{C1} BY INITIAL UNBURNED HYDROCARBONS. (FUEL : PROPANE).....	55
FIGURE 3-31 COMPARISON OF THE EVOLUTION OF THE FRACTION OF SURVIVING TOTAL HYDROCARBONS (F_{HC}) FOR VARIOUS INITIAL CORE TEMPERATURES BETWEEN THE CASES OF ETHANE (DASHED LINE) AND ETHYLENE (SOLID LINE).....	56
FIGURE 3-32 SPATIAL DISTRIBUTION OF FUEL, NON-FUEL, CARBON MONOXIDE AND RADICALS AT 25 CRANK ANGLE DEGREES AFTER START OF REACTION. (FUEL : ETHANE, INITIAL CORE TEMPERATURE : 1400 K) ..	56
FIGURE 3-33 SPATIAL DISTRIBUTION OF FUEL, NON-FUEL, CARBON MONOXIDE AND RADICALS AT 25 CRANK ANGLE DEGREES AFTER START OF REACTION. (FUEL : ETHYLENE, INITIAL CORE TEMPERATURE : 1400 K)57	57
FIGURE 3-34 REACTION RATE AS A FUNCTION OF LOCAL TEMPERATURE. (FUEL : ETHANE, INITIAL CORE TEMPERATURE : 1400 K).....	57
FIGURE 3-35 REACTION RATE AS A FUNCTION OF LOCAL TEMPERATURE. (FUEL : ETHYLENE, INITIAL CORE TEMPERATURE : 1400 K).....	58
FIGURE 3-36 SPATIAL DISTRIBUTION OF MAJOR SPECIES AT 25 CRANK ANGLE DEGREES AFTER START OF REACTION. (FUEL : PROPANE, INITIAL CORE TEMPERATURE : 1500 K).....	58
FIGURE 3-37 EVOLUTION OF THE SURVIVING FRACTION OF HYDROCARBONS FOR VARIOUS INITIAL TEMPERATURES. (FUEL : ISOCTANE).....	59
FIGURE 3-38 COMPARISON OF THE EVOLUTION OF SPATIAL INTEGRATED CONCENTRATIONS OF FUEL, NON-FUEL, CARBON MONOXIDE AND TOTAL HYDROCARBONS BETWEEN THE ORIGINAL CASE FOR ISOCTANE (SOLID LINE) AND A CASE IN WHICH THE MOLECULAR DIFFUSIVITY OF ISOCTANE WAS REPLACED WITH THAT OF PROPANE (DASHED LINE). SPECIES CONCENTRATIONS ARE NORMALIZED BY THE CONCENTRATION OF ORIGINAL TOTAL HYDROCARBONS (IN PPM _{C1}) (FUEL : ISOCTANE, INITIAL CORE TEMPERATURE : 1600 K).....	59
FIGURE 3-39 COMPARISON OF THE SURVIVING FRACTION OF FUEL AND NON-FUEL PRODUCTION AT TOP DEAD CENTER OF THE EXHAUST PROCESS BETWEEN THE CASES OF PROPANE AND ISOCTANE. (*: THE CASE THAT THE MOLECULAR DIFFUSIVITY OF ISOCTANE WAS REPLACED WITH THAT OF PROPANE) RESULTS ARE NORMALIZED BY INITIAL UNBURNED TOTAL HYDROCARBONS	60

FIGURE 4-1 MASS FLOW RATE OF HYDROCARBONS LEAVING THE CREVICE NORMALIZED BY PEAK RATE, AND PREDICTED REMAINING FRACTION OF HYDROCARBONS AT TOP DEAD CENTER OF THE EXHAUST PROCESS FOR THE CASES OF PROPANE AND ISOCTANE.....69

FIGURE 4-2 FRACTIONAL CONTRIBUTIONS OF SEGMENTS (STARTING REACTION AT VARIOUS INITIAL CORE GAS TEMPERATURES) TO THE TOTAL SURVIVING HYDROCARBONS IN THE CASES OF PROPANE AND ISOCTANE. ALL RESULTS ARE NORMALIZED BY TOTAL SURVIVING HYDROCARBON CONCENTRATION.....69

FIGURE 4-3 FRACTIONAL CONTRIBUTIONS OF SEGMENTS (STARTING REACTION AT VARIOUS INITIAL CORE TEMPERATURES) TO THE SURVIVING FUEL AND NON-FUEL SPECIES CONCENTRATIONS. ALL RESULTS ARE NORMALIZED BY TOTAL SURVIVING FUEL AND NON-FUEL SPECIES CONCENTRATION. (FUEL : PROPANE) .70

FIGURE 4-4 FRACTIONAL CONTRIBUTIONS OF SEGMENTS (STARTING REACTION AT VARIOUS INITIAL CORE TEMPERATURES) TO THE SURVIVING FUEL AND NON-FUEL SPECIES CONCENTRATIONS. NORMALIZED BY TOTAL SURVIVING FUEL AND NON-FUEL SPECIES CONCENTRATION. (FUEL : ISOCTANE).....70

FIGURE 4-5 COMPARISONS OF THE RELATIVE HYDROCARBON EMISSION LEVELS FOR DIFFERENT FUELS BASED ON PREDICTED MASS-INTEGRATED RESULTS AND EXPERIMENTAL DATA. RESULTS ARE NORMALIZED BY PROPANE EMISSIONS. (CIRCLE : DROBOT ET AL [8], SQUARE : KAYES ET AL [13], SOLID SYMBOL : TOP DEAD CENTER OF THE EXHAUST PROCESS IS CHOSEN TO CALCULATE THE SURVIVING FRACTION OF TOTAL HYDROCARBONS, BLANK SYMBOL : BOTTOM DEAD CENTER OF THE EXPANSION PROCESS IS CHOSEN TO CALCULATE THE SURVIVING FRACTION OF TOTAL HYDROCARBONS).....71

FIGURE 4-6 COMPARISON BETWEEN SIMULATIONS AND EXPERIMENTAL MEASUREMENTS [13] AT TOP DEAD CENTER OF THE EXHAUST PROCESS. (FUEL : PROPANE).....71

FIGURE 4-7 COMPARISON BETWEEN SIMULATIONS AND EXPERIMENTAL MEASUREMENTS [13] AT TOP DEAD CENTER OF THE EXHAUST PROCESS. (FUEL : ISOCTANE).....72

FIGURE 4-8 COMPARISON BETWEEN SIMULATIONS AND EXPERIMENTAL MEASUREMENTS [8] AT TOP DEAD CENTER OF THE EXHAUST PROCESS. (FUEL : ETHANE).....72

FIGURE 4-9 COMPARISON BETWEEN SIMULATIONS AND EXPERIMENTAL MEASUREMENTS [8] AT TOP DEAD CENTER OF THE EXHAUST PROCESS. (FUEL : ETHYLENE).....73

FIGURE 4-10 COMPARISON OF THE SURVIVING FRACTION OF TOTAL HYDROCARBONS AND FUEL/NON-FUEL DISTRIBUTION AT TOP DEAD CENTER OF THE EXHAUST PROCESS BETWEEN THE CASES WITH WIDTH OF HYDROCARBON LAYER OF (A) 0.1 MM (ORIGINAL CASE), (B) 0.2 MM, AND (C) 0.4 MM. RESULTS ARE NORMALIZED BY INITIAL UNBURNED HYDROCARBON CONCENTRATIONS. (FUEL : PROPANE).....73

FIGURE 4-11 COMPARISON OF SPATIAL DISTRIBUTION OF SPECIES CONCENTRATIONS BETWEEN THE ORIGINAL CASE (SOLID LINE) AND THE CASE WITH THE WIDTH OF HYDROCARBON LAYER OF 0.2 MM. (DASHED LINE) (FUEL : PROPANE, INITIAL CORE TEMPERATURE : 1400 K).....74

FIGURE 4-12 EFFECT OF WIDTH OF HYDROCARBON LAYER ON THE EXTENT OF OXIDATION AND FUEL/NON-FUEL DISTRIBUTION. RESULTS ARE NORMALIZED BY THE RESULTS IN THE BASELINE CASE (0.1 MM). (FUEL : PROPANE).....74

FIGURE 4-13 COMPARISON OF SPATIAL DISTRIBUTION OF SPECIES CONCENTRATIONS BETWEEN THE ORIGINAL CASE (SOLID LINE) AND THE CASE AT WALL TEMPERATURE OF 500K. (DASHED LINE) (FUEL : PROPANE, INITIAL CORE TEMPERATURE : 1400 K)75

FIGURE 4-14 COMPARISON OF SURVIVING FRACTION OF TOTAL HYDROCARBONS AND FUEL/NON-FUEL DISTRIBUTION AT TOP DEAD CENTER OF THE EXHAUST PROCESS BETWEEN THE (A) ORIGINAL CASE ($T_w=361$ K) (B) CASE FOR WALL TEMPERATURE $T_w=500$ K. RESULTS ARE NORMALIZED BY INITIAL UNBURNED HYDROCARBON CONCENTRATIONS. (FUEL : PROPANE).....75

FIGURE 4-15 COMPARISON OF SPATIAL DISTRIBUTION OF SPECIES CONCENTRATIONS BETWEEN THE ORIGINAL CASE (SOLID LINE) AND THE CASE AT STOICHIOMETRIC CONDITION. (DASHED LINE) (FUEL : PROPANE, INITIAL CORE TEMPERATURE : 1400 K)76

FIGURE 4-16 COMPARISON OF THE SURVIVING FRACTION OF TOTAL HYDROCARBONS AND FUEL/NON-FUEL DISTRIBUTION AT TOP DEAD CENTER OF THE EXHAUST PROCESS BETWEEN THE (A) BASELINE CASE ($\Phi=0.9$) (B) STOICHIOMETRIC CASE. RESULTS ARE NORMALIZED BY INITIAL UNBURNED HYDROCARBON CONCENTRATIONS. (FUEL : PROPANE)76

FIGURE 4-17 EFFECTS OF THE WALL TEMPERATURE AND FUEL/AIR EQUIVALENCE RATIO ON THE EXTENT OF OXIDATION AND FUEL/NON-FUEL DISTRIBUTION. THE NORMALIZED FRACTIONS ARE RELATIVE TO THE BASELINE CASE.....77

FIGURE 5-1 SIMPLIFIED PATHWAYS FOR PROPANE OXIDATION.....83

FIGURE 5-2 CONTRIBUTION OF THE IMPORTANT REACTIONS TO THE TOTAL REACTION FLUX OF PROPANE AT 25 CRANK ANGLE DEGREES AFTER START OF REACTION. (FUEL : PROPANE, INITIAL CORE TEMPERATURE : 1600 K) REACTIONS : (1) $C_3H_8+OH=NC_3H_7+H_2O$, (2) $C_3H_8+OH=iC_3H_7+H_2O$, (3) $C_3H_8+O=NC_3H_7+OH$, (4) $C_3H_8+OH=iC_3H_7+H_2$, (5) $C_3H_8+O=iC_3H_7+OH$, (6) $C_3H_8+H=NC_3H_7+H_2$, (7) $C_3H_8=C_2H_5+CH_3$83

FIGURE 5-3 CONTRIBUTION OF THE IMPORTANT REACTIONS TO THE TOTAL REACTION FLUX OF ETHYLENE AT 25 CRANK ANGLE DEGREES AFTER START OF REACTION. (FUEL : PROPANE, INITIAL CORE TEMPERATURE : 1600 K) REACTIONS : (1) $NC_3H_7=C_2H_4+CH_3$, (2) $C_2H_4+OH=C_2H_3+H_2O$, (3) $C_2H_4+OH=CH_2O+CH_3$, (4) $C_2H_4+O=CH_3+HCO$, (5) $C_2H_4+O=CH_2O+CH_2$, (6) $C_2H_5+M=C_2H_4+H+M$84

FIGURE 5-4 CONTRIBUTION OF THE IMPORTANT REACTIONS TO THE TOTAL REACTION FLUX OF PROPENE AT 25 CRANK ANGLE DEGREES AFTER START OF REACTION. (FUEL : PROPANE, INITIAL CORE TEMPERATURE : 1600 K) REACTIONS : (1) $iC_3H_7=C_3H_6+H$, (2) $C_3H_6+OH=C_2H_5+CH_2O$, (3) $C_3H_6+OH=AC_3H_5+H_2O$, (4) $C_3H_6+OH=SC_3H_5+H_2O$84

FIGURE 5-5 CONTRIBUTION OF THE IMPORTANT REACTIONS TO THE TOTAL REACTION FLUX OF CARBON MONOXIDE AT 25 CRANK ANGLE DEGREES AFTER START OF REACTION. (FUEL : PROPANE, INITIAL CORE TEMPERATURE : 1600 K) REACTIONS : (1) $HCO+M=H+CO+M$, (2) $CO+OH=CO_2+H$, (3) $HCO+O_2=CO+HO_2$85

FIGURE 5-6 SIMPLIFIED PATHWAYS FOR ISOCTANE OXIDATION.....85

FIGURE 5-7 CONTRIBUTION OF THE IMPORTANT REACTIONS TO THE TOTAL REACTION FLUX OF ISOCTANE AT 25 CRANK ANGLE DEGREES AFTER START OF REACTION. (FUEL : ISOCTANE, INITIAL CORE TEMPERATURE : 1600 K) REACTIONS : (1) $iC_8H_{18}+OH=AC_8H_{17}+H_2O$, (2) $iC_8H_{18}+OH=DC_8H_{17}+H_2O$, (3) $iC_8H_{18}+OH=BC_8H_{17}+H_2O$, (4) $iC_8H_{18}+OH=cC_8H_{18}+H_2O$, (5) $iC_8H_{18}=TC_4H_9+iC_4H_9$86

FIGURE 5-8 CONTRIBUTION OF THE IMPORTANT REACTIONS TO THE TOTAL REACTION FLUX OF ISOBUTENE AT 25 CRANK ANGLE DEGREES AFTER START OF REACTION. (FUEL : ISOCTANE, INITIAL CORE TEMPERATURE : 1600 K) REACTIONS : (1) $AC_8H_{17}=iC_4H_8+iC_4H_9$, (2) $iC_4H_9=iC_4H_8+H$, (3) $iC_4H_8=C_3H_5+CH_3$, (4) $NEOC_5H_{11}=iC_4H_8+CH_3$, (5)SUMMATION OF FOLLOWING REACTIONS : (A) $iC_4H_8+O=iC_4H_7+OH$, (B) $iC_4H_8+O=iC_3H_7+HCO$, (C) $iC_4H_8+OH=iC_4H_7+H_2O$, (D) $iC_4H_8+OH=iC_3H_7+CH_2O$, (E) $iC_4H_8+H=iC_4H_7+H_2$86

FIGURE 5-9 CONTRIBUTION OF THE IMPORTANT REACTIONS TO THE TOTAL REACTION FLUX OF ETHYLENE AT 25 CRANK ANGLE DEGREES AFTER START OF REACTION. (FUEL : ISOCTANE, INITIAL CORE TEMPERATURE : 1600 K) REACTIONS : (1) $NC_3H_7=C_2H_4+CH_3$, (2) $C_3H_4+OH=C_2H_4+HCO$, (3) $C_2H_4+OH=C_2H_3+H_2O$, (4) $C_2H_4+OH=CH_2O+CH_3$, (5) $C_2H_4+O=CH_2O+CH_2$, (6) $C_2H_5+M=C_2H_4+H+M$87

FIGURE 5-10 CONTRIBUTION OF THE IMPORTANT REACTIONS TO THE TOTAL REACTION FLUX OF HYDROXYL AT 25 CRANK ANGLE DEGREES AFTER START OF REACTION. (FUEL : PROPANE, INITIAL CORE TEMPERATURE : 1600 K) REACTIONS : (1) $O+H_2O=2OH$, (2) $H+O_2=OH+O$, (3) $CH_2O+OH=HCO+H_2O$, (4) $CH_3OH+OH=CH_2OH+H_2O$, (5) $HO_2+OH=H_2O+O_2$, (6) $H+HO_2=OH+OH$, (7) $CO+OH=CO_2+H$, (8) $CH_3+OH=CH_3OH$, (9) $H_2+OH=H_2O+H$, (10) $C_2H_4+OH=C_2H_3+H_2O$87

FIGURE 5-11 CONTRIBUTION OF THE IMPORTANT REACTIONS TO THE TOTAL REACTION FLUX OF HYDROGEN ATOM AT 25 CRANK ANGLE DEGREES AFTER START OF REACTION. (FUEL : PROPANE, INITIAL CORE TEMPERATURE : 1600 K) REACTIONS : (1) $HCO+M=H+CO+M$, (2) $H+O_2=OH+O$, (3) $C_2H_3=C_2H_2+H$, (4) $H_2+OH=H_2O+H$, (5) $iC_3H_7=C_3H_6+H$, (6) $CO+OH=CO_2+H$, (7) $H+HO_2=OH+OH$, (8) $H+O_2=HO_2$88

FIGURE 5-12 CONTRIBUTION OF THE IMPORTANT REACTIONS TO THE TOTAL REACTION FLUX OF HYDROGEN ATOM AT 25 CRANK ANGLE DEGREES AFTER START OF REACTION. (FUEL : ISOCTANE, INITIAL CORE TEMPERATURE : 1600 K) REACTIONS : (1) $HCO+M=H+CO+M$, (2) $H+O_2=OH+O$, (3) $H_2+OH=H_2O+H$, (4) $H+HO_2=OH+OH$, (5) $H+O_2=HO_2$, (6) $CO+OH=CO_2+H$88

Nomenclature

c_i	number of carbons in the i th species
$\overline{C_p}$	constant pressure specific heat of the mixture
D_i	diffusion coefficient of the i th species
$D_{i,m}$	molecular diffusion coefficient of the i th species
D_t	turbulent diffusion coefficient
m	mass
n_i	amount (mole) of the i th species
$n_{i,0}$	initial amount (mole) of the i th species
n_{HC}	amount of the total hydrocarbons
$n_{HC,0}$	initial amount of total hydrocarbons
n_c	amount (mole) of fuel/air mixture in the crevice
\dot{n}_c	molar rate of crevice outflow
L	distance between cylinder head and piston
p	pressure
R	universal gas constant (8.314 J/(mol*k))
S_p	piston speed
T	temperature
T_b	temperature of the burned gas
T_c	temperature of the crevice ($=T_w$)
T_w	wall temperature
t	time
u	velocity in x direction
v	velocity in y direction
V_c	volume of the crevice
\overline{W}	mean molecular weight of the mixture
X_i	molar fraction of the i th species
x	coordinate perpendicular to the wall; zero starting at the wall
Y_i	mass fraction of the i th species
y	coordinate in direction of axial expansion
z	$z = x - \delta_{HC}$
α_j	fractional contribution of j th segment to the overall surviving hydrocarbons
ρ	mass density
$\dot{\omega}_i$	mass rate of production by chemical reaction of the i th species
κ	thermal conductivity of the mixture
δ	thickness of the transition zone
δ_{HC}	thickness of the hydrocarbon layer
ϵ_i	extent of reaction of i th species i
ϵ_{HC}	extent of reaction of total hydrocarbons
f_i	surviving fraction (1- ϵ_i) of i th species
f_i	surviving fraction (1- ϵ_{HC}) of total hydrocarbons

Chapter 1 Introduction

1.1 Background

Hydrocarbon species emitted from automobiles pollute the environment and are harmful to human health. Specifically, hydrocarbons (HCs) react with nitrogen oxides, which are also pollutants from vehicles, to form ozone and, thus, lead to smog by photochemical reactions [1]. Not only does smog limit visibility, but it also has a deleterious effect on human health. In addition, some of the emitted hydrocarbons have been found to be toxic species*. It is estimated that cancer caused by toxic air pollutants may result in 1500 to 3000 cancer deaths each year in the United States, and that more than half of these cancers are caused by automobile emissions [2].

Consequently, government regulations for hydrocarbon emissions from automobiles are becoming more and more stringent. For instance, California requires that a significant fraction of new motor vehicles starting in 1997 meet the Ultra Low Emission Vehicle (ULEV) standard of 0.06 grams hydrocarbons per mile [3], which calls for a tremendous reduction from the 0.41 grams per mile permissible under the Clear Air Act Amendment of 1990. Therefore, considerable effort has been devoted to understanding the mechanisms of transport and the oxidation of unburned hydrocarbons in spark ignition engines. Even though the current technology of the catalytic converter can remove most of an engine's exhaust hydrocarbons, some limitations on the catalyst's performance (especially during a cold start at low temperatures) keep researchers busy in their efforts on investigations of hydrocarbon emissions mechanisms.

1.2 Hydrocarbon emissions mechanisms

Hydrocarbon emissions mechanisms have been studied for over 40 years. However, the details of the mechanisms are still unclear and quantifying the different hydrocarbon sources remains a challenge. Qualitatively speaking, a small fraction ($\leq 10\%$) of fuel inducted into an engine cylinder escapes combustion in the flame by a variety of means. Part of those unburned

* Benzene, 1,3 butadiene, formaldehyde, and acetaldehyde are toxins as defined by the United States Environmental Protection Agency (EPA).

hydrocarbons are then released from these various sources and exhausted along with the burned gas. During the transport process, the mixing of unburned hydrocarbons and burned gas provides another chance for hydrocarbons to be oxidized. A fraction of them survive the post flame oxidation, leave the exhaust system and contribute to pollution in the atmosphere.

1.2.1 Sources of unburned hydrocarbons

Substantial efforts have been devoted to identifying the mechanisms of storage and release of unburned hydrocarbons, and to quantifying their contributions to total hydrocarbon emissions. Sources of unburned hydrocarbons include crevices, oil layers, deposits, flame-quenching layers, liquid fuel, and exhaust valve leakage [4]. Depending on whether air is present in the source, these can be further divided into two categories : fuel-air and fuel-only sources.

Fuel-air sources consist of crevices, quench layers and exhaust valve leakage. Crevices, which are identified as the largest unburned hydrocarbon source, are cold narrow regions near the walls and connected to the combustion chamber. Fuel, air and residual gas mixture can enter these regions but the flame cannot because the entrance is smaller than the two-wall quench distance of hydrocarbon flames. The largest crevice volumes are in the piston-ring-liner crevice region, but the head gasket, spark plug, and valve seat crevices are also significant [5]. It is estimated that about 5 percent of the inducted fuel is captured in crevices during combustion. Wall-quench layers, results of flame-quenching at cylinder surfaces, were originally assumed to be the main contribution to the emissions, but experiments with combustion bombs [6] and numerical simulations [7] showed that wall-quench hydrocarbons diffuse quickly into burned gas and are oxidized, thus contributing very little to unburned hydrocarbons. Poor sealing of exhaust valves results in additional unburned mixture escaping from the cylinder into the exhaust port.

Fuel-only sources include oil layers, deposits and liquid fuel. Lubricating oil and deposits, which build up on the intake valves and on the combustion chamber walls of engines over extended mileage, absorb fuel hydrocarbons in the unburned mixture during intake and compression strokes and protect hydrocarbons from normal combustion. Up to 2 percent of the inducted fuel can be absorbed in oil layers or deposits under warmed-up, mid-load, mid-speed conditions. Finally, about 1 percent of the injected charge remains in the liquid phase either due to incomplete atomization or by puddling on combustion chamber walls, even under warmed-up conditions; it escapes oxidation because of the inability of the flame to completely burn the liquid fuel. The contribution of liquid fuel to unburned hydrocarbon emission is much larger

during the engine warm-up process, when large amounts of fuel are injected, and during which poor vaporization occurs.

1.2.2 Post flame oxidation

Generally speaking, the extent of oxidation of unburned hydrocarbons depends on the operating conditions and the type of fuel. More specifically, the types (fuel-air or fuel only) and locations of sources, the timing of hydrocarbon emergence into the burned gases and the residence time of unburned hydrocarbons, as well as oxidation chemistry, affect post flame oxidation. Due to the complex nature of the process, and the difficulty in conducting experimental measurements and numerical simulations, only very limited research has been devoted to the assessment of post-flame oxidation. Consequently, many details about the process remain unclear.

Post flame oxidation take places both within the cylinder and, a lesser extent, in the exhaust port. Hydrocarbons emerging from the various sources are partially oxidized while still in the cylinder. A fraction of the remaining hydrocarbon is retained in the cylinder through the next cycle, whereas the remainder leaves the cylinder with the burned gases and continues to react in the exhaust port.

Several experimental and modeling studies have addressed the extent of oxidation in the exhaust port. In experiments involving quenching of exhaust gas using carbon dioxide gas injection at the exhaust valve plane and runner [8,9], it is found that, at mid-speed and mid-load conditions, around 30 to 40 percent of exhaust hydrocarbons from the engine are oxidized within the exhaust port; and a further 5 to 10 percent in the exhaust manifold. The extent of reaction was found to be surprisingly insensitive to the reactivity of parent fuels used in the test. In addition, it was observed that the ratio of fuel to non-fuel species decreases as the exhaust gas moves downstream of the exhaust system, indicating partial oxidation. Since the flow pattern of the exhaust system is relatively simple, a numerical model for exhaust port oxidation was created, using detailed chemical kinetics for several fuels, to explore the results of different simplified models for flow, including perfectly mixed and stratified mixture models [10]. Comparisons between model and experimental results show that, even if mixing in the exhaust port is fast enough for creating a homogeneous mixture downstream of the exhaust port, the concentration of partial combustion products cannot be adequately reproduced with homogeneous mixing models, such as a plug flow or perfect mixing models. The fact that the calculation results yield closer agreement with experiments when the effects of the non-

uniformity of hydrocarbons concentrations and temperature are taken into account implies that most exhaust port oxidation (which probably happens at locations near the exhaust valve) may occur under non-uniform situations. Spatially resolved measurements [11,12] near exhaust valves support the assumption of concentration non-uniformity.

Due to difficulties in carrying out in-cylinder measurements, as well as in quantifying the magnitude of sources, the extent of in-cylinder retention, there have been only limited, indirect experiments carried out to determine the extent of post-flame oxidation inside cylinders. Engine-out speciated concentrations measured for a group of simple fuels [8,9,13,14,15,16] showed the occurrence of partial oxidation inside the engine and the effects of the type of fuel on emission levels.

Crevice [17] and oil layers [18] have been isolated as sources of unburned hydrocarbons in experiments to investigate on the extent of oxidation. These experiments have suggested that about 40 to 90 percent of the total hydrocarbons escaping the main combustion event oxidize in the post-flame environment. One-dimensional models using one-step chemistry were built to examine the process of oxidation, showing reasonable correlation with the experimental data [17]. Computational fluid dynamics (CFD) calculations on the post flame oxidation of hydrocarbons emerging from piston/liner crevices have also been carried out [19,20,21,22]. These simulations suggest that most of the hydrocarbons leaving the crevices are oxidized very quickly during the expansion stroke and that more than 80 percent of the emerging hydrocarbons are oxidized. An important shortcoming of most of these models is the use of one-step chemistry, such that those studies cannot provide any insight into the partial oxidation process and the production of non-fuel hydrocarbons. Although two CFD simulations have used multi-step chemistry [21,22], the computing effort is so large that only very limited discussions and sensitivity analysis on the process have been reported. Whereas one-step chemistry can in some cases capture the overall of the hydrocarbons, it clearly cannot capture the production of non-fuel species inside the cylinder. Furthermore, most one-step chemical models are adopted from laminar flame models, which may be significantly different from the actual hydrocarbon oxidation process, in as much as the reaction rate and heat release rate are decoupled in the latter.

At the other extreme of the computational spectrum, zero-dimensional detailed chemistry models have been used to simulate reactions during the expansion process, showing that the calculated products of reaction correlate with species concentration measured at engine-out [23,24,25]. Finally, two previous studies have addressed the problem of in-cylinder quench-layer oxidation using one-dimensional detailed chemistry models in the cases of methane, methanol

[7], and propane [26] under constant pressure and constant burned gas temperature conditions. The latter results showed additional details on the structure of the reactive layers, and demonstrated how those hydrocarbons quickly diffuse into the burned gas and completely oxidize, resulting in minor contributions to emissions levels from quench layers. However, those studies focused on the oxidation processes occurring at high temperatures and constant pressure conditions, which can give very different results from those obtained at late stages of the expansion and exhaust strokes, when temperatures are a few hundred degrees lower due to heat loss and expansion. Clearly, many details on the post flame oxidation process of unburned hydrocarbons need to be explored.

1.3 Objectives

The objective of this work is to develop and use a numerical model to carefully examine the physical and chemical processes expected to take place at the interface of the thin mixing layer between burned gas and unburned gases, and to conduct sensitivity analysis for parameters which may possibly affect oxidation. Specifically, we would like to provide plausible answers to the following questions:

- a) How do unburned hydrocarbons placed adjacently to hot burned gases in the post-flame environment oxidize?
- b) How are intermediate products formed and destroyed?
- c) How does the species distribution near the wall evolve during the oxidation process?
- d) What is the impact of the burned gas temperature, and initial burned gas radical concentration on hydrocarbon oxidation?
- e) What are the roles of convective and diffusive transport and chemical kinetics in the oxidation process?
- f) How do the following parameters affect the process and the oxidation level of total hydrocarbons? Why?
 1. fuel type
 2. initial width of hydrocarbon layer
 3. wall temperature
 4. fuel/air equivalence ratio

The following chapters address these questions in extensive detail.

Chapter 2 Methodology

In order to investigate the details of the processes which govern the oxidation of unburned hydrocarbons, a model that can capture the essential features of physics and chemical reactions must be built. A CFD simulation with detailed engine geometry coupled with a full chemical kinetic scheme is ideal for this task. However, such calculations are still very computing time intensive. For instance, Hellstrom et al. [22], performed a full scale simulation, including complex geometry and detailed chemistry, which took about one CPU month on a workstation. Accordingly, sensitivity studies for various parameters affecting the oxidation using such CPU-intensive simulations are limited, and a thorough investigation becomes very difficult. Therefore, finding methods to simplify the model in order to make the computational time acceptable without losing the important characteristics of the processes is one of the major challenges in this projects. Since a detailed description of the chemical kinetics of hydrocarbon oxidation is necessary for analyzing the formation/destruction processes of partial oxidation products, a simplification of physical conditions inside the cylinder at expansion and exhaust strokes is needed.

2.1 Experimental observations of the post-flame oxidation process

The post-flame oxidation of unburned hydrocarbon emissions in a spark ignition engine is a complicated process involving the transport of unreacted fuel-air mixture from sources into the burned gases, and its subsequent reaction. Measured concentrations and temperatures near the cylinder walls indicate steep gradients in both variables in the direction from the engine surfaces to the burned gas [11,27]. This clearly indicates that homogeneous zero-dimensional chemical reaction models are not suitable to address this process. CFD simulations [19,20,21,22] also support those observations: simulations show that hydrocarbons emerging from piston top-land crevices are confined within a layer adjacent to the walls, where temperatures are low enough to suppress oxidation reactions, and that the iso-contour lines of temperature and concentration of hydrocarbons are approximately parallel to the engine wall surfaces. Accordingly, most species and heat diffusion occurs along the direction of steepest gradients perpendicular to the walls. Further, since the engine bore is much larger than a typical unburned hydrocarbon mixture layer, the diffusive-reactive process can be approximately treated as a

planar, one-dimensional configuration during expansion process. Therefore, a one-dimensional model is appropriate to describe the process governing post-flame oxidation near the walls of the cylinder, except for the corner regions. Flow processes taking place in the engine piston/liner corner area are multi-dimensional, particularly after bottom-dead-center, when remaining unreacted hydrocarbons adjacent to the wall are scraped up into a vortex by the moving piston towards the exhaust valve [28]. However, the essential features of the reacting zone along a steep gradient are still maintained. Once the reactive-diffusive process is better understood, a simplification of the chemical mechanisms can be done for use in more complex flow configurations. With these considerations in mind, the oxidation process was simplified as a one-dimensional problem.

2.2 One-dimensional model formulation

The system to be considered consists of a thin layer of unburned air-fuel mixture, adjacent to an impermeable wall maintained at a specified temperature on one side, and to post flame combustion burned gas on the other. The system is representative of hydrocarbons emerging from different hydrocarbon sources and forming a thin layer within low-temperature regions during the expansion and exhaust processes. A piston top-land crevice is chosen as the hypothetical source for purposes of simplification, since crevices are the biggest contributors to hydrocarbon emissions; the composition of the mixture within the layer will therefore be assumed to be that of unburned fuel-air mixture. The assumed configuration is depicted in Figure 2.1. Conditions in the burned gas are governed by the adiabatic expansion of the gases, subject to the pressure history of the expansion process, in order to mimic the engine-like post flame thermodynamic environment. An initially unreacted layer of hydrocarbon-air mixture along the cylinder liner is allowed to diffuse and react during the expansion and exhaust processes.

2.2.1 Numerical model

A transient, one-dimensional, reactive-diffusive model has been formulated for simulating the oxidation processes taking place in the reactive layer between the hot, burned gases and the cold, unreacted air/fuel mixture. All the transport of species and heat is assumed to occur in the radial direction (here converted into the planar coordinate x). The gradients of concentrations of species and temperature are assumed to be negligible in the axial direction (y).

In addition, the Dufour effect, by which a heat flux is caused by concentration gradients, and the Soret effect, by which species diffusion can result from thermal gradients, are neglected [29]. All species are assumed to behave as ideal gases. The resulting mass, energy and species conservation equations, coupled with the ideal gas law, are solved for the entire process, using a detailed chemical kinetic scheme. The governing equations are shown as follows,

$$\frac{\partial \rho}{\partial t} + \frac{\partial u \rho}{\partial x} = -\Lambda(x, y) \quad (2-1)$$

$$\rho \left(\frac{\partial Y_i}{\partial t} + u \frac{\partial Y_i}{\partial x} \right) - \frac{\partial}{\partial x} \left(\rho D_i \frac{\partial Y_i}{\partial x} \right) - \dot{\omega}_i = 0 \quad (2-2)$$

$$\rho \bar{C}_p \left(\frac{\partial T}{\partial t} + u \frac{\partial T}{\partial x} \right) - \frac{\partial}{\partial x} \left(\kappa \frac{\partial T}{\partial x} \right) - \frac{dp}{dt} + \sum \dot{\omega}_i h_i = 0 \quad (2-3)$$

$$p = \frac{\rho R T}{\bar{W}} \quad (2-4)$$

The main concentration and temperature gradients occur in the radial direction (x). However, the axial expansion of the gases caused by the pressure drop and piston movement does offer a non-negligible term to the continuity equation, which must be included in the model.

The term $\Lambda(x, y) = \frac{\partial \rho v}{\partial y}$ in the mass conservation equation accounts for the volumetric expansion effect due to the downward movement of the piston. Here it is assumed that the axial expansion velocity v is proportional to the piston velocity, and that it varies linearly from the cylinder head (zero) to the piston speed (S_p). Using this assumption, the term $\frac{\partial \rho v}{\partial y}$ can be

transformed as into $\frac{\rho}{L} \frac{\partial L}{\partial t}$ as follows,

$$\frac{\partial \rho v}{\partial y} = \rho \frac{\partial v}{\partial y} = \rho \frac{\partial \left(S_p \frac{y}{L} \right)}{\partial y} = \rho \frac{S_p}{L} = \frac{\rho}{L} \frac{\partial L}{\partial t} \quad (2-5)$$

where L is defined as the instantaneous distance between the head and the piston (assume the cylinder head is flat) in order to calculate the instantaneous percentage increase in the cylinder volume due to the axial expansion $\left(\frac{1}{L} \frac{\partial L}{\partial t} \right)$. It can be calculated from a known engine geometry.

A co-ordinate transform (see Appendix 1) is carried out to eliminate the convection term in the species and energy equations such that one variable (v) and one equation (mass conservation) are removed from the original governing equations which are now expressed as the mass integrated spatial coordinate η and time τ . The resulting equations after transformation are follows:

$$\rho \frac{\partial Y_i}{\partial \tau} - \frac{\rho L}{(\rho L)_o} \frac{\partial}{\partial \eta} \left(\rho D_i \frac{\rho L}{(\rho L)_o} \frac{\partial Y_i}{\partial \eta} \right) - \dot{\omega}_i = 0 \quad (2-6)$$

$$\rho \overline{C_p} \frac{\partial T}{\partial \tau} + \sum \dot{\omega}_i h_i - \frac{\partial p}{\partial \tau} - \frac{(\rho L)}{(\rho L)_o} \frac{\partial}{\partial \eta} \left(\kappa \frac{(\rho L)}{(\rho L)_o} \frac{\partial T}{\partial \eta} \right) = 0 \quad (2-7)$$

Consequently, $n+2$ dependent variables (the mass fraction of species (Y_i , $i = 1, n$), temperature (T), and mass density (ρ)) are solved for, with respect to two independent variables (τ and η), from n species conservation equations, the energy conservation equation and the ideal gas law. The pressure p and distance L are prescribed as inputs to drive the simulations. All species reaction rates ($\dot{\omega}_i$) and physical properties (\overline{W} , h_i , $\overline{C_p}$, k , and D_i) are calculated as function of the dependent and independent variables (see discussion in section 2.3). Basically, the dependencies of these species reaction rates and physical properties on the variables are as follows,

$$\dot{\omega}_i = f(Y_i, T, p) \quad (2-8)$$

$$\overline{W} = f(Y_i) \quad (2-9)$$

$$h_i = f(T) \quad (2-10)$$

$$\overline{C_p} = f(T) \quad (2-11)$$

$$k = f(Y_i, T, p) \quad (2-12)$$

$$D_i = D_{i,m}(Y_i, T, P) + D_i(\tau, \eta) = f(Y_i, T, p, \tau, \eta) \quad (2-14)$$

A time-adaptive PDE solver was adopted from the NAG numerical library [30], which uses finite differences for the spatial discretization; the method of lines is employed to reduce the PDEs to a system of ODEs; and the resulting stiff ordinary equations are solved using a Backward Differentiation Formula (BDF) method. A fixed mesh was used in the current

computations, with the densest mesh around the initial interface between burned gas and hydrocarbon layers, as explained in detail in a subsequent section. The width between mesh points grows at a rate of 5 percent per point towards both ends (Fig. 2.2) in order to save computational time.

2.2.2 Initial and boundary conditions

One of the purposes of this study is to examine the effect of the pressure, temperature, and composition of the burned gases on the oxidation process. Since the thermodynamic environment inside an engine changes drastically during the expansion process, the unburned hydrocarbons emerging from the sources at different times face a very different environment. Accordingly, simulations must be carried out at different initial conditions corresponding to segments leaving the cold crevices at different times during the cycle to explore this effect. The baseline operating condition for the burned gas thermodynamic simulation was chosen as 1500 rpm, maximum brake torque spark timing, 3.75 bar IMEP and 361 K coolant temperature. This mid-load, mid-speed operating condition has been chosen based on experimental conditions with which current simulation results are to be compared. The temperature and pressure histories are obtained from a separate engine simulation program developed at MIT by Poulos and Heywood [31,32]. Seven different conditions were chosen, as shown in Table 1, to bracket the range of temperatures at which most hydrocarbons are oxidized survive, down to the temperature region where very little oxidation takes place.

The initial conditions consist of a near-step function in both temperature and species composition. Initial conditions within the cold hydrocarbon layer are set as the wall temperature and unburned fuel-air mixture composition; the burned gas temperature and composition of the post flame combustion gas are specified for the region outside the thin hydrocarbon layer. In the transition zone, the temperature is linearly interpolated between the temperature of the hot and the cold gases. The species composition, which is known to vary non-linearly with temperature, is assumed to be the same as that of the unburned gas at temperatures below 800 K, or is assigned to be the burned gas composition. The base width of the cold hydrocarbon layer (δ_{HC}) is assumed to be 0.1 mm, which is of the order of magnitude of the piston/liner crevice gap in spark ignition engines. The entire domain is about 200 times larger than the base width of the cold layer, to ensure that the burned gas acts as an energy and radical reservoir during the whole process. The thickness of the transition zone (δ) is chosen to be about 0.02 mm in the current calculations. As a result of the diffusive smoothing, the sensitivity of the calculated results to the

initial specifications of the transition zone has been conducted. The study shows that the effects are not significant (will be shown in detail in section 3.1.4), unless the transition zone is the order of one millimeter, thus acting as a thermal boundary layer to protect unburned hydrocarbons from being oxidized.

Since the burned gas composition is assumed to be homogeneous in space at the start of the simulation, a zero-dimensional model was adopted to calculate its composition. This calculation is made by assuming that the gas reaches chemical equilibrium at the peak pressure of the engine cycle, and then undergoes kinetically controlled changes in composition as the pressure and temperature decrease. The STANJAN program [33] was used to calculate the equilibrium composition of the mixture at a given peak pressure and temperature. A modified SENKIN program, which employs the CHEMKIN gas chemistry library [34], was then adopted to drive the non-equilibrium burned gas kinetics with the prescribed pressure and temperature histories for the results of the concentrations of species as a function of time.

For the current model, a fixed wall temperature and zero flux of species at the impermeable wall are specified on the cold layer side as boundary conditions. Zero flux conditions are also specified for all variables at the hot boundary, assuming a homogeneous burned gas composition.

2.3 Sub-models

Several sub-models must be incorporated into the numerical model to provide all the values of physical properties of mixture, molecular and turbulent transport coefficients, and chemical reaction rates. These are discussed below.

2.3.1 Physical properties

All physical properties used in the simulations, such as the mixture-averaged specific heat $\overline{C_p}$, enthalpy h_i , and mean molecular weight \overline{W} , are calculated based on the thermodynamic data for each species from the Sandia thermodynamic data base [35]. The overall transport coefficient for mass or energy diffusion is assumed to be the sum of molecular and turbulent coefficients. The mixture molecular thermal conductivity κ , and molecular diffusion coefficients $D_{i,m}$ were obtained from the Sandia transport package [36]. A simplified treatment of turbulent mixing is made by assuming turbulent transport coefficients calculated from a

simplified k-ε model with homogeneous decaying turbulence and assumption of unity turbulent Schmidt number [37], as explained in detail in the next section.

2.3.2 Turbulence model

Although numerous in-cylinder measurements of turbulence have been made in engines, there is very little information on the flow and turbulence characteristics near the wall *after* flame passage. Post-flame, near-wall boundary layer velocity measurements [38], thermal boundary layer temperature measurements [27], and recent fluorescence imaging of unburned hydrocarbons escaping the upper ring-land crevice [39], suggest that at the region near the walls (the range being in the order of millimeter) small scale turbulence near the wall is not dominant. The high molecular viscosity and diffusivity in the hot post flame environment suppresses the turbulence production and increases molecular diffusion, thereby making relative contributions of molecular and turbulent diffusion comparable in magnitude. Given the lack of experimental data on the structure of turbulence in the post-flame environment near the walls, a simplified turbulence model was created for estimating the turbulent diffusion coefficient in order to quantitatively test the transport effect on the oxidation process.

The model is based on the concept of eddy diffusivity, which assumes that the transport coefficient is proportional to the turbulent intensity and an integral length scale:

$$\alpha_t = c_\mu \sqrt{k} \ell \quad (2-15)$$

where c_μ is a proportionality constant of value $c_\mu = 0.09$ (obtained for flat plate boundary layer) [40]

The turbulent kinetic energy k is related to the turbulent intensity u' by the assumption of isotropic turbulence:

$$k = \frac{3}{2} (u')^2 \quad (2-16)$$

Experimental measurements suggest that the turbulent intensity decreases very gradually within the boundary layer as the wall is approached [38]. In this study, we adopt the approximation that the turbulent kinetic energy is uniform throughout the boundary layer. In

addition, since the region of interest is very close to the wall, it is reasonable to assume that the integral length scale ℓ is represented by the distance x away from the wall throughout the boundary layer region, asymptoting to the core integral length scale ℓ_∞ , assumed to be 3 mm [43,44], according to:

$$\frac{\ell}{\ell_\infty} = \frac{x / \ell_\infty}{1 + x / \ell_\infty} \quad (2-17)$$

Since the bulk turbulent intensity decays rapidly after combustion [38,44,46,47], the decay of turbulent kinetic energy after combustion was modeled by integrating the k - ε equations by assuming that no turbulence is produced and that turbulence is isotropic :

$$\frac{dk}{dt} = -\varepsilon \quad (2-18)$$

$$\frac{d\varepsilon}{dt} = -\frac{C_{\varepsilon_2} \varepsilon^2}{k} \quad (2-19)$$

$$\frac{k}{k_o} = \left(1 + (C_{\varepsilon_2} - 1) \frac{t}{\tau_o}\right)^{-\left(\frac{1}{C_{\varepsilon_2} - 1}\right)} \quad (2-20)$$

where

$$\tau_o = \frac{\ell_o}{\sqrt{k_o}} \quad (2-21)$$

The constant C_{ε_2} (1.9) was determined from a fit to measurements of decaying turbulence [41]. The time origin was chosen from experimental data to a point (15 CAD after TDC) when the turbulence level begins to decay [38,42]. The initial length scale was taken as 3 mm based on experimental measurements [43,44] and the initial kinetic energy was calculated assuming the following correlation between the turbulent intensity and mean piston speed [45],

$$k_o = \frac{3}{2} (u_o')^2 = \frac{3}{2} (\chi \overline{S_p})^2 \quad (2-22)$$

A value of 0.75 was selected for the constant χ , again based on a fit to experimental values of u_o' [38,42]. Using the constants described, the decay in turbulent kinetic energy then shows good agreement with experimental data in the range and conditions where measurements were made [46,47].

Figure 2.3 illustrates the predicted values of local turbulent diffusivity and molecular thermal diffusivity in the case of initial core temperature of 1500 K. Since local molecular diffusivity increases drastically about an order of magnitude from the wall regions (temperatures are around 400 K) to the burned gas zone (temperatures are above 1400 K), the molecular diffusivity remains larger than the turbulent diffusivity till the distance of 1 mm away from the wall is approached. The model predicts molecular diffusivity dominates within the distance of 0.1 mm, while the turbulent diffusivity dominates at the regions an order of magnitude of centimeter away from the wall. The transition regions are within the orders of magnitude of 0.1 mm to 1 mm away from the wall.

Examination of the experimental data shows that the effect of large scale motions such as swirl and tumble on the turbulence intensity is positive during the expansion cycle [38,44,46] so that turbulent transport is expected to increase. Near-wall temperature measurements show very similar profiles between low and high swirl cases, suggesting that swirl probably has only a small impact on energy diffusion. It is possible that tumble motion might increase species diffusion from the wall into post-flame gases, but these factors are beyond the scope of this study. In order to study the role of transport on the oxidation process, it seems reasonable to consider a range of turbulent intensities within acceptable limits for the analysis. Experimental data suggest that a factor of two increase in turbulent intensity is a reasonable extreme to account for the effect of swirl and tumble on turbulent transport.

2.3.3 Chemical kinetic models

In order to capture the important features of the processes taking place within the reactive layer, especially the formation and destruction of partial combustion products, detailed chemical reaction mechanisms are used. These mechanisms provide a description of the elementary reaction steps occurring during the conversion of the fuel and oxidizer to the final products. In reality, all detailed mechanisms are approximations based on available experimental results at relatively narrow experimental conditions. In this study we adopt mechanisms which have been tested and validated for the widest available range of conditions

Propane is chosen as the reference fuel, since it is the simplest alkane which produces an appreciable amount of intermediate products, as is the case with more complex hydrocarbons. The model for propane oxidation has been tested for years against a wealth of experimental data, so that a reasonably high accuracy of model predictions can be expected. A chemical kinetic scheme consisting of 227 elementary reactions among 48 species for propane oxidation [48] (see Appendix 2.1), which was validated under jet-stirred reactor, shock tube, and laminar flame experiments for wide temperature, pressure, and fuel/oxygen ratio ranges, was used to investigate details of the oxidation process of hydrocarbon species.

Isooctane was chosen as the next most complex compound, since it is also a major component in real gasoline. A reaction mechanism previously validated by comparison with turbulent flow reactor and laminar flame experiments was adopted for isooctane oxidation [49] (see Appendix 2.2), containing 455 reactions and 68 species. However, due to the narrow range of validation from few available experiments, the simulation results should be interpreted with caution.

In order to compare the role of chemistry and heat release, ethane and ethene were used as species with similar diffusivity. The ethane oxidation mechanism [50] (see Appendix 2.3), is a sub-mechanism of propane oxidation.

The detailed kinetic reaction mechanisms are summarized in Appendix 2, in which the forward reaction rate coefficients are given for the conventional modified Arrhenius form. The reverse reaction rate coefficients are computed from the forward rates and the appropriate equilibrium constants, which are calculated from the Sandia thermodynamic database [35], unless indicated. Due to the lack of accurate thermochemical properties of large species in the isooctane mechanism, both forward and reverse reactions are explicitly listed and calculated independently.

Table 2.1. Initial conditions for simulations*

T_{∞} (K)	P (bar)	θ_0 (°)**
2000	8.0	405
1800	5.2	420
1600	3.2	445
1500	2.4	460
1400	1.8	485
1300	1.5	505

*1500 rpm, MBT spark timing, 3.75 bar IMEP, 361 K coolant temperature

**Degrees from top dead center (TDC) of intake ($\theta_0 = 0^\circ$). TDC of is $\theta_0 = 360^\circ$

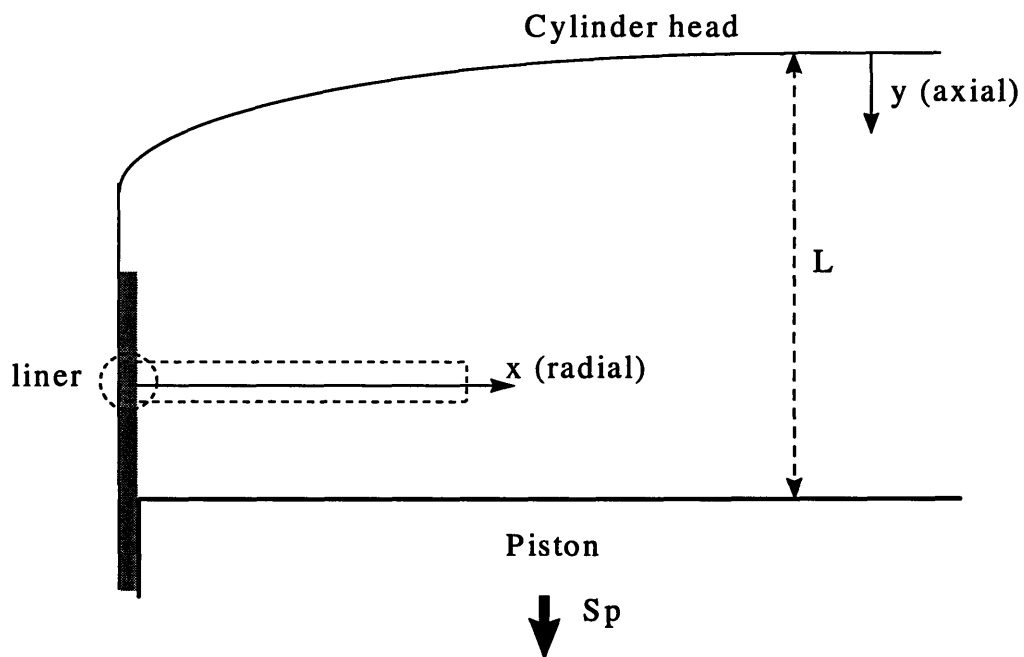


Figure 2-1 Schematic layout for the simulation

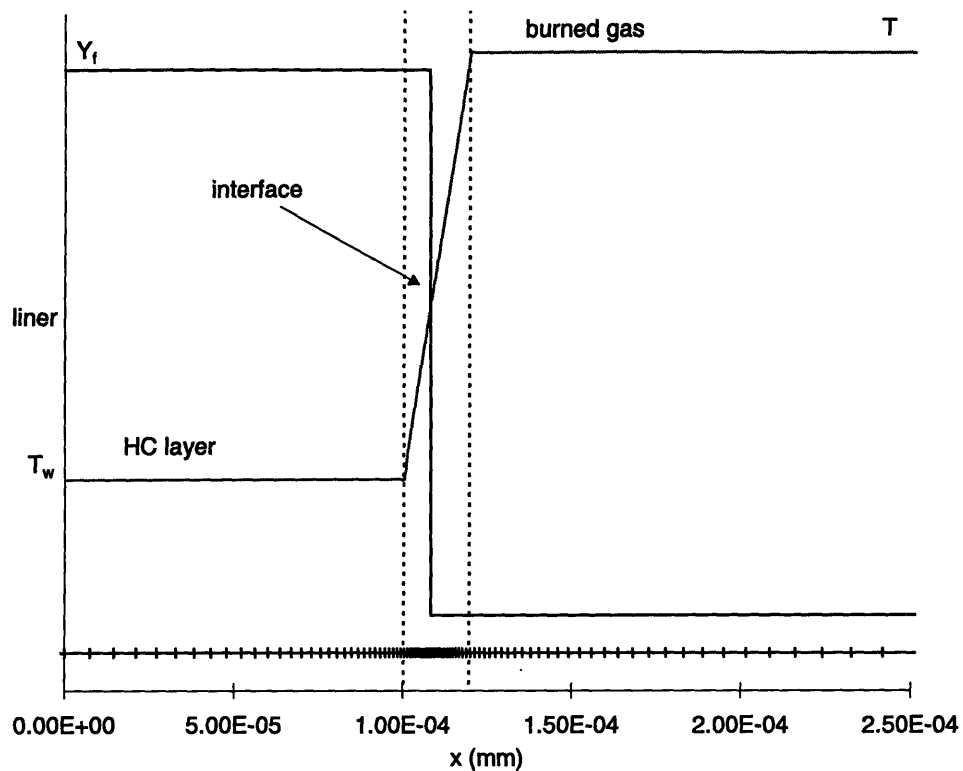


Figure 2-2 Mesh distribution for the simulation.

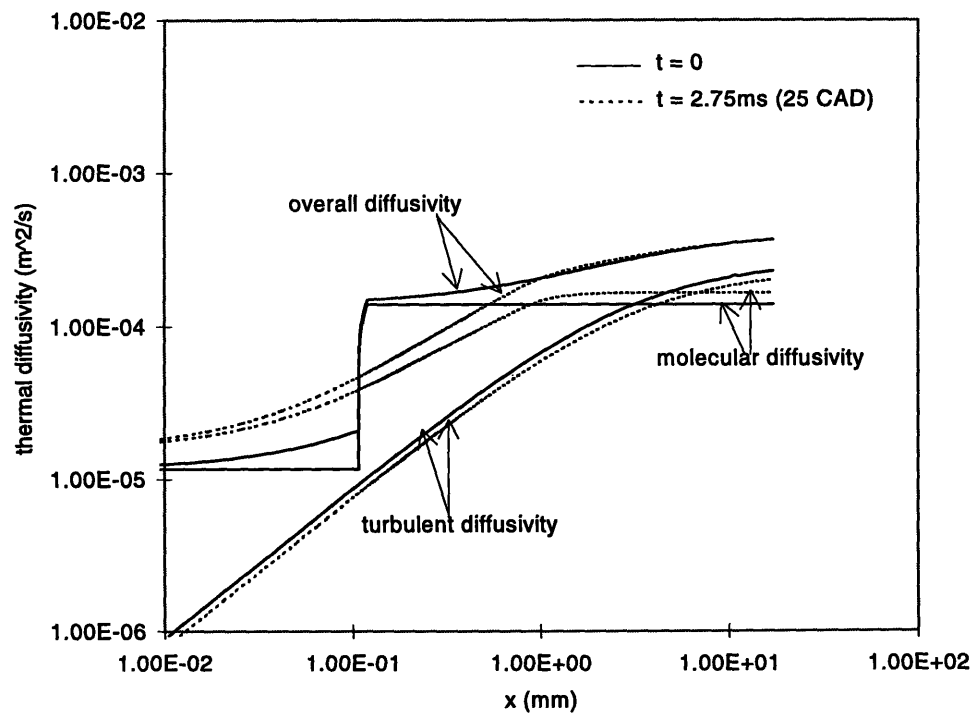


Figure 2-3 Spatial molecular diffusivity and turbulent diffusivity profiles at the start of reaction (solid line), and 25 crank angle degrees after start of reaction (dashed line) (fuel : propane, initial core temperature : 1500 K)

Chapter 3 The Reactive/Diffusive Process

Simulation results for post flame oxidation processes of unburned hydrocarbons are presented and discussed in detail in this chapter. The general features of the evolution of the reactive/diffusive process and the flux analysis of the contributions of chemical reactions and transport (diffusion and convection) to the time-evolving spatial concentration profiles of species, and the effects of the initial conditions are discussed first. The evolution of the spatially-integrated concentrations of each species through the whole computational domain is also examined. The effects of the specifications of the transition zone (the size and the temperature profile) and initial conditions on the resulting extent of oxidation and fuel/non-fuel distribution are then discussed. Finally, the roles of chemical kinetics and transport and their respective sensitivities are identified. Propane was used as a reference case to illustrate all the details; the mechanisms for isooctane, ethane, and ethylene were used for the purpose of comparison to examine the effects of reactant chemistry.

3.1 Reference model : propane

Due to the drastic changes of the thermal environment inside engines during the expansion stroke, hydrocarbons emerging from sources at different times may have distinct fates in the post flame oxidation process. Figure 3.1 shows the predicted burned gas temperature and pressure histories during the expansion process for the baseline operating condition. The core temperature of combustion products decreases from 2000 K at 405 crank angle degrees (360 crank angle degrees is top dead center of the compression stroke) to around 1200 K at bottom dead center of the expansion stroke (540 crank angle degrees). For the purpose of illustrating the general features and the details of simulated post flame diffusive-reactive process of unburned hydrocarbons, a case initiated at core gas temperature of 1500 K is chosen for the detailed examination of partial oxidation.

3.1.1 Features of the evolution of diffusive-reactive processes

Figure 3.2 shows the calculated spatial temperature profile for a case initiated at the burned gas temperature of 1500 K, corresponding to 460 crank angle degrees for the baseline engine operating condition. The fact that the temperature profiles are almost identical with those

of a non-reactive case suggests that the rate of energy release due to oxidation is much less than the rate of total energy loss to the wall and the expansion work. Consequently, the thermal boundary layer continues to grow as the result of heat loss to the wall. The core temperature continues to decrease during the expansion process due to the pressure decrease by the downward piston movement. Therefore, it would be expected that the overall oxidation should slow down due to the decreasing temperature of the entire thermodynamic environment.

Figure 3.3 shows the corresponding time-evolving profiles of propane. The fuel diffuses into the hot reaction zone, which moves outwards as peak temperatures move into the burned gas region. A molar fraction of the order of a few thousands ppmC1 of fuel species (compared to about 110,000 ppmC1 initially) is found to remain near the wall at the end of the exhaust process. Figures 3.4 and 3.5 depict time-evolving spatial distributions of ethylene, which is a major intermediate species and represents the behavior of similar stable partial combustion products, and carbon monoxide. Partial combustion products are produced quickly (in less than 1 millisecond) after the initial time, and the spatial peak concentrations of intermediate species continue to grow and move outwards. At a certain point, the peak value of the concentration starts to decrease, as the production rate cannot keep up with the diffusion rate, due to the limited supply of 'upstream' hydrocarbons and decreasing core temperatures. In contrast with the fuel species, the concentrations of intermediate hydrocarbons increase near the wall due to the diffusion of species from the reaction zone. Since the temperatures close to the wall are low enough to prevent the conversion of stable partial combustion products, the region near the wall acts as a buffer, accumulating and preserving these influx species, and releasing them as a source of hydrocarbons only when the concentration gradients of the species at the wall become negative. In this particular case (Figure 3.4), at the end of exhaust stroke, the remaining concentrations of ethylene and carbon monoxide at the wall region are a few thousand ppmC1. Therefore, this buffer mechanism provided by the cold region near the walls is found to be the main reason for the survival of partial oxidation products.

Figure 3.6 shows the evolution of spatial distributions of hydroxyl (OH), whose concentration level is the highest among the radicals at lean and stoichiometric conditions. The results indicate that oxidation of hydrocarbons in the reactive layer generates radicals at levels above those in the burned gas. The level of radical concentration in the burned gas decreases as time evolves due to recombination. Hydroxyl is also depleted in the cold regions near the wall because of recombination between radicals at these low temperatures. As the boundary layer

grows, the cold regions with low radical concentration of hydroxyl broaden and the peak concentration of hydroxyl moves away from the wall.

This self-generated radical pool offers much higher concentrations than the original burned gas radical concentrations. This implies that the abundant radicals in the burned gas *do not have a significant effect on the oxidation level of unburned hydrocarbons*, except during reaction initiation. In order to further investigate the role of the burned gas radicals on the post flame oxidation, a comparison was made between a calculation using equilibrium burned gas composition at a core temperature of 1500 K (which has an order of magnitude somewhat lower in radical concentrations than those in the non-equilibrium combustion products) and the case starting from non-equilibrium. The differences in the oxidation level and spatial concentration species profiles are trivial. Figure 3.7 shows an example of the small difference in time-evolving hydroxyl concentration profiles between two cases.

3.1.2 Flux analysis

In order to understand the influence of diffusion and chemical rates on the overall oxidation of species, an extensive analysis is made of the local contribution of diffusion, convection and reaction to the net local rate of change of species concentration. Figure 3.8 illustrates details of spatial species molar fraction concentrations at 25 crank angle degrees (2.75 milliseconds) after reaction start for an initial core temperature of 1500 K.

Figures 3.9-3.12 show the contribution of the diffusion, convection and reaction terms to the net species change at a particular location, at a time corresponding to the species profiles in Figures 3.3-3.6, for propane, ethylene, carbon monoxide, and hydroxyl, respectively. Clearly, the convective term ($\rho u \frac{\partial Y_i}{\partial x}$) can be neglected in comparison with diffusive and reactive terms.

The diffusive term is proportional to the curvature of the concentration profiles, and therefore peaks at the concentration peaks and crosses zero at the inflection point. At this point in time (the corresponding core temperature is 1400 K), peak propane diffusion rates are only slightly larger in magnitude than reaction rates, so that the overall fuel conversion is limited by reaction rate. The integrated net rate of fuel change is negative, so that integrated fuel concentration decreases over time. Ethylene (Figure 3.10) production peaks around the same location as propane destruction, whereas destruction takes place a little further into the high temperature zone. The spatially integrated mass production rate is positive but small (as will be shown in the next section), with the net effect that the total concentration changes little over time. Positive

diffusion towards the cold wall continues at later times, preventing the unburned intermediate hydrocarbons from reacting.

Carbon monoxide (Figure 3.11) is produced at peak rates where ethylene destruction peaks, but little carbon monoxide oxidation takes place in the high temperature zone, resulting in a net increase in the overall concentration of carbon monoxide. However, it is noticed that, due to the accumulation of carbon monoxide, the oxidation rate of carbon monoxide in the high temperature zone will keep up with the production rate in the low temperature region at later times, such that spatially integrated mass of carbon monoxide remains approximately constant.

Hydroxyl radical production peaks towards high temperature zone, diffusing into the low temperature zone to react with carbon monoxide and hydrocarbon species. The peak value of hydroxyl diffusion rate is slightly higher than that of the production rate, so that the net concentration of hydroxyl decreases locally at this time.

3.1.3 Spatially integrated species concentrations

The evolution of overall hydrocarbons can be calculated by integrating the hydrocarbon concentrations over the whole computation domain. The total number of moles of each species remaining per unit cross section of reactive layer was obtained by integration over the spatial layer as a function of time (or crank angle degree θ):

$$n_i = \int_0^{\bar{x}} \frac{P}{RT} X_i dx \quad (3-1)$$

The amount of total hydrocarbons was calculated by summing over the total moles of fuel and non-fuel species weighted by their carbon numbers:

$$n_{HC} = \sum_i \left(\int_0^{\bar{x}} \frac{P}{RT} X_i c_i dx \right) \quad (3-2)$$

The integrated surviving fraction of the species, and, more generally, of total hydrocarbons originally in the layer, is calculated using:

$$f_i = \frac{1}{n_{i,0}} \int_0^{\infty} \frac{p}{RT} X_i dx \quad (3-3)$$

$$f_{HC} = \frac{1}{n_{HC,0}} \sum_i \left(\int_0^{\infty} \frac{p}{RT} X_i c_i dx \right) \quad (3-4)$$

Figure 3.13 illustrates the rate of overall unburned fuel species conversion into non-fuel species and carbon monoxide as time proceeds in the case of an initial temperature of 1500 K. The simulation shows that non-fuel species and carbon monoxide are produced quickly during an initial period, then maintain an almost constant level, while the amount of fuel continues to decrease. This is because the consumption and production of intermediate species is approximately balanced in the reactive-diffusive process (as shown in previous section) in the case of initial core temperature of 1500 K. As a result, the fuel/non-fuel ratio decreases as time proceeds.

3.1.4 Effect of the initial specification of the transition zone

Figure 3.14 shows the impact of choosing a different initial temperature profile (case (b)) from original linear temperature profile (case(a)) in the transition zone, and initial transition zone thickness (δ) of 0.1 mm and 1 mm away from the wall on the overall calculated extent of oxidation and the fuel and non-fuel species distribution. The temperature profile (case (b)), which is fitted from the temperature measurements in the thermal boundary layer on an engine head [51], in the transition zone is defined as:

$$T(z) = T_w + (T_c - T_w)(z / \delta)^{0.25} \quad (3-5)$$

Simulations show that, whereas the effect of the transition temperature is not particularly dramatic, large changes in the initial transition zone thickness (δ) decrease the extent of oxidation. The impact becomes significant as the transition zone increases to the order of one millimeter in the case of initial core temperature of 1500 K, whereas the influence is little in the case of initial core temperature of 1300 K. In addition, it is noticed that the level of non-fuel species concentration is little influenced by the specification of transition zone, while the resulting concentration of the reactant fuel is more sensitive to the size of the transition zone.

3.1.5 Effect of initial burned gas temperature

The evolution of the surviving overall hydrocarbon concentration is shown in Figure 3.15 for various starting times and corresponding core gas temperatures. Each curve represents the surviving fraction of initial total hydrocarbons released at different times during the expansion cycle, demonstrating the critical role of core gas temperatures in the reactive-diffusive process. None of the hydrocarbons released from top-land crevices at core gas temperatures above 1800 K survives post-flame oxidation after the exhaust valves open (at 485 crank angle degrees) in the case of propane, whereas most of the material released at temperatures below 1300 K remains largely unreacted. In general, an inflection point in the rate of oxidation is observed at a core temperature around 1300 K, below which the reaction is practically “frozen” for residence times of the order of tens of milliseconds. Moreover, flux analysis indicates that peak propane diffusion rates start to exceed reaction rates while core temperatures drop below about 1500 K, so that the overall fuel conversion is limited by reaction.

The evolution of spatial temperature distributions for the case initiated at 1800 K burned gas temperature is illustrated in Figure 3.16. Because of the high rates of reaction at the high initial temperatures, a considerable amount of energy is released, which compensates for the energy loss to the wall, so that the temperatures in the reactive layer are raised above the burned gas temperatures within a very short period (about 0.5 milliseconds). This stimulates reactions in the hydrocarbon-rich region, so that complete oxidation of hydrocarbons is achieved very quickly. Figures 3.17-3.19 depict the time evolving spatial distributions of propane, ethylene, and carbon monoxide, respectively. Results show that the entire conversion process, in which propane decomposes into intermediate products (such as ethylene), then carbon monoxide, then into final products, is finished within about 20 crank angle degrees (about 2.2 milliseconds). In comparison with the case initiated at 1500 K, it is noticed that the effect of heat release actually narrows the reaction zone. Consequently, the high diffusion rate due to sharp gradients of hydrocarbon concentration, combined with a high conversion rate due to the high core temperatures, speeds up the process.

Figure 3.21 illustrates the temperature profiles for the starting temperature of 1300 K, and Figure 3.22 depicts the corresponding time-evolving profiles for the fuel. Results show that at a lower temperature, the fuel diffuses much farther within the same time period compared to high temperature cases due to a slow reaction rate. In addition, a slightly different pattern of the evolution of intermediate products is observed (Figures 3.23-3.24). Peak values of intermediate species continue to grow in the reaction zone, which moves away from the wall. The region

adjacent to the wall accumulates the influx partial combustion products throughout the period considered, so that the gradients never shift towards the hot region. Figure 3.25 shows no significant hydroxyl generation until much later in the oxidation process, due to the slow reaction caused by low temperatures. Clearly, the role of radicals in the burned gas is much more relevant in the case of low initial core temperature. Figure 3.26 shows the comparisons of the effect of the concentrations of radicals in the burned gas (equilibrium vs. non-equilibrium) on the extent of oxidation of hydrocarbons between the cases of initial core temperatures of 1500 and 1300 K. Results indicate the radical concentrations in the burned gas has more effect on the oxidation level in the case of 1300 K. However, due to the low extent of oxidation in the cases of low core temperatures (less than 10%), the effect of radical concentrations on the post flame oxidation is limited.

The initial temperature effect on the oxidation level of total hydrocarbons and the distribution of fuel and non-fuel species is illustrated in Figure 3.27. The mechanism which balances the consumption and production of intermediate products keeps the levels of intermediate hydrocarbons within about 10-15% of the mass of the initial total hydrocarbons in the cases of intermediate core temperatures (1400-1500 K). More fuel reactants remain intact in the cases of low initial core temperatures, so that the ratio of fuel to non-fuel is higher for reactions initiating at low core gas temperatures.

3.2 Effect of diffusion

The overall rate of oxidation in a reactive-diffusive process depends on the slowest of the diffusion and reaction rates. If chemical rates are fast, increasing diffusion rates lead to faster overall oxidation; if, however, rates of oxidation are low, increased diffusion rates will have a much smaller impact, as the reactants simply spread over wider regions. Our goal here is to investigate the effect of diffusion on the total oxidation level and overall fuel/non-fuel ratio, and how this effect varies with initial core temperatures.

As indicated in section 2.3.2, a change in the turbulence intensity by a factor of two was used to investigate this effect. The simple eddy diffusivity model implies that a change of a factor of two would also be expected in the turbulent diffusivity. A comparison between the spatial species distribution results with different diffusivity is shown in Figure 3.28, using the case of initial temperature at 1400 K. As the turbulent diffusivity increases, the spatial species distribution broadens, and the concentration of intermediate species increases. A higher transport

rate increases the reaction rate by carrying more reactants into the reaction zone. The effect of a change in the turbulent diffusivity by a factor of two on the evolution of the extent of oxidation of total hydrocarbons for various initial core temperatures is shown in Figure 3.29. Clearly, the effect of diffusivity is much greater at higher initial temperatures, which is more diffusion limited than low temperature cases.

Figure 3.30 shows the effect of diffusivity on the oxidation level and the fuel and non-fuel fractions in the surviving fraction of total hydrocarbons at various initial core temperatures. An increase of a factor of two in the turbulent diffusivity reduces the fraction of surviving hydrocarbons by 66% at a starting temperature of 1600 K, 42% at 1500 K, 12% at 1400 K, and 2.5% at 1300 K. Consequently, the reduction of unburned hydrocarbons by increased turbulent mixing would be expected to be more effective during operating conditions that can produce higher temperatures during the expansion process (such as increasing engine speed). In addition, the concentration of non-fuel species is little influenced by the change of turbulent diffusivity, such that the remaining fuel/non-fuel ratio decreases with increased diffusivity, as more fuel is transported into the reaction zone and decomposes into non-fuel species. It must be noted that, because of the finite hydrocarbon source, a high diffusion rate causes the level of hydrocarbons on the wall to drop, such that the resulting smaller gradient offsets the effect of high diffusivity to some extent. In addition, in the vicinity of the wall (within 1 millimeter), the predicted turbulent diffusivity is of the same order of the molecular diffusivity, which implies that increasing the turbulent diffusivity does not have a very large effect during the initial stages, while the hydrocarbons are confined within the region where turbulent diffusivity does not dominate. As will be shown in Chapter 4.2.3, increasing molecular diffusivity by about 80% has also a similarly moderate effect on the post flame oxidation.

3.3 Effects of reactant chemistry

The post flame oxidation process is affected by the type of reactant fuel. Experiments show that emission levels for different gaseous fuels (*i.e.*, fuels that are stored in similar sources of hydrocarbons) vary with tested fuel at the same engine operating conditions [8,14], a fact that can be attributed to the difference in either fuel chemistry or molecular diffusivity. The following section investigates the effect of fuel type on post flame oxidation.

3.3.1 Ethane versus ethylene

Ethane (C_2H_6) and ethylene (C_2H_4) have very similar molecular diffusivity due to their similar molecular weight and structure. Therefore, the effect of fuel chemistry can be more closely understood by comparing simulated results of ethane and ethylene. The same temperature and pressure histories were used for both cases to isolate the effects of hydrocarbon layer oxidation, although the adiabatic flame temperature is higher in the case of ethylene. Comparisons of the evolution of the extent of oxidation of overall unburned hydrocarbons is shown in Figure 3.31. Simulations show that ethylene leads to a higher extent of oxidation than ethane, an effect that reflects the role of chemical reactions on post flame oxidation.

Figures 3.32-3.33 show the spatial species concentration profiles in the cases of ethane and ethylene. A higher energy release and reactivity in the case of ethylene leads to a narrower reaction zone, a higher carbon monoxide concentration, and lower fuel concentration near the wall than in the case of ethane. The oxidation paths for ethane and ethylene are very similar, except for the main path for ethane decomposition into ethylene. The shorter path to oxidation in the case of ethylene results in a higher extent of oxidation for the post flame reactive/diffusive process. Figures 3.34-3.35 show the reaction rates as a function of temperature for ethane and ethylene, respectively. Similar levels of destruction rates for both reactant fuels peak at similar temperatures. However, the shorter path to oxidation in the case of ethylene leads to higher production rates of carbon monoxide and carbon dioxide, while a considerable production rate of ethylene (intermediate species), which diffuses towards either high-temperature regions for destruction or low-temperature regions for preservation, retards the conversion rates of carbon monoxide and carbon dioxide.

In addition, in comparison with the case of propane (Figure 3.15), much higher oxidation rates are observed in the cases of ethane and ethylene. Even compared to the propane cases with twice the increase in turbulent diffusivity, ethane and ethylene still show a much higher oxidation rate than propane (even in the case of an initial core temperature of 1300 K). This suggests that fuel chemistry is a more critical factor in determining the oxidation levels than transport for post flame oxidation. Shorter paths to oxidation can also be applied to explain the higher total hydrocarbon destruction rate in the cases of ethane and ethylene than propane.

3.3.2 Isooctane

Isooctane is a major component of gasoline and has much larger molecular weight and quite different chemistry from propane, ethane and ethylene. Figure 3.36 shows the spatial concentration profiles of species for the isooctane case initiated at a core temperature of 1500 K. Compared to the case of propane (Figure 3.8), a higher concentration of hydrocarbons (in terms of ppmC1) is retained near the wall and a higher concentration of intermediate compounds is produced in the case of isooctane. Major differences appear in peak CO concentrations, which are lower by a factor of two in the case of isooctane. In addition, the radical pool concentration overshoot is small in the case of isooctane, and the peak concentrations of active radicals (such as OH, H, and O) are lower by an order of magnitude.

Figure 3.37 shows the profiles of the surviving fraction total hydrocarbon for isooctane fuel at various initial core temperatures. Much lower oxidation levels are observed in the case of isooctane than propane for the same initial condition; in fact, complete oxidation cannot be achieved at initial temperatures as high as 2000 K. This can also be attributed to the slow reactivity of isooctane and a low diffusion rate.

The effect of diffusion on the oxidation process was examined by replacing the molecular diffusivity of isooctane with that of propane (test case at 1600 K). Figure 3.38 shows the comparison of the evolution of the surviving fractions of fuel and total hydrocarbons, and the normalized productions (by the amount of initial total hydrocarbons) of non-fuel and carbon monoxide. An increase of about 50% in the molecular diffusivity of isooctane boosts the total hydrocarbon extent of oxidation of from 43% to 55%, while the level of non-fuel species concentration remains unchanged. However, the final levels of oxidation are still much lower than those found in the case of propane at the same initial temperatures, showing that chemical effects are responsible for most of the difference. A more detailed analysis of the specific reaction paths to investigate the reasons for the different oxidation rates between the cases of propane and isooctane will be presented later in Chapter 5.

Figure 3.39 shows a comparison of the oxidation levels and composition of remaining hydrocarbons between propane and isooctane. Higher levels of surviving partial combustion products are found for all initial temperatures in the case of isooctane. Consequently, a higher level of emissions and a lower fuel/non-fuel ratio should be expected in the case of isooctane, which is consistent with experimental observations.

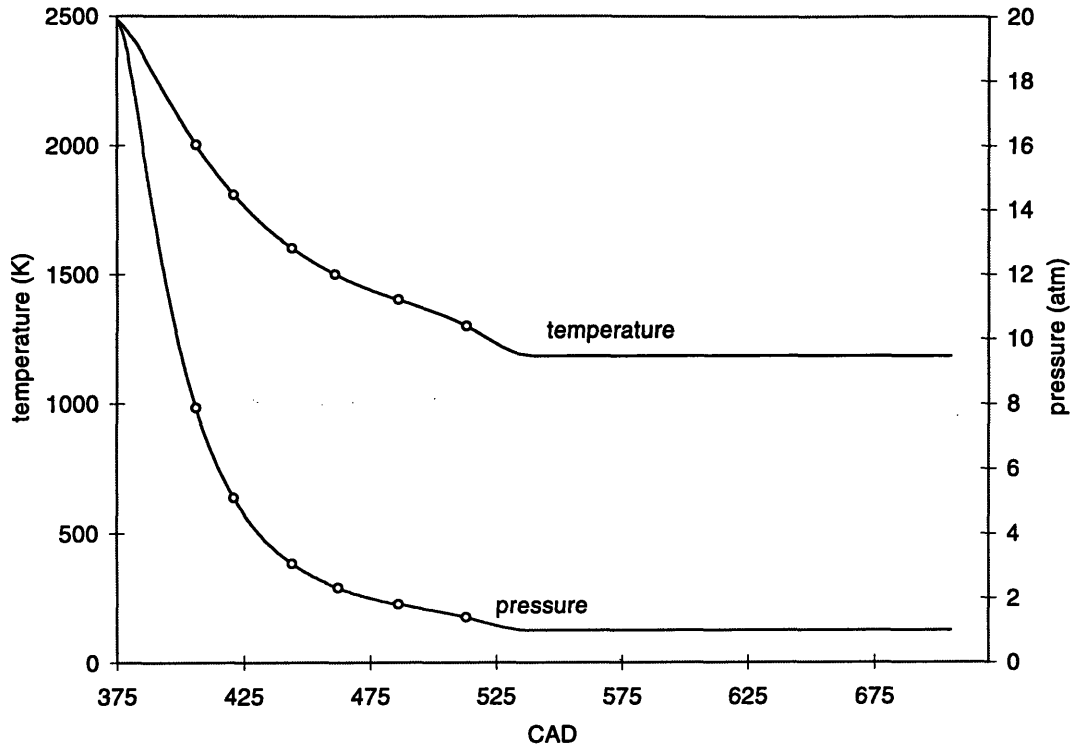


Figure 3-1 Predicted temperature and pressure histories during expansion process for the baseline operating condition. (Circles show the points where simulations start)

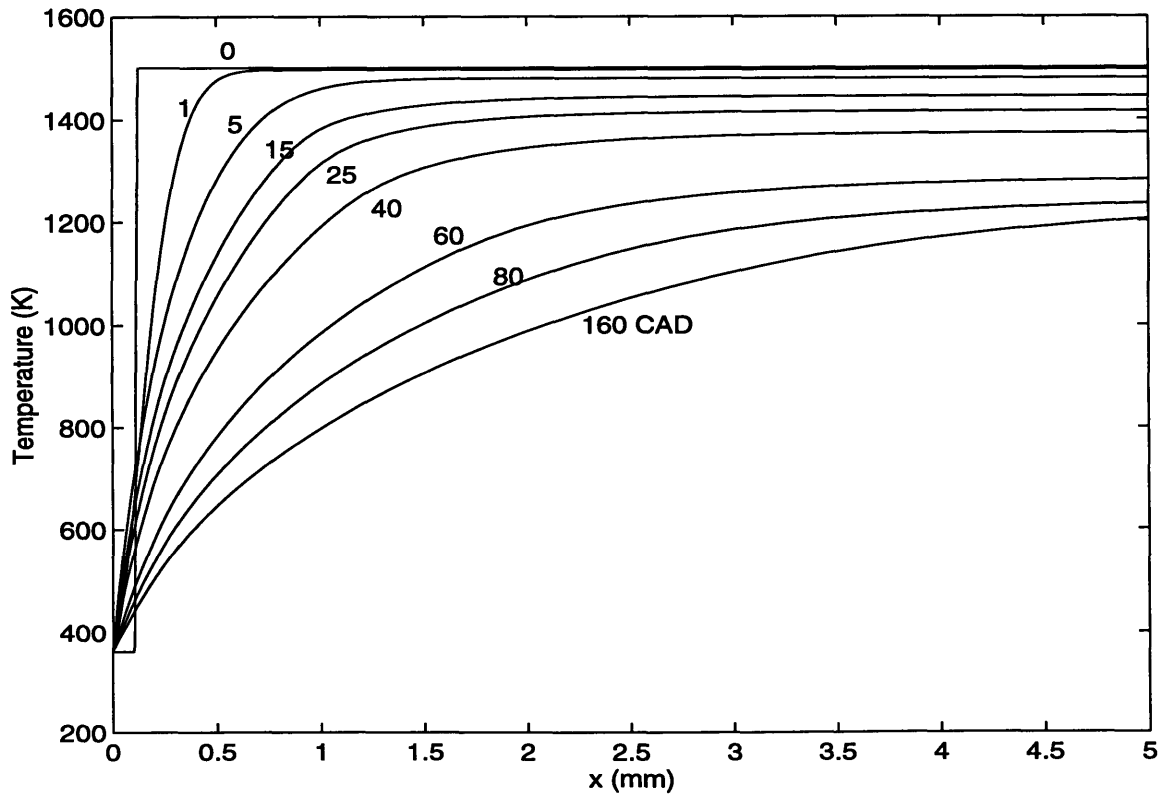


Figure 3-2 Spatial temperature profiles. (fuel : propane, initial core temperature : 1500 K)

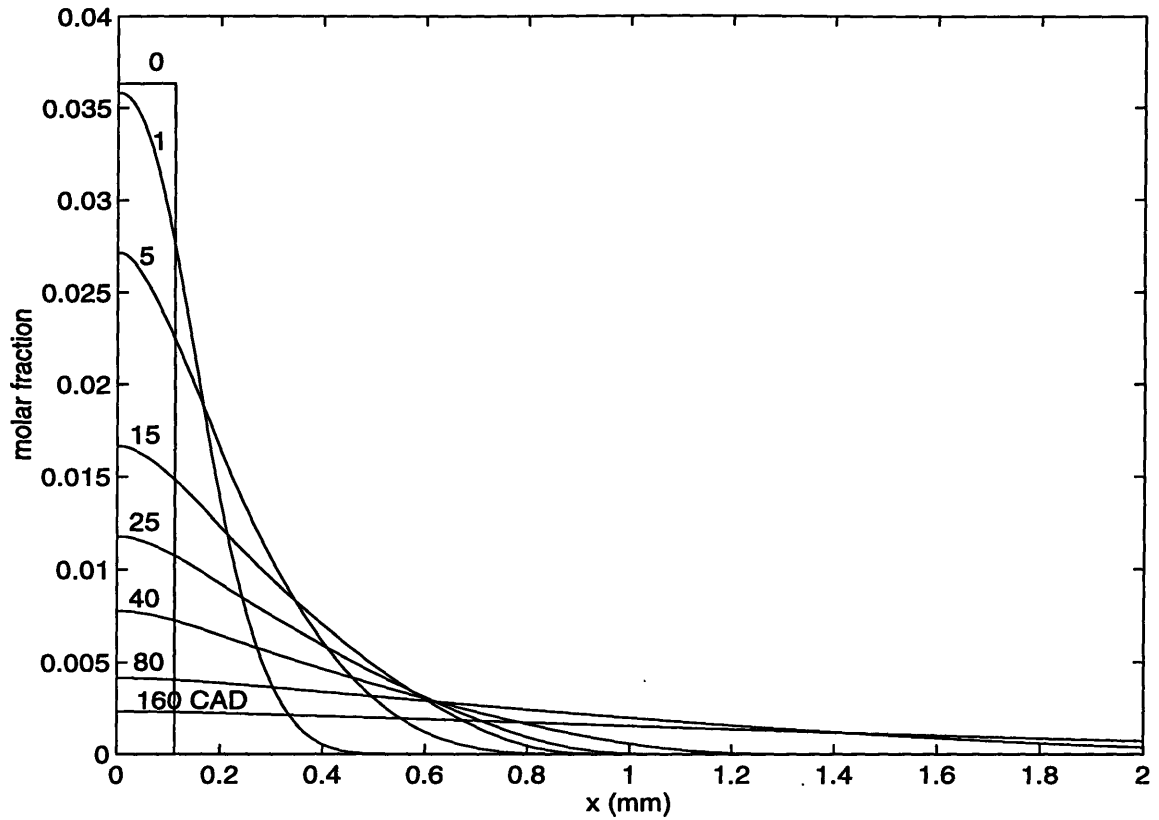


Figure 3-3 Time-evolving spatial distribution of propane. (fuel : propane, initial core temperature : 1500 K)

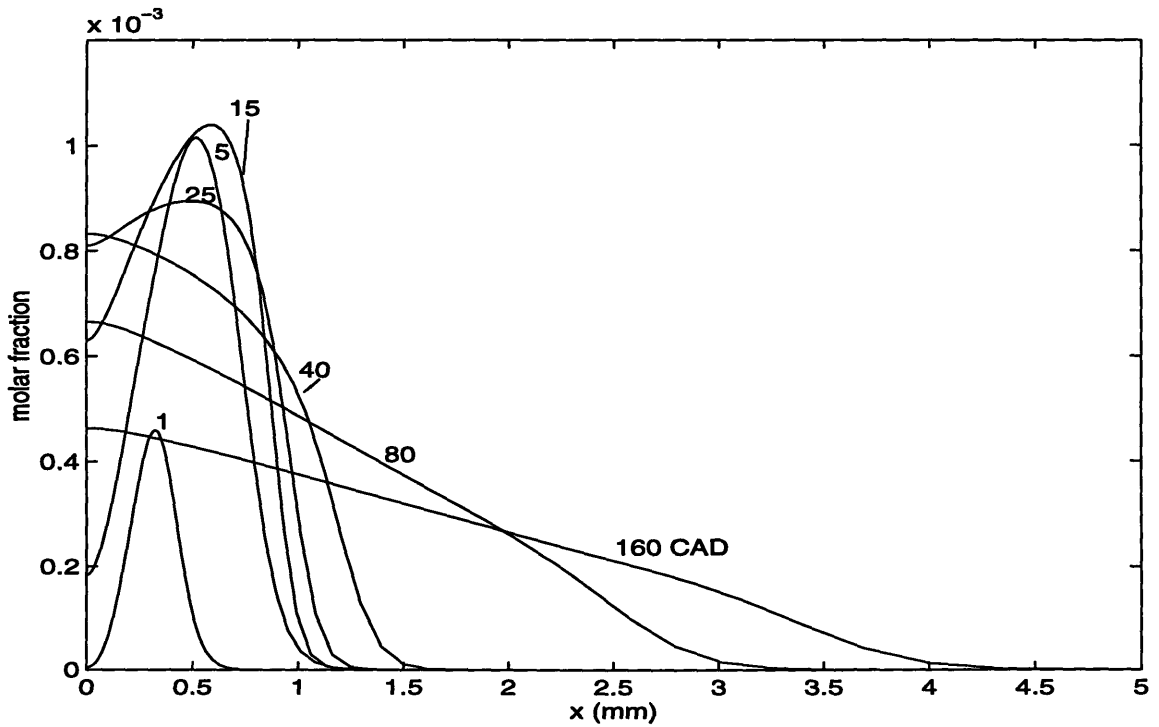


Figure 3-4 Time-evolving spatial distribution of ethylene. (fuel : propane, initial core temperature : 1500 K)

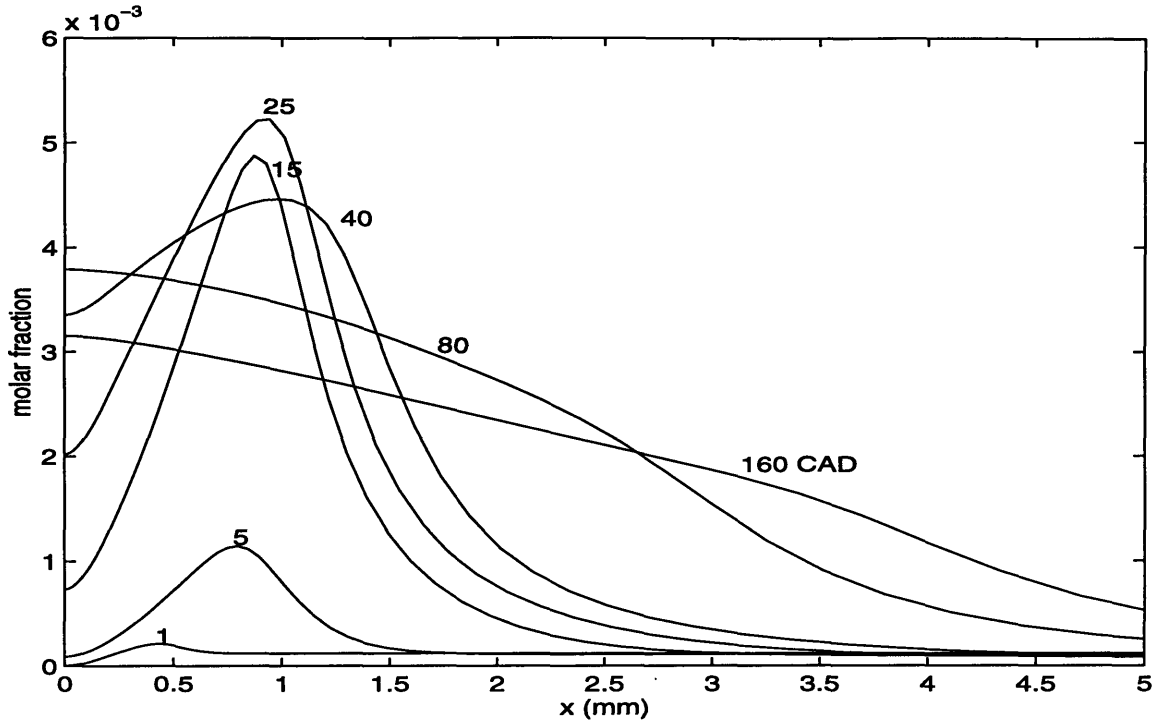


Figure 3-5 Time-evolving spatial distribution of carbon monoxide. (fuel : propane, initial core temperature : 1500 K)

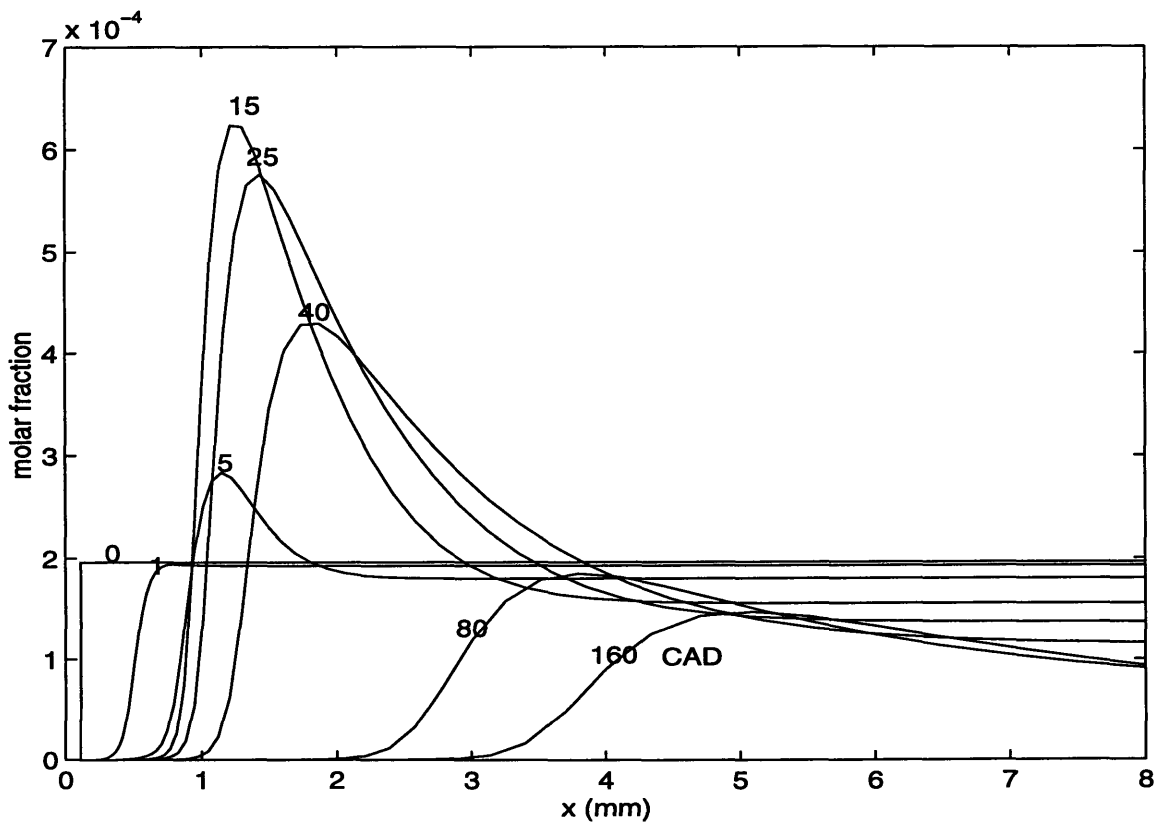


Figure 3-6 Time-evolving spatial distribution of hydroxyl. (fuel : propane, initial core temperature : 1500 K)

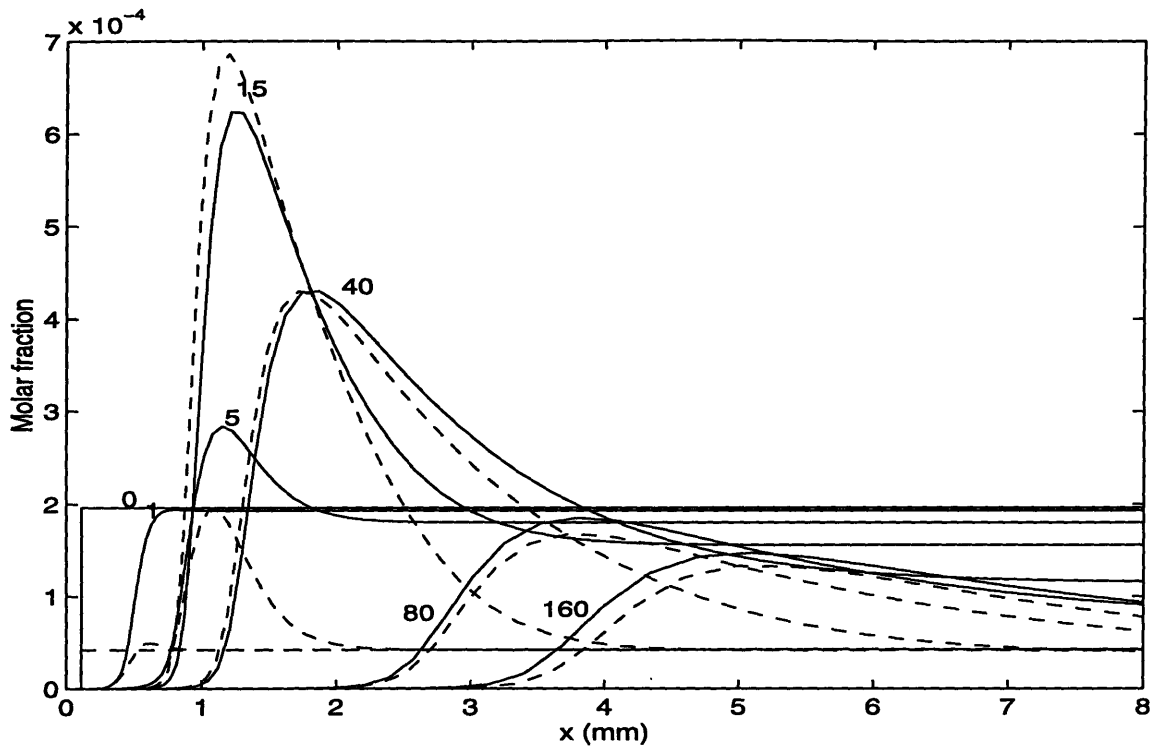


Figure 3-7 Comparison of the time-evolving spatial distribution of hydroxyl between the original case (solid line) and the case of equilibrium composition at 1500 K set on the burned gas side (dashed line). (fuel : propane, initial core temperature : 1500 K)

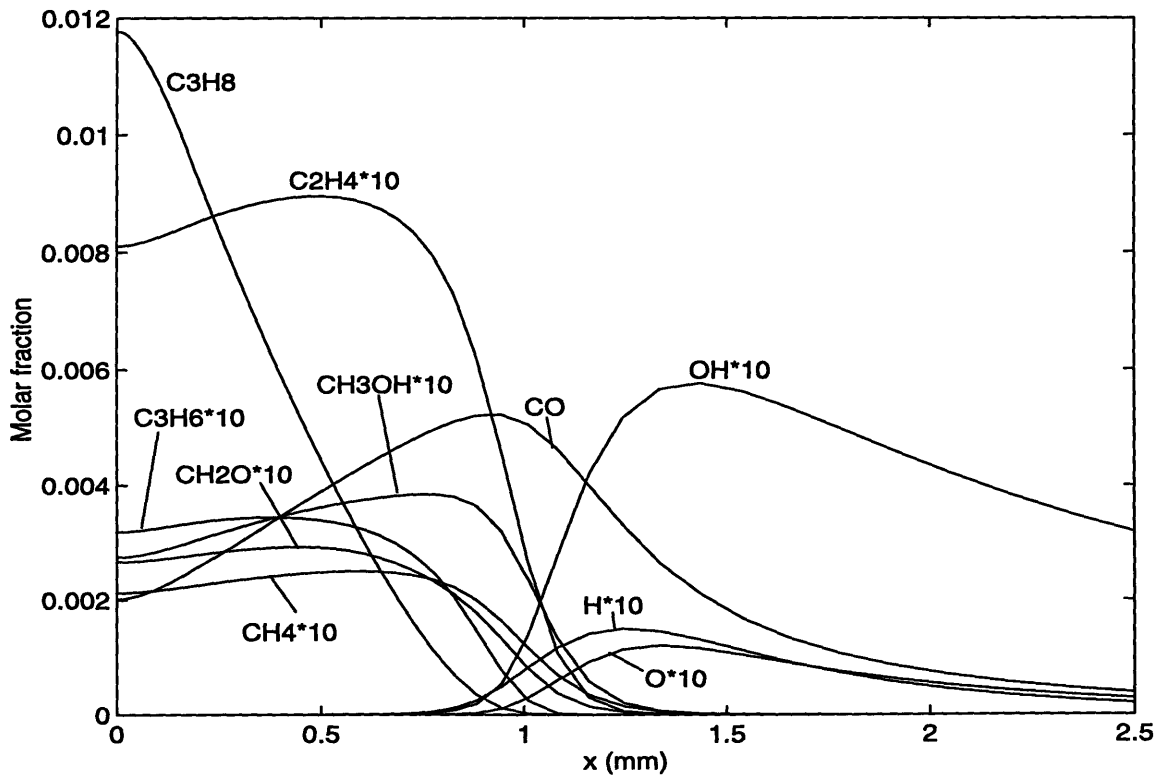


Figure 3-8 Spatial distribution of major species molar fractions at 25 crank angle degrees after start of reaction. (fuel : propane, initial core temperature : 1500 K)

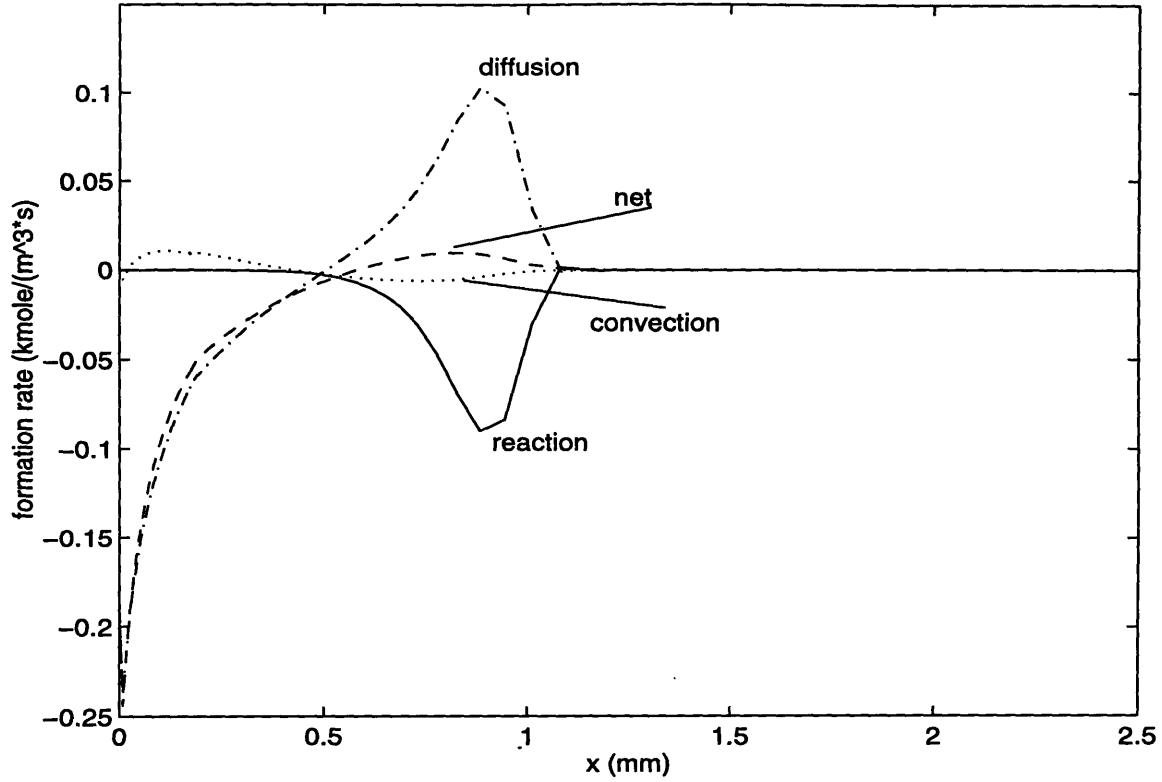


Figure 3-9 Contribution of reaction and transport to the rate of change of propane at 25 crank angle degrees after start of reaction. (fuel : propane, initial core temperature : 1500 K)

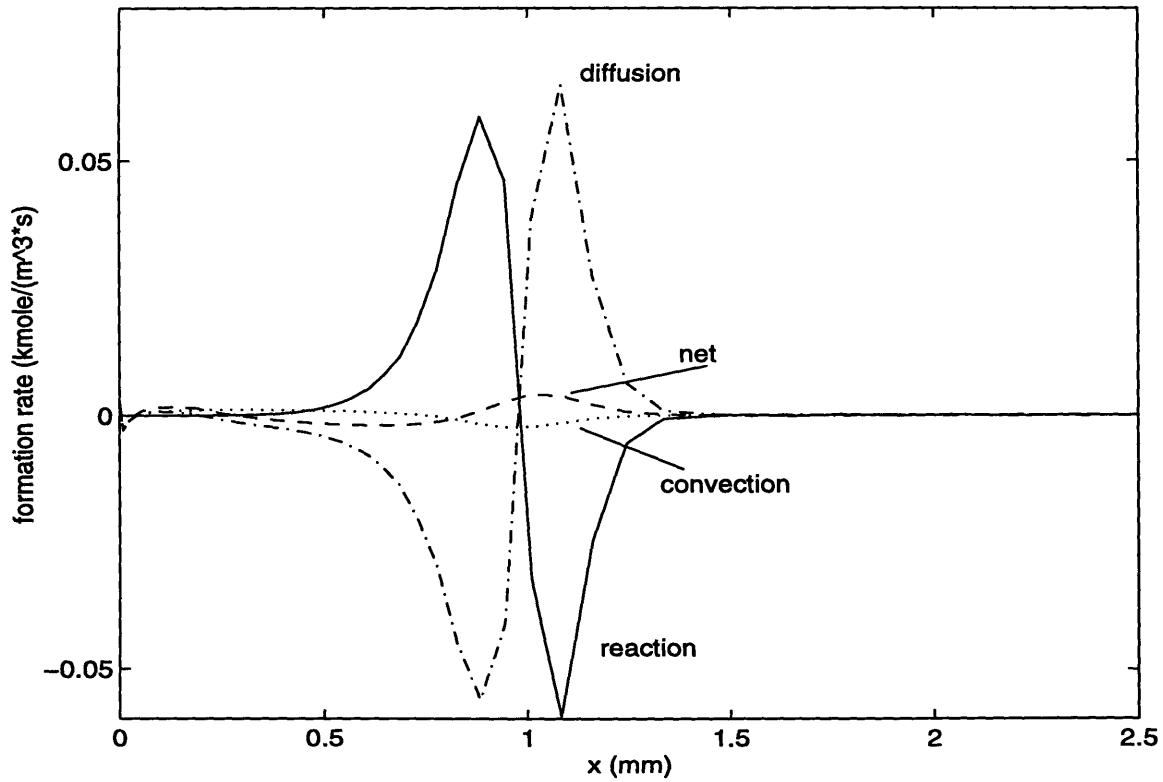


Figure 3-10 Contribution of reaction and transport to the rate of change of ethylene at 25 crank angle degrees after start of reaction. (fuel : propane, initial core temperature : 1500 K)

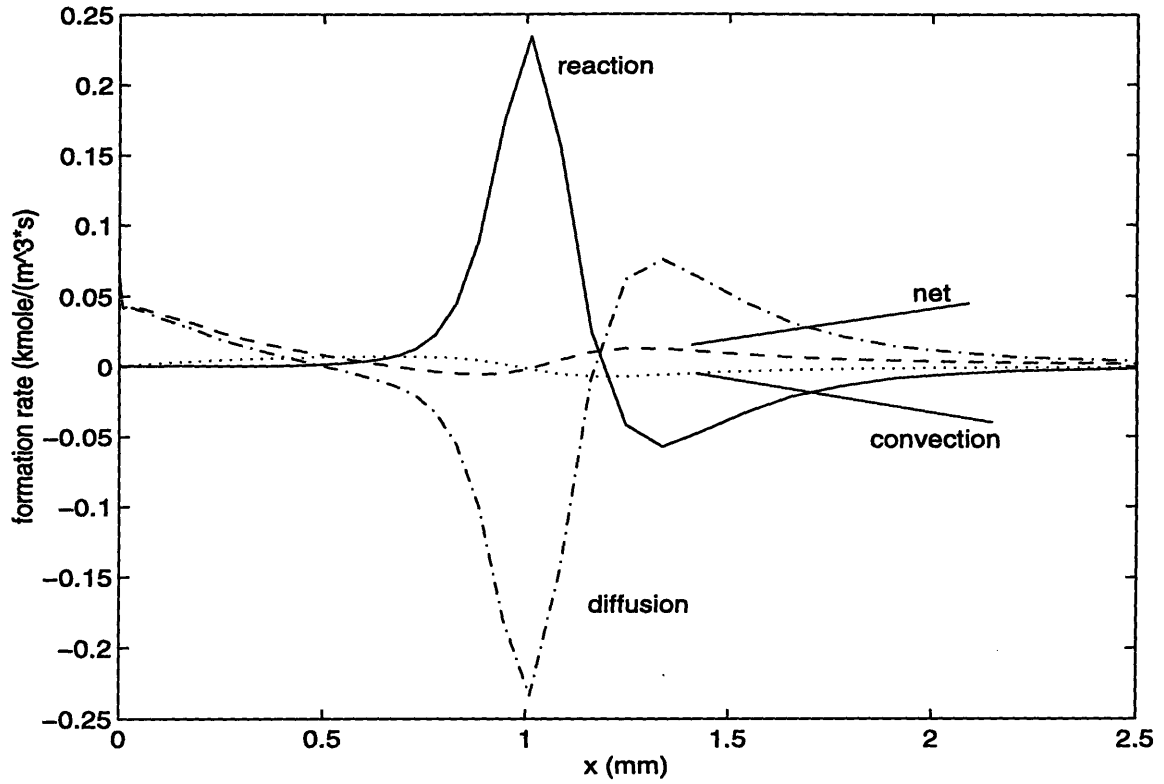


Figure 3-11 Contribution of reaction and transport to the rate of change of carbon monoxide at 25 crank angle degrees after start of reaction. (fuel : propane, initial core temperature : 1500 K)

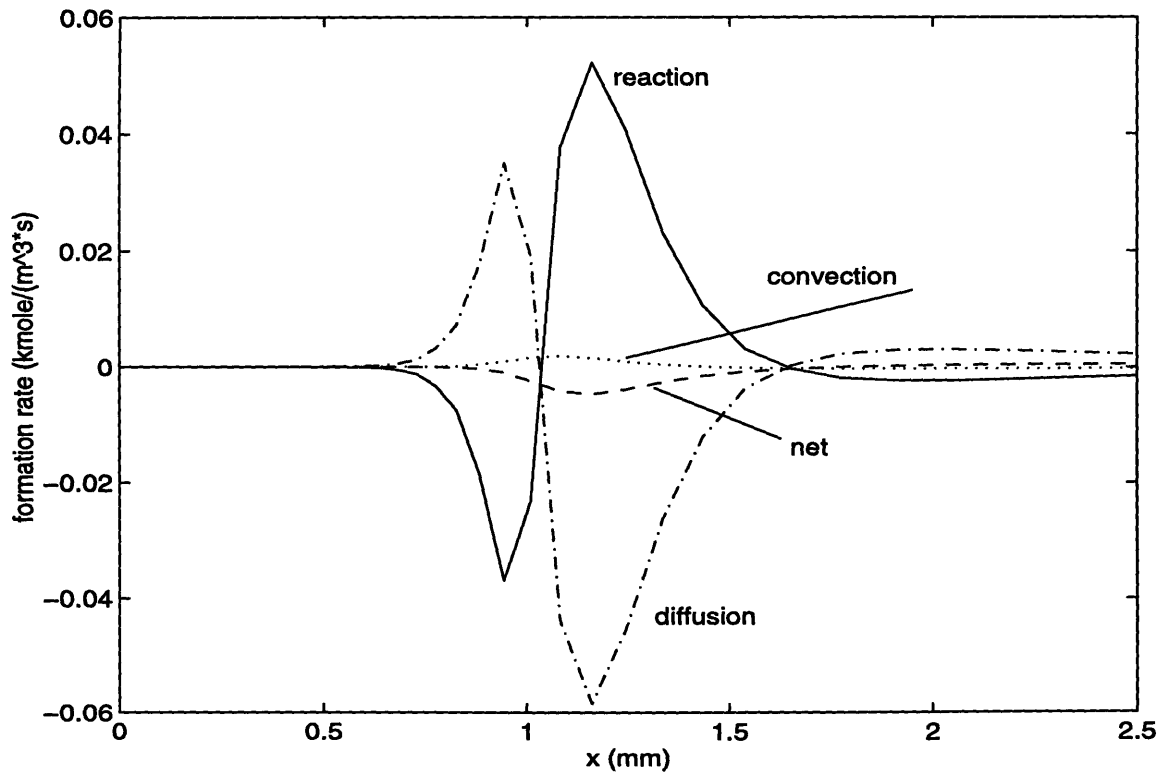


Figure 3-12 Contribution of reaction and transport to the rate of change of hydroxyl at 25 crank angle degrees after start of reaction. (fuel : propane, initial core temperature : 1500 K)

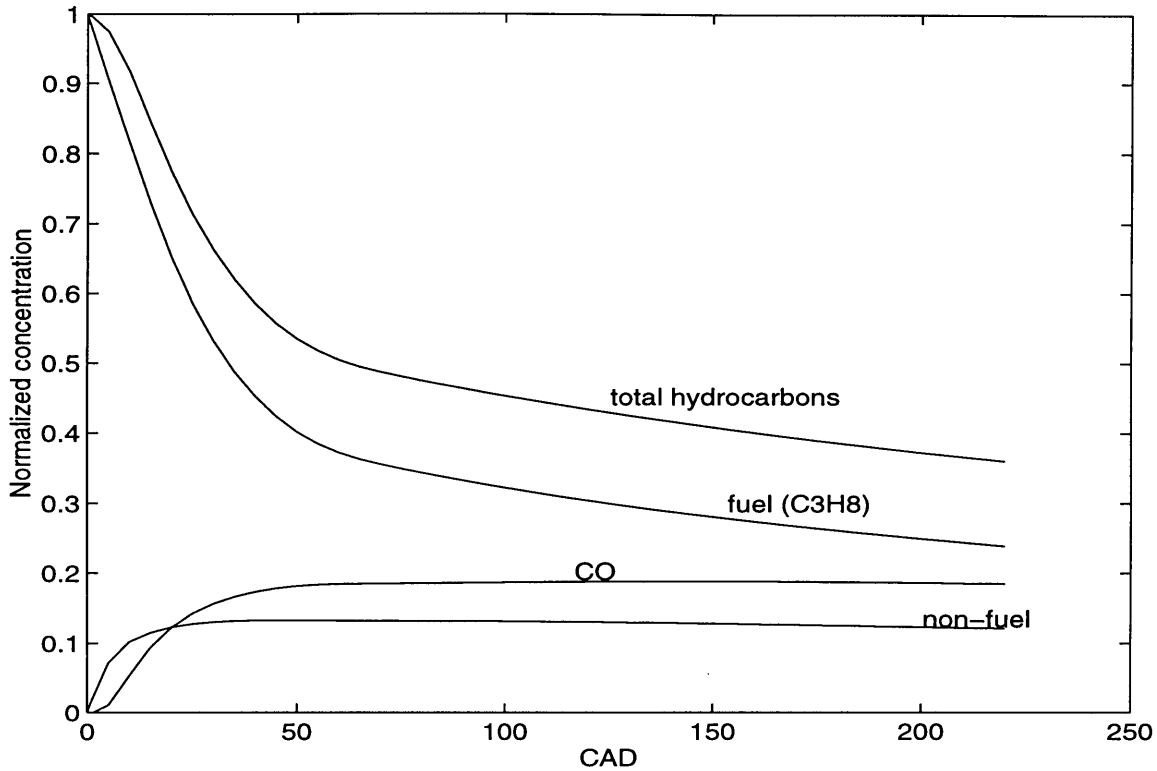


Figure 3-13 Evolution of fractional contributions to spatially integrated total hydrocarbons for fuel, non-fuel and carbon monoxide. Concentrations are normalized by the original total hydrocarbons (in ppmC1) (fuel : propane, initial core temperature : 1500 K)

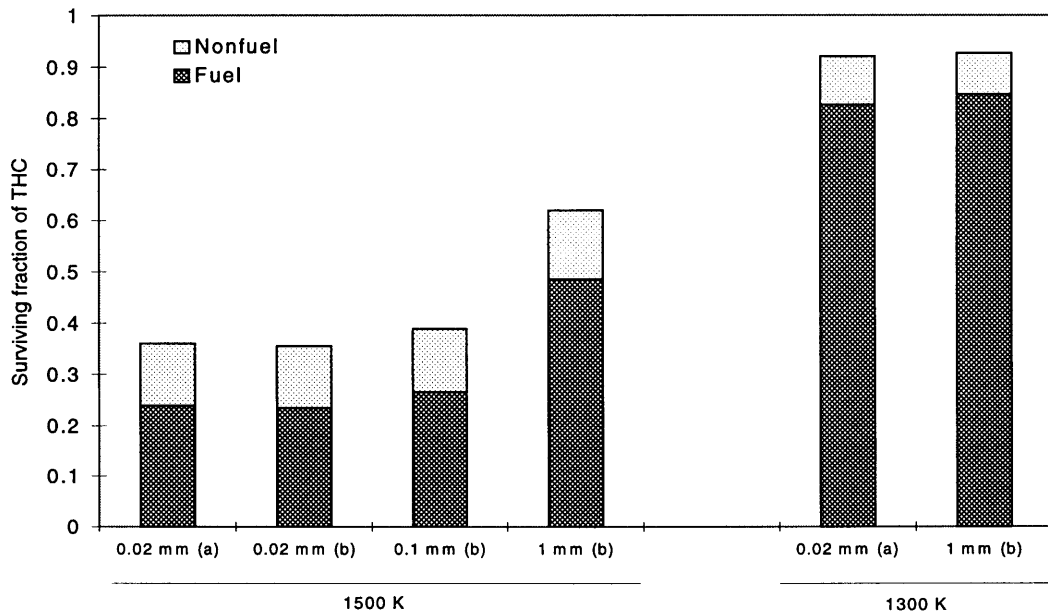


Figure 3-14 Comparison of the surviving fraction of total hydrocarbons and fuel/non-fuel distribution at top dead center of the exhaust process between the cases of the different width of transition zone and of different temperature profiles in the transition zone for two different initial burned gas temperatures. ((a) : linear temperature profile, (b) : temperature profile defined in equation (3-5)). (fuel : propane)

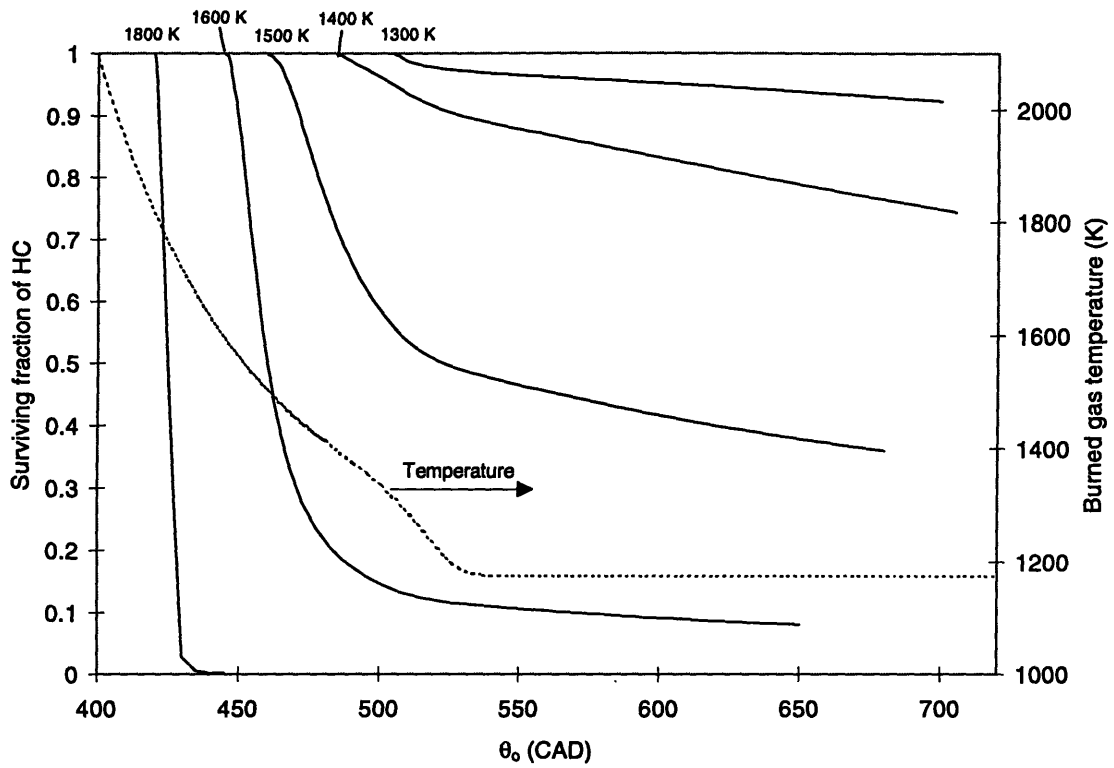


Figure 3-15 Evolution of the fraction of surviving total hydrocarbons (f_{HC}) for various initial phases. (fuel : propane)

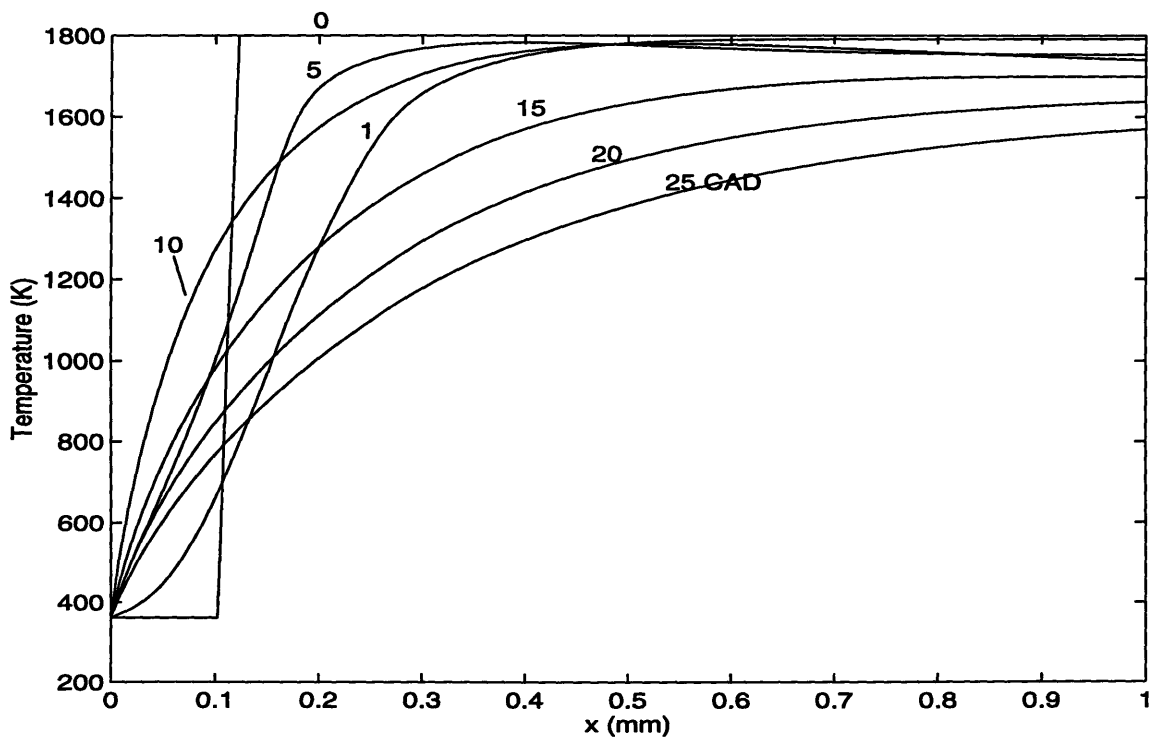


Figure 3-16 Spatial temperature profiles. (fuel : propane, initial core temperature : 1800 K)

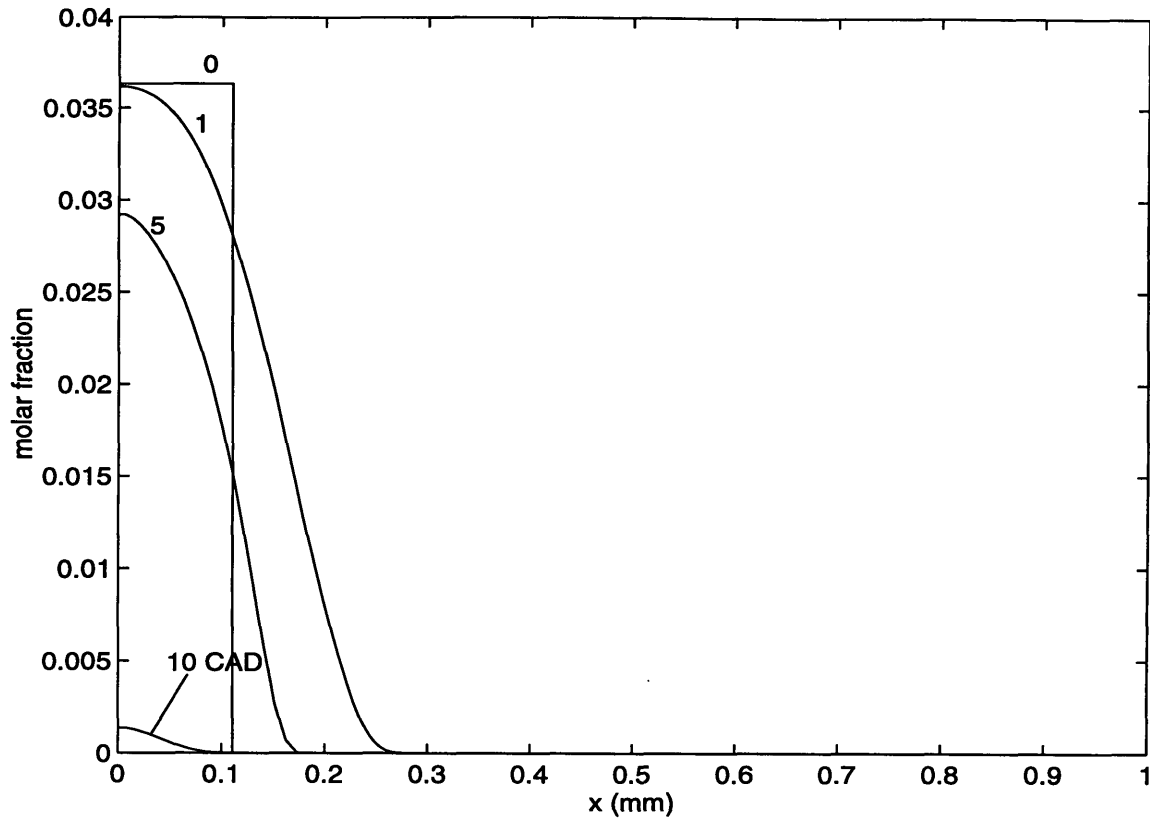


Figure 3-17 Time-evolving spatial distribution of propane. (fuel : propane, initial core temperature : 1800 K)

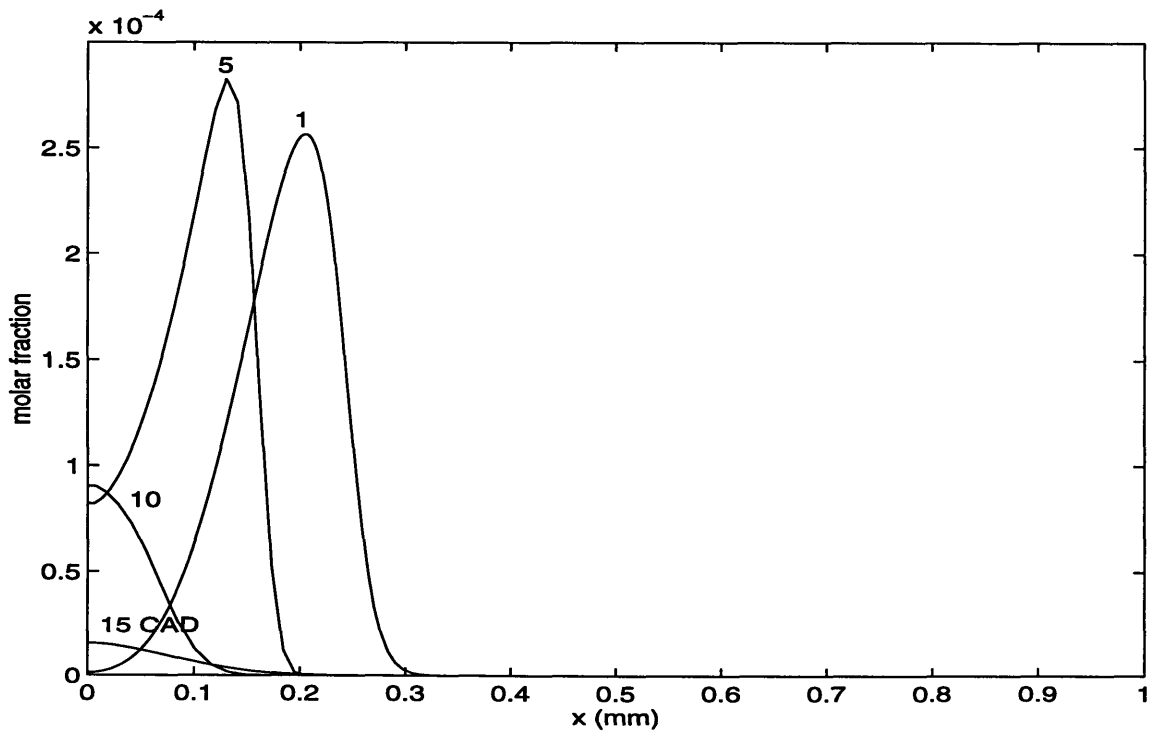


Figure 3-18 Time-evolving spatial distribution of ethylene. (fuel : propane, initial core temperature : 1800 K)

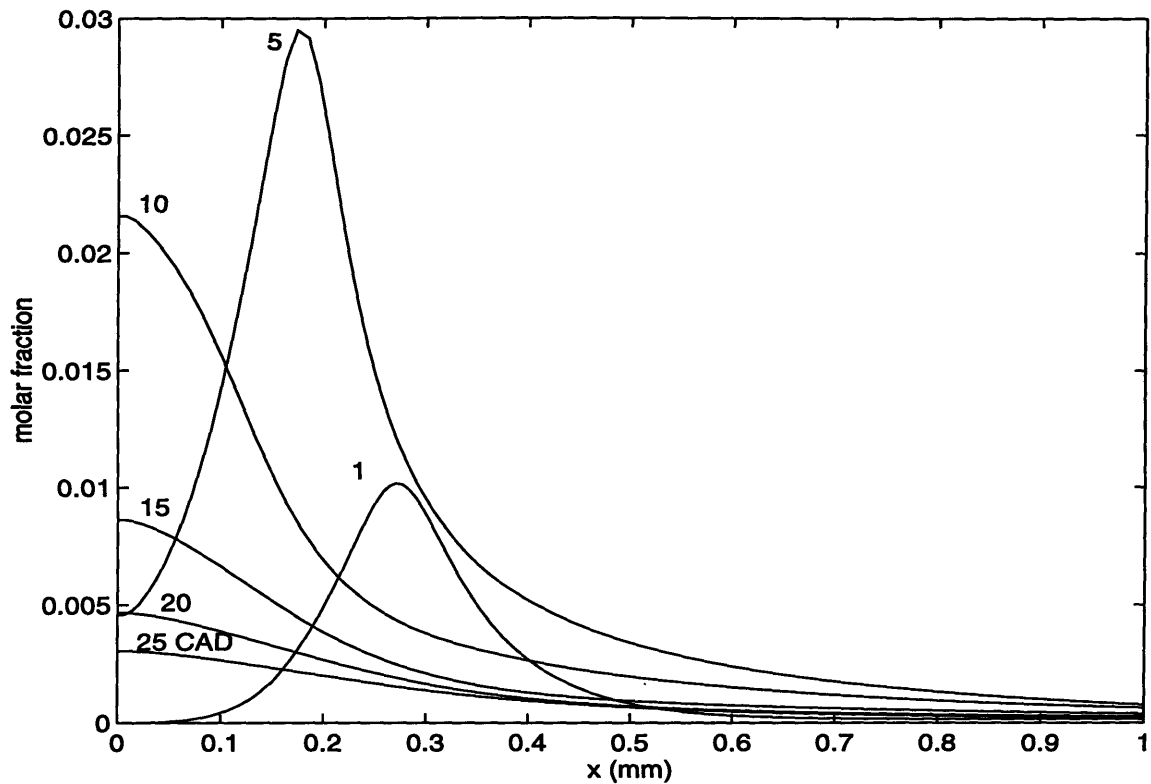


Figure 3-19 Time-evolving spatial distribution of carbon monoxide. (fuel : propane, initial core temperature : 1800 K)

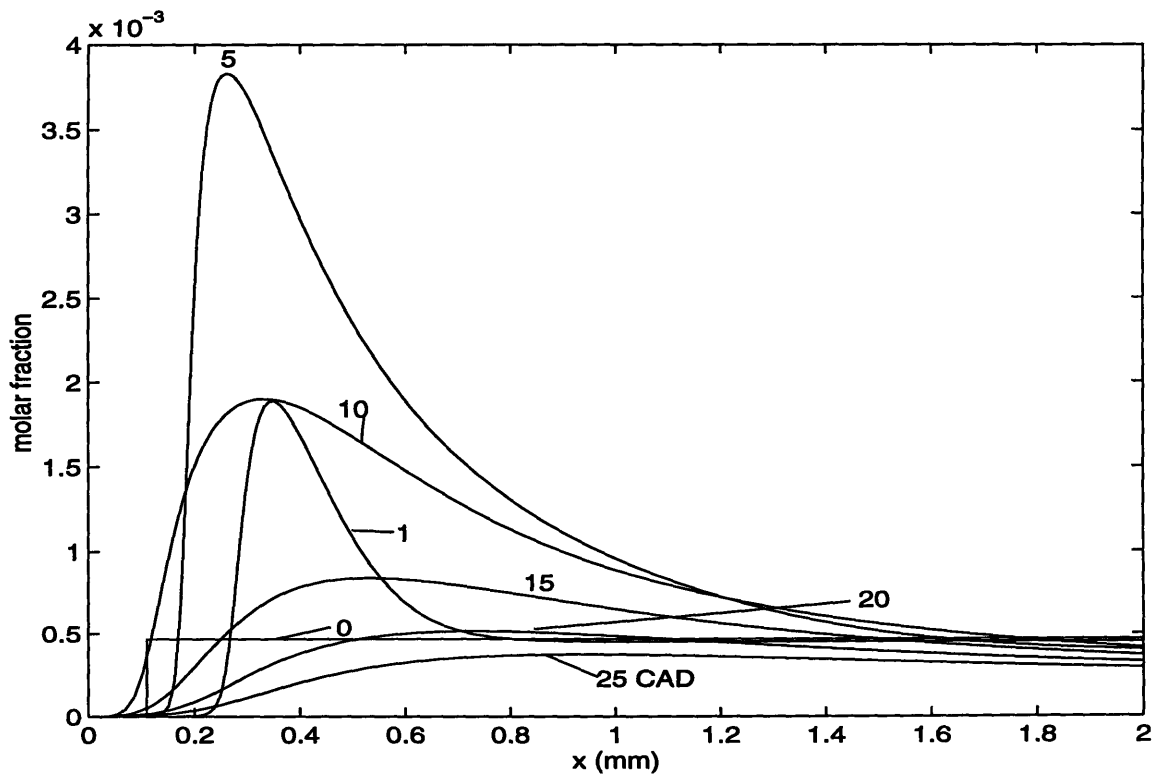


Figure 3-20 Time-evolving spatial distribution of hydroxyl. (fuel : propane, initial core temperature : 1800 K)

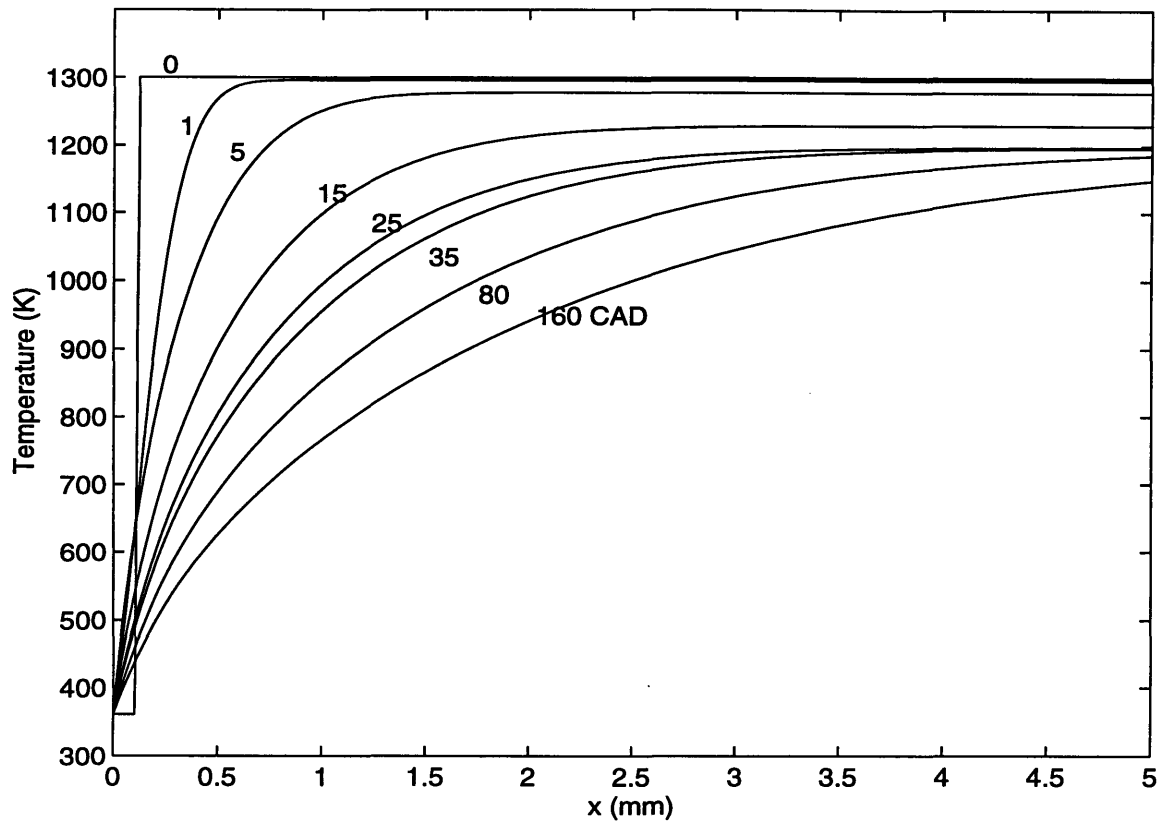


Figure 3-21 Spatial temperature profiles. (fuel : propane, initial core temperature : 1300 K)

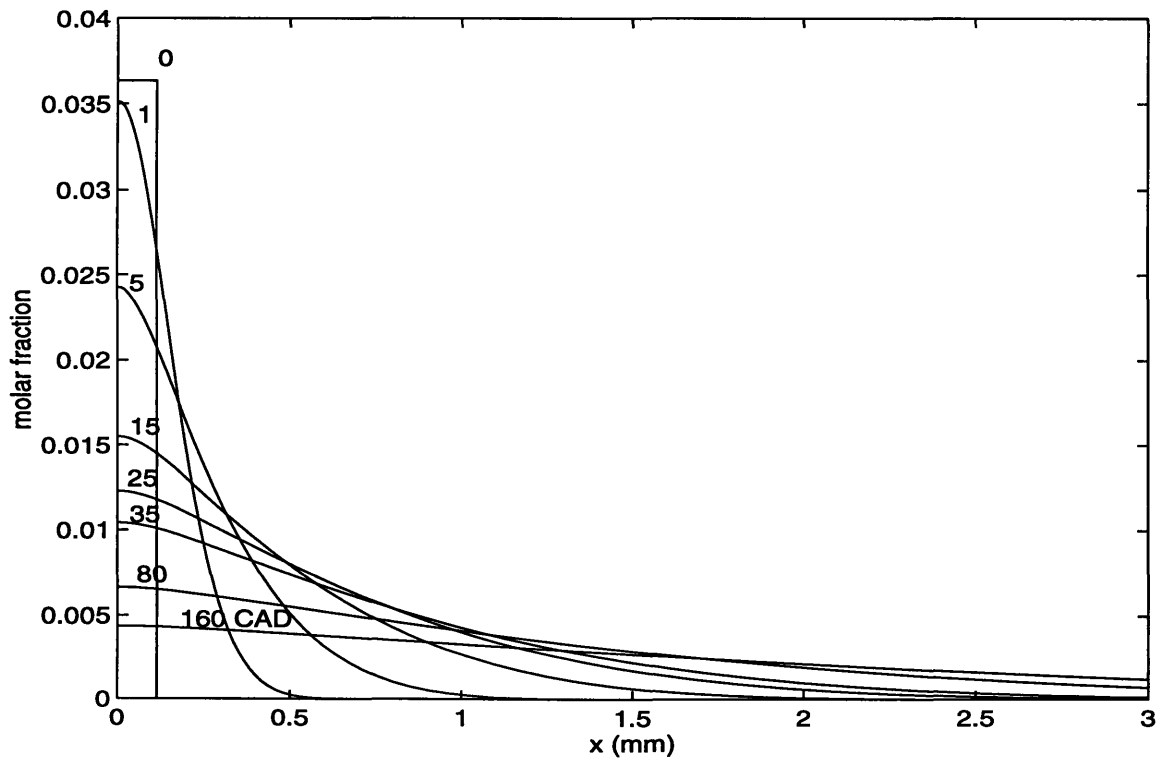


Figure 3-22 Time-evolving spatial distribution of propane. (fuel : propane, initial core temperature : 1300 K)

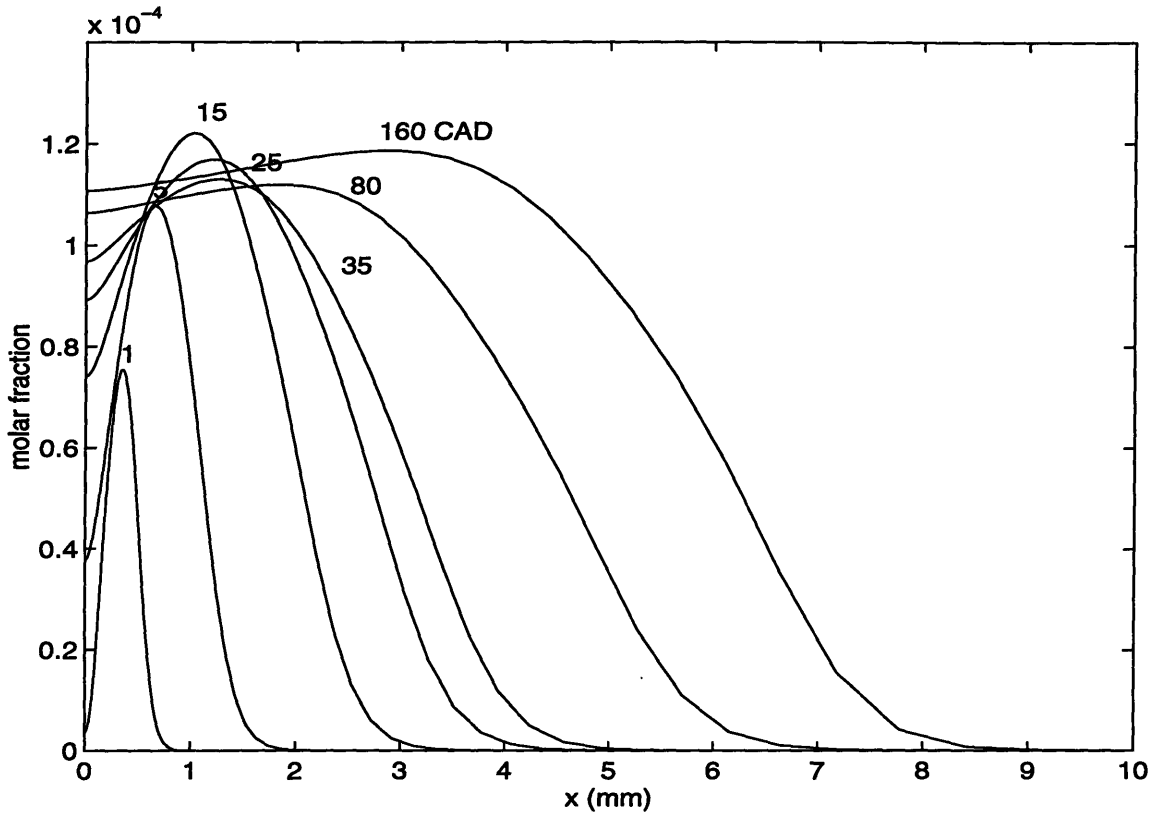


Figure 3-23 Time-evolving spatial distribution of ethylene. (fuel : propane, initial core temperature : 1300 K)

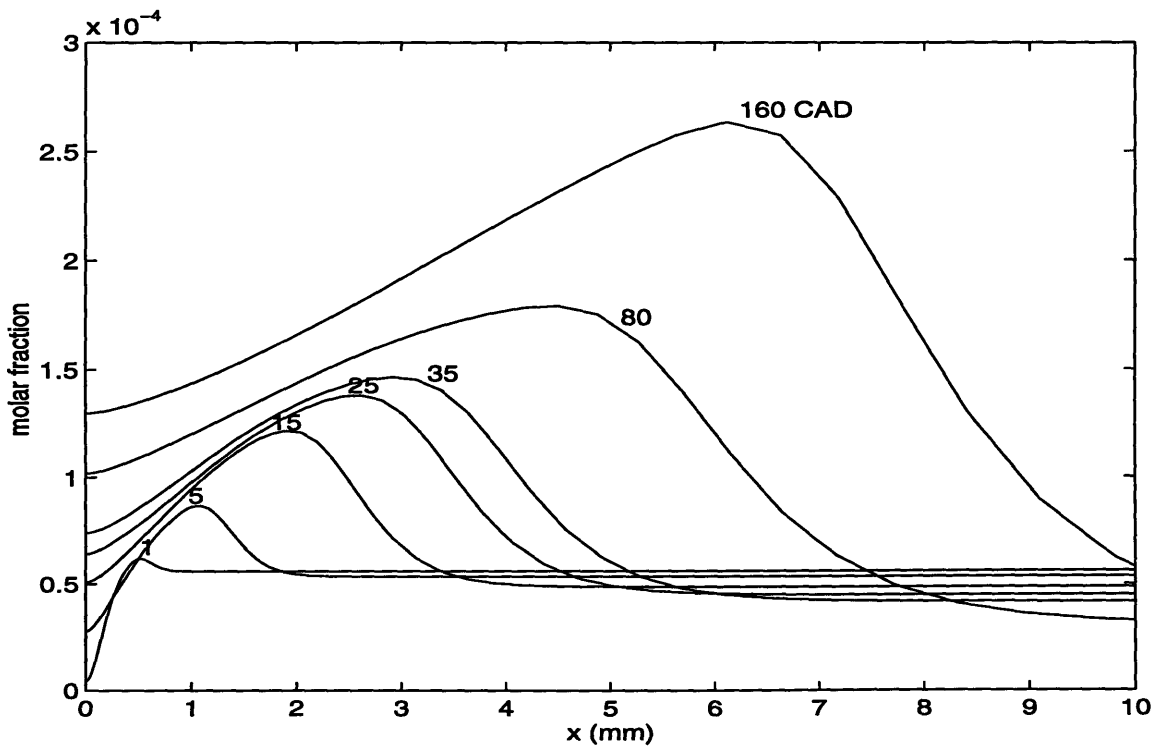


Figure 3-24 Time-evolving spatial distribution of carbon monoxide. (fuel : propane, initial core temperature : 1300 K)

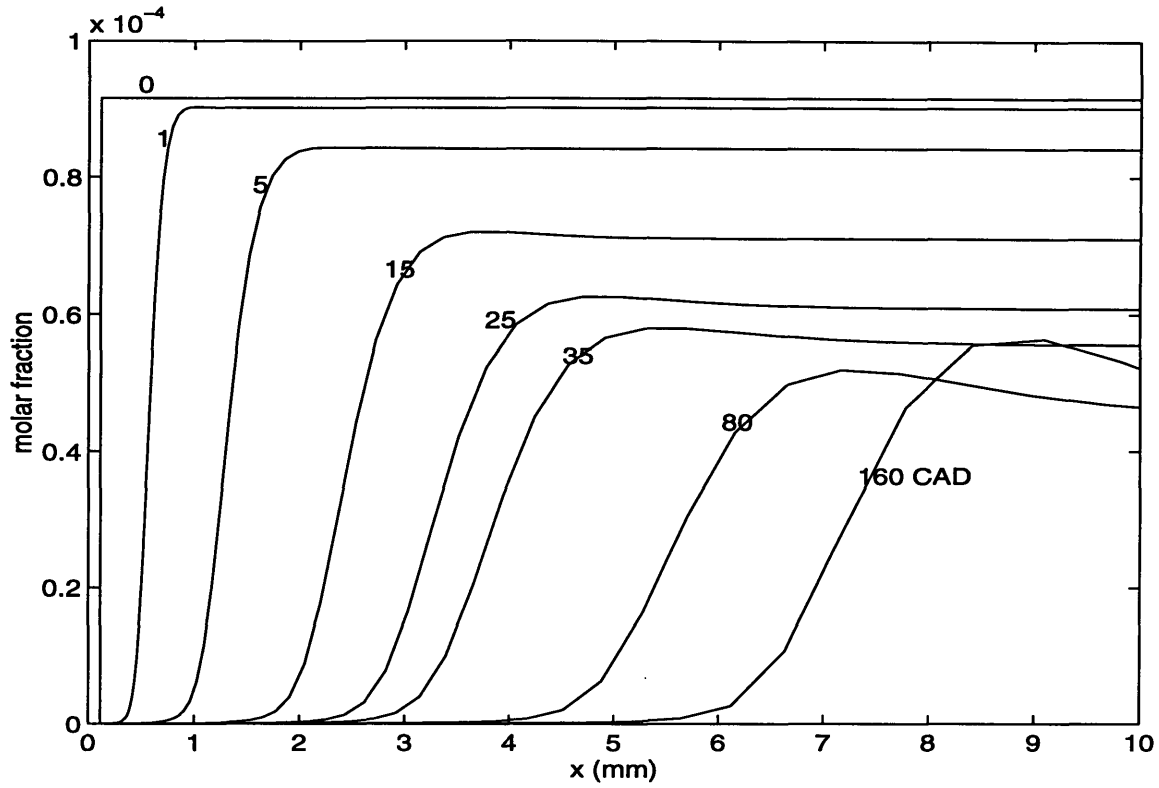


Figure 3-25 Time-evolving spatial distribution of hydroxyl. (fuel : propane, initial core temperature : 1300 K)

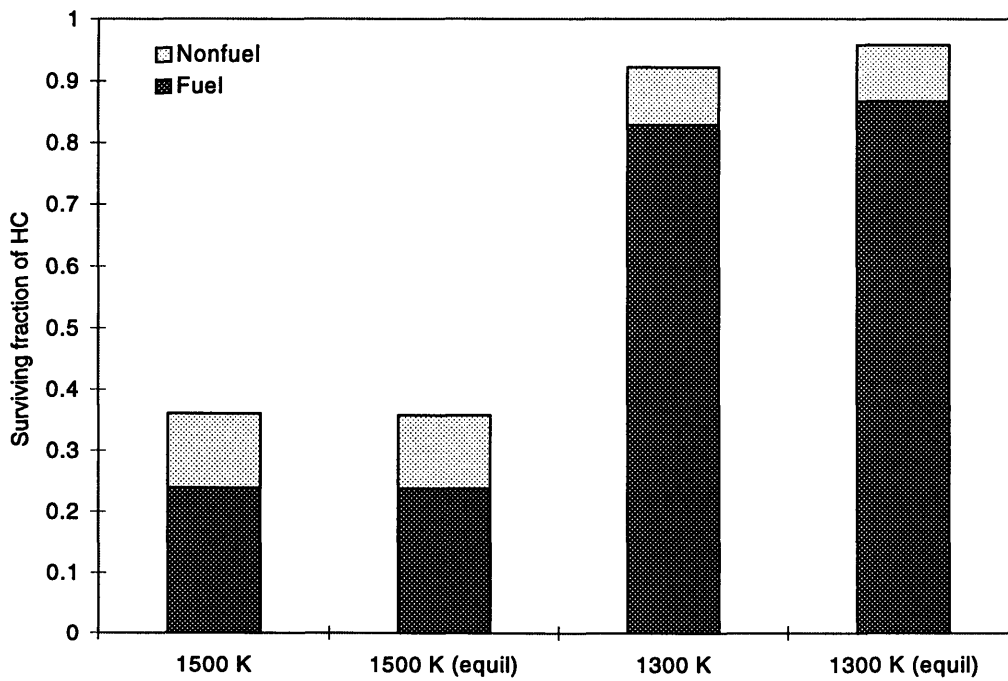


Figure 3-26 Comparisons of surviving fraction of hydrocarbons and fuel/non-fuel distribution between the cases of non-equilibrium and equilibrium burned gas composition for initial core temperatures of 1300 K and 1500 K.

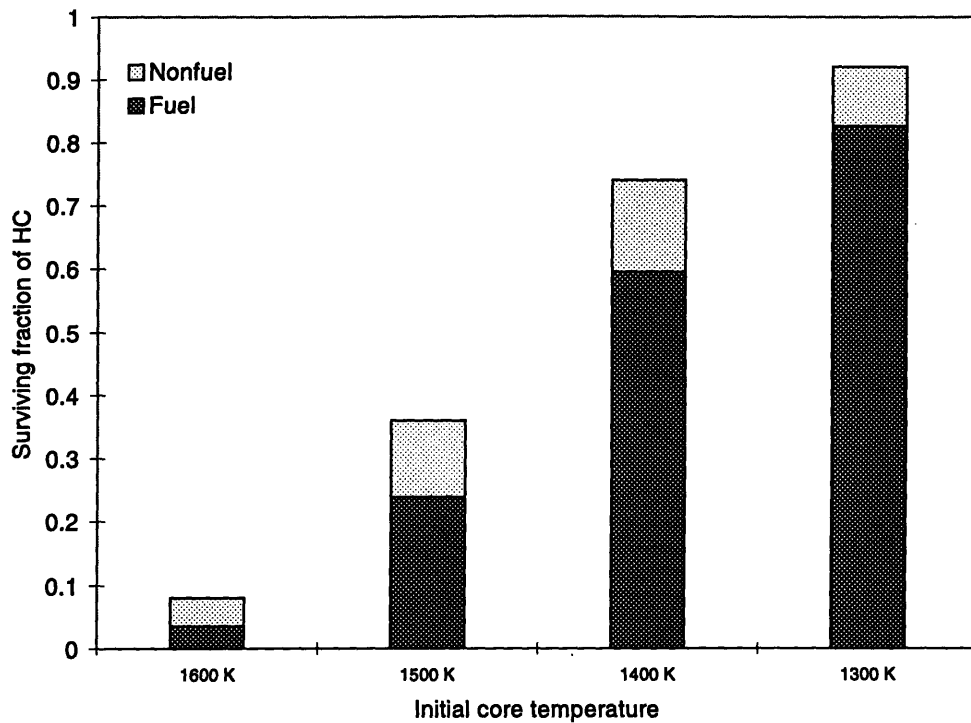


Figure 3-27 Effect of initial core temperature on the surviving fraction of hydrocarbons and fuel/non-fuel distribution at top dead center of the exhaust process. (fuel : propane)

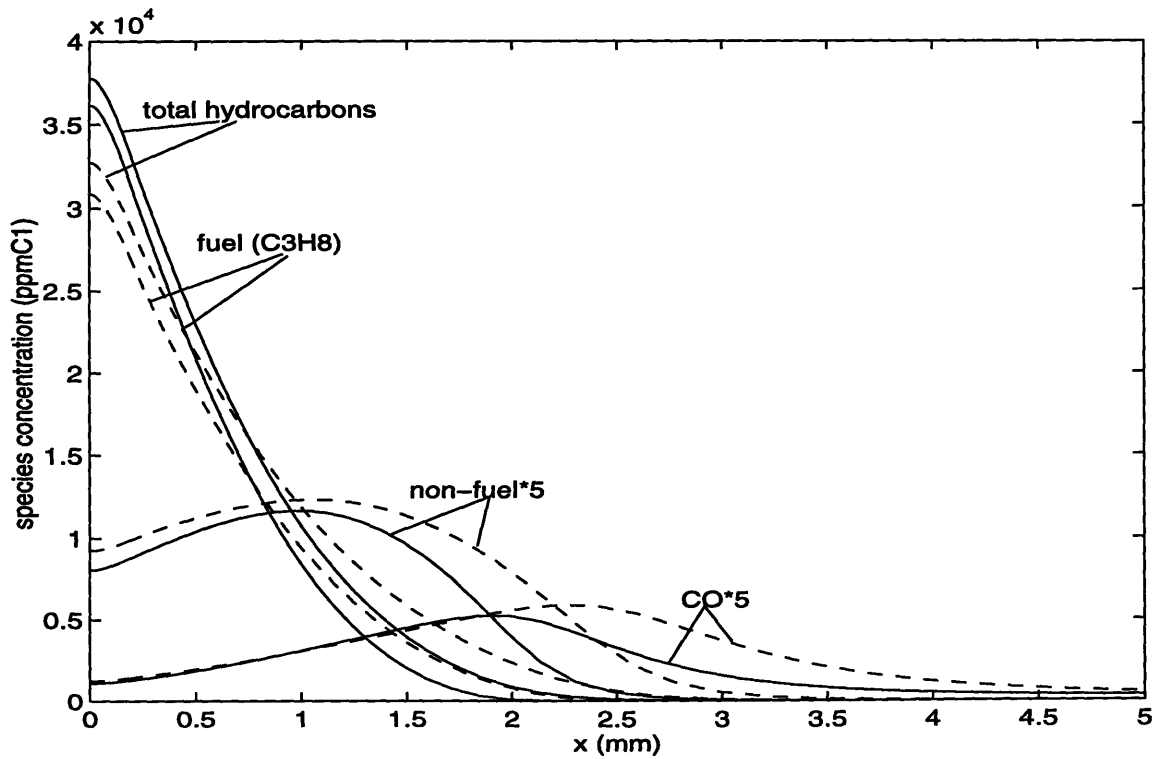


Figure 3-28 Comparison of spatial distribution of species concentrations between the original case (solid line) and high turbulent diffusivity ($2u'$) (dashed line) (fuel : propane, initial core temperature : 1400 K)

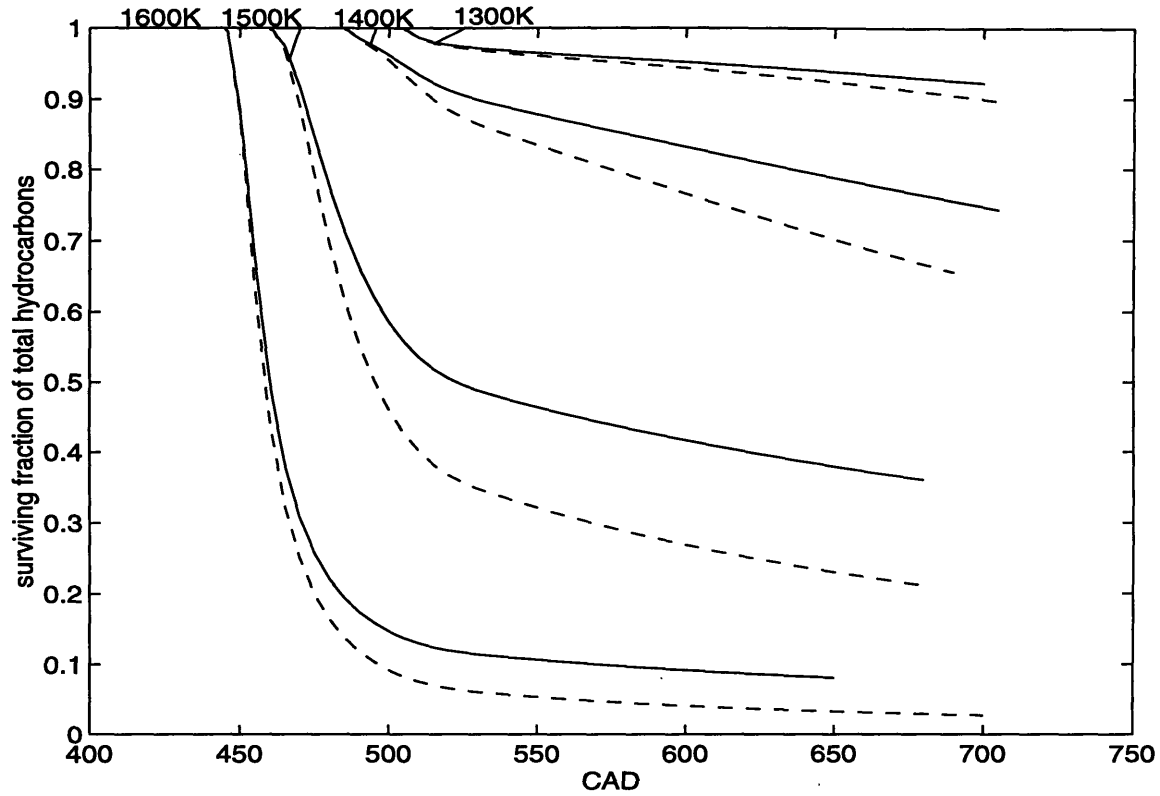


Figure 3-29 Comparison of the evolution of the fraction of surviving total hydrocarbons (f_{HC}) between the original case (solid line) and high turbulent diffusivity ($2u'$) (dashed line). (fuel : propane)

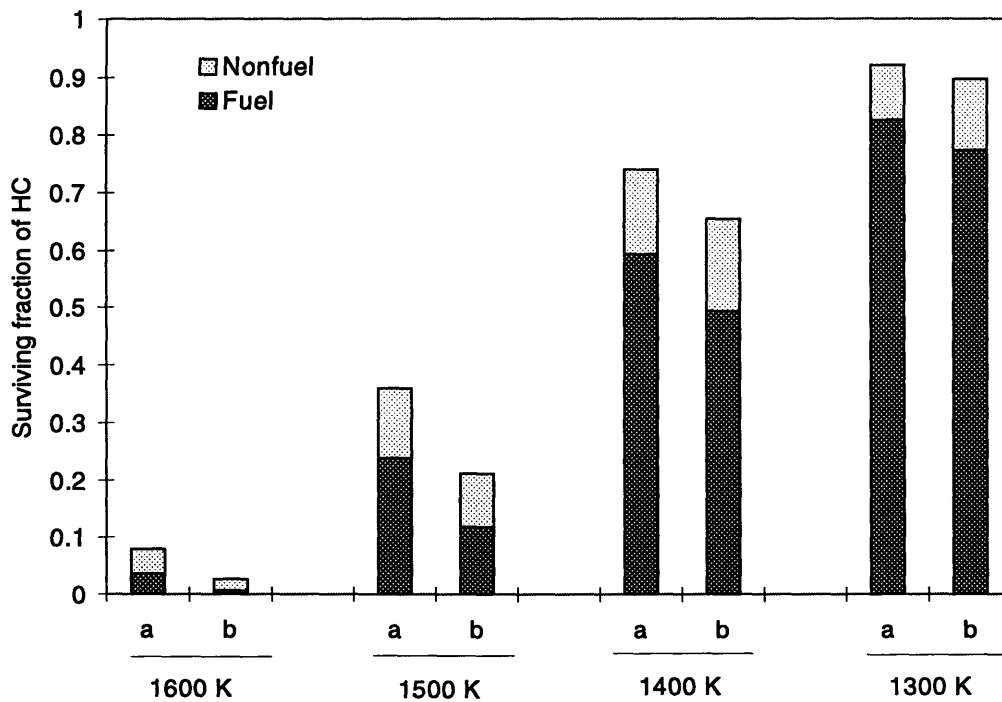


Figure 3-30 Comparison of the surviving fraction of total hydrocarbons and fuel/non-fuel distribution at top dead center of the exhaust process between the original case (a) and (b) high turbulent diffusivity ($2u'$). Results are normalized in ppmC1 by initial unburned hydrocarbons. (fuel : propane)

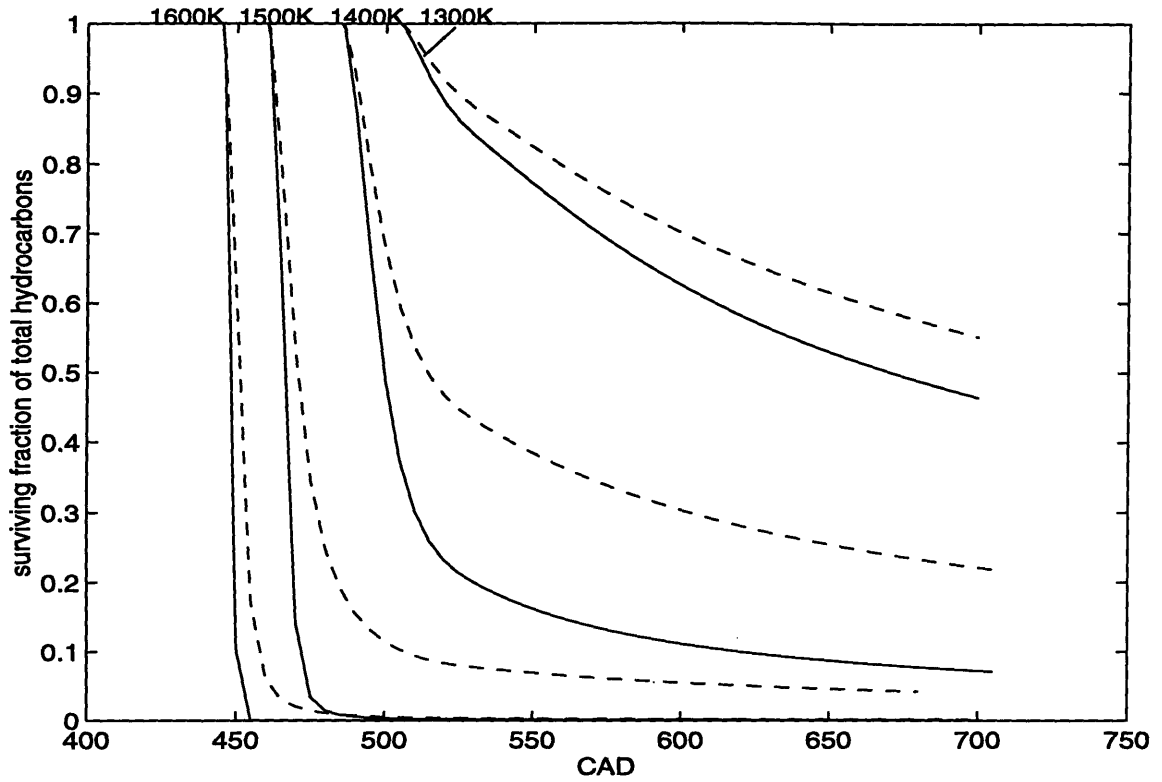


Figure 3-31 Comparison of the evolution of the fraction of surviving total hydrocarbons (f_{HC}) for various initial core temperatures between the cases of ethane (dashed line) and ethylene (solid line).

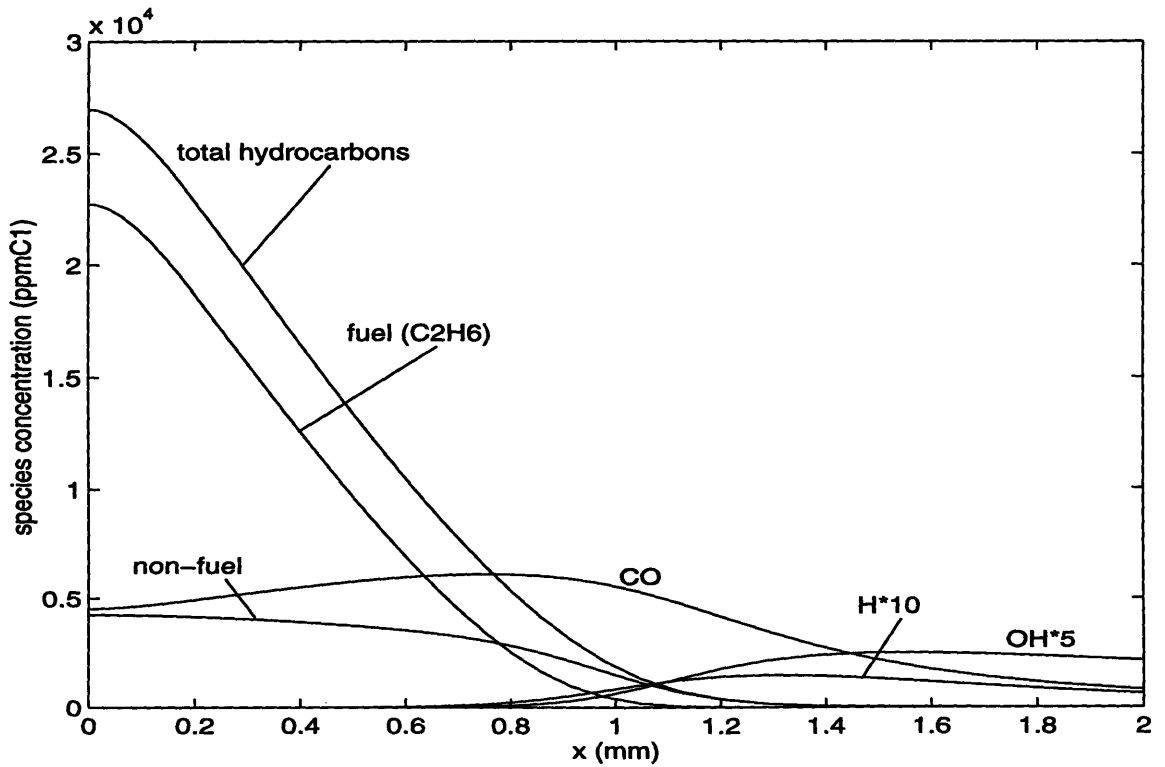


Figure 3-32 Spatial distribution of fuel, non-fuel, carbon monoxide and radicals at 25 crank angle degrees after start of reaction. (fuel : ethane, initial core temperature : 1400 K)

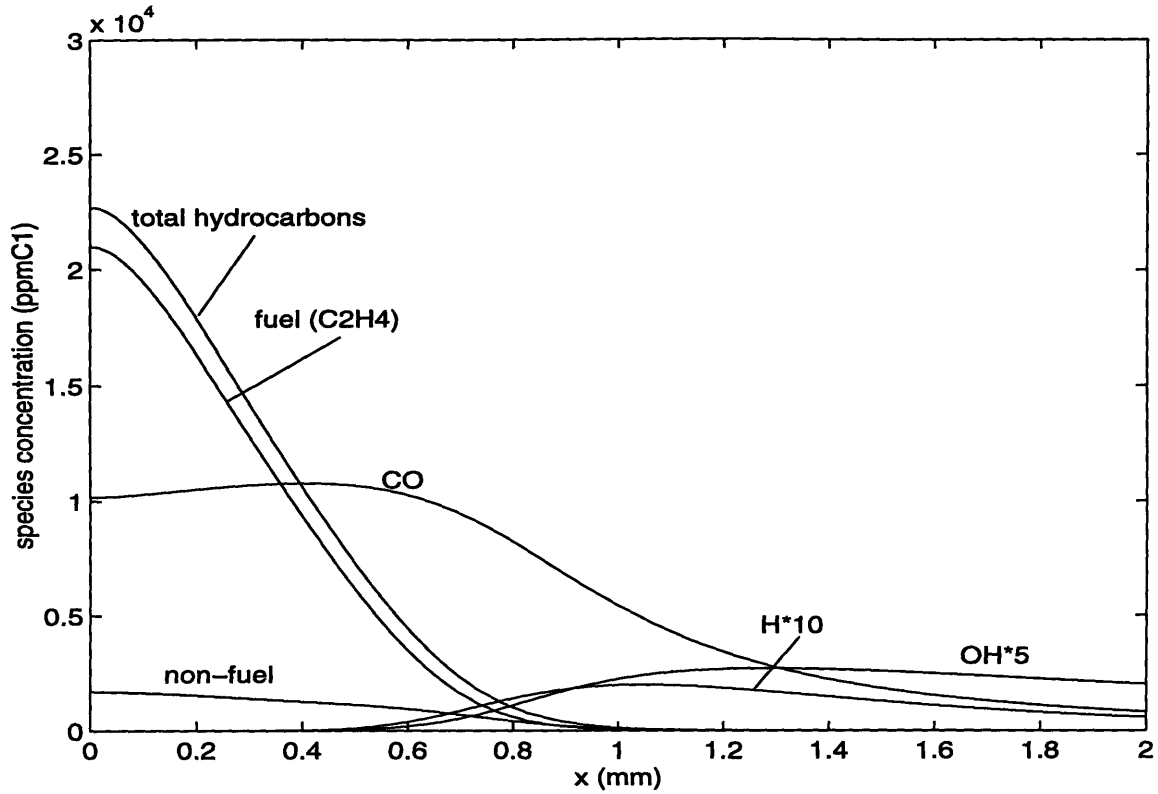


Figure 3-33 Spatial distribution of fuel, non-fuel, carbon monoxide and radicals at 25 crank angle degrees after start of reaction. (fuel : ethylene, initial core temperature : 1400 K)

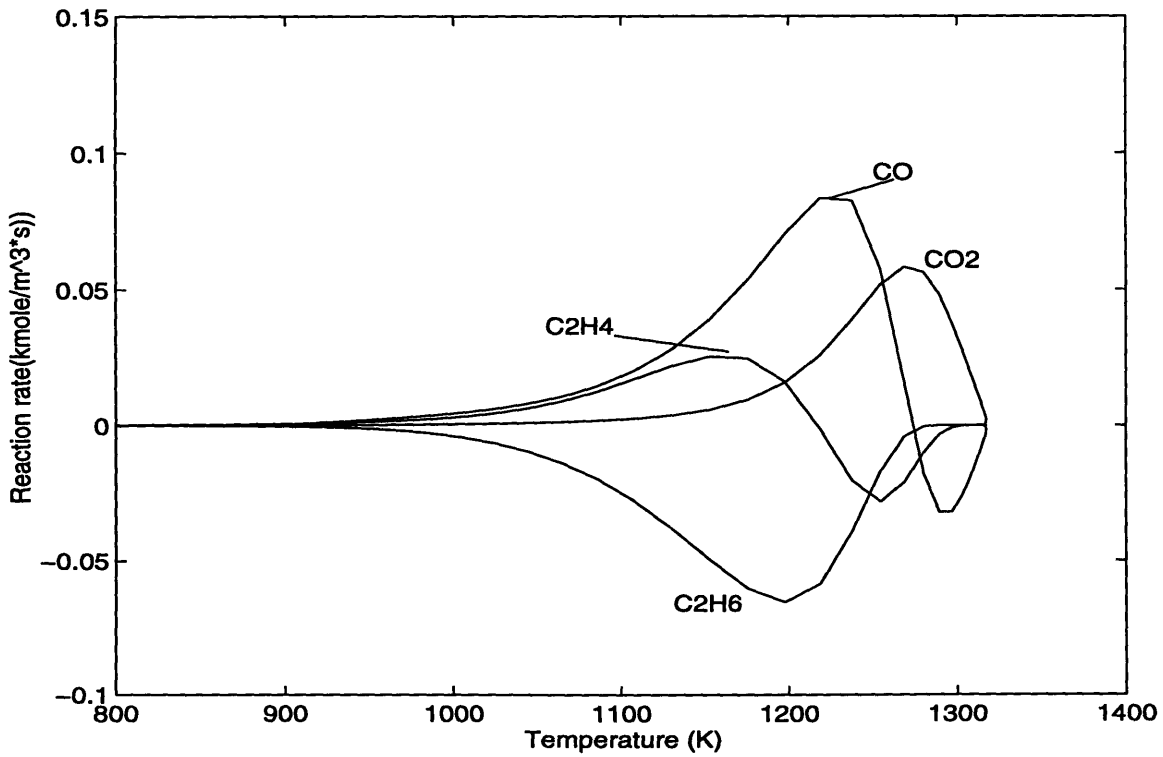


Figure 3-34 Reaction rate as a function of local temperature. (fuel : ethane, initial core temperature : 1400 K)

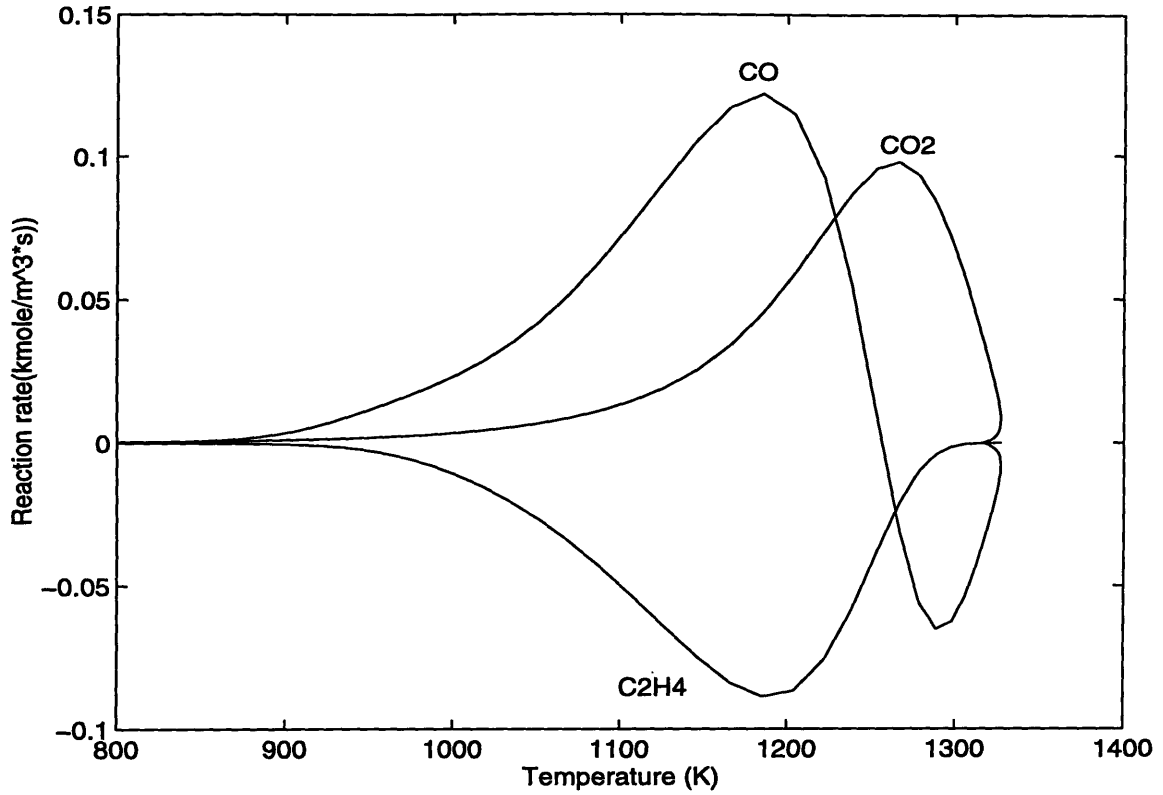


Figure 3-35 Reaction rate as a function of local temperature. (fuel : ethylene, initial core temperature : 1400 K)

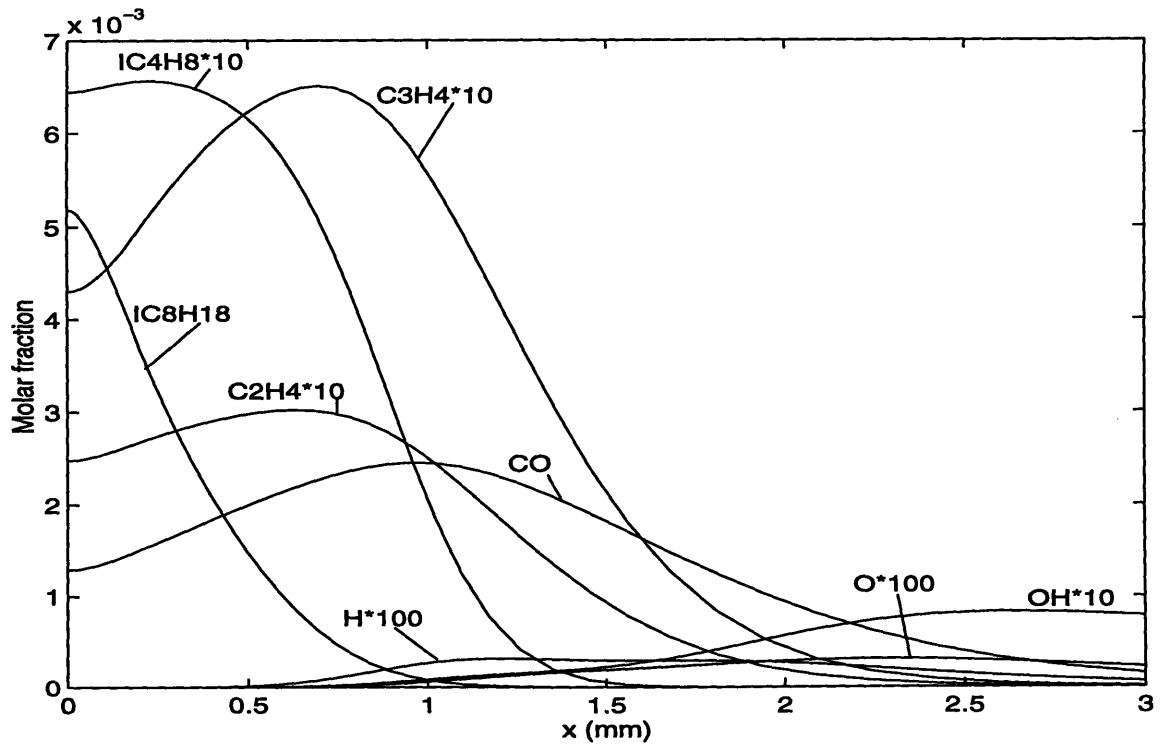


Figure 3-36 Spatial distribution of major species at 25 crank angle degrees after start of reaction. (fuel : propane, initial core temperature : 1500 K)

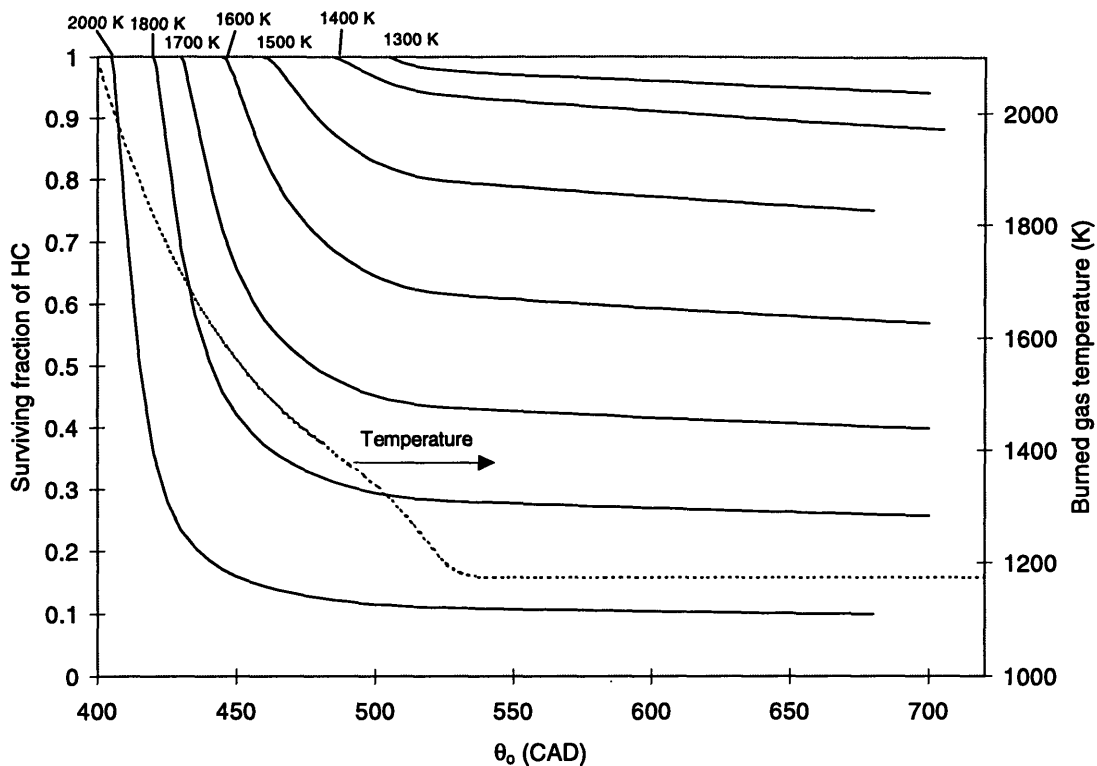


Figure 3-37 Evolution of the surviving fraction of hydrocarbons for various initial temperatures. (fuel : isooctane)

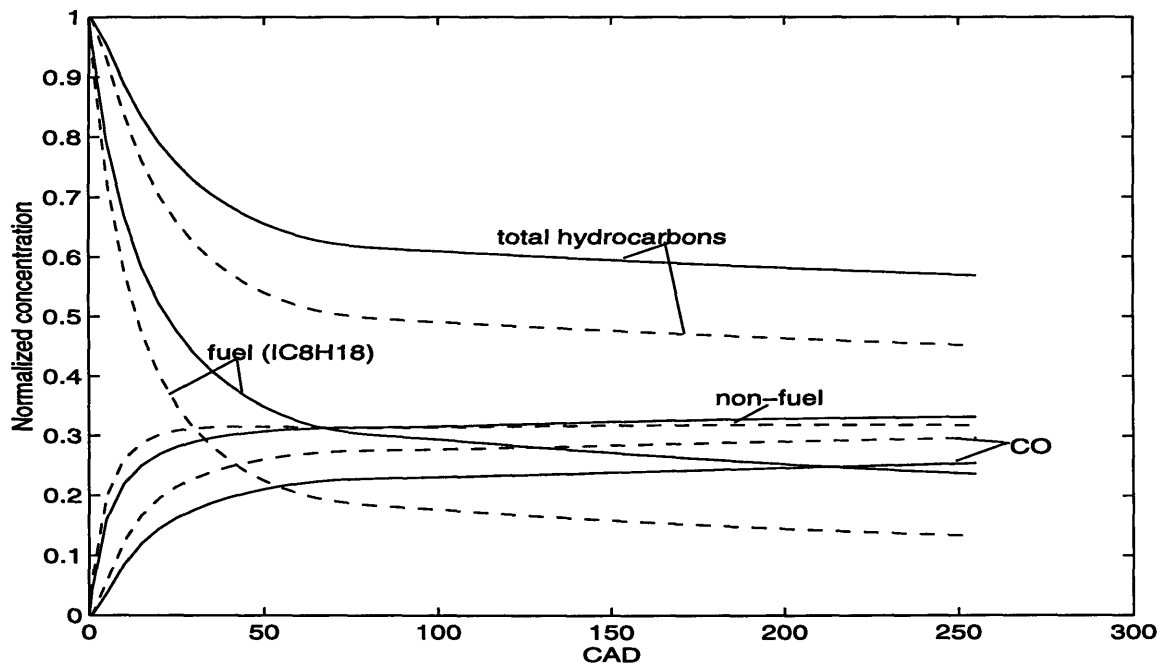


Figure 3-38 Comparison of the evolution of spatial integrated concentrations of fuel, non-fuel, carbon monoxide and total hydrocarbons between the original case for isooctane (solid line) and a case in which the molecular diffusivity of isooctane was replaced with that of propane (dashed line). Species concentrations are normalized by the concentration of original total hydrocarbons (in ppmC1) (fuel : isooctane, initial core temperature : 1600 K)

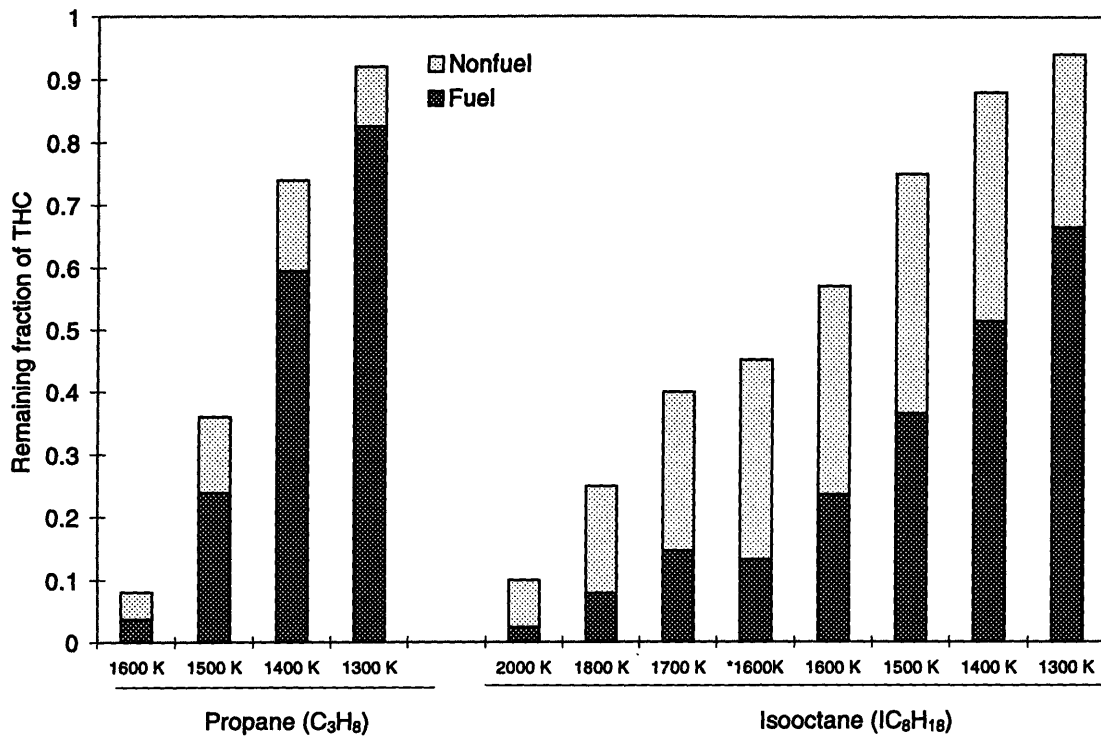


Figure 3-39 Comparison of the surviving fraction of fuel and non-fuel production at top dead center of the exhaust process between the cases of propane and isooctane. (*: the case that the molecular diffusivity of isooctane was replaced with that of propane) Results are normalized by initial unburned total hydrocarbons

Chapter 4 Hydrocarbon Emission Analysis

Many experiments have been conducted to identify the relationship between a variety of engine parameters and hydrocarbon emissions. However, concrete quantitative explanations for the observed trends are rare, especially with regards to post flame oxidation. In this chapter, the one-dimensional model described in Chapter 2 was used to examine the effects of several parameters (type of fuel, the width of hydrocarbon layer, wall temperature, and fuel/air equivalence ratio) on post-flame oxidation. By comparing simulation results with experimental measurements, one can evaluate whether the one-dimensional model captures the main features in the hydrocarbon emission data, while providing reasonable explanations for the experimental findings.

4.1 Crevice mass integrated emissions

The approximation made in this chapter is that the oxidation of crevice hydrocarbons can be represented by the one-dimensional model described in previous chapter. It is also assumed that the piston top-land crevice is the only significant source of hydrocarbon emissions. The one-dimensional model is used to calculate the transport and oxidation of individual elements of mass (“segments”) leaving the crevice normal to the liner wall. The assumptions are as follows:

1. The piston crevice is represented by a constant volume at constant temperature (equal to the wall temperature), and pressure is equal to that in the cylinder.
2. No burned gas is present in the crevice.
3. There is no axial transport between adjacent axial segments
4. The extent of reaction for segments initiated at various core gas temperatures are representative of the oxidation of hydrocarbons leaving the crevice at temperatures within ± 50 K of the initial temperature. For instance, the case of an initial core temperature of 1500 K is assumed to represent the evolution of the oxidation of hydrocarbons leaving the crevice as the core temperature changes from 1550 K to 1450 K.

The amount of fuel/air mixture flowing out of the crevice varies with time during the expansion process. The molar rate of crevice outflow is calculated from the given pressure history as:

$$\dot{n}_c = -\frac{dn_c}{dt} = -\frac{V_c}{RT_c} \frac{dp}{dt} \quad (4-1)$$

Since there is no pressure drop after bottom dead center of the expansion process, the integration was carried out from the time when the pressure reaches maximum (t_a) to bottom dead center of the expansion process (t_b). The total amount of remaining species i and total hydrocarbons at time t^* ($t^* \geq t_b$) can then be calculated as follows, respectively:

$$n_i(t^*) = \int_{t_a}^{t_b} f_i(t^*, t) \dot{n}_c(t) X_i dt \quad (4-2)$$

$$n_{HC}(t^*) = \int_{t_a}^{t_b} f_{HC}(t^*, t) \dot{n}_c(t) \left(\sum_i X_i c_i \right) dt \quad (4-3)$$

The remaining fraction of species i f_i and total hydrocarbons f_{HC} (defined in equations (3-3) and (3-4) in Chapter 3) is a function of the initial reaction time (t) and the residence time ($t^* - t$). In the present approach, the integral is approximated by discrete segments centered around given temperatures. Moreover, t^* is chosen to be top dead center of the exhaust process to determine the value of f_{HC} for each segment*:

$$n_i(t_{TDC}) = \sum_j f_{i,j}(t_{TDC}) \dot{n}_{c,j} X_i \Delta t_j \quad (4-4)$$

$$n_{HC}(t_{TDC}) = \sum_j f_{HC,j}(t_{TDC}) \dot{n}_{c,j} \left(\sum_i X_i c_i \right) \Delta t_j \quad (4-5)$$

so that the total integrated extent of oxidation at top dead center of the exhaust process can be calculated as

$$\varepsilon_{HC} = 1 - f_{HC} = \frac{n_{HC,0} - n_{HC}(t_{TDC})}{n_{HC,0}} \quad (4-6)$$

where

* Since most of surviving hydrocarbons from the piston crevice are exhausted at the end of the exhaust process, top dead center of the exhaust process is chosen to determine the surviving fraction of total hydrocarbons in order to compare with experimental data [13].

$$n_{HC,0} = \int_{t_a}^{t_b} \dot{n}_c (\sum X_i c_i) dt \quad (4-7)$$

Figure 4.1 illustrates the normalized mass flow rate of hydrocarbons leaving the crevice, and the predicted remaining fraction of hydrocarbons at top dead center of the exhaust process, in the cases of propane and isooctane. A large fraction of the crevice hydrocarbons leaves the crevice while core temperatures are above 2000 K, due to the rapidly decreasing pressure in the early stage of the expansion process. Those hydrocarbons oxidize quickly and only contribute little to hydrocarbon emissions. About 90% of the crevice outflow of hydrocarbons is completely oxidized before leaving the cylinder, in the case of propane, while only about 80% of crevice-out hydrocarbons are oxidized in the isooctane case due to a slower conversion rate.

Figure 4.2 shows the fractional contributions of segments starting at different initial core gas temperatures to the total surviving hydrocarbons in the cases of propane and isooctane. The fractional contribution of each segment is calculated as follows:

$$\alpha_j = \frac{f_{HC,j}(t_{TDC}) \dot{n}_{c,j} (\sum_i X_i c_i) \Delta t_j}{n_{HC}(t_{TDC})} \quad (4-8)$$

Results for propane indicate that about three quarters of the surviving hydrocarbons are contributed by the mass leaving the crevices at temperatures below 1400 K. In the case of isooctane, however, the fractional contributions to the surviving total hydrocarbons is distributed over a temperature range spanning from 1300 K to 2000 K, due to the slow reactivity of isooctane.

Figure 4.3 shows the fractional contributions of segments leaving at different core temperatures to the remaining fuel and non-fuel species concentrations in the case of propane: most of the unburned fuel is preserved in the mass leaving the crevices late in the cycle for initial temperatures below 1400 K. In contrast, most of the remaining intermediate hydrocarbons are produced from the segments leaving the crevice at higher temperatures around 1400 to 1500 K.

Figure 4.4 is the counterpart of Figure 4.3 for the case of isooctane. Similar trends are observed in the contribution structure for fuel and non-fuel species: most of the unburned fuel still comes from the segments leaving the crevices in the late stage; non-fuel species are

produced mostly within the intermediate temperature range, but the contributions extend to much higher core temperatures.

4.2 Effect of reactant fuel type on overall oxidation

The effect of fuel type on the post flame oxidation process appears as the combined effect of molecular diffusivity and oxidation chemistry of the fuel. Simulations indicate that oxidation chemistry is the main reason for the drastic differences in the oxidation levels between the cases of propane, isooctane, ethane and ethylene.

Figure 4.5 shows the relative remaining hydrocarbon concentrations of these four different reactant fuels between the predicted overall crevice mass remaining and experimental emission levels, the latter taken from time-resolved speciated sampling probe measurements [13] and from time-averaged exhaust port quenching experiments [8,9]. Due to the lack of the information about the crevice volume in experiments, the emission data and the predicted results are normalized by values for propane. The predictions of the magnitudes of the relative ratios of the hydrocarbon concentrations between fuels are reasonably good, although the value of the relative ratio for ethane and ethylene are somewhat under-predicted and that for isooctane is over-predicted.

Several factors may contribute to the discrepancies: first, the one dimensional assumptions break down at bottom dead center since the processes after bottom dead center involve substantial additional mixing. (simulations predicted that 15% of the surviving hydrocarbons at bottom dead center are further oxidized during the expansion process in the case of propane, 6% in the case of isooctane, 39% in the case of ethane, and 46% in the case of ethylene). Results calculated up to bottom dead center for the surviving fraction of total hydrocarbons show a better correlation with experimental data in Figure 4.5. Secondly, the fact that the processes near the corner of the piston involve a larger thermal boundary layer than just the crevice size is also neglected. Finally, no retention of hydrocarbons in the cylinder is considered in the calculation. In addition, in the case of isooctane, crevices are not the only source of hydrocarbons, with oil layers and liquid fuel probably playing a role; the core temperatures in the case of ethylene are higher (approximately 150 K) than in other cases.

Figures 4.6 through 4.9 compare the predicted fractional contributions to the total hydrocarbon emissions for individual species of propane, isooctane, ethane and ethylene, with experimental data. Results show that the current one-dimensional model with detailed chemistry

can make reasonable predictions of the fuel/non-fuel ratio and the composition of hydrocarbon emissions. The fact that the correlation seems to work reasonably well in spite of these approximations attests to the significant effect of fuel chemistry on the overall post-flame oxidation process.

4.3 Effect of the width of the hydrocarbon layer

Comparisons between the surviving fraction of total hydrocarbons and the fuel/non-fuel distribution for various widths of hydrocarbon layer (0.1 mm, 0.2 mm and 0.4 mm) for cases initiated at different initial core temperatures are illustrated in Figure 4.10. Results show that the effect of the hydrocarbon layer thickness on the oxidation level depends somewhat on the initial core temperatures. For high initial core temperatures, the extent of oxidation increases with the width of the hydrocarbon layer, since more energy can be released from the wider hydrocarbon layer during fast oxidation at high temperature, so that the resulting temperature rise accelerates the oxidation of the remaining hydrocarbons. In contrast, at lower initial core gas temperature, more hydrocarbons survive the post flame oxidation in the wider hydrocarbon layer, and a higher portion of the fuel species remains unburned in the case of wider hydrocarbon layer.

Figure 4.11 shows comparisons between the concentrations of species as a function of distance away from the wall, for the cases with 0.1 mm (reference) and 0.2 mm hydrocarbon layer thickness starting at a low initial core temperature (1400 K). The wider layer contributes to a somewhat higher concentration of intermediates and carbon monoxide, and a much higher fraction of remaining unburned fuel. The magnitude of the unburned fuel concentration at the wall is found to be approximately proportional to the initial width of the hydrocarbon layer, leading to a steeper gradient of unburned fuel concentration near the walls and thus higher diffusion rates. In spite of increased diffusion rates, the extent of oxidation of hydrocarbons is not significantly affected at a lower temperature. Non-fuel species concentrations increase near the wall as a result of higher gradients and diffusion rates. However, since remaining unburned fuel concentration near the walls are also high, the fuel/non-fuel ratio increases with the hydrocarbon layer thickness.

Figure 4.12 shows mass-integrated results for a crevice width and crevice outflow corresponding to the initial hydrocarbon layer thickness. Due to the opposite trends in the effect of width of hydrocarbon layer in cases initiated at high and low core temperatures, the overall extent of oxidation is quite insensitive to the width of the hydrocarbon layer, such that the

resulting hydrocarbon emission is approximately proportional to the width of the hydrocarbon layer, and therefore to the initial hydrocarbon mass. In addition, the fuel/nonfuel ratio increases modestly with the width of the hydrocarbon layer, as more of the fuel species are remained in the cold layer for the cases at lower initial core temperatures. The sensitivity of the emission level to the width of the hydrocarbon layer is consistent with experimental observations varying the top-land crevice radial clearance in the range of 0.05 mm to 0.18 mm, which are smaller than the two plate quench distance [52]. However, other experimental data suggest that the emission level is relatively insensitive to the radial width of the crevice size [53]. The main reasons for the discrepancies could be flame penetration into the crevice (if the crevice size is larger than the critical two-plate quench distance), and mixing effects due to the jet-like flow out of the crevice. Neither effect is included in the current model.

4.4 Effect of wall temperature on overall oxidation

Experiments indicate that the reduction of hydrocarbon emissions can be simply achieved by increasing the coolant temperature [54]. In order to investigate this effect, a change in wall temperature from 361 K (baseline condition) to 500 K for the one dimensional simulation has been carried out. In addition, the initial temperature of the hydrocarbon layer is also assumed to increase from 361 K to 500 K.

Figure 4.13 illustrates the spatial species distribution for two cases at 25 crank angle degrees after start for an initial core temperature of 1400 K. The fuel concentration near the wall drops much faster in the case of high wall temperature than for low wall temperature, with a slight increase in the concentrations of intermediates and carbon monoxide. This is a result of the increase in molecular diffusivity with the change in the temperature within the hydrocarbon layer. An increase in temperature from 361 K to 500 K raises the molecular diffusion coefficient of propane by 80%.

The surviving fractions of total hydrocarbons and fuel/non-fuel distribution in the two wall temperature cases for various initial core temperatures are shown in Figure 4.14. The result shows the effect of increased wall temperatures on the oxidation of hydrocarbons is very similar to that of increased the turbulent intensity (greater effect on the oxidation level at higher initial core temperatures and little influence on the non-fuel concentrations).

Crevice mass-integrated results (shown in Figure 4.17, along with the fuel/air equivalence ratio effect) indicate that the overall extent of oxidation is increased by 0.9% (from

93.6% at 361 K to 94.5% at 500 K), leading to a 14% reduction in the surviving fraction of total hydrocarbons (f_{HC}). Combining the effect of the decrease in the source of hydrocarbons (a 28% reduction in the density in the hydrocarbon layer) due to the increase in temperature, a 38% decrease in hydrocarbon emissions is predicted by varying temperatures from 361 K to 500 K. Consequently, the predicted hydrocarbon reduction (from the baseline case) is 0.27% per degree Kelvin, which is somewhat lower than the experimental values (0.37% per degree Kelvin for isopentane, and 0.46% for 97 RON [54]). However, the impact of a change in coolant temperature on intake, compression, combustion processes and consequent higher core temperature histories, which would result in a higher hydrocarbon reduction, has not been considered in the current analysis. In addition, because the wall temperature affects the absorption/desorption mechanism of oil layers, the hydrocarbon emissions of liquid fuels (isopentane and RON) should be more sensitive to the wall temperatures than gaseous fuel (propane). Simulations suggest that the combined effect of post-flame oxidation and a change in density provide the main contributions to the measured change in hydrocarbon emissions.

4.5 Effect of equivalence ratio

The effect of the fuel/air equivalence ratio on post-flame oxidation has been tested by varying the fuel/air ratio from 0.9 (baseline) to 1.0. It should be noticed that core gas compositions change with the initial fuel/oxygen ratio. By increasing the fuel/air ratio from slightly lean ($\phi=0.9$) to stoichiometric ($\phi=1.0$), for instance, the concentration of hydrogen atoms in the burned gas is increased by an order of magnitude; that of carbon monoxide is also increased by an order of magnitude, and that of atomic oxygen is decreased by an order of magnitude.

Figure 4.15 shows the comparisons of spatial concentration profiles of fuel, non-fuel, and carbon monoxide between the two cases. Similar species concentration profiles, except for the different 'base' concentrations of carbon monoxide in the burned gas between the two cases, indicate that the differences in burned gas composition and fuel/oxygen ratio in the cold layer do not have a significant impact on the post-flame oxidation process when the fuel/air ratio changes from 0.9 to 1.0.

Figure 4.16 shows the effect of stoichiometry on the oxidation level and the fuel and non-fuel fractions in the surviving total hydrocarbons at various initial core temperatures. A slightly lower oxidation level for the stoichiometric condition at high initial core temperatures

indicates the effect of oxygen on the fast oxidation. In contrast, a slightly higher extent of oxidation at low initial core temperatures is observed. This may be attributed to the effect of high concentrations of radicals at a stoichiometric conditions on the consumption of hydrocarbons, since the production of radicals decreases significantly at low core gas temperatures, such that the effect of radicals in the core gas becomes important.

Comparisons of final crevice mass-integrated results (along with the effect of wall temperatures) are shown in Figure 4.17. No significant change in oxidation levels and fuel and non-fuel distribution is found by varying the fuel/air equivalence ratio from slightly lean ($\phi=0.9$) to stoichiometric ($\phi=1.0$), which is consistent with experimental observations [55]. More drastic changes in emission levels would be expected in simulations into the fuel-rich range due to the effect of oxygen shortage.

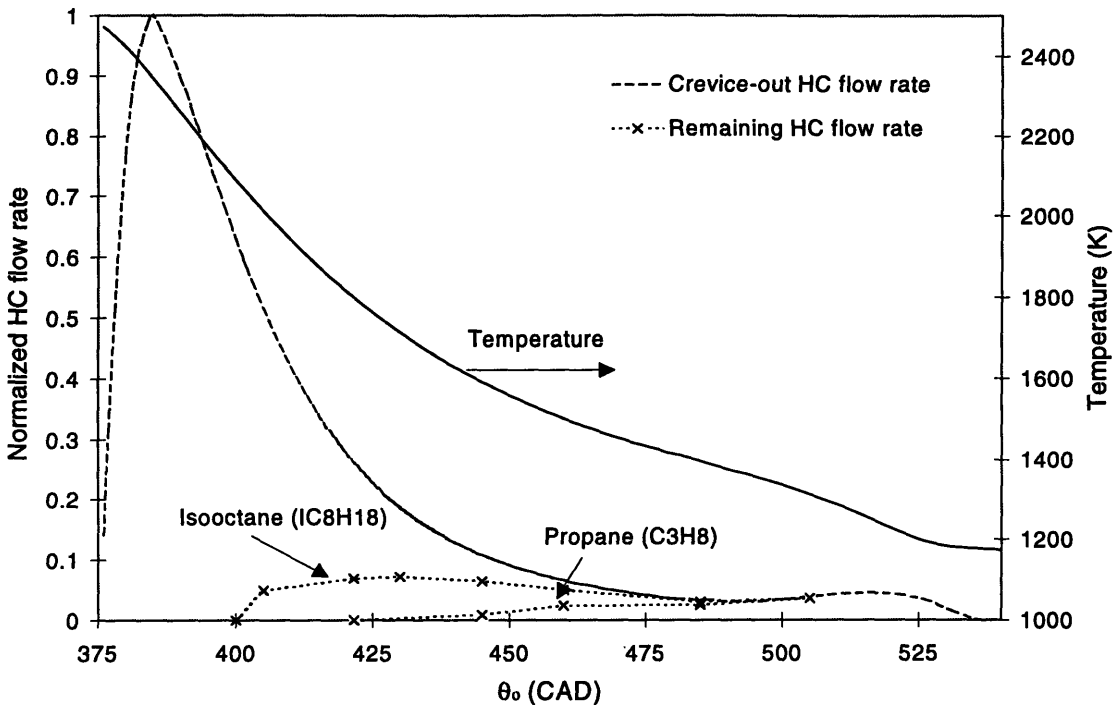


Figure 4-1 Mass flow rate of hydrocarbons leaving the crevice normalized by peak rate, and predicted remaining fraction of hydrocarbons at top dead center of the exhaust process for the cases of propane and isooctane.

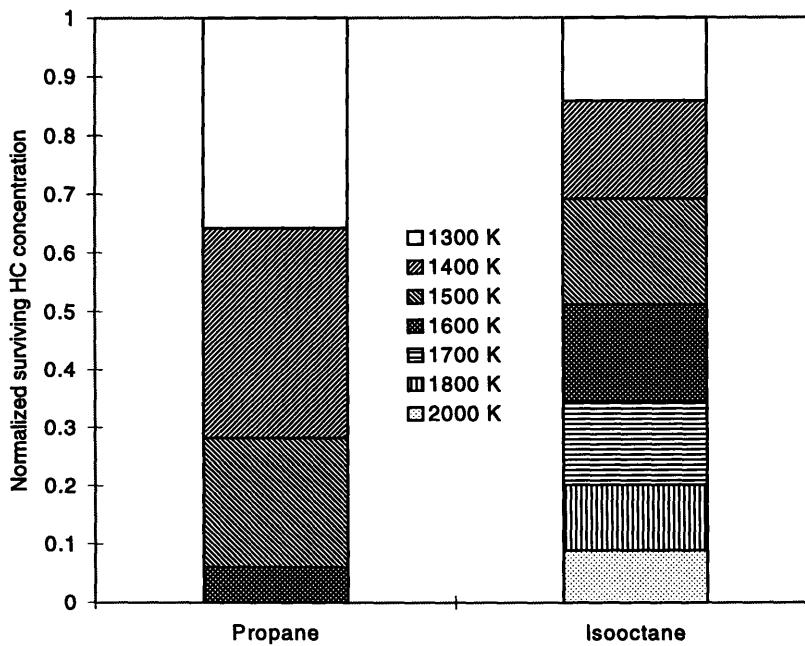


Figure 4-2 Fractional contributions of segments (starting reaction at various initial core gas temperatures) to the total surviving hydrocarbons in the cases of propane and isooctane. All results are normalized by total surviving hydrocarbon concentration.

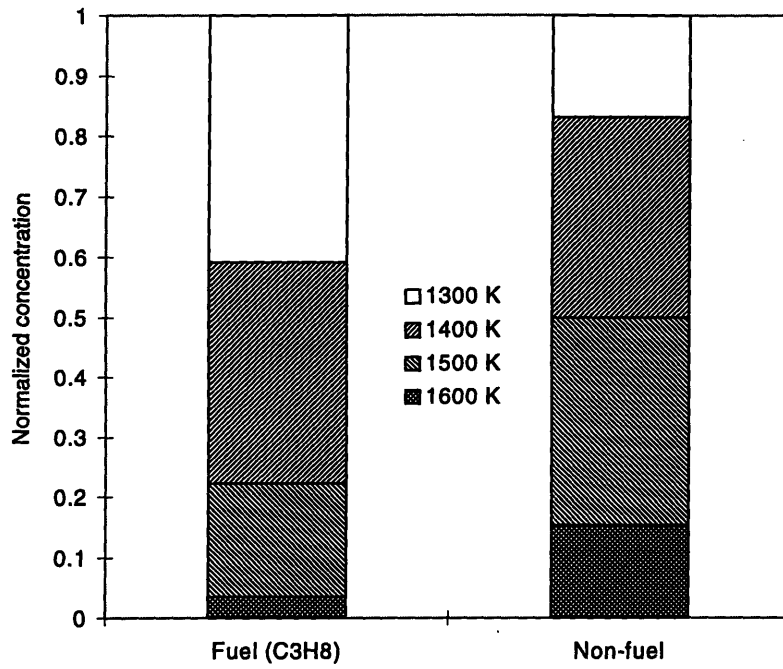


Figure 4-3 Fractional contributions of segments (starting reaction at various initial core temperatures) to the surviving fuel and non-fuel species concentrations. All results are normalized by total surviving fuel and non-fuel species concentration. (fuel : propane)

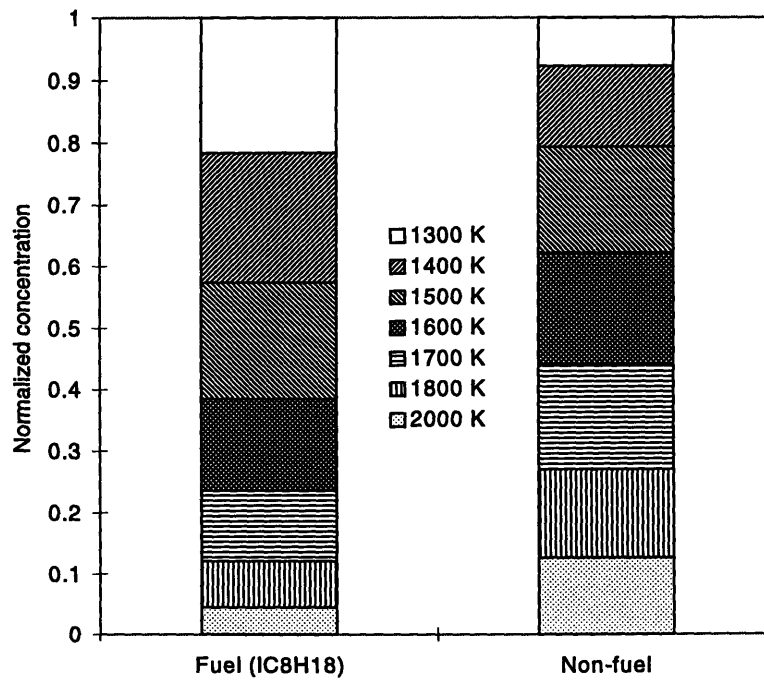


Figure 4-4 Fractional contributions of segments (starting reaction at various initial core temperatures) to the surviving fuel and non-fuel species concentrations. Normalized by total surviving fuel and non-fuel species concentration. (fuel : isooctane)

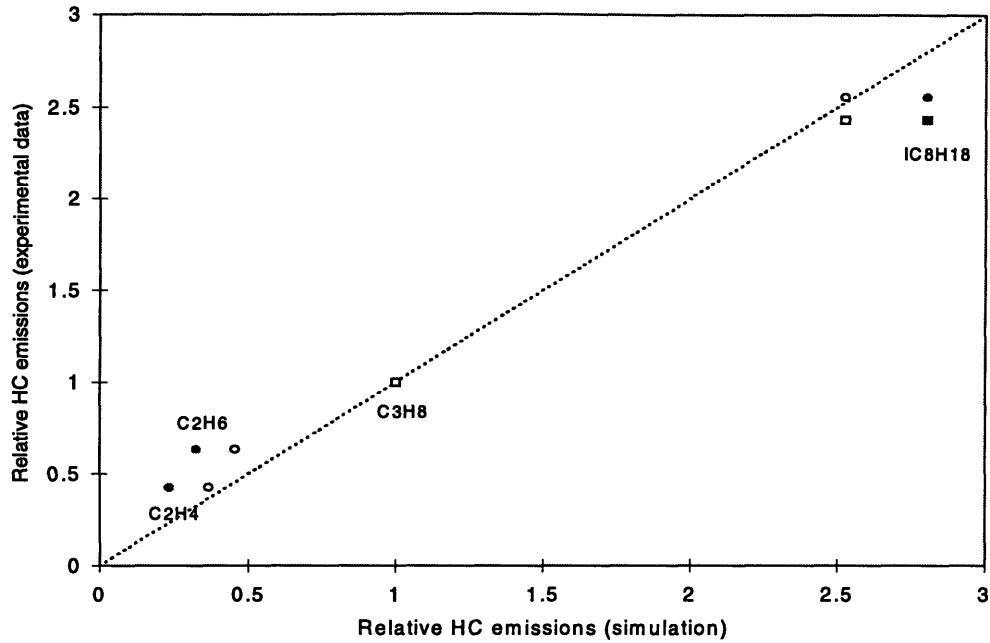


Figure 4-5 Comparisons of the relative hydrocarbon emission levels for different fuels based on predicted mass-integrated results and experimental data. Results are normalized by propane emissions. (circle : Drobot et al [8], square : Kayes et al [13], solid symbol : top dead center of the exhaust process is chosen to calculate the surviving fraction of total hydrocarbons, blank symbol : bottom dead center of the expansion process is chosen to calculate the surviving fraction of total hydrocarbons)

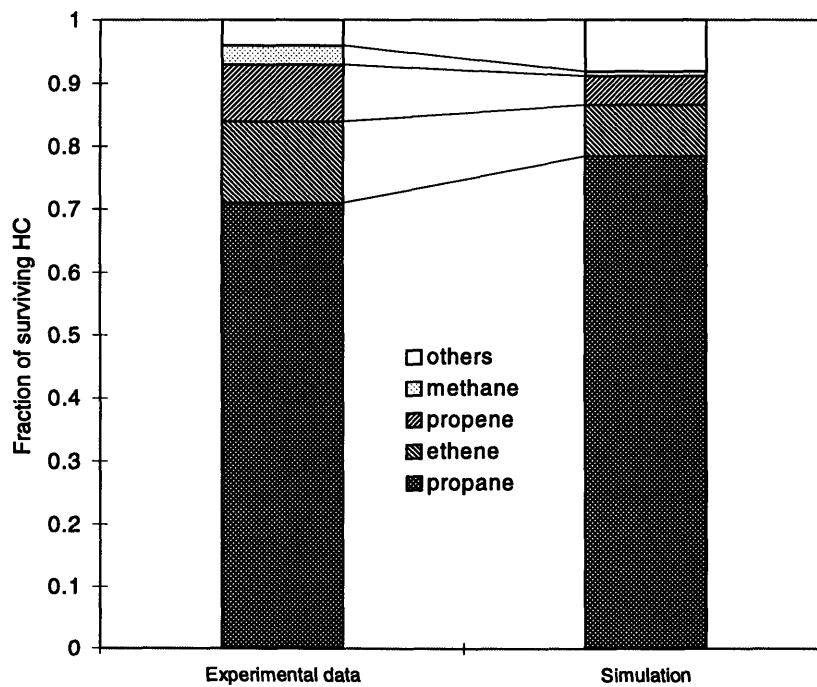


Figure 4-6 Comparison between simulations and experimental measurements [13] at top dead center of the exhaust process. (fuel : propane)

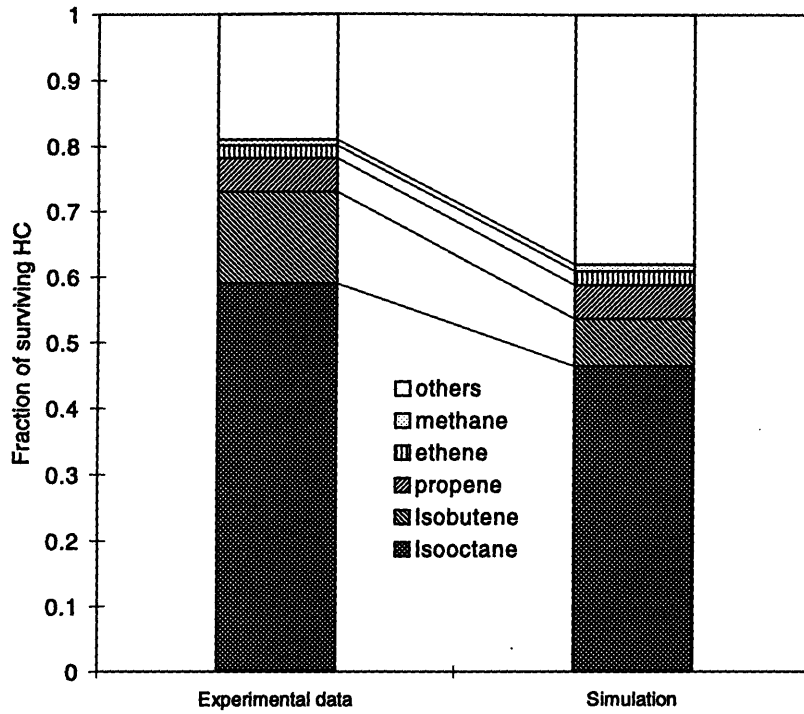


Figure 4-7 Comparison between simulations and experimental measurements [13] at top dead center of the exhaust process. (fuel : isooctane)

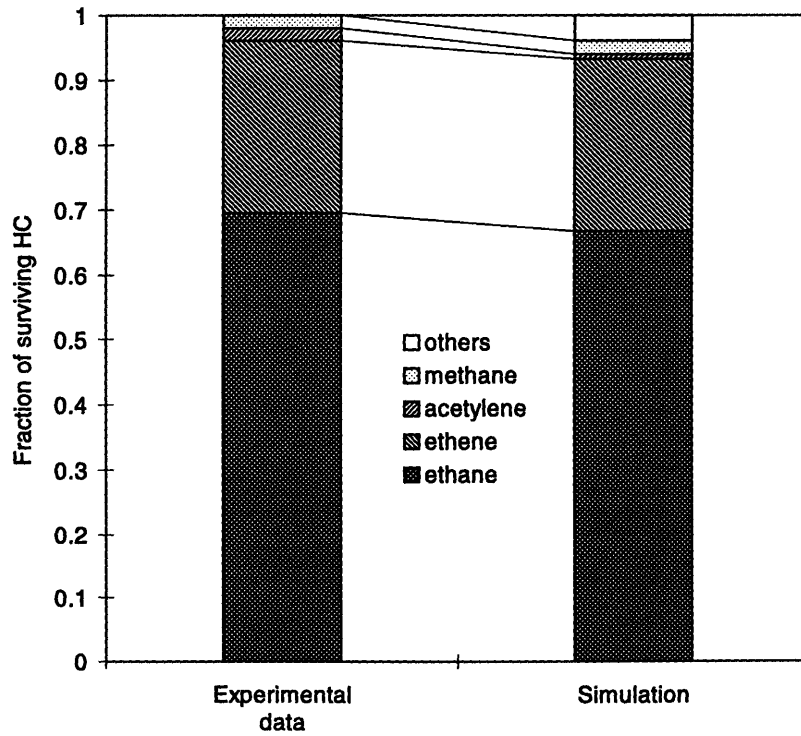


Figure 4-8 Comparison between simulations and experimental measurements [8] at top dead center of the exhaust process. (fuel : ethane)

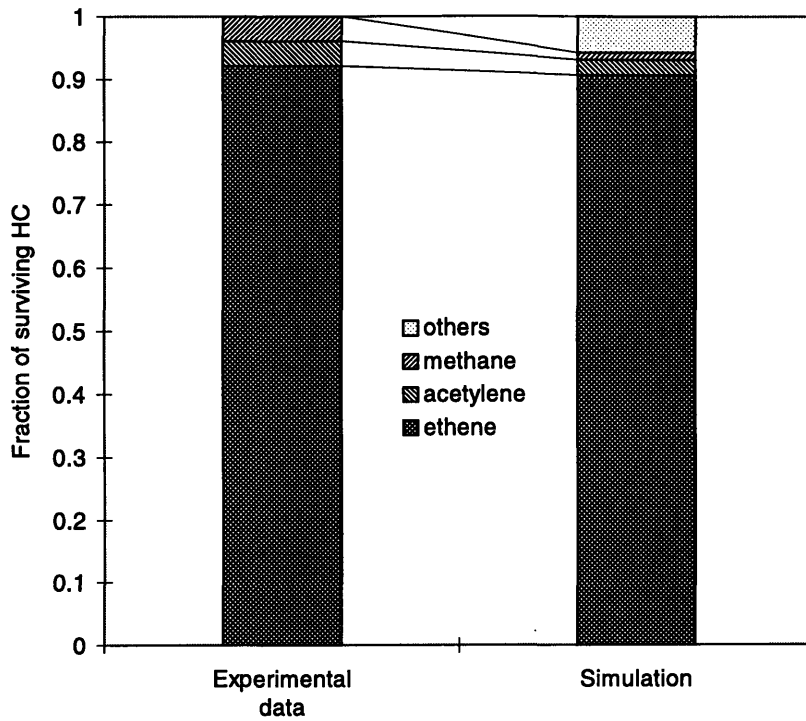


Figure 4-9 Comparison between simulations and experimental measurements [8] at top dead center of the exhaust process. (fuel : ethylene)

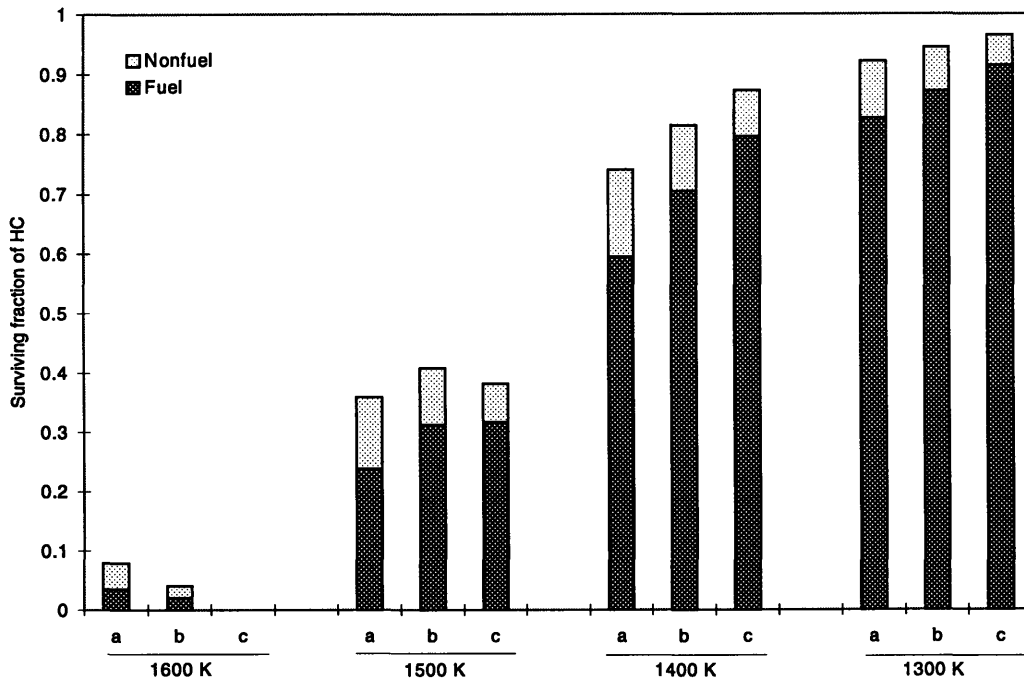


Figure 4-10 Comparison of the surviving fraction of total hydrocarbons and fuel/non-fuel distribution at top dead center of the exhaust process between the cases with width of hydrocarbon layer of (a) 0.1 mm (original case), (b) 0.2 mm, and (c) 0.4 mm. Results are normalized by initial unburned hydrocarbon concentrations. (fuel : propane)

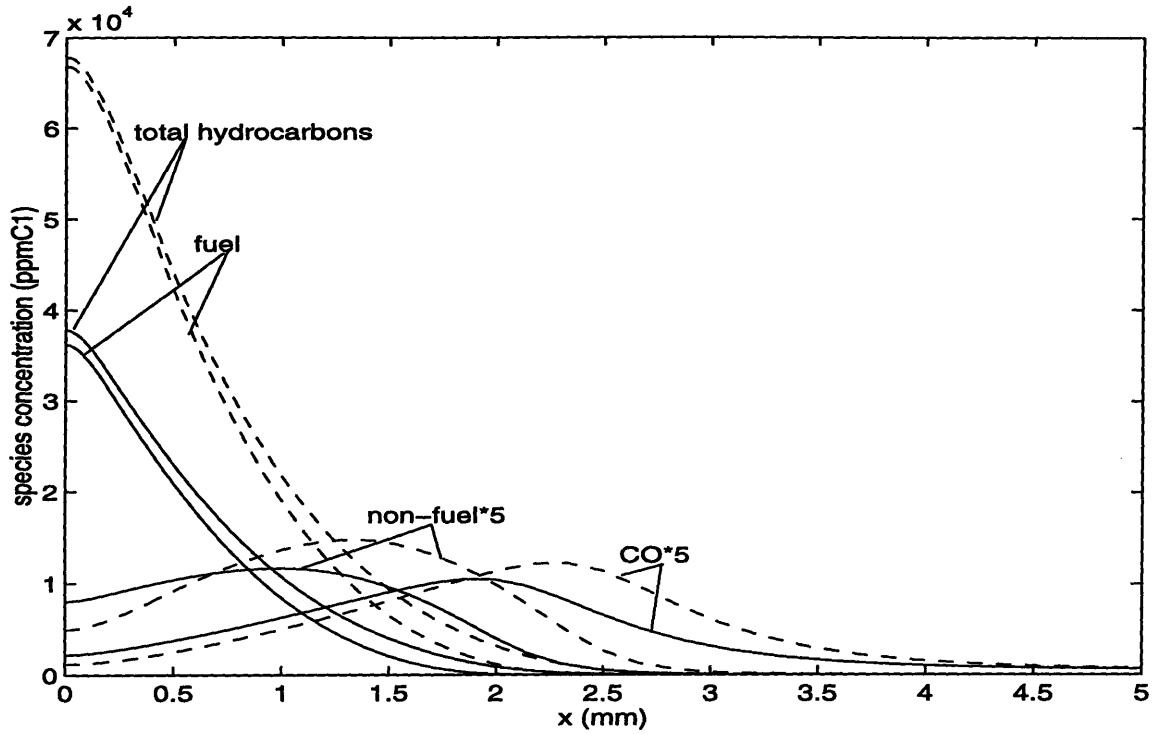


Figure 4-11 Comparison of spatial distribution of species concentrations between the original case (solid line) and the case with the width of hydrocarbon layer of 0.2 mm. (dashed line) (fuel : propane, initial core temperature : 1400 K)

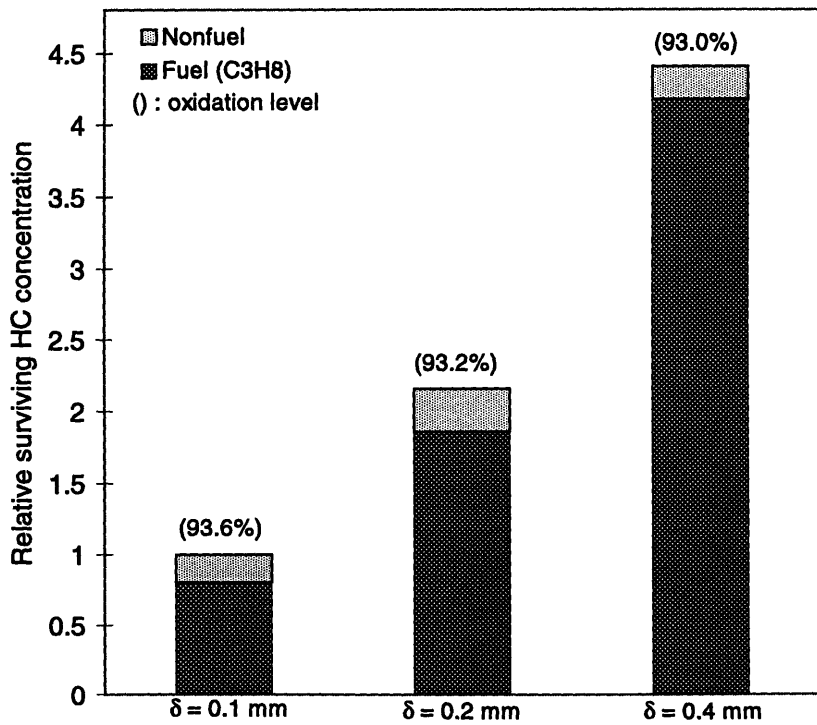


Figure 4-12 Effect of width of hydrocarbon layer on the extent of oxidation and fuel/non-fuel distribution. Results are normalized by the results in the baseline case (0.1 mm). (fuel : propane)

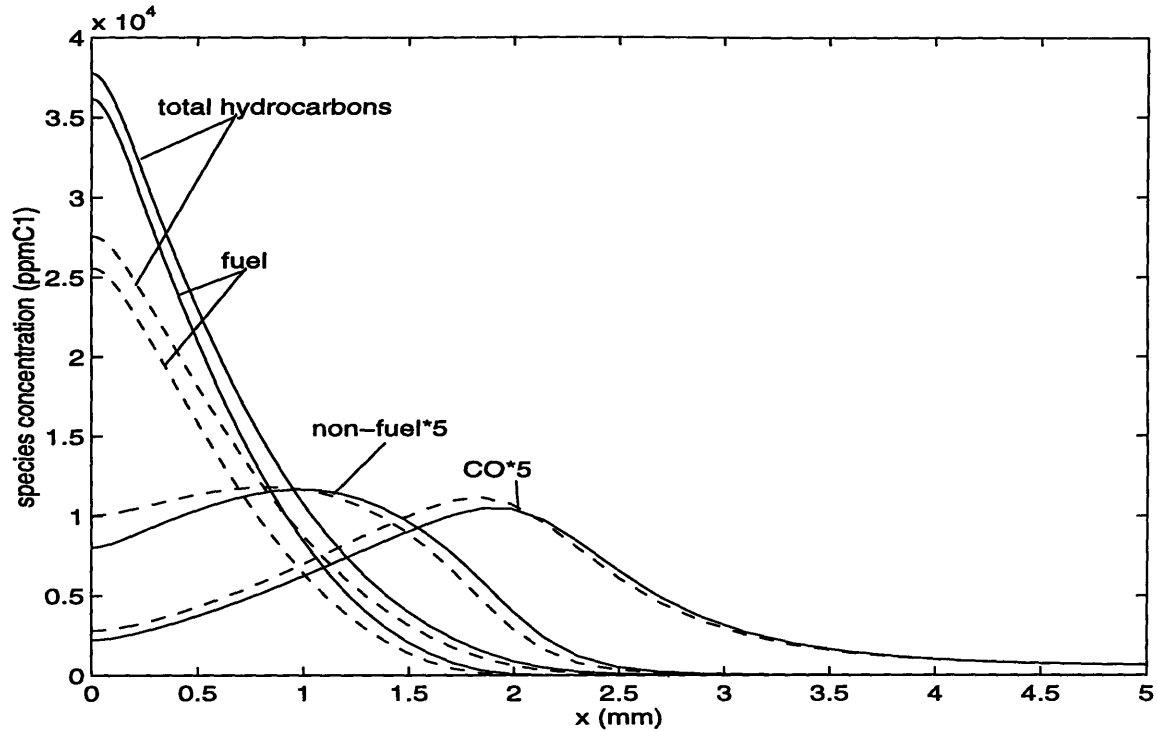


Figure 4-13 Comparison of spatial distribution of species concentrations between the original case (solid line) and the case at wall temperature of 500K. (dashed line) (fuel : propane, initial core temperature : 1400 K)

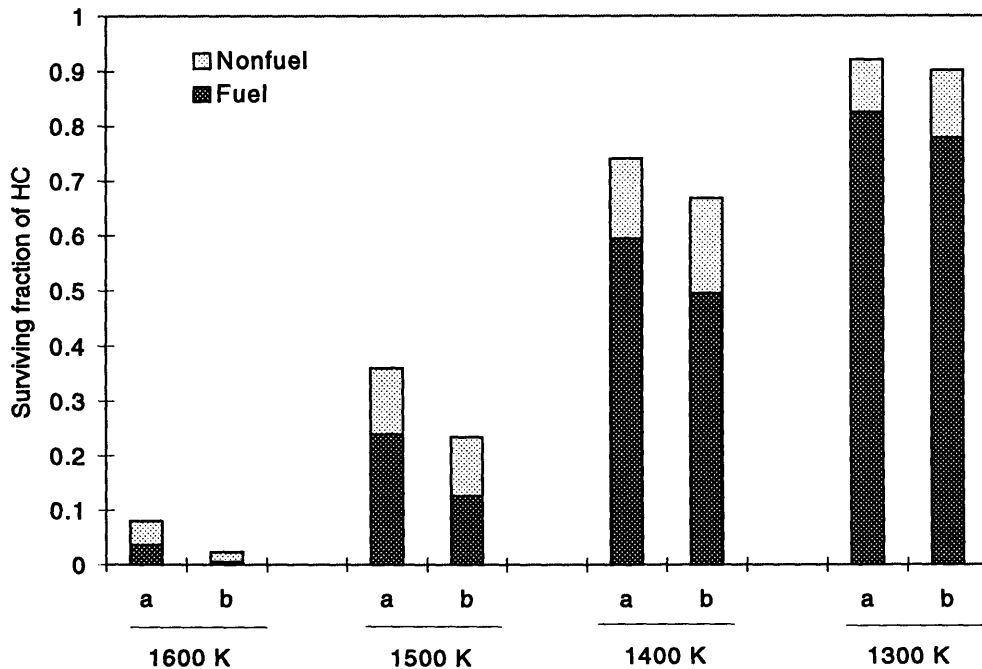


Figure 4-14 Comparison of surviving fraction of total hydrocarbons and fuel/non-fuel distribution at top dead center of the exhaust process between the (a) original case ($T_w = 361$ K) (b) case for wall temperature $T_w = 500$ K. Results are normalized by initial unburned hydrocarbon concentrations. (fuel : propane)

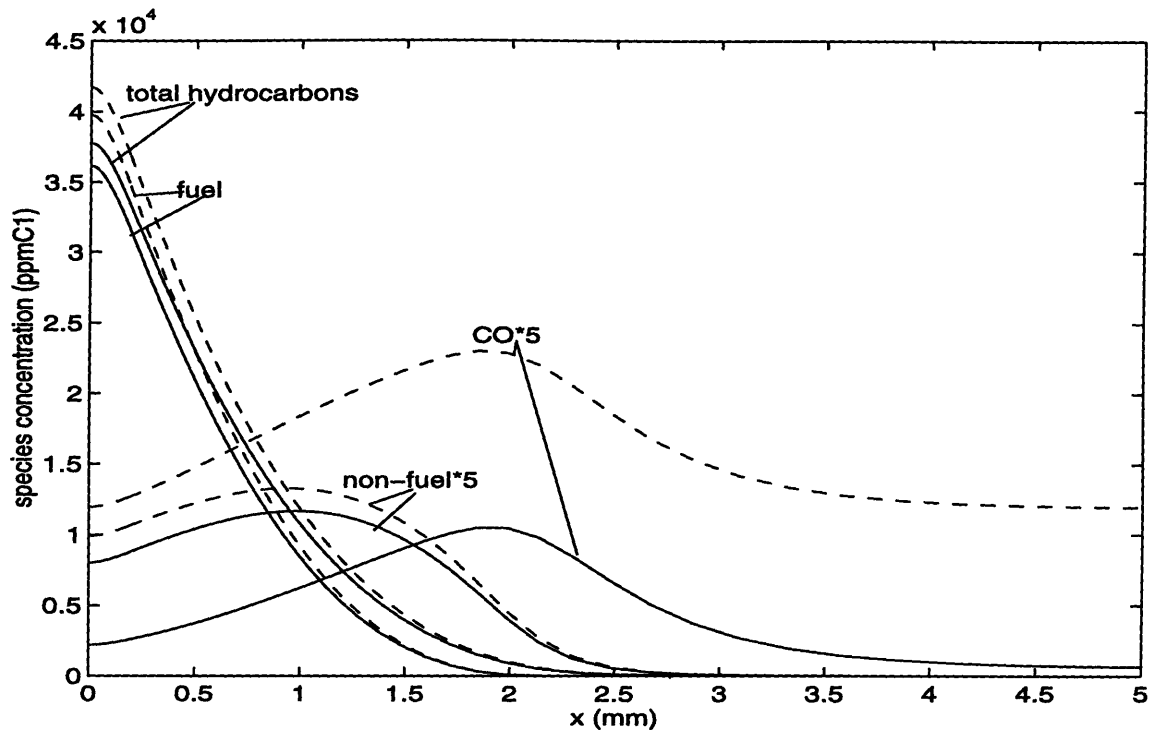


Figure 4-15 Comparison of spatial distribution of species concentrations between the original case (solid line) and the case at stoichiometric condition. (dashed line) (fuel : propane, initial core temperature : 1400 K)

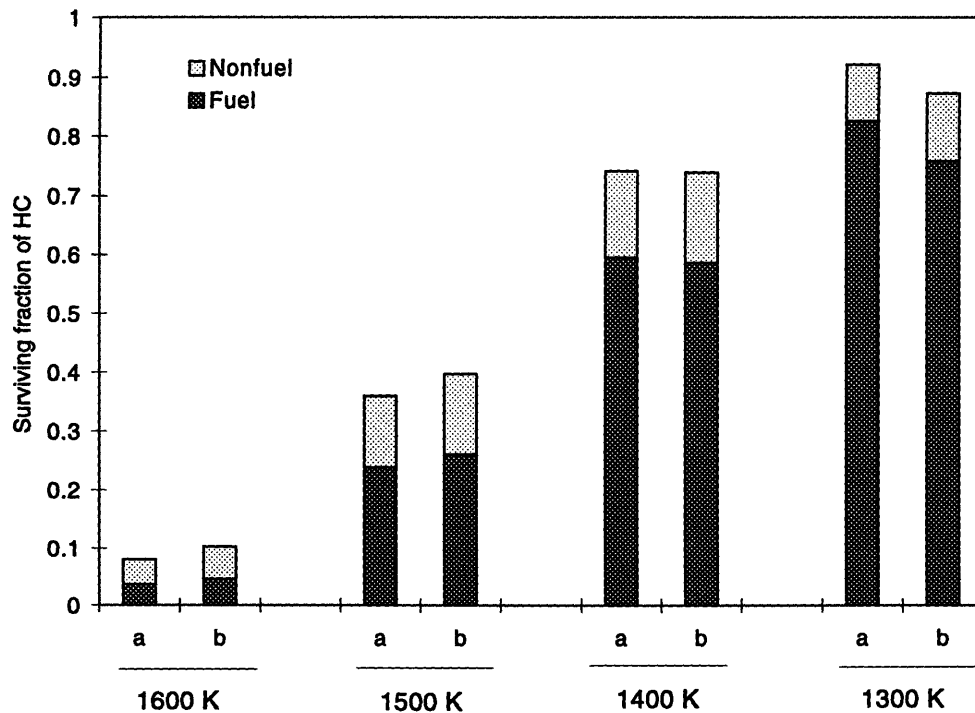


Figure 4-16 Comparison of the surviving fraction of total hydrocarbons and fuel/non-fuel distribution at top dead center of the exhaust process between the (a) baseline case ($\Phi=0.9$) (b) stoichiometric case. Results are normalized by initial unburned hydrocarbon concentrations. (fuel : propane)

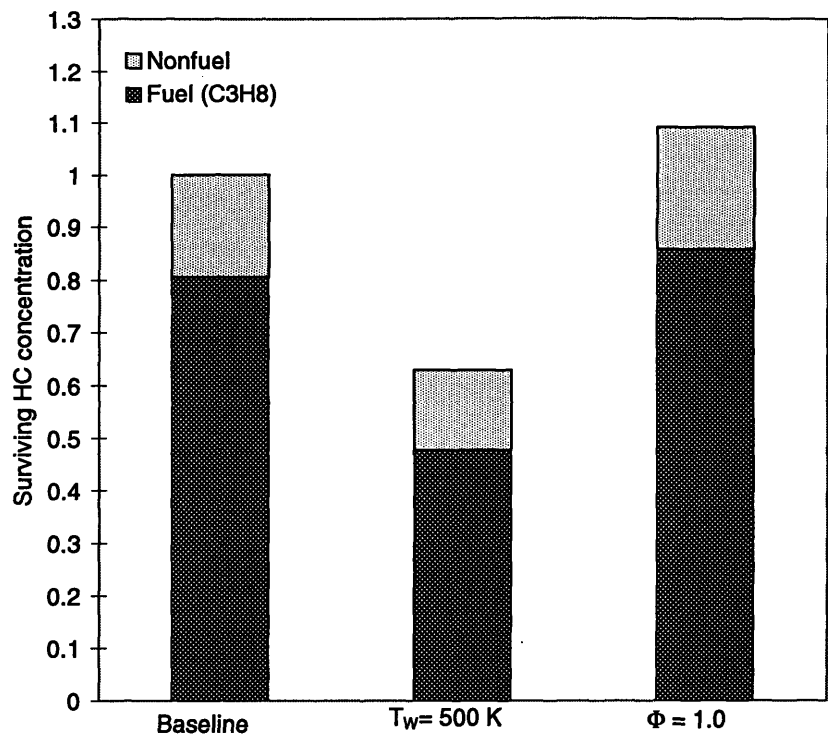


Figure 4-17 Effects of the wall temperature and fuel/air equivalence ratio on the extent of oxidation and fuel/non-fuel distribution. The normalized fractions are relative to the baseline case.

Chapter 5 Reaction Path Analysis

The local contribution of diffusion, convection and reaction to the net local rate of change of species concentration has been analyzed in Chapter 3, in order to understand the roles of diffusion and chemical rates on the overall oxidation of species. In this chapter, chemical reaction path analysis was conducted to identify the main pathways of hydrocarbon oxidation and radical pool generation. Through detailed reaction flux analysis, the reasons for the different oxidation rates between the cases of propane and isooctane is investigated

5.1 Reaction path analysis for oxidation of hydrocarbon species

The oxidation of a hydrocarbon fuel takes place by the sequential fragmentation of the initial fuel molecule into smaller intermediate species, which are ultimately converted to final products, H₂O and CO₂. The reaction path analysis identifies the main pathways of the sequence of fragmentation of hydrocarbons for the case of propane and isooctane.

5.1.1 Propane

Figure 5.1 shows the simplified main pathways for propane oxidation. Most of the propane is consumed by attack of OH, O, and H radicals to form propyl radicals, which then decompose into major intermediate species, ethylene (C₂H₄) and propene (C₃H₆). These intermediate species then further oxidize into smaller hydrocarbon fragments such as formaldehyde (CH₂O) and formyl radical (HCO), which are and finally converted into carbon monoxide and carbon dioxide. The detailed reaction flux analysis for the main paths are described as follows.

Figure 5.2 shows the consumption pathways of propane are dominated by reactions (1) - (6) via OH, O, and H radical attack, the latter generated in the reaction zone.



Reactions fluxes (1) to (4) are higher than reactions (5) and (6) for lean and stoichiometric conditions. The initial thermal decomposition reaction



does not effectively compete with radical-fuel reactions (less than 10% of the top reaction rate) because of low temperature (high activation energy in reaction (7)) and the abundance of radicals in the reaction zone.

The propyl radicals (C_3H_7) are almost entirely consumed by thermal decomposition



which are the main paths for producing ethylene (C_2H_4) and propene (C_3H_6) as important intermediate species.

Ethylene and propene are further consumed by reaction with active radicals (Figures 5.3-4) to yield formaldehyde (CH_2O), formyl radical (HCO) and smaller allyl radicals (CH_3 , etc).



Carbon monoxide is finally formed via reactions (16) and (17), and is converted to a final combustion product CO_2 by reaction (18) (Figure 5.5),



5.1.2 Isooctane

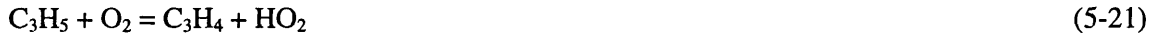
Isooctane has a larger and more complicated molecular structure than propane. Consequently, there are more reaction flux paths available for isooctane oxidation and more intermediate products involved. Figure 5.6 depicts the main isooctane oxidation pathways. Due to the hierarchical structure of chemical kinetics, the reaction flux paths of the byproducts of propane oxidation can be viewed as part of that of isooctane. Therefore, only the paths outside the scope of the oxidation paths of the byproduct of propane are discussed in this section.

As in the case of propane, H atom abstraction reactions with OH radicals are the most important for the consumption of isooctane to form isooctyl radicals, which then decompose into major intermediate species isobutene (IC₄H₈). Important fuel consumption reactions are showed in Figure 5.7 as a function of local temperature. Again, the thermal decomposition reaction (19)



is not the main initiation reaction for isooctane post flame oxidation, even though a large molecule like isooctane can decompose more easily than propane.

Through several pathways, all the isooctyl radicals promptly undergo β -scission to form a large amount of isobutene (IC₄H₈). Subsequently, propene (C₃H₆), allene (C₃H₄), and smaller fragments are produced from the decomposition of and radical attack on isobutene (Figure 5.8).



The conversion rates of both fuel and intermediate species in the case of isooctane are much lower than in the case of propane. (For instance, compare Figure 5.2 with Figure 5.7 for the rates of fuel decomposition; compare Figure 5.3 with Figure 5.9 for the rates of production/destruction of intermediate species (ethylene)). Since the reaction constants of the main decomposition reactions are approximately within the same range for propane and isooctane (for the same temperature range), the low concentrations of reactants (fuel (or intermediate species) and radicals in the reaction zone, see Figure 3.8 and Figure 3.36) are found to be the main reason for the lower oxidation rate in the case of isooctane.

5.2 Flux analysis for radical pool generation

Since the low concentrations of radicals in the reaction zone result in the low hydrocarbon conversion rate in the case of isooctane, it is important to find out why lower concentrations of radicals are generated in the case of isooctane. Figure 5.10 illustrates the main reaction rates leading to OH formation/consumption in the case of propane. Flux analysis shows that the important chain-branching and chain propagating reactions for OH in the radical pool are



Most of the OH is consumed by diffusing into the adjacent zone and reacting with locally rich partial combustion products such as CH₂O



and CO (reaction (18)), which are produced near the radical pool, or by the termination reaction (reaction (31)).

Figures 5.11 show the contributions to the formation and destruction of H radicals. The primary pathway for hydrogen atom production is the decomposition of formyl radical HCO (reaction (17)) and the oxidation of carbon monoxide (reaction (18)). It is observed that H is consumed mostly in the important chain-propagating and chain-branching reactions (27), (29), and (30).

In laminar flame simulations at high pressures, the recombination reaction



competes with reaction (27) to reduce the radical concentrations and slow down the combustion [29]. In the present cases, the recombination reaction (33) only has a moderate contribution to suppress the generation of radicals due to the relatively low pressure environment of post-flame oxidation. In most cases, the net production rate of reaction (33) is less than 30% than that of reaction (27).

The pathway analysis above indicates that the hydrogen atom is the key radical for the production of hydroxyl radicals by triggering the main chain-branching reactions (27), (29), and (30), and generating oxygen atoms (through reaction (27) to further promote another main chain-branching reaction (28)). Moreover, the rates of formyl radicals decomposition (reaction(17)) and carbon monoxide oxidation (reaction (18)) determine the rate of production of hydrogen atom. Therefore, the generation of radicals actually depends on the rate of hydrocarbon conversion (into HCO and further CO). Higher concentrations of radicals are generated in the case of propane than isooctane for two reasons : the higher initial fuel concentrations in the case of propane, and the shorter oxidation pathways.

Figure 5.12 depicts the reaction rates of formation and destruction of hydrogen atom in the isooctane case. The peak production rate of hydrogen atoms through the decomposition of

carbonyl radicals (HCO) in the isooctane case is about an order of magnitude lower than in the case of propane (Figure 5.11) demonstrating the much slower conversion of hydrocarbon species in the case of isooctane.

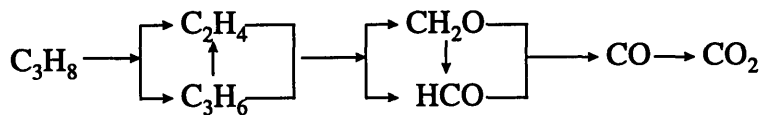


Figure 5-1 Simplified pathways for propane oxidation.

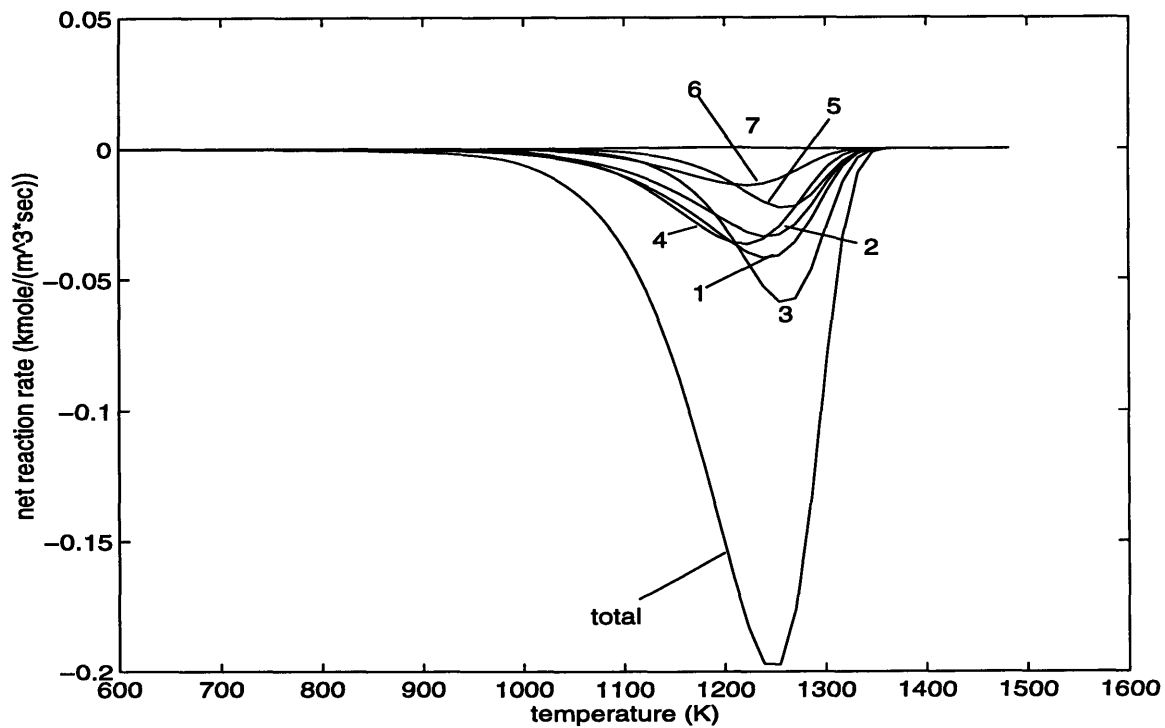


Figure 5-2 Contribution of the important reactions to the total reaction flux of propane at 25 crank angle degrees after start of reaction. (fuel : propane, initial core temperature : 1600 K) Reactions : (1) $\text{C}_3\text{H}_8 + \text{OH} = \text{nC}_3\text{H}_7 + \text{H}_2\text{O}$, (2) $\text{C}_3\text{H}_8 + \text{OH} = \text{iC}_3\text{H}_7 + \text{H}_2\text{O}$, (3) $\text{C}_3\text{H}_8 + \text{O} = \text{nC}_3\text{H}_7 + \text{OH}$, (4) $\text{C}_3\text{H}_8 + \text{OH} = \text{iC}_3\text{H}_7 + \text{H}_2$, (5) $\text{C}_3\text{H}_8 + \text{O} = \text{iC}_3\text{H}_7 + \text{OH}$, (6) $\text{C}_3\text{H}_8 + \text{H} = \text{nC}_3\text{H}_7 + \text{H}_2$, (7) $\text{C}_3\text{H}_8 = \text{C}_2\text{H}_5 + \text{CH}_3$.

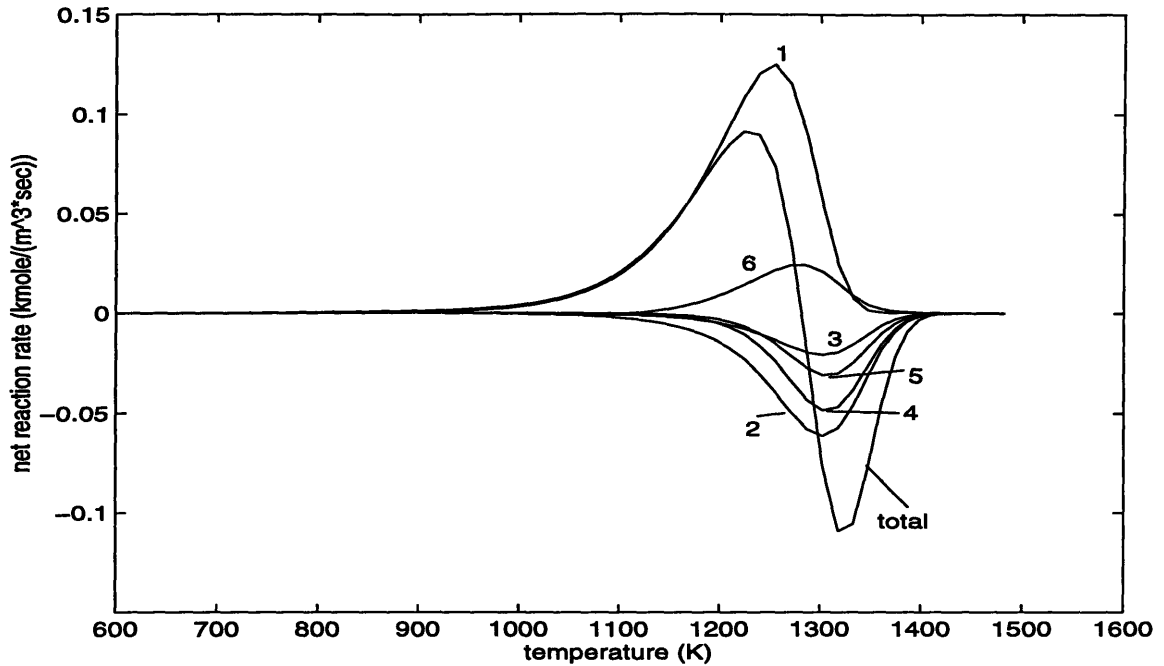


Figure 5-3 Contribution of the important reactions to the total reaction flux of ethylene at 25 crank angle degrees after start of reaction. (fuel : propane, initial core temperature : 1600 K) Reactions : (1) $nC_3H_7=C_2H_4+CH_3$, (2) $C_2H_4+OH=C_2H_3+H_2O$, (3) $C_2H_4+OH=CH_2O+CH_3$, (4) $C_2H_4+O=CH_3+HCO$, (5) $C_2H_4+O=CH_2O+CH_2$, (6) $C_2H_5+M=C_2H_4+H+M$.

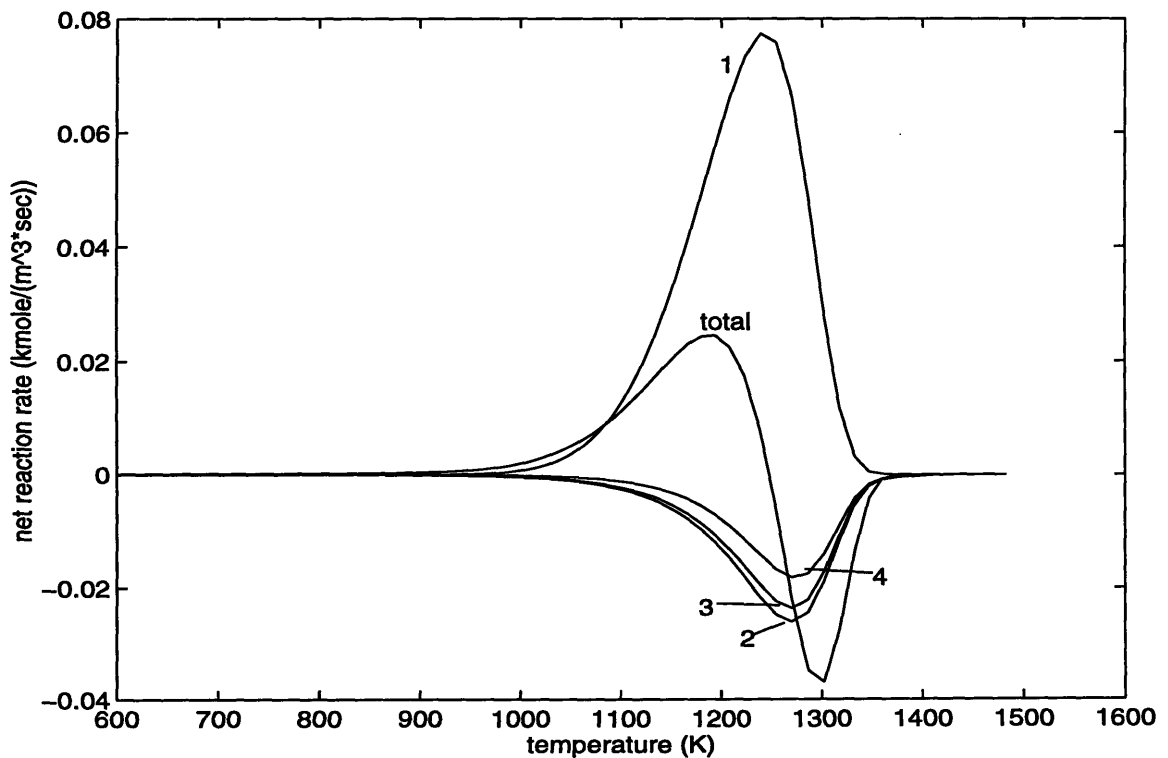


Figure 5-4 Contribution of the important reactions to the total reaction flux of propene at 25 crank angle degrees after start of reaction. (fuel : propane, initial core temperature : 1600 K) Reactions : (1) $iC_3H_7=C_3H_6+H$, (2) $C_3H_6+OH=C_2H_5+CH_2O$, (3) $C_3H_6+OH=AC_3H_5+H_2O$, (4) $C_3H_6+OH=SC_3H_5+H_2O$.

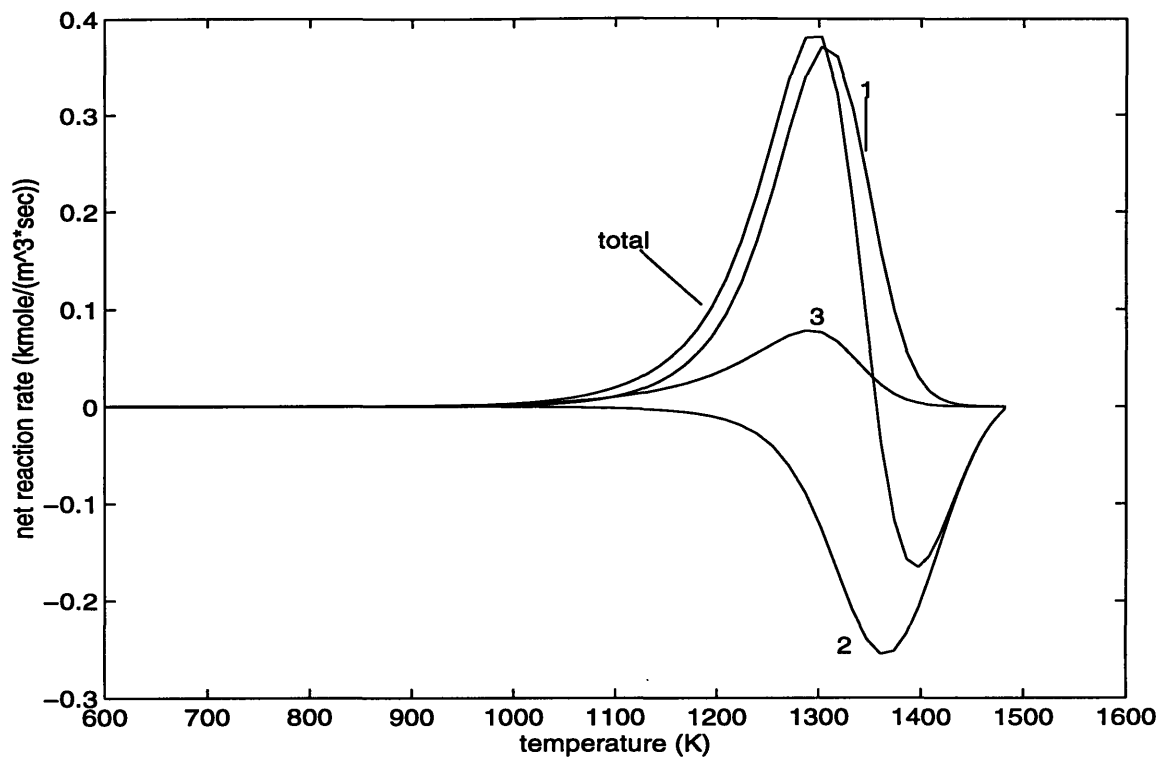


Figure 5-5 Contribution of the important reactions to the total reaction flux of carbon monoxide at 25 crank angle degrees after start of reaction. (fuel : propane, initial core temperature : 1600 K) Reactions : (1) $\text{HCO} + \text{M} = \text{H} + \text{CO} + \text{M}$, (2) $\text{CO} + \text{OH} = \text{CO}_2 + \text{H}$, (3) $\text{HCO} + \text{O}_2 = \text{CO} + \text{HO}_2$.

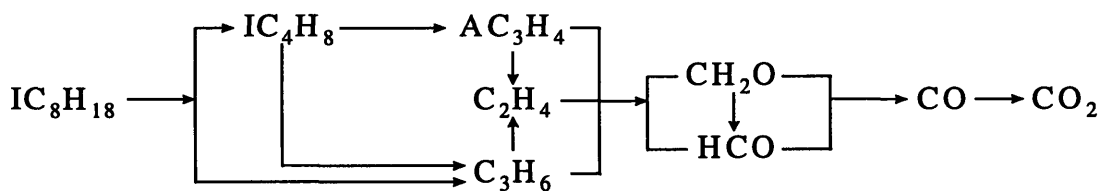


Figure 5-6 Simplified pathways for isooctane oxidation

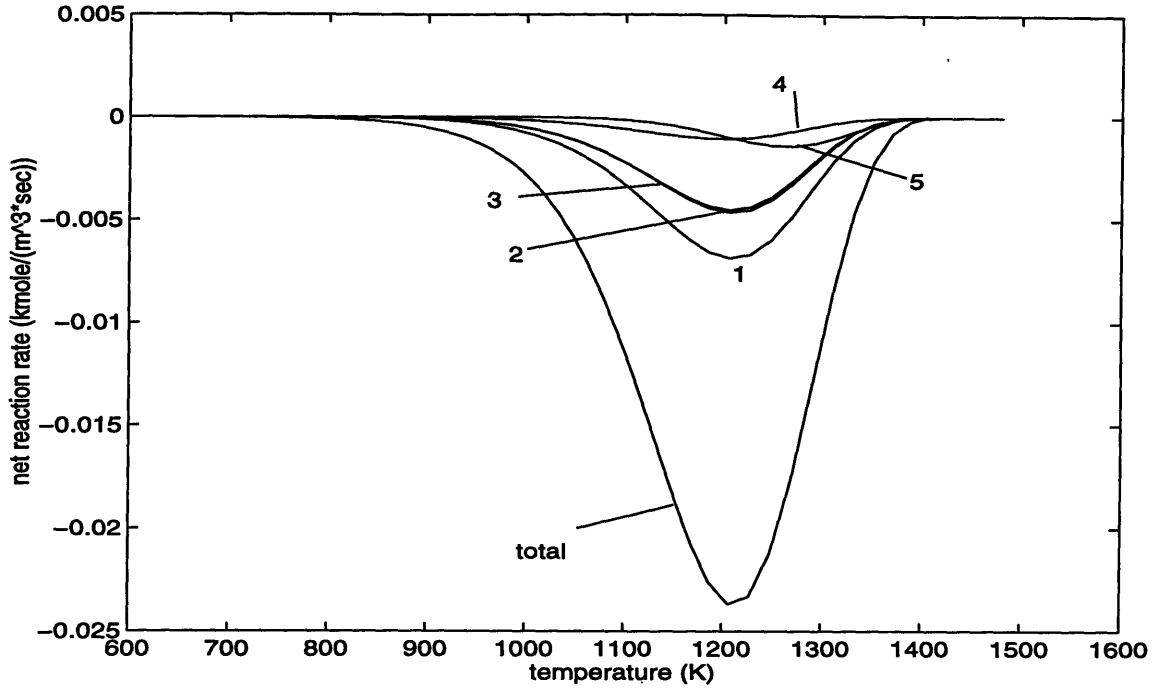


Figure 5-7 Contribution of the important reactions to the total reaction flux of isooctane at 25 crank angle degrees after start of reaction. (fuel : isooctane, initial core temperature : 1600 K) Reactions : (1) $iC_8H_{18}+OH=aC_8H_{17}+H_2O$, (2) $iC_8H_{18}+OH=dC_8H_{17}+H_2O$, (3) $iC_8H_{18}+OH=bC_8H_{17}+H_2O$, (4) $iC_8H_{18}+OH=cC_8H_{18}+H_2O$, (5) $iC_8H_{18}=tC_4H_9+iC_4H_9$.

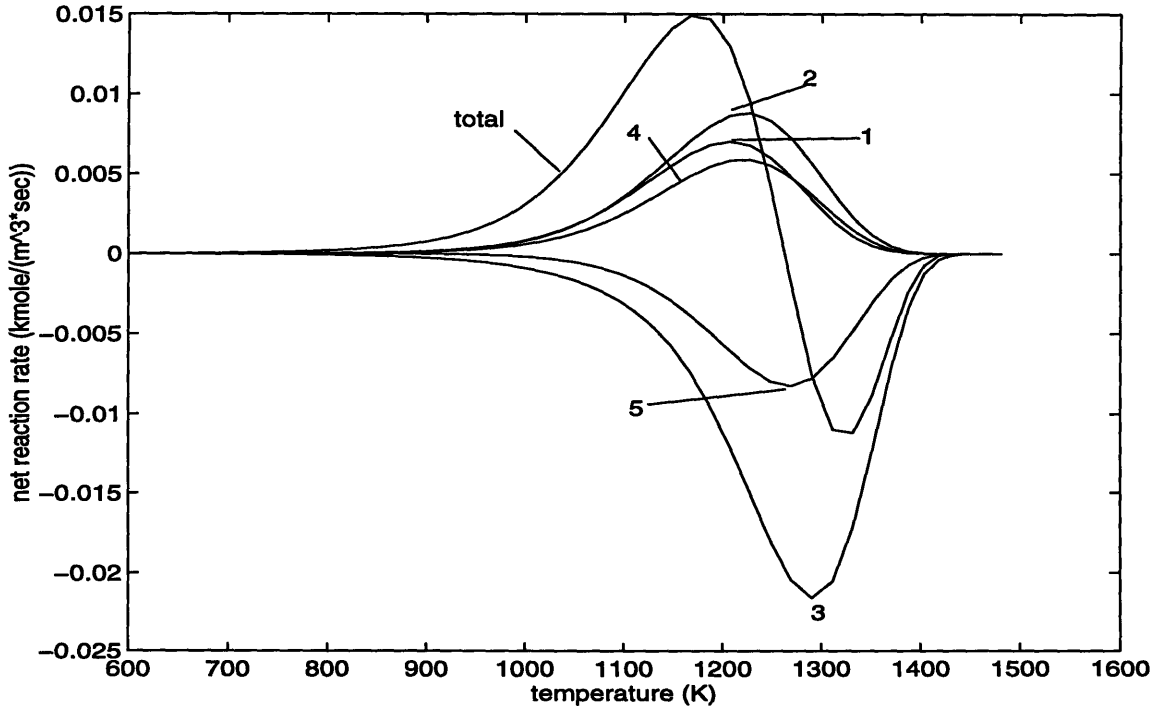


Figure 5-8 Contribution of the important reactions to the total reaction flux of isobutene at 25 crank angle degrees after start of reaction. (fuel : isooctane, initial core temperature : 1600 K) Reactions : (1) $aC_8H_{17}=iC_4H_8+iC_4H_9$, (2) $iC_4H_9=iC_4H_8+H$, (3) $iC_4H_8=C_3H_5+CH_3$, (4) $neoC_5H_{11}=iC_4H_8+CH_3$, (5)summation of following reactions : (a) $iC_4H_8+O=iC_4H_7+OH$, (b) $iC_4H_8+O=iC_3H_7+HCO$, (c) $iC_4H_8+OH=iC_4H_7+H_2O$, (d) $iC_4H_8+OH=iC_3H_7+CH_2O$, (e) $iC_4H_8+H=iC_4H_7+H_2$.

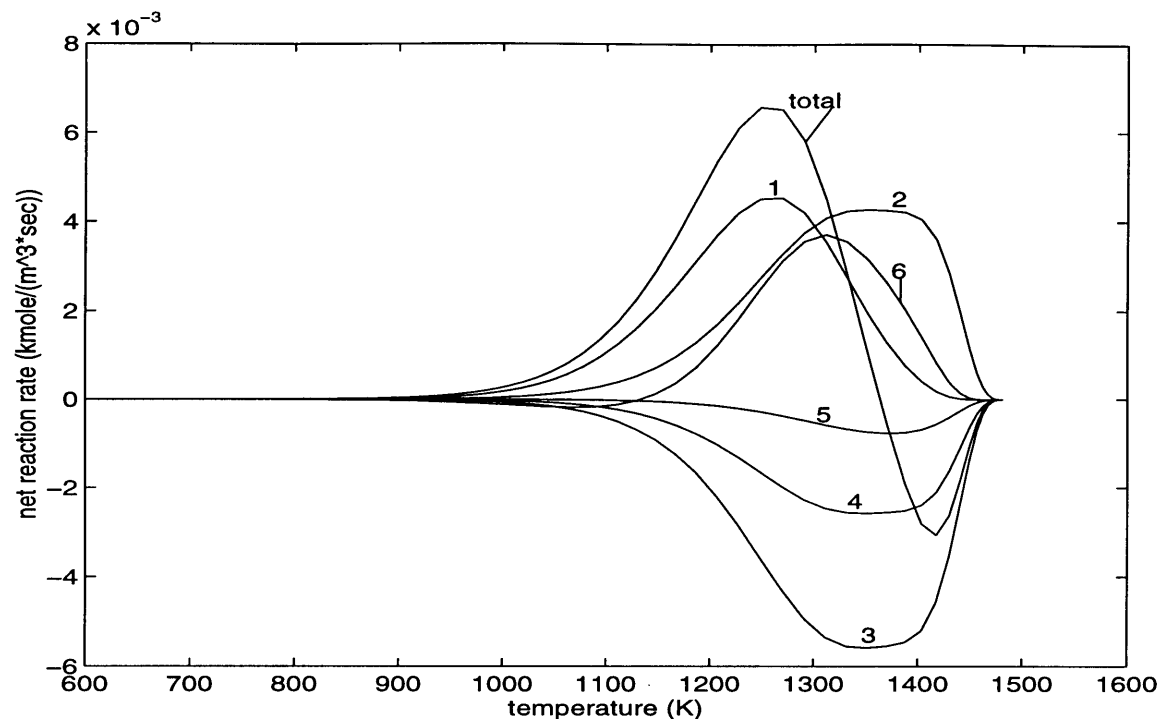


Figure 5-9 Contribution of the important reactions to the total reaction flux of ethylene at 25 crank angle degrees after start of reaction. (fuel : isooctane, initial core temperature : 1600 K) Reactions : (1) $nC_3H_7=C_2H_4+CH_3$, (2) $C_3H_4+OH=C_2H_4+HCO$, (3) $C_2H_4+OH=C_2H_3+H_2O$ (4) $C_2H_4+OH=CH_2O+CH_3$, (5) $C_2H_4+O=CH_2O+CH_2$, (6) $C_2H_5+M=C_2H_4+H+M$.

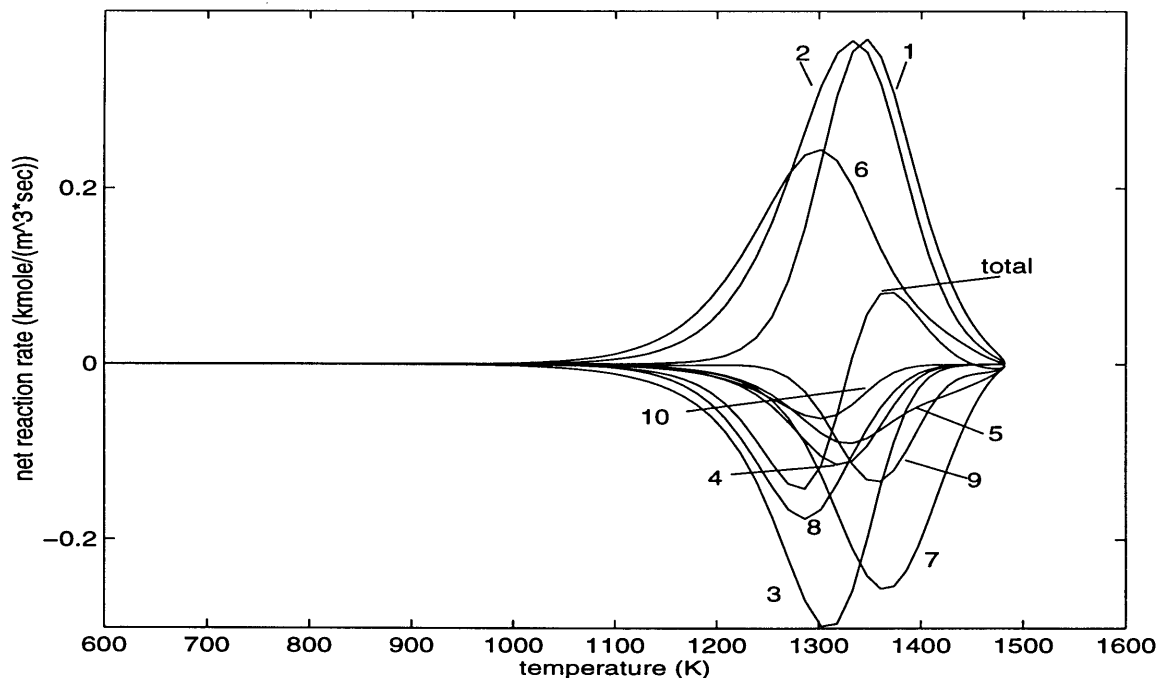


Figure 5-10 Contribution of the important reactions to the total reaction flux of hydroxyl at 25 crank angle degrees after start of reaction. (fuel : propane, initial core temperature : 1600 K) Reactions : (1) $O+H_2O=2OH$, (2) $H+O_2=OH+O$, (3) $CH_2O+OH=HCO+H_2O$, (4) $CH_3OH+OH=CH_2OH+H_2O$, (5) $HO_2+OH=H_2O+O_2$, (6) $H+HO_2=OH+OH$, (7) $CO+OH=CO_2+H$, (8) $CH_3+OH=CH_3OH$, (9) $H_2+OH=H_2O+H$, (10) $C_2H_4+OH=C_2H_3+H_2O$.

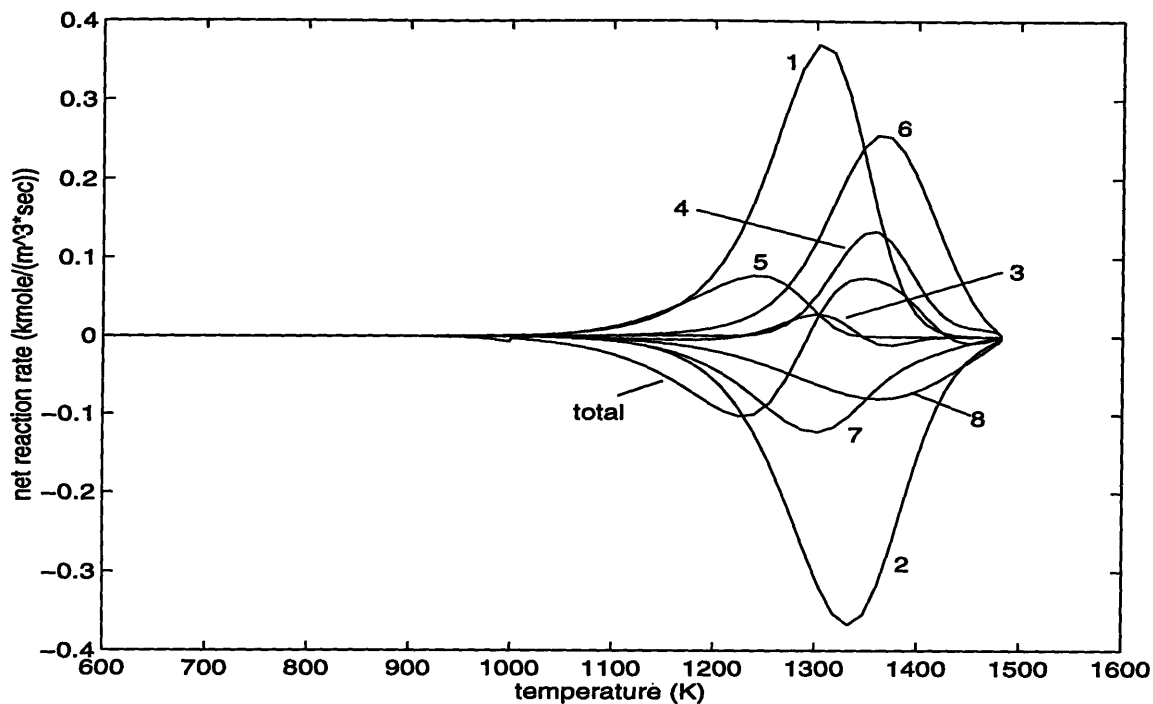


Figure 5-11 Contribution of the important reactions to the total reaction flux of hydrogen atom at 25 crank angle degrees after start of reaction. (fuel : propane, initial core temperature : 1600 K) Reactions : (1) $\text{HCO}+\text{M}=\text{H}+\text{CO}+\text{M}$, (2) $\text{H}+\text{O}_2=\text{OH}+\text{O}$, (3) $\text{C}_2\text{H}_3=\text{C}_2\text{H}_2+\text{H}$, (4) $\text{H}_2+\text{OH}=\text{H}_2\text{O}+\text{H}$, (5) $\text{C}_3\text{H}_7=\text{C}_3\text{H}_6+\text{H}$, (6) $\text{CO}+\text{OH}=\text{CO}_2+\text{H}$, (7) $\text{H}+\text{HO}_2=\text{OH}+\text{OH}$, (8) $\text{H}+\text{O}_2=\text{HO}_2$.

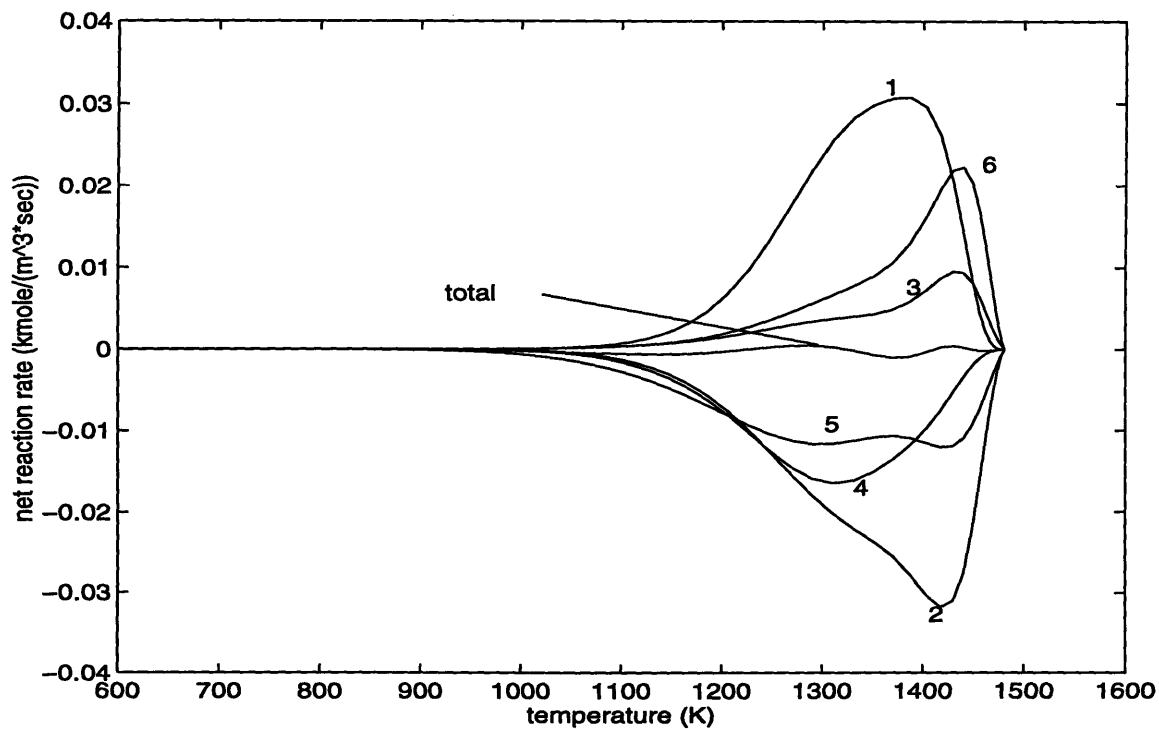


Figure 5-12 Contribution of the important reactions to the total reaction flux of hydrogen atom at 25 crank angle degrees after start of reaction. (fuel : isooctane, initial core temperature : 1600 K) Reactions : (1) $\text{HCO}+\text{M}=\text{H}+\text{CO}+\text{M}$, (2) $\text{H}+\text{O}_2=\text{OH}+\text{O}$, (3) $\text{H}_2+\text{OH}=\text{H}_2\text{O}+\text{H}$, (4) $\text{H}+\text{HO}_2=\text{OH}+\text{OH}$, (5) $\text{H}+\text{O}_2=\text{HO}_2$, (6) $\text{CO}+\text{OH}=\text{CO}_2+\text{H}$.

Chapter 6 Summary and Conclusions

A one-dimensional, detailed chemistry and transport numerical model has been established to simulate the post-flame oxidation process of unburned hydrocarbons in a spark ignition engine, for the purpose of investigating in detail the roles of oxidation chemistry and transport on the oxidation process. Varying pressures and temperatures, as well as turbulent transport, have been included in the current model in order to simulate the environment inside an engine, where oxidation reactions occur between a thin layer of unburned hydrocarbons adjacent to the walls and the surrounding hot burned gas. The important results are summarized as follows.

1. *General features of the reactive/diffusive process* : simulations show that unburned fuel is transported towards the hot burned gases, where intermediate species are quickly generated. The cold region near the walls acts as a reservoir that preserves the intermediate species from quick oxidation. Radicals are generated close to the burned gas during the oxidation process, at much higher concentrations than the original burned gas radical concentrations, indicating that radicals in the burned gas do not have a significant effect on the oxidation level of unburned hydrocarbons.

2. *Roles of diffusion, convection, and reaction* : flux analysis indicates that the convective term ($\rho u \frac{\partial Y_i}{\partial x}$) can be neglected in comparison with diffusive and reactive terms.

Diffusion plays the role of transporting radicals generated at higher temperatures towards lower temperature regions, and generated intermediate species towards higher temperature regions for destruction. The mechanism of generation (at lower temperatures) and destruction (at higher temperatures) of intermediate species keeps the overall concentrations of intermediate species approximately constant after the intermediate species initially increase.

3. *Effect of the burned gas temperature* : the burned gas temperature is the critical factor determining the oxidation level. Fast energy release raises the local temperatures near the walls, simulating the oxidation rate of unburned hydrocarbons in the cases of high initial core temperatures (of the order of 1800 K). In contrast, at low initial core temperatures (< 1400 K), radical generation near the burned gas is not significant, such that the influence of radicals already present in the burned gas becomes more important, and the whole conversion process is very slow.

4. *Effect of diffusion* : molecular diffusivity dominates in the regions close to the wall (within 0.1 mm) and throughout the reaction zone. Sensitivity analysis of the effect of diffusion on the oxidation process has been conducted by increasing turbulent diffusivity by a factor of two. The effect of diffusion strongly depends on the initial burned gas temperature : a large increase in oxidation is possible by increasing diffusion rates at high initial temperatures. The overall concentrations of non-fuel species is little influenced by the change of turbulent diffusivity, so that the remaining fuel/nonfuel ratio decreases with increasing diffusivity.
5. *Effect of reactant chemistry* : The effect of reactant chemistry on the oxidation process has been investigated by comparing the oxidation results between the cases of propane, ethane, ethylene, and isooctane.
 - a) *Ethane vs. ethylene* : Comparisons between the results of ethane and ethylene, which have similar molecular diffusivity and oxidation chemistry, show that the shorter path to oxidation in the case of ethylene, and the subsequent diffusion of non-fuel species (especially ethylene) towards the cold wall in the case of ethane, are responsible for the higher overall oxidation rate of ethylene.
 - b) *Isooctane vs. propane* : Higher concentrations of intermediate species concentrations, lower radical concentrations and much slower oxidation rate of unburned hydrocarbons is observed in the case of isooctane. Even increasing the molecular diffusivity of isooctane to the same level of that of propane, there is still a drastic difference in the oxidation level between propane and isooctane. This demonstrates the critical role of reaction chemistry on the oxidation level of unburned hydrocarbons. The factors resulting in the difference in reaction rates between the cases of propane and isooctane was investigated through reaction path analysis (see summary (8)).
6. *Effect of operating parameters* :
 - a) *Width of initial hydrocarbon layer* : the width of the hydrocarbon layer is a measure of the capacity of hydrocarbon supply. In the high temperature cases, more energy is released, raising local temperatures and promoting oxidation rates. In the cases of low initial core temperatures, the slow conversion rate results in more unburned hydrocarbons remaining near the wall.
 - b) *Wall temperature* : increasing the wall temperature (and consequently the temperatures in the reactive layer) raises the molecular diffusivity of unburned

fuel in the hydrocarbon layer and shortens the distance to the high temperature reaction zone, which results in higher extent of oxidation of unburned hydrocarbons, while the overall concentrations of intermediate species remain approximately constant..

c) *Fuel/air equivalence ratio* : Increasing fuel/air equivalence ratio from slightly lean ($\phi=0.9$) to stoichiometric ($\phi=1.0$) drastically changes the burned gas composition, but has little influence on the oxidation level.

7. *Crevice mass-integration and correlation with experiments* : An approximation was made that the oxidation of crevice hydrocarbons can be represented by the one-dimensional model, by integrating overall oxidation levels for crevice masses leaving at different core gas temperatures. Calculations indicate that over 90% of the crevice outflow of hydrocarbons is completely oxidized at top dead center of the exhaust process in the case of propane, and about 80% for the case of isooctane. Comparison with experimental data for various fuels shows a reasonable correlation with the relative emission levels, as well as with fractional contributions of individual species to the overall emissions.

8. *Factors determining the oxidation rate* : Reaction path analysis indicates most of hydrocarbons decompose by the attack of radicals (OH, O, and H). The drastic difference in the oxidation rate of unburned hydrocarbons between the cases of propane and isooctane are mainly due to the difference in the reactant concentrations (especially radicals) in the reaction zone. Hydrogen atom is the key radical for triggering most of the important chain-branching reactions. The main pathways of hydrogen atom production are through HCO decomposition and the reaction of carbon monoxide and hydroxyl. The rate of hydrocarbon conversion (to HCO) determines the rates of radical generation. It provides the explanation for the higher concentrations of radicals and higher oxidation level of unburned hydrocarbons in the case of propane than isooctane since there are a higher initial fuel concentration as well as shorter pathways to oxidation in the case of propane than isooctane.

References

- [1] Seinfeld, J. H., "Atmospheric Chemistry and Physics of Air Pollution", John Wiley & Sons, New York, pp. 58, 61 (1986).
- [2] McNeill, E., *Clean Air Act*, EESC Issue Paper (1992).
- [3] Owen, K., and Coley, T., "Automotive Fuels Reference Book", 2nd ed. Society of Automotive Engineers, Inc., Warrendale, PA, p 648 (1995).
- [4] Cheng, W. K., Hamrin, D., Heywood, J. B., Hochgreb, S., Min, K., and Norris, M. G., "An Overview of Hydrocarbon Emissions Mechanisms in Spark-Ignition Engines", *SAE Paper* 932708 (1993).
- [5] Namazian, M. and Heywood, J. B., "Flow in the Piston-Cylinder-Ring Crevices of a Spark Ignition Engine: Effect on Hydrocarbon Emissions, Efficiency and Power", *SAE Trans.*, vol. 91, (1982).
- [6] Adamczyk, A. A., Kaiser, E. W., Cavolowsky, J. A., and Lavoie, G. A., "An Experimental Study of Hydrocarbon Emissions from Closed Vessel Explosions", *Eighteenth Symposium (International) on Combustion*, The Combustion Institute (1981).
- [7] Westbrook, C. K., Adamczyk, A. A., and Lavoie, G. A., "A Numerical Study of Laminar Flame Wall Quenching", *Combust. Flame*. 40:81 (1981).
- [8] Drobot, K., Cheng, W. K., Trinker, F. H., Kaiser, E. W., Siegl, W. O., Cotton, D. F., and Underwood, J., "Hydrocarbon Oxidation in the Exhaust Port and Runner of a Spark Ignition Engine", *Combust. Flame*. 99:422 (1994).
- [9] Kaiser, E. W., Siegl, W. O., Trinker, F. H., Cotton, D. F., Cheng, W. K., and Drobot, K., "Effect of Engine Operating Parameters on Hydrocarbon Oxidation in the Exhaust Port and Runner of a Spark-Ignited Engine", *SAE Paper*. 950159 (1995).
- [10] Wu, K. C., and Hochgreb, S., "Chemical Kinetic Simulation of Hydrocarbon Oxidation Through the Exhaust Port of a Spark Ignition Engine", *Combust. Flame*. 107:383 (1996).
- [11] Peckham, M., and Collings, N., "Study of Engine Wall Layer Hydrocarbons with a Fast-Response FID", *SAE Paper*. 922237 (1992).
- [12] Min, K., "The Effects of Crevices on the Engine-out Hydrocarbon Emissions in Spark Ignition Engines", Ph.D. Thesis, Department of Mechanical Engineering, Massachusetts Institute of Technology, (1994).
- [13] Kayes, D. J., and Hochgreb, S., "Development of a Time and Space Resolved Sampling Probe diagnostic for Engine Exhaust Hydrocarbons", *SAE Paper*. 961002 (1996).

- [14] Kaiser, E. W., Siegl, W. O., Henig, Y. I., Anderson, R. W., and Trinker, F. H., "Effect of Fuel Structure on Emissions from a Spark-Ignited Engine", *Eviron. Sci. Tech.* 25:2005 (1991). Cotton, D. F.,
- [15] Kaiser, E. W., Siegl, W. O., Cotton, D. F., Henig, Y. I., and Anderson, R. W., "Effect of Fuel Structure on Emissions from a Spark-Ignited Engine 2. Naphthene and Aromatic Fuels", *Eviron. Sci. Tech.* 26:1581 (1992).
- [16] Kaiser, E. W., Siegl, W. O., Cotton, D. F., Henig, Y. I., and Anderson, R. W., "Effect of Fuel Structure on Emissions from a Spark-Ignited Engine. 3. Olefinic Fuels" *Eviron. Sci. Tech.* 27:1440 (1993).
- [17] Min, K., and Cheng, W. K., "Oxidation of the Piston Crevice Hydrocarbon during the Expansion Process in a Spark Ignition Engine", *Combust. Sci. Tech.* 106:307 (1995).
- [18] Norris, M. G., and Hochgreb, S., "Extent of Oxidation of Hydrocarbons Desorbing from the Lubricants Oil Layer in Spark-Ignition Engines", *SAE Paper* 960069 (1996).
- [19] Reitz, R. D., and Kuo, T. W., "Modeling of HC Emissions due to Crevice Flows in Premixed Charge Engines", *SAE Paper* 892085 (1989).
- [20] Das, S., and Dent, J. C., "Simulation of Exhaust Unburned Hydrocarbons from a Spark Ignition Engine, Originating from In-Cylinder Crevices", *SAE Paper* 961956 (1996).
- [21] Tonse, S. R., "Numerical Simulations of Emerging Piston Crevice Gases", *SAE Paper* 961968 (1996).
- [22] Hellstrom, T., and Chomiak, J., "Oxidation of Hydrocarbons Released from Piston Crevices of S.I. Engines", *SAE Paper* 952539 (1995).
- [23] Wu, K. C., Hochgreb, S. and Norris, M., "Chemical Kinetic Modeling of Exhaust Hydrocarbon Oxidation", *Combust. Flame.* 100:193 (1995).
- [24] Wu, K. C., "Chemical Kinetic Modeling of Oxidation of Hydrocarbon Emissions in Spark Ignition Engines", M. S. Thesis, Department of Mechanical Engineering, Massachusetts Institute of Technology (1994).
- [25] Lee, G. R., and Morley, C., "Chemical Modelling of Hydrocarbon Exhaust Emissions", *SAE Paper* 941958 (1994).
- [26] Kiehne, T. M., Rorald, D. M., and Wilson, D. E., "The Significance of Intermediate Hydrocarbons During Wall Quench of Propane Flames", *Twenty-first Symposium (International) on Combustion.* (1986).

- [27] Lucht, R. P., Dunn-Rankin, D., Walter, T., Dreier, T., and Bopp, S.C., "Heat Transfer in Engines: Comparison of CARS Thermal Boundary Layer Measurements and Heat Flux Measurements", *SAE Paper* 910722 (1991).
- [28] Lavoie, G., Lorusso, J. A., Adamczyk, A. A., "Hydrocarbon Emissions Modeling for SI Engines", ed. By Mattavi, J. N. and Amann, C. A., Plenum Press (1978).
- [29] Westbrook, C. K., and Dryer, F. L., "Chemical Kinetic Modeling of Hydrocarbon Combustion", *Prog. Energy Combust Sci.* 10:1 (1984).
- [30] The Numerical Algorithm Group Limited, NAG Fortran Library, D03PPF subroutine, Mark 16 (1995).
- [31] Poulos, S. G., "The Effect of Combustion Chamber Geometry on S.I. Engine Combustion Rates : A Modeling Study", M. S. Thesis, Department of Mechanical Engineering, Massachusetts Institute of Technology (1982).
- [32] Poulos, S. G. and Heywood, J. B., "The Effect of Chamber Geometry on Spark Ignition Engine Combustion", *SAE Paper* 830334 (1983).
- [33] Reynolds, W. C., " The Element Potential Method for Chemical Equilibrium Analysis : Implementation in the Interactive Program STANJAN Version 3" Department of Mechanical Engineering, Stanford University, (1986).
- [34] Kee, R. J., Rupley, F. M., and Miller, J. A., "CHEMKIN-II: A FORTRAN Chemical Kinetics Package for the Analysis of Gas-Phase Chemical Kinetics", *Sandia National Laboratories Report* SAND89-8009 (1989).
- [35] Kee, R. J., Rupley, F. M., and Miller, J. A., "The Chemical Thermodynamic Data Base", *Sandia National Laboratories Report* SAND87-8215 (1987).
- [36] Kee, R. J., Dixon-Lewis, D., Warnatz, J., Coltrin, M. E., and Miller, J. A., "A FORTRAN Computer Code Package for the Evaluation of Gas-Phase, Multicomponent Transport Properties" *Sandia National Laboratories Report* SAND86-8246 (1986).
- [37] Norris, M. G., Bauer, W., and Hochgreb, S., "Oxidation of Hydrocarbons from Lubricant Oil Layers in a Spark-Ignition Engines", *Twenty-sixth Symposium (International) on Combustion*. The Combustion Institute. (1996).
- [38] Foster, D. E., and Witze P. O., "Velocity Measurements in the Wall Boundary Layer of a Spark-Ignited Research Engine", *SAE Paper* 872105 (1987).
- [39] Green, R. M., and Cloutman, L. D., "Planar LIF Observations of Unburned Fuel Escaping the Upper Ring-Land Crevice in an SI Engine", *SAE Paper* 970823 (1997).

- [40] Launder, B. E., and Spalding, D. B., "Lectures in Mathematical Models of Turbulence", Academic Press, London. (1972).
- [41] Comte-Bellot, G. and Corrsin, S., "The Use of a Contraction to Improve the Isotropy of Grid-Generated Turbulence" *J. Fluid Mech.* 25:657 (1966).
- [42] Hall, M. J., Bracco, F. V., and Santavicca, D. A., "Cycle-Resolved Velocity and Turbulence Measurements in an I.C. Engine with Combustion", *SAE Paper* 860320 (1986).
- [43] Fraser, R. A. and Bracco, F. V., "Cycle-Resolved LDV Integral Length Scale Measurements in an I.C. Engine", *SAE Paper* 880381 (1988).
- [44] Haddad, O., and Denbratt, I., "Turbulence Characteristics of Tumbling Air Motion in Four Valve S.I. Engines and their Correlation with Combustion Parameters", *SAE Paper* 910478 (1991).
- [45] Heywood, J. B., "Internal Combustion Engine Fundamentals", McGraw-Hill, New York. (1988).
- [46] Dimopoulos, P. and Boulouchos, K., "Reynolds Stress Components in the Flow Field of a Motored Reciprocating Engine", *SAE Paper* 950725 (1995).
- [47] Gilaber, P. and Pinchon, P., "Measurements and Multidimensional Modeling of Gas-Wall Heat Transfer in an S.I. Engine", *SAE Paper* 880516 (1988).
- [48] Dagaut, P., Cathonnet, M., Boettner, J. C. and Gaillard, F., "Kinetic Modeling of Propane Oxidation", *Combust. Sci. Tech.* 56:23 (1987).
- [49] Axelsson, E. I., Brezinsky, K., Dryer, F. L., Pitz, W. J. and Westbrook, C. K., "Chemical Kinetic Modeling of the Oxidation of Large Alkane Fuels: N-Octane and Iso-octane", *Twenty-First Symposium (International) on Combustion*. The Combustion Institute. (1988).
- [50] Dagaut, P., Cathonnet, M., and Boettner, J. C., "Kinetics of Ethane Oxidation", *Int. J. Chem. Kinet.* 23:437 (1991).
- [51] Lucht, R. P., and Maris, M. A., "CARS Measurements of Temperature Profiles Near a Wall in an Internal Combustion Engine", *SAE Paper* 870459 (1987).
- [52] Haskell, W. W., and Legate, C. E., "Exhaust Hydrocarbon Emissions from Gasoline Engines-Surface Phenomena", *SAE Paper* 720255 (1972).
- [53] Alkidas, A. C., Drews, R. J., and Miller, W. F., "Effects of Piston Crevice Geometry on the Steady-State Engine-Out Hydrocarbons Emissions of a S.I. Engine", *SAE Paper* 952537 (1995).

- [54] Russ, S. G., Kaiser, E. K., Siegl, W. O., "Effect of Cylinder Head and Engine Block Temperature on HC Emissions from a Single Cylinder Spark Ignition Engine", *SAE Paper* 952536 (1995).
- [55] Drobot, K., "Hydrocarbon Oxidation in the Exhaust Port and Runner of a Spark Ignition Engine", M. S. Thesis, Department of Mechanical Engineering, Massachusetts Institute of Technology (1994).

Appendix 1 Coordinate Transform

New coordinates are given by the coordinate transformation,

$$\eta = \int_0^x \frac{\rho L}{(\rho L)_o} dx$$

$$\tau = t$$

where subscript o denotes initial state. Therefore,

$$\frac{\partial \eta}{\partial t} = \int_0^x \frac{1}{(\rho L)_o} \frac{\partial(\rho L)}{\partial t} dx \quad (\text{A.1})$$

$$\frac{\partial \eta}{\partial x} = \frac{\rho L}{(\rho L)_o} \quad (\text{A.2})$$

From the continuity equation,

$$\frac{\partial \rho}{\partial t} + \frac{\partial(u\rho)}{\partial x} + \frac{\partial(v\rho)}{\partial y} = \frac{\partial \rho}{\partial t} + \frac{\partial(u\rho)}{\partial x} + \frac{\rho}{L} \frac{\partial L}{\partial t} = 0 \quad (\text{A.3})$$

Therefore,

$$\frac{\partial(\rho L)}{\partial t} + \frac{\partial(u\rho L)}{\partial x} = 0$$

so that

$$\frac{1}{(\rho L)_o} \int_0^x \left(\frac{\partial(\rho L)}{\partial t} + \frac{\partial(u\rho L)}{\partial x} \right) dx = \frac{\partial \eta}{\partial t} + u \frac{(\rho L)}{(\rho L)_o} = 0 \quad (\text{A.4})$$

Hence,

$$\frac{D}{Dt} = \frac{\partial}{\partial t} + u \frac{\partial}{\partial x} = \frac{\partial}{\partial \tau} + \left(-u \frac{(\rho L)}{(\rho L)_o} \right) \frac{\partial}{\partial \eta} + \left(u \frac{(\rho L)}{(\rho L)_o} \right) \frac{\partial}{\partial \eta} = \frac{\partial}{\partial \tau} \quad (\text{A.5})$$

Therefore, the governing equations in the new co-ordinate system are

$$\frac{\partial(\rho L)}{\partial t} + \frac{\partial(u\rho L)}{\partial x} = \frac{\partial(\rho L)}{\partial \tau} + \frac{(\rho L)^2}{(\rho L)_o} \frac{\partial u}{\partial \eta} = 0 \quad (\text{A.6})$$

$$\rho \left(\frac{\partial Y_i}{\partial t} + u \frac{\partial Y_i}{\partial x} \right) - \frac{\partial}{\partial x} (\rho D_i \frac{\partial Y_i}{\partial x}) - \dot{\omega}_i = \rho \frac{\partial Y_i}{\partial \tau} - \frac{\rho L}{(\rho L)_o} \frac{\partial}{\partial \eta} (\rho D_i \frac{\rho L}{(\rho L)_o} \frac{\partial Y_i}{\partial \eta}) - \dot{\omega}_i = 0 \quad (\text{A.7})$$

$$\rho C_p \left(\frac{\partial T}{\partial t} + \frac{\partial(uT)}{\partial x} \right) + \left(\sum \dot{\omega}_i h_i - \frac{\partial p}{\partial t} - \frac{\partial}{\partial x} (\kappa \frac{\partial T}{\partial x}) \right) =$$

$$\rho C_p \frac{\partial T}{\partial \tau} + \sum \dot{\omega}_i h_i - \frac{\partial p}{\partial \tau} - \frac{(\rho L)}{(\rho L)_o} \frac{\partial}{\partial \eta} (\kappa \frac{(\rho L)}{(\rho L)_o} \frac{\partial T}{\partial \eta}) = 0 \quad (\text{A.8})$$

The old co-ordinate can be restored from equation (A.2).

$$x = \int_0^{\eta} \frac{(\rho L)_o}{(\rho L)} d\eta \quad (\text{A.9})$$

Appendix 2 Chemical Kinetic Reaction Mechanisms

Appendix 2.1 Propane chemical kinetic reaction mechanism

REACTIONS CONSIDERED	(k = A T**b exp(-E/RT))			Source/Modification
	A	b	E	
1 H+H+M=H2+M	7.31E+17	-1	0	# All reactions : Ref(49)
2 O+O+M=O2+M	1.14E+17	-1	0	
3 O+H+M=OH+M	6.20E+16	-0.6	0	
4 H2+O2=OH+OH	1.70E+13	0	47780	
5 O+H2=OH+H	1.50E+07	2	7550	
6 H+O2=OH+O	1.20E+17	-0.9	16520	
7 H+O2+M=HO2+M	8.00E+17	-0.8	0	
8 H+O2+O2=HO2+O2	6.70E+19	-1.4	0	
9 H+OH+M=H2O+M	8.62E+21	-2	0	
10 H2+OH=H2O+H	1.00E+08	1.6	3300	
11 H2O+O=OH+OH	1.50E+10	1.1	17260	
12 HO2+OH=H2O+O2	5.00E+13	0	1000	
13 HO2+O=OH+O2	2.00E+13	0	0	
14 H+HO2=H2+O2	2.50E+13	0	690	
15 H+HO2=OH+OH	1.50E+14	0	1000	
16 HO2+HO2=H2O2+O2	2.80E+12	0	0	
17 H2O2+M=OH+OH+M	1.30E+17	0	45410	
18 H2O2+OH=HO2+H2O	7.00E+12	0	1430	
19 H2O2+H=H2O+OH	1.00E+13	0	3590	
20 H2O2+H=HO2+H2	1.70E+12	0	3750	
21 H2O2+O=HO2+OH	2.80E+13	0	6400	
22 CO+HO2=CO2+OH	4.57E+14	0	25240	
23 CO+OH=CO2+H	4.40E+06	1.5	-740	
24 CO+O+M=CO2+M	2.83E+13	0	-4540	
25 CO+O2=CO2+O	2.53E+12	0	47700	
26 HCO+M=H+CO+M	2.86E+14	0	16800	
27 HCO+OH=CO+H2O	5.00E+13	0	0	
28 HCO+O=CO+OH	3.00E+13	0	0	
29 HCO+O=CO2+H	3.00E+13	0	0	
30 HCO+H=CO+H2	7.22E+13	0	0	
31 HCO+O2=CO+HO2	3.31E+13	-0.3	0	
32 HCO+CH3=CO+CH4	3.00E+11	0.5	0	
33 CH4=CH3+H	1.00E+15	0	100380	
34 CH4+HO2=CH3+H2O2	4.00E+12	0	19360	
35 CH4+OH=CH3+H2O	1.09E+05	2.4	2110	
36 CH4+O=CH3+OH	1.40E+07	2.1	7620	
37 CH4+H=CH3+H2	2.60E+04	3	8750	
38 CH4+CH2=CH3+CH3	6.00E+14	0	14000	

39	CH ₃ +M=CH ₂ +H+M	1.90E+16	0	91600
40	CH ₃ +HO ₂ =CH ₃ O+OH	3.00E+13	0	1080
41	CH ₃ +HO ₂ =CH ₄ +O ₂	1.00E+12	0	400
42	CH ₃ +OH=CH ₂ O+H ₂	4.00E+12	0	0
43	CH ₃ +OH=CH ₃ O+H	9.00E+14	0	15400
44	CH ₃ +OH=CH ₂ +H ₂ O	3.00E+13	0	3000
45	CH ₃ +O=CH ₂ O+H	6.00E+13	0	0
46	CH ₃ +O=CH ₂ +OH	5.00E+13	0	12000
47	CH ₃ +H=CH ₂ +H ₂	7.00E+13	0	15100
48	CH ₃ +O ₂ =CH ₃ O+O	2.24E+14	0	33700
49	CH ₃ +CH ₃ =C ₂ H ₅ +H	8.00E+14	0	26530
50	CH ₃ +CH ₃ =C ₂ H ₄ +H ₂	2.10E+14	0	19200
51	C ₂ H ₆ =CH ₃ +CH ₃	1.40E+16	0	87480
52	CH ₂ +OH=CH+H ₂ O	4.00E+13	0	0
53	CH ₂ +OH=CH ₂ O+H	2.00E+13	0	0
54	CH ₂ +O=CO+H+H	3.00E+13	0	0
55	CH ₂ +O=CO+H ₂	5.00E+13	0	0
56	CH ₂ +O=CH+OH	5.00E+13	0.7	12000
57	CH ₂ +O=HCO+H	5.00E+13	0	0
58	CH ₂ +H=CH+H ₂	4.00E+13	0	0
59	CH ₂ +O ₂ =HCO+OH	4.30E+10	0	-500
60	CH ₂ +O ₂ =CO ₂ +H ₂	6.90E+11	0	500
61	CH ₂ +O ₂ =CO ₂ +H+H	1.60E+12	0	1000
62	CH ₂ +O ₂ =CO+H ₂ O	1.87E+10	0	-1000
63	CH ₂ +O ₂ =CO+OH+H	8.64E+10	0	-500
64	CH ₂ +O ₂ =CH ₂ O+O	5.00E+13	0	9000
65	CH ₂ +CO ₂ =CH ₂ O+CO	1.10E+11	0	1000
66	CH ₂ +CH ₂ =C ₂ H ₂ +H ₂	3.20E+13	0	0
67	CH ₂ +CH ₃ =C ₂ H ₄ +H	4.00E+13	0	0
68	CH ₂ +CH=C ₂ H ₂ +H	4.00E+13	0	0
69	CH+OH=HCO+H	3.00E+13	0	0
70	CH+O=CO+H	4.00E+13	0	0
71	CH+O ₂ =HCO+O	3.30E+13	0	0
72	CH+O ₂ =CO+OH	2.00E+13	0	0
73	CH+CO ₂ =HCO+CO	3.40E+12	0	690
74	CH+CH ₄ =C ₂ H ₄ +H	6.00E+13	0	0
75	CH+CH ₃ =C ₂ H ₃ +H	3.00E+13	0	0
76	CH ₃ O+M=CH ₂ O+H+M	1.80E+14	0	25100
77	CH ₃ O+OH=CH ₂ O+H ₂ O	1.00E+13	0	0
78	CH ₃ O+O=CH ₂ O+OH	1.00E+13	0	0
79	CH ₃ O+H=CH ₂ O+H ₂	2.00E+13	0	0
80	CH ₃ O+O ₂ =CH ₂ O+HO ₂	1.50E+13	0	7170
81	CH ₃ O+CH ₂ O=CH ₃ OH+HCO	1.15E+11	0	1280
82	CH ₃ O+CH ₄ =CH ₃ OH+CH ₃	2.00E+11	0	7000
83	CH ₂ O+M=HCO+H+M	5.72E+16	0	76480
84	CH ₂ O+HO ₂ =HCO+H ₂ O ₂	1.00E+12	0	9600
85	CH ₂ O+OH=HCO+H ₂ O	7.00E+13	0	1250
86	CH ₂ O+O=HCO+OH	3.50E+13	0	3510
87	CH ₂ O+H=HCO+H ₂	2.50E+13	0	3990
88	CH ₂ O+O ₂ =HCO+HO ₂	2.04E+13	0	39000

89	$\text{CH}_2\text{O}+\text{CH}_3=\text{HCO}+\text{CH}_4$	1.00E+11	0	6100
90	$\text{C}_2\text{H}_6+\text{HO}_2=\text{C}_2\text{H}_5+\text{H}_2\text{O}_2$	1.69E+13	0	20460
91	$\text{C}_2\text{H}_6+\text{OH}=\text{C}_2\text{H}_5+\text{H}_2\text{O}$	5.13E+05	2.1	860
92	$\text{C}_2\text{H}_6+\text{O}=\text{C}_2\text{H}_5+\text{OH}$	4.40E+07	2	5120
93	$\text{C}_2\text{H}_6+\text{H}=\text{C}_2\text{H}_5+\text{H}_2$	5.40E+02	3.5	5210
94	$\text{C}_2\text{H}_6+\text{O}_2=\text{C}_2\text{H}_5+\text{HO}_2$	1.00E+13	0	51000
95	$\text{C}_2\text{H}_6+\text{CH}_3\text{O}=\text{C}_2\text{H}_5+\text{CH}_3\text{OH}$	3.02E+11	0	7000
96	$\text{C}_2\text{H}_6+\text{CH}_3=\text{C}_2\text{H}_5+\text{CH}_4$	5.50E-01	4	8290
97	$\text{C}_2\text{H}_5+\text{O}=\text{CH}_3\text{CHO}+\text{H}$	5.00E+13	0	0
98	$\text{C}_2\text{H}_5+\text{H}=\text{C}_2\text{H}_4+\text{H}_2$	1.25E+14	0	8000
99	$\text{C}_2\text{H}_5+\text{O}_2=\text{C}_2\text{H}_4+\text{HO}_2$	1.58E+10	0	-1900
100	$\text{C}_2\text{H}_5+\text{C}_2\text{H}_5=\text{C}_2\text{H}_4+\text{C}_2\text{H}_6$	1.40E+12	0	0
101	$\text{C}_2\text{H}_4+\text{M}=\text{C}_2\text{H}_2+\text{H}_2+\text{M}$	3.00E+17	0	79350
102	$\text{C}_2\text{H}_4+\text{M}=\text{C}_2\text{H}_3+\text{H}+\text{M}$	2.97E+17	0	96560
103	$\text{C}_2\text{H}_4+\text{HO}_2=\text{C}_2\text{H}_4\text{O}+\text{OH}$	1.00E+13	0	18280
104	$\text{C}_2\text{H}_4+\text{OH}=\text{C}_2\text{H}_3+\text{H}_2\text{O}$	4.90E+12	0	1230
105	$\text{C}_2\text{H}_4+\text{OH}=\text{CH}_2\text{O}+\text{CH}_3$	1.50E+12	0	960
106	$\text{C}_2\text{H}_4+\text{O}=\text{CH}_2\text{O}+\text{CH}_2$	4.00E+13	0	5000
107	$\text{C}_2\text{H}_4+\text{O}=\text{CH}_3+\text{HCO}$	2.20E+09	1.2	740
108	$\text{C}_2\text{H}_4+\text{H}=\text{C}_2\text{H}_3+\text{H}_2$	4.00E+06	2	6000
109	$\text{C}_2\text{H}_5+\text{M}=\text{C}_2\text{H}_4+\text{H}+\text{M}$	2.00E+15	0	30120
110	$\text{C}_2\text{H}_4+\text{O}_2=\text{C}_2\text{H}_3+\text{HO}_2$	4.00E+13	0	61500
111	$\text{C}_2\text{H}_4+\text{C}_2\text{H}_4=\text{C}_2\text{H}_5+\text{C}_2\text{H}_3$	5.00E+14	0	64700
112	$\text{C}_2\text{H}_4+\text{CH}_3=\text{C}_2\text{H}_3+\text{CH}_4$	5.60E+11	0	11110
113	$\text{C}_2\text{H}_4\text{O}=\text{CH}_4+\text{CO}$	2.00E+14	0	58000
114	$\text{C}_2\text{H}_3=\text{C}_2\text{H}_2+\text{H}$	2.20E+14	0	38000
115	$\text{C}_2\text{H}_3+\text{OH}=\text{C}_2\text{H}_2+\text{H}_2\text{O}$	5.00E+12	0	0
116	$\text{C}_2\text{H}_3+\text{O}=\text{CH}_2\text{CO}+\text{H}$	3.30E+13	0	0
117	$\text{C}_2\text{H}_3+\text{H}=\text{C}_2\text{H}_2+\text{H}_2$	2.50E+13	0	0
118	$\text{C}_2\text{H}_3+\text{O}_2=\text{CH}_2\text{O}+\text{HCO}$	3.20E+12	0	-350
119	$\text{C}_2\text{H}_3+\text{C}_2\text{H}_6=\text{C}_2\text{H}_4+\text{C}_2\text{H}_5$	1.50E+13	0	10000
120	$\text{C}_2\text{H}_2+\text{M}=\text{C}_2\text{H}+\text{H}+\text{M}$	4.57E+16	0	106840
121	$\text{C}_2\text{H}_2+\text{OH}=\text{C}_2\text{H}+\text{H}_2\text{O}$	1.00E+13	0	7000
122	$\text{C}_2\text{H}_2+\text{OH}=\text{CH}_2\text{CO}+\text{H}$	3.20E+10	0	200
123	$\text{C}_2\text{H}_2+\text{H}=\text{C}_2\text{H}+\text{H}_2$	6.00E+13	0	23660
124	$\text{C}_2\text{H}_2+\text{O}=\text{CH}_2+\text{CO}$	4.10E+08	1.5	1700
125	$\text{C}_2\text{H}_2+\text{O}=\text{C}_2\text{H}+\text{OH}$	3.20E+15	-0.6	15000
126	$\text{C}_2\text{H}_2+\text{O}=\text{HCCO}+\text{H}$	4.30E+14	0	12120
127	$\text{C}_2\text{H}_2+\text{O}_2=\text{HCCO}+\text{OH}$	2.00E+08	1.5	30100
128	$\text{C}_2\text{H}_2+\text{O}_2=\text{HCO}+\text{HCO}$	4.00E+12	0	28000
129	$\text{C}_2\text{H}+\text{OH}=\text{HCCO}+\text{H}$	2.00E+13	0	0
130	$\text{C}_2\text{H}+\text{O}=\text{CO}+\text{CH}$	1.00E+13	0	0
131	$\text{C}_2\text{H}+\text{O}_2=\text{HCCO}+\text{O}$	5.00E+13	0	1500
132	$\text{C}_2\text{H}+\text{O}_2=\text{HCO}+\text{CO}$	5.00E+13	0	1510
133	$\text{CH}_2\text{CO}+\text{M}=\text{CH}_2+\text{CO}+\text{M}$	4.11E+15	0	59270
134	$\text{CH}_2\text{CO}+\text{OH}=\text{CH}_2\text{O}+\text{HCO}$	1.00E+13	0	0
135	$\text{CH}_2\text{CO}+\text{O}=\text{HCO}+\text{HCO}$	2.00E+13	0	2300
136	$\text{CH}_2\text{CO}+\text{O}=\text{CH}_2\text{O}+\text{CO}$	2.00E+13	0	0
137	$\text{CH}_2\text{CO}+\text{H}=\text{CH}_3+\text{CO}$	7.00E+12	0	3010
138	$\text{HCCO}+\text{OH}=\text{HCO}+\text{CO}+\text{H}$	1.00E+13	0	0

139	HCCO+O=CO+CO+H	1.93E+14	0	590
140	HCCO+H=CH2+CO	3.00E+13	0	0
141	HCCO+O2=CO+CO+OH	1.46E+12	0	2500
142	HCCO+CH2=C2H+CH2O	1.00E+13	0	2000
143	HCCO+CH2=C2H3+CO	3.00E+13	0	0
144	CH3OH=CH3+OH	6.00E+16	0	91060
145	CH3OH+HO2=CH2OH+H2O2	6.30E+12	0	19360
146	CH3OH+OH=CH2OH+H2O	1.00E+13	0	1700
147	CH3OH+O=CH2OH+OH	1.00E+13	0	4690
148	CH3OH+H=CH2OH+H2	4.00E+13	0	6100
149	CH3OH+CH2O=CH3O+CH3O	1.55E+12	0	79570
150	CH3OH+CH3=CH2OH+CH4	1.82E+11	0	9800
151	CH2OH+M=CH2O+H+M	1.00E+14	0	25100
152	CH2OH+H=CH2O+H2	3.00E+13	0	0
153	CH2OH+O2=CH2O+HO2	1.00E+13	0	7170
154	CH3CHO=CH3+HCO	2.00E+15	0	79110
155	CH3CHO+HO2=CH3+CO+H2O2	1.70E+12	0	10700
156	CH3CHO+OH=CH3+CO+H2O	1.00E+13	0	0
157	CH3CHO+O=CH3+CO+OH	5.00E+12	0	1790
158	CH3CHO+H=CH3+CO+H2	4.00E+13	0	4210
159	CH3CHO+O2=CH3+CO+HO2	2.00E+13	0.5	42200
160	CH3CHO+CH3=CH3+CO+CH4	8.50E+11	0	6000
161	C3H8=C2H5+CH3	7.94E+16	0	85100
162	C3H8+HO2=NC3H7+H2O2	4.50E+11	0	14900
163	C3H8+HO2=IC3H7+H2O2	2.00E+11	0	12500
164	C3H8+OH=NC3H7+H2O	4.71E+05	2.4	390
165	C3H8+OH=IC3H7+H2O	3.58E+02	3.2	-1600
166	C3H8+O=NC3H7+OH	3.72E+06	2.4	1390
167	C3H8+O=IC3H7+OH	5.50E+05	2.5	790
168	C3H8+H=NC3H7+H2	1.35E+14	0	9680
169	C3H8+H=IC3H7+H2	2.00E+14	0	8300
170	C3H8+O2=NC3H7+HO2	4.00E+13	0	47500
171	C3H8+O2=IC3H7+HO2	4.00E+13	0	47500
172	C3H8+IC3H7=NC3H7+C3H8	1.00E+11	0	12900
173	C3H8+AC3H5=NC3H7+C3H6	7.94E+11	0	20500
174	C3H8+AC3H5=IC3H7+C3H6	7.94E+11	0	16200
175	C3H8+C2H5=NC3H7+C2H6	3.16E+11	0	12300
176	C3H8+C2H5=IC3H7+C2H6	5.01E+10	0	10400
177	C3H8+C2H3=NC3H7+C2H4	1.00E+11	0	10400
178	C3H8+C2H3=IC3H7+C2H4	1.00E+11	0	10400
179	C3H8+CH3O=NC3H7+CH3OH	3.18E+11	0	7050
180	C3H8+CH3O=IC3H7+CH3OH	7.20E+10	0	4470
181	C3H8+CH3=NC3H7+CH4	3.00E+12	0	11710
182	C3H8+CH3=IC3H7+CH4	8.07E+11	0	10110
183	NC3H7=C2H4+CH3	3.00E+14	0	33220
184	NC3H7=C3H6+H	1.00E+14	0	37280
185	NC3H7+O2=C3H6+HO2	1.00E+12	0	5000
186	IC3H7=C2H4+CH3	1.00E+14	0	45000
187	C3H6+H=IC3H7	3.00E+12	0	960
188	IC3H7+O2=C3H6+HO2	3.00E+12	0	3000

189	C3H6=AC3H5+H	1.00E+15	0	88040
190	C3H6=SC3H5+H	3.33E+14	0	88040
191	C3H6=C2H3+CH3	7.00E+15	0	85800
192	C3H6+HO2=C3H6O+OH	1.05E+12	0	14190
193	C3H6+HO2=AC3H5+H2O2	1.50E+11	0	14190
194	C3H6+HO2=SC3H5+H2O2	7.50E+09	0	12570
195	C3H6+HO2=TC3H5+H2O2	3.00E+09	0	9930
196	C3H6+OH=AC3H5+H2O	1.15E+13	0	600
197	C3H6+OH=SC3H5+H2O	9.00E+13	0	6450
198	C3H6+OH=C2H5+CH2O	1.00E+13	0	0
199	C3H6+OH+O2=CH3CHO+CH2O+OH	3.00E+10	0	-8230
200	C3H6+O=C2H5+HCO	6.83E+04	2.6	-1130
201	C3H6+O=C2H4+CH2O	6.83E+04	2.6	-1130
202	C3H6+O=CH3+CH3+CO	6.83E+04	2.6	-1130
203	C3H6+H=AC3H5+H2	2.50E+12	0	1100
204	C3H6+O2=SC3H5+HO2	4.00E+13	0	47560
205	C3H6+O2=TC3H5+HO2	4.00E+13	0	44000
206	C3H6+O2=AC3H5+HO2	4.00E+13	0	50900
207	C3H6+C2H5=AC3H5+C2H6	1.00E+11	0	9800
208	C3H6+CH3=AC3H5+CH4	1.40E+11	0	8800
209	C3H6+CH3=SC3H5+CH4	6.60E+11	0	10110
210	C3H6+CH3=TC3H5+CH4	2.40E+11	0	8030
211	C3H6O=C2H6+CO	1.26E+14	0	58000
212	SC3H5=C2H2+CH3	3.00E+10	0	36200
213	SC3H5+O2=CH3CHO+HCO	3.00E+12	0	-250
214	SC3H5+O2=CH3+CO+CH2O	2.00E+12	0	-250
215	AC3H5=AC3H4+H	8.91E+12	0	59000
216	AC3H5+H=AC3H4+H2	3.33E+12	0	0
217	AC3H5+CH3=AC3H4+CH4	5.00E+11	0	0
218	AC3H5+O2+O2=CO+OH+CH2O+CH2O	1.50E+13	0	-250
219	TC3H5+O2=CH3+CO+CH2O	3.20E+12	0	-250
220	AC3H4+HO2=C2H4+CO+OH	1.00E+12	0	14000
221	AC3H4+HO2=C3H3+H2O2	3.00E+13	0	14000
222	AC3H4+OH=CH2CO+CH3	2.00E+12	0	860
223	AC3H4+OH=C2H4+HCO	1.00E+12	0	900
224	AC3H4+O=CO+C2H4	7.80E+12	0	1600
225	AC3H4+H=TC3H5	8.50E+12	0	2000
226	AC3H4+H=SC3H5	4.00E+12	0	2700
227	PC3H4=AC3H4	7.76E+11	0	55700
228	PC3H4+OH=C3H3+H2O	1.85E+12	0	1650
229	PC3H4+OH=CH2CO+CH3	4.50E+11	0	0
230	PC3H4+O=C2H2+H2+CO	1.60E+13	0	2010
231	PC3H4+H=TC3H5	6.63E+12	0	2000
232	PC3H4+H=SC3H5	5.78E+12	0	3100
233	C2H2+CH2=C3H3+H	1.80E+12	0	0
234	C2H2+CH=C3H3	3.00E+13	0	0
235	C3H3+H=PC3H4	2.00E+13	0	0
236	C3H3+O=C2H3+CO	3.80E+13	0	0
237	C3H3+O2=CH2CO+HCO	3.01E+10	0	2870
238	C2H3+C2H4=C4H6+H	1.00E+12	0	7300

239	C2H2+C2H2=C4H3+H	2.00E+12	0	45900
240	C2H2+C2H=C4H2+H	3.50E+13	0	0
241	C4H3+M=C4H2+H+M	1.00E+16	0	59700
242	C4H2+M=C4H+H+M	3.50E+17	0	80000
243	C4H7=C4H6+H	1.20E+14	0	49300
244	C4H7=C2H4+C2H3	1.00E+12	0	28000
245	C4H7+H=C4H6+H2	3.16E+13	0	0
246	C4H7+O2=C4H6+HO2	1.00E+11	0	0
247	C4H7+C2H3=C4H6+C2H4	4.00E+12	0	0
248	C4H7+C2H5=C4H6+C2H6	4.00E+12	0	0
249	C4H7+C2H5=PC4H8+C2H4	5.00E+11	0	0
250	C4H7+C2H5=TRAC4H8+C2H4	5.00E+11	0	0
251	C4H6=C2H3+C2H3	3.98E+19	-1	98150
252	C4H6+OH=C2H5+CH2CO	1.00E+12	0	0
253	C4H6+OH=SC3H5+CH2O	1.00E+12	0	0
254	C4H6+OH=CH3CHO+C2H3	1.00E+12	0	0
255	C4H6+O=C2H4+CH2CO	1.00E+12	0	0
256	C4H6+O=PC3H4+CH2O	1.00E+12	0	0
257	PC4H8=C4H7+H	4.08E+18	-1	97350
258	TRAC4H8=C4H7+H	4.07E+18	-1	97350
259	PC4H8+H=C4H7+H2	1.00E+14	0	3900
260	TRAC4H8+H=C4H7+H2	2.00E+14	0	3500
261	PC4H8+OH=C4H7+H2O	1.41E+13	0	3060
262	TRAC4H8+OH=C4H7+H2O	2.29E+13	0	3060
263	PC4H8+CH3=C4H7+CH4	1.00E+11	0	7300
264	TRAC4H8+CH3=C4H7+CH4	1.00E+11	0	8200
265	PC4H8+O=C3H6+CH2O	5.01E+12	0	0
266	TRAC4H8+O=IC3H7+HCO	6.03E+12	0	0
267	TRAC4H8+O=CH3CHO+C2H4	1.00E+12	0	0
268	PC4H8+OH=NC3H7+CH2O	1.51E+12	0	0
269	TRAC4H8+OH=CH3CHO+C2H5	3.02E+12	0	0
270	PC4H8=AC3H5+CH3	1.00E+16	0	73400
271	PC4H8=C2H3+C2H5	1.00E+19	-1	96770
272	PC4H8+O=CH3CHO+C2H4	1.50E+13	0	850
273	PC4H8+O=C2H5+CH3+CO	1.29E+13	0	850
274	PC4H8+OH=CH3CHO+C2H5	1.00E+11	0	0
275	PC4H8+OH=C2H6+CH3+CO	1.00E+10	0	0
276	C2H5+CH3=C2H4+CH4	4.37E-04	5	8300
277	C2H3+CH3=C2H2+CH4	4.37E-04	5	8300

NOTE : A units mole-cm-sec-K, E units cal/mole

= : reversible reaction

=> : irreversible reaction

PC4H8: 1-butene

TRAC4H8: trans-2-butene

IC3H7: iso-propyl radical

NC3H7: n-propyl radical

SC3H5: 2-methylvinyl radical

AC3H5: allyl radical

TC3H5: 1-methylvinyl radical

PC3H4: propyne

AC3H4: allene

Appendix 2.2 Isooctane chemical kinetic reaction mechanism

REACTIONS CONSIDERED	(k = A T**b exp(-E/RT))			Source/Modification
	A	b	E	
1 H+O2=O+OH	5.13E+16	-0.8	16510	# All reactions : Ref(49)
2 H2+O=H+OH	1.82E+10	1	8900	#(Reactions 351 - 455
3 H2O+O=OH+OH	6.76E+13	0	18350	# are reverse reactions
4 H2O+H=H2+OH	9.55E+13	0	20300	# for reactions 244 - 350)
5 H2O2+OH=H2O+HO2	1.00E+13	0	1800	
6 H2O+M=H+OH+M	2.19E+16	0	105000	
H2O Enhanced by	2.000E+01			
7 H+O2+M=HO2+M	1.66E+15	0	-1000	
H2O Enhanced by	2.100E+01			
CO2 Enhanced by	5.000E+00			
CO Enhanced by	2.000E+00			
H2 Enhanced by	3.300E+00			
8 HO2+O=OH+O2	5.01E+13	0	1000	
9 HO2+H=OH+OH	2.51E+14	0	1900	
10 HO2+H=H2+O2	2.51E+13	0	700	
11 HO2+OH=H2O+O2	5.01E+13	0	1000	
12 H2O2+O2=HO2+HO2	3.98E+13	0	42640	
13 H2O2+M=OH+OH+M	1.20E+17	0	45500	
H2O Enhanced by	6.000E+00			
O2 Enhanced by	7.800E-01			
H2O2 Enhanced by	6.600E+00			
14 H2O2+H=HO2+H2	1.70E+12	0	3750	
15 O+H+M=OH+M	1.00E+16	0	0	
16 O2+M=O+O+M	5.13E+15	0	115000	
17 H2+M=H+H+M	2.19E+14	0	96000	
H2O Enhanced by	6.000E+00			
H Enhanced by	2.000E+00			
H2 Enhanced by	3.000E+00			
18 CO+OH=CO2+H	1.51E+07	1.3	-770	
19 CO+HO2=CO2+OH	1.51E+14	0	23650	
20 CO+O+M=CO2+M	5.89E+15	0	4100	
21 CO2+O=CO+O2	2.75E+12	0	43830	
22 HCO+OH=CO+H2O	1.00E+14	0	0	
23 HCO+M=H+CO+M	1.45E+14	0	19000	
24 HCO+H=CO+H2	2.00E+14	0	0	
25 HCO+O=CO+OH	1.00E+14	0	0	
26 HCO+HO2=CH2O+O2	1.00E+14	0	3000	
27 HCO+O2=CO+HO2	3.98E+12	0	0	
28 CH2O+M=HCO+H+M	3.31E+16	0	81000	
29 CH2O+OH=HCO+H2O	7.59E+12	0	170	
30 CH2O+H=HCO+H2	3.31E+14	0	10500	
31 CH2O+O=HCO+OH	5.01E+13	0	4600	
32 CH2O+HO2=HCO+H2O2	2.00E+11	0	8000	

33	CH4+M=CH3+H+M	1.41E+17	0	88400
34	CH4+H=CH3+H2	1.26E+14	0	11900
35	CH4+OH=CH3+H2O	3.47E+03	3.1	2000
36	CH4+O=CH3+OH	2.14E+06	2.2	6480
37	CH4+HO2=CH3+H2O2	2.00E+13	0	18000
38	CH3+HO2=CH3O+OH	3.24E+13	0	0
39	CH3+OH=CH2O+H2	3.98E+12	0	0
40	CH3+O=CH2O+H	1.29E+14	0	2000
41	CH3+O2=CH3O+O	4.79E+13	0	29000
42	CH2O+CH3=CH4+HCO	1.00E+10	0.5	6000
43	CH3+HCO=CH4+CO	3.02E+11	0.5	0
44	CH3+HO2=CH4+O2	1.00E+12	0	400
45	CH3O+M=CH2O+H+M	5.01E+13	0	21000
46	CH3O+O2=CH2O+HO2	7.59E+10	0	2700
47	C2H6=CH3+CH3	2.24E+19	-1	88310
48	C2H6+CH3=C2H5+CH4	5.50E-01	4	8280
49	C2H6+H=C2H5+H2	5.37E+02	3.5	5200
50	C2H6+OH=C2H5+H2O	8.71E+09	1.1	1810
51	C2H6+O=C2H5+OH	1.12E+14	0	7850
52	C2H5+M=C2H4+H+M	2.00E+15	0	30000
53	C2H5+O2=C2H4+HO2	1.00E+12	0	5000
54	C2H4+C2H4=C2H5+C2H3	5.01E+14	0	64700
55	C2H4+M=C2H2+H2	9.33E+16	0	77200
56	C2H4+M=C2H3+H+M	6.31E+18	0	108720
57	C2H4+O=CH3+HCO	3.31E+12	0	1130
58	C2H4+O=CH2O+CH2	2.51E+13	0	5000
59	C2H4+H=C2H3+H2	1.51E+07	2	6000
60	C2H4+OH=C2H3+H2O	4.79E+12	0	1230
61	C2H4+OH=CH3+CH2O	2.00E+12	0	960
62	C2H3+M=C2H2+H+M	7.94E+14	0	31500
63	C2H3+O2=C2H2+HO2	1.00E+12	0	10000
64	C2H2+M=C2H+H+M	1.00E+14	0	114000
65	C2H2+O2=HCO+HCO	3.98E+12	0	28000
66	C2H2+H=C2H+H2	2.00E+14	0	19000
67	C2H2+OH=C2H+H2O	6.03E+12	0	7000
68	C2H2+OH=CH2CO+H	3.24E+11	0	200
69	C2H2+O=C2H+OH	3.24E+15	-0.6	17000
70	C2H2+O=CH2+CO	6.76E+13	0	4000
71	C2H+O2=HCO+CO	1.00E+13	0	7000
72	C2H+O=CO+CH	5.01E+13	0	0
73	CH2+O2=HCO+OH	1.00E+14	0	3700
74	CH2+O=CH+OH	1.91E+11	0.7	25000
75	CH2+H=CH+H2	2.69E+11	0.7	25700
76	CH2+OH=CH+H2O	2.69E+11	0.7	25700
77	CH+O2=CO+OH	1.35E+11	0.7	25700
78	CH+O2=HCO+O	1.00E+13	0	0
79	CH3OH+M=CH3+OH+M	3.02E+18	0	80000
80	CH3OH+OH=CH2OH+H2O	3.98E+12	0	1370
81	CH3OH+O=CH2OH+OH	1.70E+12	0	2290
82	CH3OH+H=CH2OH+H2	3.02E+13	0	7000

83	CH3OH+H=CH3+H2O	5.25E+12	0	5340
84	CH3OH+CH3=CH2OH+CH4	1.82E+11	0	9800
85	CH3OH+HO2=CH2OH+H2O2	6.31E+12	0	19360
86	CH2OH+M=CH2O+H+M	2.51E+13	0	29000
87	CH2OH+O2=CH2O+HO2	8.31E+11	0	0
88	C2H2+C2H2=C4H3+H	1.00E+13	0	45000
89	C4H3+M=C4H2+H+M	1.00E+16	0	60000
90	C2H2+C2H=C4H2+H	3.98E+13	0	0
91	C4H2+M=C4H+H+M	3.47E+17	0	80000
92	C2H3+H=C2H2+H2	2.00E+13	0	2500
93	C3H8=CH3+C2H5	1.70E+16	0	84840
94	CH3+C3H8=CH4+IC3H7	1.10E+15	0	25140
95	CH3+C3H8=CH4+NC3H7	1.10E+15	0	25140
96	H+C3H8=H2+IC3H7	8.71E+06	2	5000
97	H+C3H8=H2+NC3H7	5.62E+07	2	7700
98	IC3H7=H+C3H6	6.31E+13	0	36900
99	IC3H7=CH3+C2H4	2.00E+10	0	29500
100	NC3H7=CH3+C2H4	9.55E+13	0	31000
101	NC3H7=H+C3H6	1.26E+14	0	37000
102	IC3H7+C3H8=NC3H7+C3H8	3.02E+10	0	12900
103	C2H3+C3H8=C2H4+IC3H7	1.00E+11	0	10400
104	C2H3+C3H8=C2H4+NC3H7	1.00E+11	0	10400
105	C2H5+C3H8=C2H6+IC3H7	1.00E+11	0	10400
106	C2H5+C3H8=C2H6+NC3H7	1.00E+11	0	10400
107	C3H8+O=IC3H7+OH	2.81E+13	0	5200
108	C3H8+O=NC3H7+OH	1.12E+14	0	7850
109	C3H8+OH=IC3H7+H2O	4.79E+08	1.4	850
110	C3H8+OH=NC3H7+H2O	5.75E+08	1.4	850
111	C3H8+HO2=IC3H7+H2O2	3.39E+12	0	17000
112	C3H8+HO2=NC3H7+H2O2	1.12E+13	0	19400
113	C3H6+O=C2H4+CH2O	6.76E+04	2.6	-1130
114	IC3H7+O2=C3H6+HO2	1.00E+12	0	5000
115	NC3H7+O2=C3H6+HO2	1.00E+12	0	5000
116	C3H8+O2=IC3H7+HO2	3.98E+13	0	47500
117	C3H8+O2=NC3H7+HO2	3.98E+13	0	47500
118	C3H6+OH=C2H5+CH2O	1.00E+12	0	0
119	C3H6+O=C2H5+HCO	6.76E+04	2.6	-1130
120	C3H6+OH=CH3+CH3CHO	1.00E+12	0	0
121	C3H6+O=CH3+CH3CO	6.67E+04	2.6	-1130
122	CH3CHO+H=CH3CO+H2	3.98E+13	0	4200
123	CH3CHO+OH=CH3CO+H2O	1.00E+13	0	0
124	CH3CHO+O=CH3CO+OH	5.01E+12	0	1790
125	CH3CHO+CH3=CH3CO+CH4	1.73E+12	0	8440
126	CH3CHO+HO2=CH3CO+H2O2	1.70E+12	0	10700
127	CH3CHO=CH3+HCO	7.08E+15	0	81780
128	CH3CHO+O2=CH3CO+HO2	2.00E+13	0.5	42200
129	CH3CO+M=CH3+CO+M	4.37E+15	0	10500
130	C3H6+H=C3H5+H2	5.01E+12	0	1500
131	C3H6+CH3=C3H5+CH4	1.58E+12	0	8800
132	C3H6+C2H5=C3H5+C2H6	1.00E+11	0	9800

133	$C_3H_6+OH=C_3H_5+H_2O$	1.00E+13	0	3060
134	$C_3H_8+C_3H_5=IC_3H_7+C_3H_6$	2.00E+11	0	16100
135	$C_3H_8+C_3H_5=NC_3H_7+C_3H_6$	7.94E+11	0	20500
136	$C_3H_5=C_3H_4+H$	3.98E+13	0	70000
137	$C_3H_5+O_2=C_3H_4+HO_2$	6.03E+11	0	10000
138	$PC_4H_8=C_3H_5+CH_3$	1.51E+19	-1	73400
139	$PC_4H_8=C_2H_3+C_2H_5$	1.00E+19	-1	96770
140	$PC_4H_8+O=CH_3CHO+C_2H_4$	1.29E+13	0	850
141	$PC_4H_8+O=CH_3CO+C_2H_5$	1.29E+13	0	850
142	$PC_4H_8+OH=CH_3CHO+C_2H_5$	1.00E+11	0	0
143	$PC_4H_8+OH=CH_3CO+C_2H_6$	1.00E+10	0	0
144	$C_3H_4+O=CH_2O+C_2H_2$	1.00E+12	0	0
145	$C_3H_4+O=HCO+C_2H_3$	1.00E+12	0	0
146	$C_3H_4+OH=CH_2O+C_2H_3$	1.00E+12	0	0
147	$C_3H_4+OH=HCO+C_2H_4$	1.00E+12	0	0
148	$C_3H_6=C_3H_5+H$	1.00E+13	0	78000
149	$C_2H_2+O=HCCO+H$	3.55E+04	2.7	1390
150	$CH_2CO+H=CH_3+CO$	1.10E+13	0	3400
151	$CH_2CO+O=HCO+HCO$	1.00E+13	0	2400
152	$CH_2CO+OH=CH_2O+HCO$	2.82E+13	0	0
153	$CH_2CO+M=CH_2+CO+M$	2.00E+16	0	60000
154	$CH_2CO+O=HCCO+OH$	5.01E+13	0	8000
155	$CH_2CO+OH=HCCO+H_2O$	7.59E+12	0	3000
156	$CH_2CO+H=HCCO+H_2$	7.59E+13	0	8000
157	$HCCO+OH=HCO+HCO$	1.00E+13	0	0
158	$HCCO+H=CH_2+CO$	5.01E+13	0	0
159	$HCCO+O=HCO+CO$	3.39E+13	0	2000
160	$C_3H_6=C_2H_3+CH_3$	6.31E+15	0	85800
161	$C_3H_5+H=C_3H_4+H_2$	1.00E+13	0	0
162	$C_3H_5+CH_3=C_3H_4+CH_4$	1.00E+12	0	0
163	$C_2H_6+O_2=C_2H_5+HO_2$	1.00E+13	0	51000
164	$C_2H_6+HO_2=C_2H_5+H_2O_2$	1.12E+13	0	19400
165	$CH_3+C_2H_3=CH_4+C_2H_2$	1.00E+12	0	0
166	$CH_3+C_2H_5=CH_4+C_2H_4$	7.94E+11	0	0
167	$C_2H_5+C_3H_5=C_3H_6+C_2H_4$	1.26E+12	0	0
168	$C_2H_5+C_2H_5=C_2H_6+C_2H_4$	5.01E+11	0	0
169	$CH_3OH+CH_2O=CH_3O+CH_3O$	1.55E+12	0	79570
170	$CH_2O+CH_3O=CH_3OH+HCO$	6.03E+11	0	3300
171	$CH_4+CH_3O=CH_3OH+CH_3$	2.00E+11	0	7000
172	$C_2H_6+CH_3O=CH_3OH+C_2H_5$	3.02E+11	0	7000
173	$C_3H_8+CH_3O=CH_3OH+IC_3H_7$	3.02E+11	0	7000
174	$C_3H_8+CH_3O=CH_3OH+NC_3H_7$	3.02E+11	0	7000
175	$C_4H_{10}=C_2H_5+C_2H_5$	2.00E+16	0	81300
176	$C_4H_{10}=NC_3H_7+CH_3$	1.00E+17	0	85400
177	$C_4H_{10}+O_2=PC_4H_9+HO_2$	2.51E+13	0	49000
178	$C_4H_{10}+O_2=SC_4H_9+HO_2$	3.98E+13	0	47600
179	$C_4H_{10}+H=PC_4H_9+H_2$	5.62E+07	2	7700
180	$C_4H_{10}+H=SC_4H_9+H_2$	1.74E+07	2	5000
181	$C_4H_{10}+OH=PC_4H_9+H_2O$	8.71E+09	1.1	1810
182	$C_4H_{10}+OH=SC_4H_9+H_2O$	2.57E+09	1.3	700

183	C4H10+O=PC4H9+OH	1.12E+14	0	7850
184	C4H10+O=SC4H9+OH	5.62E+13	0	5200
185	C4H10+CH3=PC4H9+CH4	1.29E+12	0	11600
186	C4H10+CH3=SC4H9+CH4	7.94E+11	0	9500
187	C4H10+C2H3=PC4H9+C2H4	1.00E+12	0	18000
188	C4H10+C2H3=SC4H9+C2H4	7.94E+11	0	16800
189	C4H10+C2H5=PC4H9+C2H6	1.00E+11	0	13400
190	C4H10+C2H5=SC4H9+C2H6	1.00E+11	0	10400
191	C4H10+C3H5=PC4H9+C3H6	7.94E+11	0	20500
192	C4H10+C3H5=SC4H9+C3H6	3.16E+11	0	16400
193	C4H10+HO2=PC4H9+H2O2	1.12E+13	0	19400
194	C4H10+HO2=SC4H9+H2O2	6.76E+12	0	17000
195	C4H10+CH3O=PC4H9+CH3OH	3.02E+11	0	7000
196	C4H10+CH3O=SC4H9+CH3OH	6.03E+11	0	7000
197	PC4H9=C2H5+C2H4	2.51E+13	0	28800
198	PC4H9=PC4H8+H	1.26E+13	0	38600
199	PC4H9+O2=PC4H8+HO2	1.00E+12	0	2000
200	SC4H9=SC4H8+H	5.01E+12	0	37900
201	SC4H9=PC4H8+H	2.00E+13	0	40400
202	SC4H9=C3H6+CH3	2.00E+14	0	33200
203	SC4H9+O2=PC4H8+HO2	1.00E+12	0	4500
204	SC4H9+O2=SC4H8+HO2	2.00E+12	0	4250
205	PC4H8=C4H7+H	4.07E+18	-1	97350
206	SC4H8=C4H7+H	4.07E+18	-1	97350
207	PC4H8+H=C4H7+H2	5.01E+13	0	3900
208	SC4H8+H=C4H7+H2	5.01E+13	0	3800
209	PC4H8+OH=C4H7+H2O	1.41E+13	0	3060
210	SC4H8+OH=C4H7+H2O	2.29E+13	0	3060
211	PC4H8+CH3=C4H7+CH4	1.00E+11	0	7300
212	SC4H8+CH3=C4H7+CH4	1.00E+11	0	8200
213	PC4H8+O=C3H6+CH2O	5.01E+12	0	0
214	SC4H8+O=IC3H7+HCO	6.03E+12	0	0
215	SC4H8+O=C2H4+CH3CHO	1.00E+12	0	0
216	PC4H8+OH=NC3H7+CH2O	1.51E+12	0	0
217	SC4H8+OH=C2H5+CH3CHO	3.02E+12	0	0
218	C4H7=C4H6+H	1.20E+14	0	49300
219	C4H7=C2H4+C2H3	1.00E+11	0	37000
220	C4H7+O2=C4H6+HO2	1.00E+11	0	0
221	C4H7+H=C4H6+H2	3.16E+13	0	0
222	C4H7+C2H3=C4H6+C2H4	3.98E+12	0	0
223	C4H7+C2H5=C4H6+C2H6	3.98E+12	0	0
224	C4H7+C2H5=PC4H8+C2H4	5.01E+11	0	0
225	C4H7+C2H5=SC4H8+C2H4	5.01E+11	0	0
226	C4H7+C3H5=C4H6+C3H6	6.31E+12	0	0
227	C4H6=C2H3+C2H3	3.98E+19	-1	98150
228	C4H6+OH=C2H5+CH2CO	1.00E+12	0	0
229	C4H6+OH=C3H5+CH2O	1.00E+12	0	0
230	C4H6+OH=C2H3+CH3CHO	1.00E+12	0	0
231	C4H6+O=C2H4+CH2CO	1.00E+12	0	0
232	C4H6+O=C3H4+CH2O	1.00E+12	0	0

233	$C_2H_3 + C_2H_4 = C_4H_6 + H$	5.01E+11	0	7300
234	$C_5H_{10} = CH_3 + C_4H_7$	1.00E+19	-1	81550
235	$C_5H_{10} + O = PC_4H_8 + CH_2O$	8.51E+12	0	0
236	$C_5H_{10} + O = C_3H_6 + CH_3CHO$	8.51E+12	0	0
237	$C_5H_{10} + OH = PC_4H_9 + CH_2O$	1.00E+12	0	0
238	$C_5H_{10} + OH = NC_3H_7 + CH_3CHO$	1.00E+12	0	0
239	$C_2H_5 + H = CH_3 + CH_3$	3.16E+13	0	0
240	$CH_3OH + O_2 = CH_2OH + HO_2$	3.98E+13	0	50900
241	$C_2H_4 + O_2 = C_2H_3 + HO_2$	3.98E+13	0	61500
242	$C_2H_4 + CH_3 = C_2H_3 + CH_4$	1.00E+13	0	13000
243	$C_3H_6 + O_2 = C_3H_5 + HO_2$	1.00E+14	0	39000
244	$IC_8H_{18} => TC_4H_9 + IC_4H_9$	2.00E+16	0	78000
245	$IC_8H_{18} => IC_3H_7 + NEOC_5H_{11}$	2.00E+16	0	78000
246	$IC_8H_{18} + H => AC_8H_{17} + H_2$	8.51E+07	2	7700
247	$IC_8H_{18} + H => BC_8H_{17} + H_2$	8.91E+06	2	5000
248	$IC_8H_{18} + H => CC_8H_{17} + H_2$	1.26E+13	0	7300
249	$IC_8H_{18} + H => DC_8H_{17} + H_2$	5.62E+07	2	7700
250	$IC_8H_{18} + O => AC_8H_{17} + OH$	1.51E+14	0	7850
251	$IC_8H_{18} + O => BC_8H_{17} + OH$	2.82E+13	0	5200
252	$IC_8H_{18} + O => CC_8H_{17} + OH$	1.00E+13	0	3280
253	$IC_8H_{18} + O => DC_8H_{17} + OH$	1.00E+14	0	7850
254	$IC_8H_{18} + OH => AC_8H_{17} + H_2O$	1.29E+10	1.1	1810
255	$IC_8H_{18} + OH => BC_8H_{17} + H_2O$	1.29E+09	1.3	700
256	$IC_8H_{18} + OH => CC_8H_{17} + H_2O$	1.95E+12	0	440
257	$IC_8H_{18} + OH => DC_8H_{17} + H_2O$	8.71E+09	1.1	1810
258	$IC_8H_{18} + O_2 => AC_8H_{17} + HO_2$	3.72E+13	0	49000
259	$IC_8H_{18} + O_2 => BC_8H_{17} + HO_2$	2.00E+13	0	48000
260	$IC_8H_{18} + O_2 => CC_8H_{17} + HO_2$	2.00E+12	0	46000
261	$IC_8H_{18} + O_2 => DC_8H_{17} + HO_2$	2.51E+13	0	49000
262	$IC_8H_{18} + HO_2 => AC_8H_{17} + H_2O_2$	1.70E+13	0	19400
263	$IC_8H_{18} + HO_2 => BC_8H_{17} + H_2O_2$	3.39E+12	0	17000
264	$IC_8H_{18} + HO_2 => CC_8H_{17} + H_2O_2$	3.02E+12	0	14400
265	$IC_8H_{18} + HO_2 => DC_8H_{17} + H_2O_2$	1.12E+13	0	19400
266	$IC_8H_{18} + CH_3 => AC_8H_{17} + CH_4$	1.17E+13	0	11600
267	$IC_8H_{18} + CH_3 => BC_8H_{17} + CH_4$	2.40E+12	0	9500
268	$IC_8H_{18} + CH_3 => CC_8H_{17} + CH_4$	2.00E+11	0	7900
269	$IC_8H_{18} + CH_3 => DC_8H_{17} + CH_4$	7.76E+12	0	11600
270	$AC_8H_{17} => AC_7H_{14} + CH_3$	1.00E+10	0	26000
271	$AC_8H_{17} => IC_4H_8 + IC_4H_9$	1.29E+13	0	29500
272	$BC_8H_{17} => CC_7H_{14} + CH_3$	1.00E+13	0	26000
273	$CC_8H_{17} => IC_4H_8 + IC_4H_9$	5.01E+12	0	29000
274	$CC_8H_{17} => IC_8H_{16} + H$	1.00E+13	0	38000
275	$DC_8H_{17} => AC_7H_{14} + CH_3$	1.26E+13	0	32800
276	$DC_8H_{17} => C_3H_6 + NEOC_5H_{11}$	1.29E+13	0	29500
277	$DC_8H_{17} => IC_8H_{16} + H$	3.31E+13	0	36000
278	$AC_8H_{17} + O_2 => IC_8H_{16} + HO_2$	1.51E+10	0	10000
279	$BC_8H_{17} + O_2 => IC_8H_{16} + HO_2$	1.00E+10	0	10000
280	$CC_8H_{17} + O_2 => IC_8H_{16} + HO_2$	1.00E+10	0	10000
281	$DC_8H_{17} + O_2 => IC_8H_{16} + HO_2$	1.00E+10	0	10000
282	$IC_8H_{16} + O => IC_4H_8 + IC_4H_7 + OH$	2.82E+13	0	5200 # no reverse reacton

283	IC8H16+OH=>IC4H8+IC4H7+H2O	1.29E+09	1.3	700 # no reverse reacton
284	IC8H16+O=>IC7H15+HCO	1.00E+11	0	0
285	IC7H15=>IC4H8+IC3H7	2.51E+13	0	28000
286	IC7H15=>AC7H14+H	3.98E+13	0	40000
287	IC7H15=>TC4H9+C3H6	2.51E+13	0	28200
288	IC7H15=>CC7H14+H	3.98E+13	0	40400
289	AC7H14+H=>IC7H13+H2	2.82E+13	0	4000
290	CC7H14+H=>IC7H13+H2	5.62E+13	0	4000
291	AC7H14+O=>IC7H13+OH	5.13E+05	2.6	-1100
292	CC7H14+O=>IC7H13+OH	5.13E+05	2.6	-1100
293	AC7H14+OH=>IC7H13+H2O	1.35E+14	0	3100
294	CC7H14+OH=>IC7H13+H2O	1.35E+14	0	3100
295	AC7H14+O=>IC6H13+HCO	2.00E+11	0	0
296	CC7H14+O=>NEOC5H11+CH3CO	1.00E+11	0	0
297	AC7H14+OH=>IC6H13+CH2O	1.00E+11	0	0
298	CC7H14+OH=>NEOC5H11+CH3CHO	1.00E+11	0	0
299	IC8H16=>IC4H7+TC4H9	2.51E+16	0	71000
300	IC8H16=>C6H11+C2H5	2.51E+16	0	71000
301	AC7H14=>IC4H7+IC3H7	5.01E+16	0	71000
302	AC7H14=>TC4H9+C3H5	2.51E+16	0	71000
303	CC7H14=>C6H11+CH3	2.51E+16	0	71000
304	IC8H16+OH=>IC7H15+CH2O	1.00E+11	0	0
305	IC7H13=>IC4H8+C3H5	5.01E+13	0	30000
306	IC7H13=>IC4H7+C3H6	5.01E+13	0	30000
307	IC7H13=>C6H10+CH3	2.00E+14	0	32800
308	IC6H13=>IC3H7+C3H6	2.51E+13	0	28200
309	IC6H13=>TC4H9+C2H4	2.51E+13	0	28800
310	IC6H13=>IC4H9+C2H4	2.51E+13	0	28800
311	C6H11=>C3H5+C3H6	2.51E+13	0	30000
312	C6H11=>C6H10+H	1.26E+14	0	49300
313	C6H11+O2=>C6H10+HO2	1.00E+11	0	0
314	C6H10=>C3H5+C3H5	2.51E+14	0	5940
315	NEOC5H11=>IC4H8+CH3	1.00E+11	0	26000
316	IC4H10=>IC3H7+CH3	2.00E+17	0	83400
317	IC4H10=>TC4H9+H	1.00E+15	0	83400
318	IC4H10=>IC4H9+H	1.00E+15	0	83400
319	IC4H10+H=>TC4H9+H2	1.26E+14	0	7300
320	IC4H10+H=>IC4H9+H2	1.00E+14	0	8400
321	IC4H10+OH=>TC4H9+H2O	1.95E+12	0	440
322	IC4H10+OH=>IC4H9+H2O	4.90E+03	3	-700
323	IC4H10+O=>TC4H9+OH	1.10E+13	0	3280
324	IC4H10+O=>IC4H9+OH	3.16E+13	0	5760
325	IC4H10+CH3=>TC4H9+CH4	1.00E+11	0	7900
326	IC4H10+CH3=>IC4H9+CH4	8.91E+11	0	10340
327	IC4H10+HO2=>TC4H9+H2O2	3.16E+12	0	14400
328	IC4H10+HO2=>IC4H9+H2O2	1.70E+13	0	19400
329	IC4H10+O2=>TC4H9+HO2	2.00E+12	0	46000
330	IC4H10+O2=>IC4H9+HO2	3.72E+13	0	49000
331	IC4H10+C2H5=>TC4H9+C2H6	1.00E+11	0	7900
332	IC4H10+C2H5=>IC4H9+C2H6	1.51E+12	0	10400

333	IC4H9=>C3H6+CH3	1.00E+14	0	32800
334	IC4H9=>IC4H8+H	3.31E+14	0	36000
335	TC4H9=>IC4H8+H	1.00E+15	0	43600
336	TC4H9=>C3H6+CH3	1.58E+15	0	46300
337	TC4H9+O2=>IC4H8+HO2	1.00E+12	0	5000
338	IC4H9+O2=>IC4H8+HO2	1.00E+12	0	5000
339	IC4H8=>C3H5+CH3	1.51E+19	-1	73400
340	IC4H8=>IC4H7+H	1.00E+17	0	88000
341	IC4H8+H=>IC4H7+H2	1.00E+13	0	3800
342	IC4H8+O=>IC4H7+OH	2.51E+05	2.6	-1130
343	IC4H8+OH=>IC4H7+H2O	1.91E+12	0	1230
344	IC4H8+O=>IC3H7+HCO	7.24E+05	2.3	-1050
345	IC4H8+OH=>IC3H7+CH2O	1.51E+12	0	0
346	IC4H8+CH3=>IC4H7+CH4	6.03E+11	0	8900
347	IC4H7=>C3H4+CH3	1.00E+13	0	32600
348	C2H3+O2=>CH2O+HCO	3.98E+12	0	-250
349	AC8H17=>DC8H17	6.03E+11	0	14100
350	AC8H17=>CC8H17	1.00E+11	0	16100
351	TC4H9+IC4H9=>IC8H18	1.00E+12	0	0
352	IC3H7+NEOC5H11=>IC8H18	1.00E+12	0	0
353	AC8H17+H2=>IC8H18+H	1.00E+12	0	30000
354	BC8H17+H2=>IC8H18+H	1.00E+12	0	30000
355	CC8H17+H2=>IC8H18+H	1.00E+12	0	30000
356	DC8H17+H2=>IC8H18+H	1.00E+12	0	30000
357	AC8H17+OH=>IC8H18+O	1.00E+12	0	30000
358	BC8H17+OH=>IC8H18+O	1.00E+12	0	30000
359	CC8H17+OH=>IC8H18+O	1.00E+12	0	30000
360	DC8H17+OH=>IC8H18+O	1.00E+12	0	30000
361	AC8H17+H2O=>IC8H18+OH	1.00E+12	0	30000
362	BC8H17+H2O=>IC8H18+OH	1.00E+12	0	30000
363	CC8H17+H2O=>IC8H18+OH	1.00E+12	0	30000
364	DC8H17+H2O=>IC8H18+OH	1.00E+12	0	30000
365	AC8H17+HO2=>IC8H18+O2	2.00E+12	0	30000
366	BC8H17+HO2=>IC8H18+O2	5.01E+12	0	30000
367	CC8H17+HO2=>IC8H18+O2	2.00E+12	0	30000
368	DC8H17+HO2=>IC8H18+O2	2.00E+12	0	30000
369	AC8H17+H2O2=>IC8H18+HO2	1.00E+12	0	30000
370	BC8H17+H2O2=>IC8H18+HO2	1.00E+12	0	30000
371	CC8H17+H2O2=>IC8H18+HO2	1.00E+12	0	30000
372	DC8H17+H2O2=>IC8H18+HO2	1.00E+12	0	30000
373	AC8H17+CH4=>IC8H18+CH3	1.00E+12	0	30000
374	BC8H17+CH4=>IC8H18+CH3	1.00E+12	0	30000
375	CC8H17+CH4=>IC8H18+CH3	1.00E+12	0	30000
376	DC8H17+CH4=>IC8H18+CH3	1.00E+12	0	30000
377	AC7H14+CH3=>AC8H17	6.31E+09	0	7000
378	IC4H8+IC4H9=>AC8H17	1.00E+11	0	8000
379	CC7H14+CH3=>BC8H17	6.31E+10	0	7000
380	IC4H8+IC4H9=>CC8H17	6.03E+10	0	7000
381	IC8H16+H=>CC8H17	1.00E+10	0	1500
382	AC7H14+CH3=>DC8H17	1.58E+10	0	7000

383	C3H6+NEOC5H11=>DC8H17	1.00E+10	0	7000
384	IC8H16+H=>DC8H17	1.00E+09	0	1200
385	IC8H16+HO2=>AC8H17+O2	2.00E+11	0	20000
386	IC8H16+HO2=>BC8H17+O2	2.00E+11	0	20000
387	IC8H16+HO2=>CC8H17+O2	2.00E+11	0	20000
388	IC8H16+HO2=>DC8H17+O2	2.00E+11	0	20500
389	IC7H15+HCO=>IC8H16+O	1.00E+10	0	30000
390	IC4H8+IC3H7=>IC7H15	3.98E+10	0	6900
391	AC7H14+H=>IC7H15	1.58E+13	0	1200
392	TC4H9+C3H6=>IC7H15	1.20E+11	0	8000
393	CC7H14+H=>IC7H15	1.58E+13	0	1200
394	IC7H13+H2=>AC7H14+H	1.00E+12	0	14000
395	IC7H13+H2=>CC7H14+H	2.00E+12	0	14000
396	IC7H13+OH=>AC7H14+O	1.41E+12	0	30000
397	IC7H13+OH=>CC7H14+O	1.41E+12	0	30000
398	IC7H13+H2O=>AC7H14+OH	1.00E+13	0	27000
399	IC7H13+H2O=>CC7H14+OH	1.00E+13	0	27000
400	IC6H13+HCO=>AC7H14+O	1.00E+12	0	30000
401	NEOC5H11+CH3CO=>CC7H14+O	1.00E+12	0	30000
402	IC6H13+CH2O=>AC7H14+OH	5.01E+12	0	27000
403	NEOC5H11+CH3CHO=>CC7H14+OH	1.00E+12	0	27000
404	IC4H7+TC4H9=>IC8H16	1.00E+13	0	0
405	C6H11+C2H5=>IC8H16	1.00E+13	0	0
406	IC4H7+IC3H7=>AC7H14	1.00E+13	0	0
407	TC4H9+C3H5=>AC7H14	1.00E+13	0	0
408	C6H11+CH3=>CC7H14	1.00E+13	0	0
409	IC7H15+CH2O=>IC8H16+OH	1.00E+12	0	0
410	IC4H8+C3H5=>IC7H13	1.26E+11	0	17000
411	IC4H7+C3H6=>IC7H13	1.26E+11	0	17000
412	C6H10+CH3=>IC7H13	6.46E+11	0	9100
413	IC3H7+C3H6=>IC6H13	3.98E+10	0	6900
414	TC4H9+C2H4=>IC6H13	3.98E+10	0	6900
415	IC4H9+C2H4=>IC6H13	3.98E+10	0	6900
416	C3H5+C3H6=>C6H11	6.31E+10	0	17000
417	C6H10+H=>C6H11	7.94E+12	0	1200
418	C6H10+HO2=>C6H11+O2	1.00E+11	0	17000
419	C3H5+C3H5=>C6H10	6.31E+12	0	0
420	IC4H8+CH3=>NEOC5H11	1.00E+11	0	7200
421	IC3H7+CH3=>IC4H10	1.58E+13	0	0
422	TC4H9+H=>IC4H10	1.00E+11	0	0
423	IC4H9+H=>IC4H10	1.00E+11	0	0
424	TC4H9+H2=>IC4H10+H	1.00E+12	0	16000
425	IC4H9+H2=>IC4H10+H	3.16E+12	0	15700
426	TC4H9+H2O=>IC4H10+OH	3.98E+12	0	22000
427	IC4H9+H2O=>IC4H10+OH	8.91E+03	3	20800
428	TC4H9+OH=>IC4H10+O	2.00E+12	0	9600
429	IC4H9+OH=>IC4H10+O	2.00E+12	0	9600
430	TC4H9+CH4=>IC4H10+CH3	2.00E+11	0	21000
431	IC4H9+CH4=>IC4H10+CH3	2.00E+11	0	15000
432	TC4H9+H2O2=>IC4H10+HO2	3.16E+12	0	7400

433	IC4H9+H2O2=>IC4H10+HO2	3.16E+12	0	7400
434	TC4H9+HO2=>IC4H10+O2	2.00E+12	0	2000
435	IC4H9+HO2=>IC4H10+O2	2.00E+12	0	2000
436	TC4H9+C2H6=>IC4H10+C2H5	3.02E+11	0	21000
437	IC4H9+C2H6=>IC4H10+C2H5	3.16E+11	0	12300
438	C3H6+CH3=>IC4H9	3.16E+11	0	9100
439	IC4H8+H=>IC4H9	1.00E+13	0	1200
440	IC4H8+H=>TC4H9	3.16E+13	0	1500
441	C3H6+CH3=>TC4H9	1.00E+11	0	7000
442	IC4H8+HO2=>TC4H9+O2	2.00E+11	0	17500
443	IC4H8+HO2=>IC4H9+O2	2.00E+11	0	17500
444	C3H5+CH3=>IC4H8	3.98E+12	0	0
445	IC4H7+H=>IC4H8	2.00E+13	0	0
446	IC4H7+H2=>IC4H8+H	3.02E+13	0	25000
447	IC4H7+OH=>IC4H8+O	7.08E+11	0	29900
448	IC4H7+H2O=>IC4H8+OH	4.79E+12	0	26470
449	IC3H7+HCO=>IC4H8+O	2.00E+05	2.3	80280
450	IC3H7+CH2O=>IC4H8+OH	1.95E+13	0	13230
451	IC4H7+CH4=>IC4H8+CH3	6.03E+11	0	29900
452	C3H4+CH3=>IC4H7	2.00E+11	0	7500
453	CH2O+HCO=>C2H3+O2	3.98E+12	0	86300
454	DC8H17=>AC8H17	8.91E+11	0	14100
455	CC8H17=>AC8H17	8.91E+11	0	21100

NOTE : A units mole-cm-sec-K, E units cal/mole

= : reversible reaction

=> : irreversible reaction

AC8H17: primary iso-octyl radical
 BC8H17: secondary iso-octyl radical
 CC8H17: tertiary iso-octyl radical
 DC8H17: primary iso-octyl radical
 IC8H16: 2,4,4-trimethyl-2-pentene
 IC7H15: 2,4-dimethyl-1-pentyl radical
 AC7H14: 2,4-dimethyl-2-pentene
 CC7H14: 4,4-dimethyl-2-pentene
 IC4H9: isobutyl radical
 PC4H9: primary butyl radical
 SC4H9: secondary butyl radical
 TC4H9: tertiary butyl radical
 PC4H8: 1-butene
 SC4H8: 2-butene
 IC3H7: iso-propyl radical
 NC3H7: n-propyl radical

Appendix 2.3 Ethane (ethylene) chemical kinetic reaction mechanism

REACTIONS CONSIDERED	(k = A T**b exp(-E/RT))			Source/Modification
	A	b	E	
1 H+H+M=H2+M	7.31E+17	-1	0	# All Reactions : Ref(51)
2 O+O+M=O2+M	1.14E+17	-1	0	
3 O+H+M=OH+M	6.20E+16	-0.6	0	
4 H2+O2=OH+OH	1.70E+13	0	47780	
5 O+H2=OH+H	3.87E+04	2.7	6260	
6 H+O2=OH+O	1.90E+14	0	16812	
7 H+O2+M=HO2+M	8.00E+17	-0.8	0	
8 H+OH+M=H2O+M	8.62E+21	-2	0	
9 H2+OH=H2O+H	2.16E+08	1.5	3430	
10 H2O+O=OH+OH	1.50E+10	1.1	17260	
11 HO2+OH=H2O+O2	2.89E+13	0	-497	
12 HO2+O=OH+O2	1.81E+13	0	-400	
13 H+HO2=H2+O2	4.22E+13	0	1411	
14 H+HO2=OH+OH	4.95E+13	0	143	
15 H+HO2=H2O+O	1.18E+14	0	2730	
16 HO2+HO2=H2O2+O2	1.46E+13	0	5088	
17 OH+OH=H2O2	1.56E+16	-1.5	149	
18 H2O2+OH=HO2+H2O	1.78E+12	0	326	
19 H2O2+H=HO2+H2	1.70E+12	0	3750	
20 H2O2+H=H2O+OH	1.00E+13	0	3590	
21 H2O2+O=HO2+OH	2.80E+13	0	6400	
22 CO+HO2=CO2+OH	1.50E+14	0	23650	
23 CO+OH=CO2+H	4.40E+06	1.5	-740	
24 CO+O+M=CO2+M	2.83E+13	0	-4540	
25 CO+O2=CO2+O	2.53E+12	0	47700	
26 HCO+M=H+CO+M	1.85E+17	-1	17000	
27 HCO+OH=CO+H2O	1.00E+14	0	0	
28 HCO+O=CO+OH	3.00E+13	0	0	
29 HCO+O=CO2+H	3.00E+13	0	0	
30 HCO+H=CO+H2	7.22E+13	0	0	
31 HCO+O2=CO+HO2	4.22E+12	0	0	
32 HCO+CH3=CO+CH4	1.20E+14	0	0	
33 HCO+HO2=CO2+OH+H	3.00E+13	0	0	
34 HCO+C2H6=CH2O+C2H5	4.70E+04	2.7	18235	
35 HCO+HCO=CH2O+CO	1.80E+13	0	0	
36 HCO+HCO=H2+CO+CO	3.00E+12	0	0	
37 CH4=CH3+H	5.99E+30	-4.9	108553	
38 CH4+HO2=CH3+H2O2	1.12E+13	0	24641	
39 CH4+OH=CH3+H2O	1.55E+07	1.8	2774	
40 CH4+O=CH3+OH	6.92E+08	1.6	8486	
41 CH4+H=CH3+H2	8.58E+03	3.1	7941	
42 CH4+CH2=CH3+CH3	4.30E+12	0	10038	
43 CH3+M=CH2+H+M	1.90E+16	0	91600	

44	CH3+HO2=CH3O+OH	4.00E+13	0	5000
45	CH4+O2=CH3+HO2	7.63E+13	0	58590
46	CH3+OH=CH2OH+H	2.64E+19	-1.8	8068
47	CH3+OH=CH3O+H	5.74E+12	-0.2	13931
48	CH3+OH=CH2+H2O	8.90E+18	-1.8	8067
49	CH3+OH=CH2O+H2	3.19E+12	-0.5	10810
50	CH3+O=CH2O+H	8.43E+13	0	0
51	CH3+H=CH2+H2	7.00E+13	0	15100
52	CH3+O2=CH3O+O	6.00E+12	0	33700
53	CH3+O2=CH2O+OH	3.05E+30	-4.7	36571
54	CH3+CH3=C2H5+H	3.01E+13	0	13513
55	CH3+CH3=C2H6	2.39E+38	-7.6	11359
56	CH3+CH3O=CH4+CH2O	2.41E+13	0	0
57	CH3+CH2OH=CH4+CH2O	2.41E+12	0	0
58	CH2+OH=CH+H2O	1.13E+07	2	3000
59	CH2+OH=CH2O+H	2.50E+13	0	0
60	CH2+O=CO+H+H	9.08E+13	0	656
61	CH2+O=CO+H2	3.89E+13	0	-149
62	CH2+H=CH+H2	5.52E+12	0	-2026
63	CH2+O2=HCO+OH	4.30E+10	0	-500
64	CH2+O2=CO2+H2	6.90E+11	0	500
65	CH2+O2=CO2+H+H	1.60E+12	0	1000
66	CH2+O2=CO+H2O	1.87E+10	0	-1000
67	CH2+O2=CO+OH+H	8.64E+10	0	-500
68	CH2+O2=CH2O+O	1.00E+14	0	4500
69	CH2+CO2=CH2O+CO	1.10E+11	0	1000
70	CH2+CH2=C2H2+H2	3.20E+13	0	0
71	CH2+CH3=C2H4+H	4.00E+13	0	0
72	CH2+CH=C2H2+H	4.00E+13	0	0
73	CH2+C2H2=H+C3H3	1.20E+13	0	6620
74	CH2+C2H4=C3H6	4.30E+12	0	10038
75	CH2+C2H6=CH3+C2H5	6.50E+12	0	7911
76	CH2+C3H8=CH3+IC3H7	2.19E+12	0	6405
77	CH2+C3H8=CH3+NC3H7	1.79E+12	0	6405
78	CH+OH=HCO+H	3.00E+13	0	0
79	CH+O=CO+H	1.00E+14	0	0
80	CH+O2=HCO+O	3.30E+13	0	0
81	CH+O2=CO+OH	2.00E+13	0	0
82	CH+CO2=HCO+CO	3.40E+12	0	690
83	CH+CH4=C2H4+H	6.00E+13	0	0
84	CH+CH3=C2H3+H	3.00E+13	0	0
85	CH3O+M=CH2O+H+M	4.88E+15	0	22773
86	CH3O+HO2=CH2O+H2O2	3.00E+11	0	0
87	CH3O+OH=CH2O+H2O	1.00E+13	0	0
88	CH3O+O=CH2O+OH	1.30E+13	0	0
89	CH3O+H=CH2O+H2	2.00E+13	0	0
90	CH3O+O2=CH2O+HO2	2.35E+10	0	1788
91	CH3O+CH2O=CH3OH+HCO	1.15E+11	0	1280
92	CH3O+CO=CH3+CO2	1.57E+13	0	2981
93	CH3O+HCO=CH3OH+CO	9.00E+13	0	0

94	CH3O+C2H5=CH2O+C2H6	2.41E+13	0	0
95	CH3O+C2H3=CH2O+C2H4	2.41E+13	0	0
96	CH3O+C2H4=CH2O+C2H5	1.20E+11	0	7000
97	CH2O+M=HCO+H+M	5.72E+16	0	76480
98	CH2O+HO2=HCO+H2O2	4.00E+12	0	11665
99	CH2O+OH=HCO+H2O	3.43E+09	1.2	-447
100	CH2O+O=HCO+OH	1.81E+13	0	3088
101	CH2O+H=HCO+H2	1.12E+08	1.7	2127
102	CH2O+O2=HCO+HO2	2.04E+13	0	39000
103	CH2O+CH3=HCO+CH4	8.91E-13	7.4	-960
104	C2H6=C2H5+H	2.08E+38	-7.1	106507
105	C2H6+HO2=C2H5+H2O2	1.21E+12	0	17600
106	C2H6+OH=C2H5+H2O	5.13E+06	2.1	860
107	C2H6+O=C2H5+OH	1.14E-07	6.5	274
108	C2H6+H=C2H5+H2	5.00E+02	3.5	5210
109	C2H6+O2=C2H5+HO2	1.00E+13	0	51000
110	C2H6+CH3O=C2H5+CH3OH	3.02E+11	0	7000
111	C2H6+CH3=C2H5+CH4	3.97E+05	2.5	17684
112	C2H5+HO2=C2H4+H2O2	3.00E+11	0	0
113	C2H5+HO2=>CH3+CH2O+OH	2.50E+13	0	0
114	C2H5+OH=C2H4+H2O	2.41E+13	0	0
115	C2H5+OH=>CH3+CH2O+H	2.41E+13	0	0
116	C2H5+O=CH2O+CH3	4.24E+13	0	0
117	C2H5+O=CH3CHO+H	5.30E+13	0	0
118	C2H5+O=C2H4+OH	3.05E+13	0	0
119	C2H5+H=C2H4+H2	1.25E+14	0	8000
120	C2H5+O2=C2H4+HO2	1.70E+10	0	-670
121	C2H5+CH3=C2H4+CH4	4.37E-04	5	8300
122	C2H5+C2H5=C2H4+C2H6	1.40E+12	0	0
123	C2H4+M=C2H2+H2+M	3.00E+17	0	79350
124	C2H4+M=C2H3+H+M	2.97E+17	0	96560
125	C2H4+HO2=>C2H4O+OH	6.22E+12	0	18962
126	C2H4+OH=C2H3+H2O	2.02E+13	0	5960
127	C2H4+O=CH3+HCO	1.08E+14	0	7432
128	C2H4+O=>CH2+HCO+H	5.66E+12	0	1488
129	C2H4+H=C2H3+H2	3.36E-07	6	1692
130	C2H4+H=C2H5	1.05E+14	-0.5	655
131	C2H4+O2=C2H3+HO2	4.00E+13	0	61500
132	C2H4+C2H4=C2H5+C2H3	5.00E+14	0	64700
133	C2H4+CH3=C2H3+CH4	3.97E+05	2.5	20000
134	C2H4O=CH4+CO	3.16E+14	0	57000
135	C2H3=C2H2+H	2.10E+44	-8.4	51106
136	C2H3+HO2=>CH3+CO+OH	3.00E+13	0	0
137	C2H3+OH=C2H2+H2O	3.00E+13	0	0
138	C2H3+OH=CH3CHO	3.00E+13	0	0
139	C2H3+O=CH3+CO	3.00E+13	0	0
140	C2H3+H=C2H2+H2	3.00E+13	0	0
141	C2H3+O2=CH2O+HCO	3.00E+12	0	-250
142	C2H3+CH3=C2H2+CH4	4.37E-04	5	8300
143	C2H3+C2H6=C2H4+C2H5	1.50E+13	0	10000

144	$C_2H_3+HCO=C_2H_4+CO$	9.03E+13	0	0
145	$C_2H_3+CH_2O=C_2H_4+HCO$	5.42E+03	2.8	5862
146	$C_2H_3+C_2H_3=C_2H_2+C_2H_4$	1.08E+13	0	0
147	$C_2H_3+C_2H_3=C_4H_6$	4.94E+13	0	0
148	$C_2H_2=C_2H+H$	2.37E+32	-5.3	130688
149	$C_2H_2+HO_2=CH_2CO+OH$	1.00E+13	0	18280
150	$C_2H_2+OH=C_2H+H_2O$	3.39E+07	2	14000
151	$C_2H_2+OH=HCCOH+H$	5.06E+05	2.3	13500
152	$C_2H_2+OH=CH_2CO+H$	2.19E-04	4.5	-1000
153	$C_2H_2+OH=CH_3+CO$	4.85E-04	4	-2000
154	$C_2H_2+H=C_2H+H_2$	6.02E+13	0	22257
155	$C_2H_2+O=CH_2+CO$	1.52E+04	2.8	497
156	$C_2H_2+O=HCCO+H$	6.50E+03	2.8	497
157	$C_2H_2+O_2=HCCO+OH$	2.00E+08	1.5	30100
158	$C_2H_2+O_2=C_2H+HO_2$	1.20E+13	0	74520
159	$C_2H_2+CH_3=SC_3H_5$	1.61E+40	-8.6	20331
160	$C_2H_2+CH_3=PC_3H_4+H$	2.73E+17	-2	20592
161	$C_2H_2+CH_3=AC_3H_5$	2.61E+46	-9.8	36951
162	$C_2H_2+CH_3=AC_3H_4+H$	6.74E+19	-2.1	31591
163	$HCCOH+H=CH_2CO+H$	1.00E+13	0	0
164	$C_2H+OH=HCCO+H$	2.00E+13	0	0
165	$C_2H+O=CO+CH$	1.00E+13	0	0
166	$C_2H+O_2=CO+CO+H$	5.00E+13	0	1510
167	$CH_2CO+M=CH_2+CO+M$	4.11E+15	0	59270
168	$CH_2CO+O_2=CH_2O+CO_2$	1.00E+08	0	0
169	$CH_2CO+OH=HCCO+H_2O$	7.50E+12	0	2000
170	$CH_2CO+O=CH_2+CO_2$	1.76E+12	0	1349
171	$CH_2CO+O=HCCO+OH$	1.00E+13	0	8000
172	$CH_2CO+H=CH_3+CO$	4.54E+09	1.3	3160
173	$CH_2CO+H=HCCO+H_2$	5.00E+13	0	8000
174	$HCCO+M=CH+CO+M$	6.00E+15	0	58821
175	$HCCO+OH=HCO+CO+H$	1.00E+13	0	0
176	$HCCO+O=CO+CO+H$	1.93E+14	0	590
177	$HCCO+H=CH_2+CO$	1.50E+14	0	0
178	$HCCO+O_2=CO+CO+OH$	1.46E+12	0	2500
179	$HCCO+CH_2=C_2H+CH_2O$	1.00E+13	0	2000
180	$HCCO+CH_2=C_2H_3+CO$	3.00E+13	0	0
181	$CH_3OH=CH_3+OH$	1.57E+46	-9.3	103522
182	$CH_3OH+HO_2=CH_2OH+H_2O_2$	6.30E+12	0	19360
183	$CH_3OH+OH=CH_2OH+H_2O$	4.53E+11	0.3	1160
184	$CH_3OH+OH=CH_3O+H_2O$	3.63E+11	0.7	5868
185	$CH_3OH+O=CH_2OH+OH$	1.00E+13	0	4690
186	$CH_3OH+H=CH_2OH+H_2$	4.00E+13	0	6100
187	$CH_3OH+CH_2O=CH_3O+CH_3O$	1.55E+12	0	79570
188	$CH_3OH+CH_3=CH_2OH+CH_4$	3.57E+11	0	8663
189	$CH_3OH+CH_3=CH_3O+CH_4$	4.68E+05	2.3	12764
190	$CH_2OH+M=CH_2O+H+M$	1.00E+14	0	25100
191	$CH_2OH+H=CH_2O+H_2$	3.00E+13	0	0
192	$CH_2OH+O_2=CH_2O+HO_2$	2.17E+14	0	4690
193	$CH_3CHO=CH_3+HCO$	2.45E+16	0	84128

194	CH3CHO+HO2=CH3CO+H2O2	1.70E+12	0	10700
195	CH3CHO+OH=CH3CO+H2O	1.00E+13	0	0
196	CH3CHO+O=CH3CO+OH	5.00E+12	0	1790
197	CH3CHO+H=CH3CO+H2	4.00E+13	0	4210
198	CH3CHO+O2=CH3CO+HO2	2.00E+13	0.5	42200
199	CH3CHO+CH3=CH3CO+CH4	2.00E-06	5.6	2464
200	CH3CO+M=CH3+CO+M	8.64E+15	0	14400

NOTE : A units mole-cm-sec-K, E units
cal/mole

= : reversible reaction

=> : irreversible reaction

IC3H7: iso-propyl radical

NC3H7: n-propyl radical

SC3H5: 2-methylvinyl radical

AC3H5: allyl radical

PC3H4: propyne

AC3H4: allene

Appendix 3 One Dimensional Program

Appendix 3.1 One dimensional transport/chemistry program

The one dimensional transport/chemistry program consists of main.f, interp.f (interpreter), ck_1d.f (thermodynamic properties and chemical reactions), and tran_1d.f (transport properties). In addition, CHEMKIN gas-phase subroutines are also needed to be linked while the code is compiled.

(a) main.f

PROGRAM MAIN

```
*=====
* One dimensional transport/chemistry code
*
* Solution of PDEs governing the temperature and species concentrations.
* Determines concentration profiles away from the wall as a function of time.
* The numerical solver for solving PDEs (d03ppf) is obtained from the NAG numerical library.
* Please refer to the NAG numerical library for the parameters used in this program.
*
* All the units in this code are converted into MKS unit (kg, m, s).
*
* Author:      Kuo-Chun Wu, MIT
*=====
```

implicit none

```
*=====
* Constant Declarations
*=====
```

* NUMERICAL

```
integer      npde, npdemx, npts, ncode, m, nxi, nxfix,
+           neqn, neqnmx, niw, nptsmx,
+           nwkres, lenode, nw, intpts, itype, mlu
parameter    ( npdemx = 80, ncode = 0, m = 0, nptsmx = 205,
+           nxi = 0, nxfix = 0, intpts = 2, itype = 2,
+           neqnmx = npdemx*nptsmx + ncode,
+           niw = neqnmx + 25 + nxfix,
+           nwkres = npdemx*(nptsmx + 3*npdemx + 21) + 7*nptsmx + nxfix + 3,
+           lenode = 11*neqnmx + 50,
+           mlu = 2*npdemx - 1,
+           nw = (3*mlu + 1)*neqnmx + neqnmx + nwkres + lenode )
```

```
*=====
```

* BOUNDARY LAYER

double precision	hx,tout,tinc,tmax,ts,dxmesh,rmesh,xratio,gasconst,
+	const,time_ini,pressure,length,dpdt,avespeed,tconst
integer	i, ii, j, ifail, ind, iteration, itol, itask, itrace, ipminf
double precision	u(neqnm _x),w(nw),x(nptsm _x),atol(neqnm _x),rtol(1),y(npdem _x),
+	temp(nptsm _x), algopt(30), xfix(1), v(1),sumspec(neqnm _x),
+	wtm(nptsm _x),xi(1),rho(nptsm _x)
integer	iw(niw), nrmesh
logical	remesh, more
character	laopt, norm
real	time(2)
real	dtime, elapsed
external	d03pck
external	bndary, pdedef, uvinit, monitf
external	dtime

* CHEMKIN DECLARATIONS

integer	LINKCK,LINKMC,LCADPL,LINIT,LMESH,LINTEG,LOUT,
+	LSCREEN,LDATA,LRESULT,leniwk, lenrwk, lencwk
parameter	(LINKCK=25,LINKMC=35,LCADPL=10,LINIT=15,LMESH=12,
+	LINTEG=20,LOUT=30,LSCREEN=6,LDATA=18,
+	LRESULT=8,leniwk=7500,lenrwk=90000,lencwk=500)
integer	ickwrk(leniwk), imcwrk(leniwk)
double precision	rckwrk(lenrwk), rmcwrk(lenrwk)
character	cckwrk(lencwk)*(16)
common /ckspi/	ickwrk,imcwrk
common /ckspr/	rckwrk, rmcwrk
common /ckspc/	cckwrk

double precision	xnew(nptsm _x)
integer	index,nptss,nspecies
common /pointers/	index, nptss, nspecies
double precision	timeold, timenew, xcheck
common /timedif/	timeold, timenew, xcheck
double precision	init_rhol(nptsm _x)
common /transform/	init_rhol
logical	firsttime(nptsm _x)
common /starttime/	firsttime
common /gconst/	gasconst
double precision	temp_l, temp_r, x_l(100), x_r(100)
common /INITDAT/	temp_l, temp_r, tmax, tinc, x_l, x_r

* =====
* Executable Statements
* =====

* Open files

open(UNIT=LINKCK, status='old', file='cklink', form='unformatted')

```

open(UNIT=LINKMC, status='old', file='tlink', form='unformatted')
open(UNIT=LCADPL, status='old', file='cad-p-l', form='formatted')
open(UNIT=LINIT, status='old', file='initial', form='formatted')
open(UNIT=LMESH, status='old', file='mesh', form='formatted')
open(UNIT=LINTEG, status='new', file='1d_int', form='formatted')
open(UNIT=LDATA, status='new', file='1d_dat', form='unformatted')
open(UNIT=LOUT, status='new', file='1d_out', form='formatted')
open(UNIT=LRESULT, status='new', file='result', form='formatted')

```

* Initialize CHEMKIN AND TRANSPORT LINK FILE

```

call ckinit(leniwrk, lenrwrk, lencwrk, LINKCK, LOU, ickwrk, rckwrk, cckwrk)
call mcinit(LINKMC, LOU, leniwrk, lenrwrk, imcwrk, rmcwrk)
call ck_initial_knui(ickwrk)

```

* Read all input data and store in arrays for later use

```

call read_init(LINIT, LOU, cckwrk, nspecies)
call read_cadpl(LCADPL, LOU)
call read_mesh(LMESH, LOU)

```

* Set up initial mesh distribution

```

call set_mesh(LSCREEN, LOU, x, xnew, npts)
nptss = npts - 1
xcheck = x(npts-1)
if(npts .GT. nptsmx) then
  write (6,*) npts
  stop ' Number of mesh points has exceeded maximum
: limit'
endif

```

* Determine the number of PDEs, which include K species and temperature

```

npde = nspecies + 1

gasconst = 8.31431d3      /* unit is J/(Kmol*k) */

remesh = .false.
nrmesh = 3
dxmesh = 0.0d0
trmesh = 0.0d0
const = 2.0d0/(npts - 1.0d0)
xratio = 1.5d0
xi(1) = 0.0d0
norm = 'A'
laopt = 'B'

neqn = npde*npts + ncode

do i = 1, 30
  algopt(i) = 0.0d0
enddo

```

```
algot(1) = 1.0d0
algot(2) = 5.0d0
algot(3) = 1.0d0
algot(4) = 2.0d0
algot(12) = 1.0d-20
algot(13) = 1.0d-1
algot(14) = 1.0d-12
```

```
ind = 0
itask = 1
itrace = 0
ipminf = 0
itol = 1
```

```
atol(1) = 1.0d-10
rtol(1) = 1.0d-3
```

* SET INITIAL CONDITIONS

```
call uvinit(npde, npts, nxi, x, xi, u, ncode, v)
```

```
time_ini = 0.0d0
timeold = 0.0d0
timenew = 0.0d0
```

```
do i = 1, npts
  firsttime(i) = .true.
enddo
```

```
index = 1
```

```
call interpolate(time_ini, pressure, dpdt, length, avspeed, tconst)
```

```
do 10 j = 1, npts
  do 20 i = 1, nspecies
    y(i) = u(npde*(j - 1) + i)
20 continue
  call ck_mmwy(y, ickwrk, rckwrk, wtm(j))
10 continue
```

```
do i = 1, npts
  temp(i) = u(npde*(i - 1) + npde)
  rho(i) = pressure*wtm(i)/(gasconst*temp(i))
enddo
```

```
call integrate_x(nspecies, npts, npde, rho, length, rckwrk, u, x, sumspec)
```

```
write(LDATA) npts, npde
```

```
write(LDATA) time_ini
write(LDATA) (x(i), i = 1, npts)
write(LDATA) (u(i), i = 1, npde*npts)
write(LDATA) pressure
```

```

write(LINTEG,1000) time_ini, (sumspec(i), i = 1 , nspecies)

ts = 0.0d0

* set the first data point to be 1.0d-6 sec

tout = 1.0d-6

more = .TRUE.
iteration = 0

do 30 while (more)

    iteration = iteration + 1
    ifail = 0

    if( tout .LT. tinc ) then
        tout = tout*10.0
        if( tout .GE. tinc ) tout = tinc
    else
        tout = tout + tinc
    endif

    elapsed = dtime(time)

* call PDE solver

    call d03ppf(npde, m, ts, tout, pdedef, bndary, uvinit, u, npts,
+           x, ncode, d03pck, nxi, xi, neqn, rtol, atol, itol,
+           norm, laopt, algopt, remesh, nxfix, xfix, nrmesh,
+           dxmesh, trmesh, ipminf, xratio, const, monitf, w,
+           nw, iw, niw, itask, itrace, ind, ifail)

    elapsed = dtime(time)

    write(LRESULT, '(i4,f10.1,1pe12.3)') iteration, elapsed, tout

    call interpolate(tout,pressure,dpdt,length,avespeed,tconst)

    do 40 j = 1 , npts
        do 50 i = 1 , nspecies
            y(i) = u(npde*(j - 1) + i)
50 continue
            call ck_mmwy(y,ickwrk,rckwrk,wtm(j))
40 continue

    do i = 1 , npts
        temp(i) = u(npde*(i - 1) + npde)
        rho(i) = pressure*wtm(i)/(gasconst*temp(i))
    enddo

    call coord_tran(npts, length, rho, x, xnew)
    call integrate_x(nspecies,npts,npde,rho,length,rckwrk,u,xnew,sumspec)

```

```

write(LDATA) tout
write(LDATA) (xnew(i), i = 1 , npts)
write(LDATA) (u(i), i = 1 , npde*npts)
write(LDATA) pressure
write(LINTEG,1000) tout, (sumspec(i), i = 1,nspecies)

```

```

more = tout .lt. tmax

```

```

30 continue

```

*** PRINT INTEGRATION STATISTICS**

```

write (LRESULT, 2000) iw(1), iw(2), iw(3), iw(5)
write (LRESULT,*) (u(npde*(i-1)+npde), i = 1 , npts)
stop

```

```

1000 format (<nspecies+1>(1pe13.4))
2000 format (/i4, ' integration steps in time',
+ /i4, ' residual evaluations of resulting ODE system',
+ /i4, ' Jacobian evaluations',
+ /i4, ' iterations of nonlinear solver', /)

```

```

end

```

* =====

```

subroutine uvinit(npde, npts, nxi, x, xi, u, ncode, v)

```

```

*
* This subroutine specifies initial profiles of temperatures and mass fraction
* of all species. Users might modify this subroutine to meet their special
* initial profiles
*

```

```

integer      npde,nxi,npts,ncode,resInt,nptsmx,leniwk,lenrwk,lencwk
double precision      x(npts),xi(*), u(npde, npts), v(*)

```

```

logical      woc,cold

```

```

parameter      (leniwk = 7500, lenrwk = 90000, lencwk = 500 )
integer      ickwrk(leniwk), imcwrk(leniwk)
double precision      rckwrk(lenrwk), rmcwrk(lenrwk)
character      cckwrk(lencwk)*(16)

```

```

common /ckspi/ ickwrk,imcwrk
common /ckspr/ rckwrk, rmcwrk
common /ckspc/ cckwrk

```

```

integer      i, j, ii, index, nptss, nspecies
common /pointers/ index, nptss, nspecies

```

```

double precision      temp_l, temp_r, tmax, tinc, cri_temp, x_l(100),
:      x_r(100),y_l(100), y_r(100)

```

```

common /initdat/ temp_l, temp_r, tmax, tinc, x_l, x_r

integer l_point, i_point, r_point
double precision wid_c, wid_bl, wid_i, factor, steep
COMMON /meshdat/ wid_c, wid_bl, wid_i, factor, l_point, i_point, r_point

parameter (cri_temp = 800.0)

i = 1
woc = .false.

* Change molar fraction to mass fraction

call ck_x2y(x_l,ickwrk,rckwrk,y_l)
call ck_x2y(x_r,ickwrk,rckwrk,y_r)

do 10 while (i .LE. l_point+1)

    do j = 1,nspecies
        u(j,i) = y_l(j) /* mass fraction of species */
    enddo
    u(npde,i) = temp_l /* initial temperature */
    i = i + 1

10 continue

ii = i
*
*----- Temperature profile (SAE 870459) fitted to CARS
*----- measurement by Lucht et al.
*
cold = .true.

do 50 i = ii, npts
    do 60 j = 1, nspecies
        if (cold) then
            u(j,i) = y_l(j)
        else
            u(j,i) = y_r(j)
        endif
    60 continue

    if(x(i) .GE. wid_c) then
        if(x(i) .LE. wid_bl) then
            u(npde,i) = temp_l+(temp_r-temp_l)*((x(i)-x(ii-1))/
:            (wid_bl-x(ii-1)))*0.25
        else
            u(npde,i) = temp_r
        endif
    else
        u(npde,i) = temp_l
    endif

    if(u(npde,i) .GE. cri_temp) cold = .false.

```

50 continue

ii = i

do 70 i = ii, npts

do 80 j = 1, nspecies

u(j,i) = y_r(j)

80 continue

u(npde,i) = temp_r

70 continue

return

end

```
*=====
* P D E  d e f i n i t i o n s
*=====
```

subroutine pdedef(npde, time, x, u, dudx, ncode, v, vdot, p, q, r, ires)

integer npdemx, maxpts, leniwk, lenrwk, lencwk

parameter (npdemx = 80, nptsmx = 205, leniwk = 7500, lenrwk = 90000, lencwk = 500)

double precision time, x

integer ires, npde, ncode

double precision dudx(npde), v(*), vdot(*), p(npde, npde), q(npde), r(npde), u(npde)

integer i, j

double precision time_ini, rho, rhol, length, dpdt, avspeed, sumwh,

: sumnhv, wtm, temperature, pressure, cpbar, conmix,

: init_kin, init_tau, init_l, kin, tconst, turb_diff,

: a_total

parameter (init_l = 3.0d-3)

double precision diffmc(npdemx), hml(npdemx), wi(npdemx), molarf(npdemx)

integer ickwrk(leniwk), imcwrk(leniwk)

double precision rckwrk(lenrwk), rmcwrk(lenrwk)

character cckwrk(lencwk)*(16)

common /ckspi/ ickwrk, imcwrk

common /ckspr/ rckwrk, rmcwrk

common /ckspc/ cckwrk

integer index, nptss, nspecies

common /pointers/ index, nptss, nspecies

double precision timeold, timenew, xcheck

common /timedif/ timeold, timenew, xcheck

logical firsttime(nptsmx)

common /starttime/ firsttime

double precision init_rhol(nptsmx), gasconst

common /transform/ init_rhol

common /gconst/ gasconst


```

temperature = u(npde)

C Calculate product of initial length and density

if (firsttime(index)) then
  time_ini = 0.0d0
  call ck_mmwy(u,ickwrk,rckwrk,wtm)
  call interpolate(time_ini,pressure,dpdt,length,avespeed,tconst)
  init_rhol(index) = pressure*wtm/(gasconst*temperature)*length
  firsttime(index) = .false.
endif

call interpolate(time,pressure,dpdt,length,avespeed,tconst) /* unit of pressure is pa (N/m^2) */

call ck_mmwy(u,ickwrk,rckwrk,wtm) /* unit of mean molar weight is Kg/Kmole */
rho = pressure*wtm/(gasconst*temperature) /* Unit of density is Kg/m^3 */
rhol = rho*length

call ck_species_source(pressure, temperature, u, ickwrk, rckwrk, wi)
/* Unit of wi (production rate of species) is Kg/(m^3*sec) */

do 90 i = 1, nspecies
  q(i) = -(init_rhol(index)*wi(i)/rhol)
90 continue

C*****
C*-----
C*
C* Sandia CHEMKIN and TRANSPORT subroutine libraries are called
C* to return the thermodynamic and transport properties of species
C*
C*-----

call ck_y2x(u,ickwrk,rckwrk,molarf) /* convert mass fraction to molar fraction */
call ck_cpbl(temperature,molarf,ickwrk,rckwrk,cpbar)
cpbar = cpbar/wtm /* convert from unit J/(Kmole*k) to J/(Kg*K) */
call ck_hml(temperature, ickwrk, rckwrk, hml) /* Unit of enthalpy is J/Kmole */
call ck_react_heat(wi,hml,rckwrk,sumwh) /* Unit of reaction heat is J/m**3s */

call mc_acion(temperature, molarf, rmcwrk, conmix)
call mc_adif(pressure, temperature, molarf, rmcwrk, diffmc)

q(npde) = init_rhol(index)*(sumwh-dpdt)/rhol

*
* Calculate the turbulent transport coefficients
*

init_kin = 1.5*(0.75*avespeed)*(0.75*avespeed)
init_tau = init_l/sqrt(init_kin)
kin = init_kin*(1+0.9*(tconst+time)/init_tau)**(-1.11)
turb_diff = 0.09*x/(1+x/init_l)*sqrt(kin)

sumnhv = 0.0d0

```

```

do 100 i = 1, nspecies
  r(i) = rhol*rho*(diffmc(i)+turb_diff)*dudx(i)/init_rhol(index)
100 continue

```

```

a_total = turb_diff + conmix/(rho*cpbar)
a_total = a_total*rho*cpbar

```

```

r(npde) = rhol*(a_total*dudx(npde))/init_rhol(index)

```

```

do 110 i = 1, npde
  do 120 j = 1, npde
    if (i .eq. j) then
      if (i .eq. npde) then
        p(i, j) = cpbar*init_rhol(index)/length
      else
        p(i, j) = init_rhol(index)/length
      endif
    else
      p(i, j) = 0.0d0
    endif
  120 continue
110 continue

```

```

index = index + 1
if(index .gt. nptss) then
  if(x .lt. xcheck) stop 'counting index is not correct !'
  if(time .ne. timeold) then
    write(8,*) time
    call flush(8)
    timeold = time
  endif
  index = 1
endif

return
end

```

```

* =====
* Boundary conditons
* =====

```

```

subroutine bndary(npde, time, u, ux, ncode, v, vdot, ibnd, beta, gamma, ires)

```

```

double precision      time
integer               npde, ncode, ibnd, ires
double precision      v(*), vdot(*), beta(npde), gamma(npde), u(npde), ux(npde)

```

```

integer               i

```

```

double precision      temp_l, temp_r, tmax, tinc, x_l(100), x_r(100)
common                /initdat/ temp_l, temp_r, tmax, tinc, x_l, x_r

```

```

do i = 1, npde
  beta(i) = 0.0d0

```

```

        enddo

        if (ibnd .eq. 0) then

* LEFT BOUNDARY /* cold wall boundary condition */

        do i = 1, npde-1
            gamma(i) = ux(i)
        enddo

        gamma(npde) = u(npde) - temp_l

        else

* RIGHT BOUNDARY /* burned gas side boundary condition */

        do i = 1, npde
            gamma(i) = ux(i)
        enddo

        endif

        return
    end

* =====
* Remesh Monitor Function
* =====

subroutine monitf(t, npts, npde, x, u, r, fmon)

integer            npdemx
parameter          ( npdemx = 80 )

double precision   t
integer            npde, npts
double precision   fmon(npts), r(npde, npts), u(npde, npts), x(npts)
double precision   drdx, maxdrdx, h, extremes(2, npdemx), diff
integer            i, k, l
intrinsic          abs, max, min

* FIND EXTREME VALUES

do i = 1, npde
    extremes(1, i) = 0.0d0
    extremes(2, i) = 0.0d0
enddo

do 130 i = 1, npts
    do 140 j = 1, npde
        extremes(1, j) = min(extremes(1, j), u(j, i))
        extremes(2, j) = max(extremes(2, j), u(j, i))
    enddo
enddo

```

```
140 continue
130 continue
```

*** CALCULATE DERIVATIVES**

```
do 150 i = 1, npts - 1

  k = max(1, i - 1)
  l = min(npts, i + 1)
  h = (x(l) - x(k))*0.5d0
```

```
  maxdrdx = 0
```

*** Calculate second derivative of temperature only**

```
  if (extremes(1, npde) .eq. extremes(2, npde)) then
    drdx = 0.0d0
  else
    diff = extremes(2, npde) - extremes(1, npde)
    drdx = ((u(npde, i + 1) - extremes(1, npde))/diff - (u(npde, i) - extremes(1, npde))/diff)/h
  endif
```

```
  maxdrdx = max(maxdrdx, abs(drdx))
```

```
  fmon(i) = maxdrdx**(0.25)
```

```
150 continue
```

```
  fmon(npts) = fmon(npts - 1)
```

```
  write(6, '(1pe17.8)') t
```

```
  return
  end
```

***----- SETUP MESH**

```
*=====
* Initialize mesh points distribution
* This subroutine can be modified to meet special needs
*=====
```

```
  subroutine set_mesh(LSCREEN, LOUT, x, xnew, npts)
```

```
  double precision x(*), xnew(*)
  integer LSCREEN, LOUT, npts
```

```
  integer maxpoint
  double precision hx, sum_dist, interval, criterion
  parameter (maxpoint = 100, criterion = 0.05)
```

```
  logical exceed
  integer i
  integer l_point, i_point, r_point
```

```
double precision wid_c, wid_bl, wid_i, factor
COMMON /meshdat/ wid_c, wid_bl, wid_i, factor, l_point, i_point, r_point
```

* calculate the distance between two mesh points in interface region

```
hx = wid_i/i_point
```

* calculate the mesh points on left side of interface region

```
sum_dist = 0.0d0
interval = hx
```

```
exceed = .True.
```

```
do 160 i = 1 , maxpoint
  sum_dist = sum_dist + interval
  if(sum_dist .ge. wid_c) then
    l_point = i
    exceed = .False.
    goto 170
  endif
  interval = interval*factor
```

```
160 continue
```

```
170 if(exceed) stop ' maxpoint limit (on left boundary zone) has
:been exceeded, please check your mesh input file'
```

```
write(LSCREEN,2500) sum_dist
write(LOUT,2500) sum_dist
x(2) = interval
interval = interval/factor
```

* Set up mesh distribution for left boundary zone

```
x(1) = 0.0d0
do i = 3, l_point+1
  x(i) = x(i-1)+interval
  interval = interval/factor
enddo
```

* Set up mesh distribution for interface zone

```
do i = l_point+2 , l_point+i_point+2
  x(i) = x(i-1)+hx
enddo
```

* Set up mesh distribution for right boundary zone, in current case the final
* distance of right boundary (i.e. Xinf) depends on the number of points in the
* right boundary zone (user's input)

```
interval = hx
do i = l_point+i_point+3 , l_point+i_point+r_point+1
  x(i) = x(i-1)+ interval
  interval = interval*factor
enddo
```

```

npts = l_point+i_point+r_point+1

do i = 1 , npts
  xnew(i) = x(i)
enddo

write(LOUT,3000)
write(LOUT,4000) (x(i) , i = 1, npts)
write(LOUT,5000) npts

2500 format('Exact width of left boundary zone is :', 1PE12.4, '(M)')
3000 format('----- Details of mesh distribution -----')
4000 format(5(1PE11.4,3x))
5000 format('Number of mesh points :',I4)

end

*----- coordinate transform (back to original spatial coordinate)
*=====
* Co-ordinate transformation
*=====

subroutine coord_tran(npts, length, rho, x, xnew)

integer npts
double precision length
double precision rho(*), x(*), xnew(*)

integer nptsmx
parameter (nptsmx = 205)
double precision init_rhol(nptsmx)
common /transform/ init_rhol

integer i , j

do i = 1 , npts
  xnew(i) = 0.0d0
enddo

do i = 2 , npts
  xnew(i) = xnew(i-1)+(init_rhol(i)+init_rhol(i-1))*0.5/
:      (length*(rho(i)+rho(i-1))*0.5)*(x(i)-x(i-1))
enddo

return
end

*----- calculate integrated results
*=====
* Integrate species concentration from x=0 to xinf
* Transfer results based on mass basis into the ones of molar basis
*=====

subroutine integrate_x(nspecies,npts,npde,rho,length,rckwrk,u,xnew,sumspec)

```

```

integer nspecies, npts, npde
double precision length
double precision rho(*), u(*), xnew(*), sumspec(*), rckwrk(*)

```

```

integer i , j

```

```

COMMON /CKSTRT/ NMM , NKK , NII , MXSP, MXTB, MXTP, NCP , NCP1,
1      NCP2, NCP2T,NPAR, NLAR, NFAR, NLAN, NFAL, NREV,
2      NTHB, NRLT, NWL,  IcMM, IcKK, IcNC, IcPH, IcCH,
3      IcNT, IcNU, IcNK, IcNS, IcNR, IcLT, IcRL, IcRV,
4      IcWL, IcFL, IcFO, IcKF, IcTB, IcKN, IcKT, NcAW,
5      NcWT, NcTT, NcAA, NcCO, NcRV, NcLT, NcRL, NcFL,
6      NcKT, NcWL, NcRU, NcRC, NcPA, NcKF, NcKR, NcK1,
7      NcK2, NcK3, NcK4, NcI1, NcI2, NcI3, NcI4

```

```

do i = 1 , nspecies
  sumspec(i) = 0.0d0
enddo

```

```

do 180 i = 1, nspecies
  do 190 j = 2, npts
    sumspec(i)=sumspec(i)+((rho(j)+rho(j-1))*0.5)*
:      ((u(npde*(j-1)+i)+u(npde*(j-2)+i))*0.5)*
:      length*(xnew(j)-xnew(j-1))/rckwrk(NcWT+i-1)

```

```

190 continue

```

```

180 continue

```

```

return
end

```

```

*----- Interpolate pressure

```

```

*=====
* Interpolate corresponding pressure accroding to the input (time)
*=====

```

```

Subroutine interpolate(time,p,dpdt,l,barsp,t)

```

```

double precision time, p, dpdt, l, barsp,t
double precision ca, stroke
parameter (stroke = 8.8d-2)
integer i
double precision speed(1),cad(360), pressure(360), length(360)
COMMON /CADPLDAT/ speed, cad, pressure, length

```

```

*
* Convert input (time) into corresponding crank angle
*

```

```

If(time .EQ. 0.0d0) then
  p = pressure(1)
  dpdt = (pressure(2)-pressure(1))/(cad(2)-cad(1))
: *(speed(1)/60.0*360.0)
  l = length(1)
  barsp = speed(1)/60.0*2.0*stroke

```

```

    t = (cad(1)-375)/(speed(1)/60.0*360.0)
    return
else
    ca = cad(1) + time * (speed(1)/60.0*360.0)
endif

*
* Interpolation
*
do i = 1 , 359
    if(ca .GE. cad(i) .AND. ca .LE. cad(i+1)) then
        p = pressure(i) + (ca-cad(i))/(cad(i+1)-cad(i))*
:         (pressure(i+1)-pressure(i))
        dpdt = (pressure(i+1)-pressure(i))/(cad(i+1)-cad(i))
:         *(speed(1)/60.0*360.0)
        l = length(i) + (ca-cad(i))/(cad(i+1)-cad(i))*(length(i+1)
:         -length(i))
        goto 100
    endif
enddo

stop 'Current crank angle degree cannot be bracketed by input crank angle
: list!'

100 continue

*
* Calculate average engine speed and time constant used for turbulent model
*

barsp = speed(1)/60.0*2.0*stroke
t = (cad(1)-375)/(speed(1)/60.0*360.0)

return
end

```

(b) interp.f

```

Subroutine READ_INIT(LINIT, LOUT, CCKWRK, NSPECIES)
C
C BEGIN PROLOGUE
C
C Read initial condition file and store all input into arrays
C
C Input: LINIT, LOUT are indexes of input/output files
C
C CCKWRK - Array of character work space in cklink file
C Data type - character array
C Dimension CCKWRK(*) at least LENCWK
C Output: NSPECIES - Number of species in Chemical mechanism
C

```



```

C END PROLOGUE
C*****precision > double
  IMPLICIT DOUBLE PRECISION (A-H,O-Z), INTEGER (I-N)

  INTEGER LOUT
  CHARACTER CCKWRK(*)*(*)
  CHARACTER LINE*80, SUB(80)*80, UPCASE*10
  LOGICAL exist
  DIMENSION x_l(100),x_r(100)

  COMMON /CKSTRT/ NMM , NKK , NII , MXSP, MXTB, MXTP, NCP , NCP1,
1      NCP2, NCP2T,NPAR, NLAR, NFAR, NLAN, NFAL, NREV,
2      NTHB, NRLT, NWL, IcMM, IcKK, IcNC, IcPH, IcCH,
3      IcNT, IcNU, IcNK, IcNS, IcNR, IcLT, IcRL, IcRV,
4      IcWL, IcFL, IcFO, IcKF, IcTB, IcKN, IcKT, NcAW,
5      NcWT, NcTT, NcAA, NcCO, NcRV, NcLT, NcRL, NcFL,
6      NcKT, NcWL, NcRU, NcRC, NcPA, NcKF, NcKR, NcK1,
7      NcK2, NcK3, NcK4, NcI1, NcI2, NcI3, NcI4
  COMMON /INITDAT/ temp_l,temp_r,tmax, tinc, x_l,x_r

C
C Read initial conditions
C
  exist = .FALSE.

C
C Print the list of species in CKLINK file and the number of species
C
  write(LOUT,'(A)') '--- Species ordering --- (same as the cklink file)'
  do i = 1 , NKK
    write(LOUT,9020) CCKWRK(IcKK+i-1), i
  enddo
  write(LOUT,9030) NKK

30 continue

  read(LINIT,'(A)',END=6000) LINE
  ILEN = IPPLEN(LINE)
  if(ILEN .EQ. 0) GOTO 30
  exist = .TRUE.
  call CKISUB(LINE(:ILEN), SUB, NSUB)

C
C Match main key words : LEFT, RIGHT, TMAX, TINC, and END
C
35 continue

  if(UPCASE(SUB(1),4) .EQ. 'LEFT') then
    write(LOUT,'(/,A)') '--- INITIAL CONDITIONS AT LEFT BOUNDARY ---'
40  read(LINIT,'(A)') LINE
    ILEN = IPPLEN(LINE)
    if(ILEN .EQ. 0) GOTO 40
    call CKISUB(LINE(:ILEN), SUB, NSUB)

  if(UPCASE(SUB(1),4) .EQ. 'TEMP') then
    call IPPARR(SUB(2),1,1,temp_l,nval,ier,LOUT)
    write(LOUT,9040) temp_l

```

```

    if(ier .eq. 2) stop 'Left temperature is missing in
:file initial'
    else if(UPCASE(SUB(1),4) .EQ. 'REAC') then
        do i = 1 , NKK
            lsub = ILASCH(SUB(2))-IFIRCH(SUB(2))+1
            IFIR = IFIRCH(CCKWRK(IcKK+i-1))
            ILAS = ILASCH(CCKWRK(IcKK+i-1))
            if(UPCASE(SUB(2),lsub) .EQ. CCKWRK(IcKK+i-1)(IFIR:ILAS))
:then
                call IPPARR(SUB(3),1,1,x_l(i),nval,ier,LOUT)
                write(LOUT,9050) SUB(2),x_l(i)
                if(ier .eq. 2) stop 'Left molar fraction is missing in
:file initial'
                    goto 40
                endif
            enddo
            stop 'Left species name can not be matched !'
        else
            goto 35
        endif

        goto 40

    else if(UPCASE(SUB(1),5) .EQ. 'RIGHT') then
        write(LOUT,'(/,A)') '-- INITIAL CONDITIONS AT RIGHT BOUNDARY ---'
50 read(LINIT,'(A)') LINE
        ILEN = IPPLEN(LINE)
        if(ILEN .EQ. 0) GOTO 50
        call CKISUB(LINE(:ILEN), SUB, NSUB)

        if(UPCASE(SUB(1),4) .EQ. 'TEMP') then
            call IPPARR(SUB(2),1,1,temp_r,nval,ier,LOUT)
            write(LOUT,9040) temp_r
            if(ier .eq. 2) stop 'Right temperature is missing in
: file initial'
        else if(UPCASE(SUB(1),4) .EQ. 'REAC') then
            do i = 1 , NKK
                lsub = ILASCH(SUB(2))-IFIRCH(SUB(2))+1
                IFIR = IFIRCH(CCKWRK(IcKK+i-1))
                ILAS = ILASCH(CCKWRK(IcKK+i-1))
                if(UPCASE(SUB(2),lsub) .EQ. CCKWRK(IcKK+i-1)(IFIR:ILAS))
: then
                    call IPPARR(SUB(3),1,1,x_r(i),nval,ier,LOUT)
                    write(LOUT,9050) SUB(2),x_r(i)
                    if(ier .eq. 2) stop 'Right molar fraction is missing in file
: initial'
                        goto 50
                    endif
                enddo
                stop 'Right species name can not be matched !'
            else
                goto 35
            endif

            goto 50

```

```

else if(UPCASE(SUB(1),4) .EQ. 'TMAX') then
  call IPPARR(SUB(2),1,1,tmax,nval,ier,LOUT)
  write(LOUT,9060) tmax
  goto 30

else if(UPCASE(SUB(1),4) .EQ. 'TINC') then
  call IPPARR(SUB(2),1,1,tinc,nval,ier,LOUT)
  write(LOUT,9070) tinc
  goto 30

else if(UPCASE(SUB(1),3) .EQ. 'END') then
  write(LOUT,'(A,/)') '----- End of initial file -----'
  goto 6000

else
  stop 'Key words can not be matched, please check initial file'

endif

```

```

6000 if(.NOT. exist) stop 'Check initial file, it is empty !'
      close(LINIT)

```

```

NSPECIES = NKK

```

```

9020 format(' REAC ',A, I3)
9030 format(' TOTAL NUMBER OF SPECIES : ', I4,/)
9040 format(' TEMPERATURE : ', 1PE12.4,'(K)')
9050 format(' SPECIES : ',A12,1PE12.4)
9060 format(' MAX. TIME: ', 1PE12.4,'(S)')
9070 format(' INCREMENTAL TIME STEP : ', 1PE12.4,'(S)')

```

```

return
end

```

```

C
C-----C
C Subroutine READ_CADPL(LCADPL, LOUT)
C
C BEGIN PROLOGUE
C
C Read cad-pressure-length input files and store information into arrays
C
C Input: LCADPL, and LOUT are indexes of input/output files
C
C
C END PROLOGUE
C****precision > double
      IMPLICIT DOUBLE PRECISION (A-H,O-Z), INTEGER (I-N)

      CHARACTER LINE*80, SUB(80)*80, UPCASE*10
      LOGICAL exist
      double precision length(360)
      DIMENSION speed(1),cad(360), pressure(360)

```

COMMON /CADPLDAT/ speed, cad, pressure, length

```
CC
CC READ CAD-PRESSURE-LENGTH INPUT DATA
CC
  exist = .FALSE.
  10 continue
  read(LCADPL,'(A)',END=5000) LINE
  ILEN = IPPLEN(LINE)
  if( ILEN .EQ. 0) GOTO 10
  call CKISUB(LINE(:ILEN), SUB, NSUB)
C
C Read engine speed
C
  if(UPCASE(SUB(1),5) .NE. 'SPEED') stop 'Please put engine speed(RPM)
: in the first line of input file (cad-p-l)'
  call IPPARR(SUB(2),1,1,speed,nfound,ier,LOUT)
  if(ier .eq. 2) stop 'Engine speed is missing in file cad-p-l'
  write(LOUT,9000)
  write(LOUT,9010) speed
  exist = .TRUE.
C
C Read crankangle(degree)-pressure(n/m^2)-length(m) data
C
  write(LOUT,9020)
  do i = 1 , 1000
  20 continue
  read(LCADPL,'(A)',END=5000) LINE
  ILEN = IPPLEN(LINE)
  if(ILEN .EQ. 0) GOTO 20

  call CKISUB(LINE(:ILEN), SUB, NSUB)
  call IPPARR(SUB(1),1,1,cad(i),nval,ier,LOUT)
  call IPPARR(SUB(2),1,1,pressure(i),nval,ier,LOUT)
  call IPPARR(SUB(3),1,1,length(i),nval,ier,LOUT)
  write(LOUT,9030)cad(i),pressure(i),length(i)
  if(NSUB .NE. 3) stop 'Something is missing in cad-p-l file'
  enddo

5000 if(.NOT. exist) stop 'Check cad-p-l file, it is empty !'
  write(LOUT, '(A,/)') '----- End of cad-p-l file -----'
  close(LCADPL)

9000 format('* Length : distance between cylinder head and piston *')
9010 format(' Engine Speed :, 1PE12.4)
9020 format('__Crankangle__Pressure__Length__')
9030 format(3(1PE12.4))
  end
C
C-----C
  Subroutine READ_MESH(LMESH, LOUT)
C
C BEGIN PROLOGUE
```

```

C
C Read initial mesh file and store information
C
C   Input: LMESS, and LOU are indexes of input/output files
C
C
C END PROLOGUE
C****precision > double
  IMPLICIT DOUBLE PRECISION (A-H,O-Z), INTEGER (I-N)
  LOGICAL exist
  CHARACTER LINE*80, SUB(80)*80, UPCASE*10
  integer r_point
  COMMON /meshdat/ wid_c, wid_bl, wid_i, factor, l_point, i_point, r_point

  exist = .FALSE.
  write(LOUT,'(A)') '----- MESH SETUP (input) -----'
10 continue
  read(LMESS,'(A)',END=5000) LINE
  ILEN = IPPLEN(LINE)
  if( ILEN .EQ. 0) GOTO 10
  call CKISUB(LINE(:ILEN), SUB, NSUB)

  exist = .TRUE.

  if(UPCASE(SUB(1),2) .EQ. 'BL') then
    call IPPARR(SUB(2),1,1,wid_bl,nval,ier,LOUT)
    write(LOUT,9000) wid_bl
    goto 10

  else if(UPCASE(SUB(1),2) .EQ. 'WC') then
    call IPPARR(SUB(2),1,1,wid_c,nval,ier,LOUT)
    write(LOUT,9000) wid_c
    goto 10

  else if(UPCASE(SUB(1),2) .EQ. 'IW') then
    call IPPARR(SUB(2),1,1,wid_i,nval,ier,LOUT)
    write(LOUT,9010) wid_i
    goto 10

  else if(UPCASE(SUB(1),2) .EQ. 'IP') then
    read(SUB(2),'(I4)') i_point
    write(LOUT,9020)i_point
    goto 10

  else if(UPCASE(SUB(1),2) .EQ. 'RP') then
    read(SUB(2),'(I4)') r_point
    write(LOUT,9025)r_point
    goto 10

  else if(UPCASE(SUB(1),2) .EQ. 'GF') then
    call IPPARR(SUB(2),1,1,factor,nval,ier,LOUT)
    write(LOUT,9030) factor
    goto 10

  else if(UPCASE(SUB(1),3) .EQ. 'END') then

```

```

write(LOUT,'(A,/)') '----- End of mesh file -----'
goto 5000

else
  stop 'Key word can not be matched, please check mesh
:file again !'
endif

5000 if(.NOT. exist) stop 'Check cad-p-l file, it is empty !'
close(LCADPL)

9000 format ('Width of left-side-zone of a step function ',1PE12.4)
9010 format ('Width of interface of a step function ',1PE12.4)
9020 format ('Number of mesh points in interface zone of a step
  1 function ',I4)
9025 format ('Number of mesh points in right boundary zone of a step
  1 function ',I4)
9030 format ('Growth Factor of the interval width between two
  1 mesh points ',1PE12.4)
end

C
C-----C
SUBROUTINE CKISUB (LINE, SUB, NSUB)
C
C Generates an array of CHAR*(*) substrings from a CHAR*(*) string,
C using blanks or tabs as delimiters
C
C Input: LINE - a CHAR*(*) line
C Output: SUB - a CHAR*(*) array of substrings
C NSUB - number of substrings found
C A '!' will comment out a line, or remainder of the line.
C F. Rupley, Div. 8245, 5/15/86
C-----C
C*****precision > double
IMPLICIT DOUBLE PRECISION (A-H,O-Z), INTEGER (I-N)
C*****END precision > double
C*****precision > single
C IMPLICIT REAL (A-H,O-Z), INTEGER (I-N)
C*****END precision > single
C
CHARACTER*(*) SUB(*), LINE
NSUB = 0
C
DO 5 N = 1, LEN(LINE)
  IF (ICHAR(LINE(N:N)) .EQ. 9) LINE(N:N) = ' '
5 CONTINUE
C
IF (IPPLEN(LINE) .LE. 0) RETURN
C
ILEN = ILASCH(LINE)
C
NSTART = IFIRCH(LINE)
10 CONTINUE

```

```

ISTART = NSTART
NSUB = NSUB + 1
SUB(NSUB) = ''
C
DO 100 I = ISTART, ILEN
  ILAST = INDEX(LINE(ISTART:),' ') - 1
  IF (ILAST .GT. 0) THEN
    ILAST = ISTART + ILAST - 1
  ELSE
    ILAST = ILEN
  ENDIF
  SUB(NSUB) = LINE(ISTART:ILAST)
  IF (ILAST .EQ. ILEN) RETURN
C
  NSTART = ILAST + IFIRCH(LINE(ILAST+1:))
C
C   Does SUB have any slashes?
C
  I1 = INDEX(SUB(NSUB),'/')
  IF (I1 .LE. 0) THEN
    IF (LINE(NSTART:NSTART) .NE. '/') GO TO 10
    NEND = NSTART + INDEX(LINE(NSTART+1:),'/')
    IND = INDEX(SUB(NSUB),' ')
    SUB(NSUB)(IND:) = LINE(NSTART:NEND)
    IF (NEND .EQ. ILEN) RETURN
    NSTART = NEND + IFIRCH(LINE(NEND+1:))
    GO TO 10
  ENDIF
C
C   Does SUB have 2 slashes?
C
  I2 = INDEX(SUB(NSUB)(I1+1:),'/')
  IF (I2 .GT. 0) GO TO 10
C
  NEND = NSTART + INDEX(LINE(NSTART+1:),'/')
  IND = INDEX(SUB(NSUB),' ') + 1
  SUB(NSUB)(IND:) = LINE(NSTART:NEND)
  IF (NEND .EQ. ILEN) RETURN
  NSTART = NEND + IFIRCH(LINE(NEND+1:))
  GO TO 10
100 CONTINUE
  RETURN
  END
C
C
C-----
C
C   CHARACTER*(*) FUNCTION UPCASE(ISTR, ILEN)
C
C   START PROLOGUE
C
C   FUNCTION UPCASE(ISTR, ILEN)
C   return an uppercase character string according to the assigned length
C
C   INPUT

```

```

C  ISTR   - Input character string
C          data type - character array
C  ILEN   - length of the character string returned
C          data type - integer
C
C  OUTPUT
C  UPCASE - Returned uppercase character string
C          data type - character array
C
C  END PROLOGUE
C
C  CHARACTER ISTR*(*), LCASE(26)*1, UCASE(26)*1
C  DATA LCASE /'a','b','c','d','e','f','g','h','i','j','k','l','m',
1         'n','o','p','q','r','s','t','u','v','w','x','y','z'/,
2  UCASE /'A','B','C','D','E','F','G','H','I','J','K','L','M',
3         'N','O','P','Q','R','S','T','U','V','W','X','Y','Z'/
C
C  UPCASE = ''
C  UPCASE = ISTR(:ILEN)
C  JJ = MIN (LEN(UPCASE), LEN(ISTR), ILEN)
C  DO 10 J = 1, JJ
C     DO 10 N = 1,26
C        IF (ISTR(J:J) .EQ. LCASE(N)) UPCASE(J:J) = UCASE(N)
10 CONTINUE
C  RETURN
C  END

```

(c) ck_1d.f

```

C
C-----C
C
C  SUBROUTINE CK_CPBL (T, X, ICKWRK, RCKWRK, CPBML)
C
C  START PROLOGUE
C
C  SUBROUTINE CK_CPBL (T, X, ICKWRK, RCKWRK, CPBML)
C  Returns the mean specific heat at constant pressure;
C  see Eq. (33).
C
C  INPUT
C  T   - Temperature.
C       cgs units - K
C       Data type - real scalar
C  X   - Mole fractions of the species.
C       cgs units - none
C       Data type - real array
C       Dimension X(*) at least KK, the total number of
C       species.
C  ICKWRK - Array of integer workspace.
C       Data type - integer array

```



```

C      Dimension ICKWRK(*) at least LENIWK.
C      RCKWRK - Array of real work space.
C      Data type - real array
C      Dimension RCKWRK(*) at least LENRWK.
C
C      OUTPUT
C      CPBML - Mean specific heat at constant pressure in molar units.
C      Units - J/(Kmole*K), which is converted from
C      cgs units - ergs/(mole*K)
C      Data type - real scalar
C
C      END PROLOGUE
C
C*****double precision
      IMPLICIT DOUBLE PRECISION (A-H, O-Z), INTEGER (I-N)
C*****END double precision
C*****single precision
      IMPLICIT REAL (A-H, O-Z), INTEGER (I-N)
C*****END single precision
C
      DIMENSION ICKWRK(*), RCKWRK(*), X(*)
      COMMON /CKSTRT/ NMM , NKK , NII , MXSP, MXTB, MXTP, NCP , NCP1,
1      NCP2, NCP2T, NPAR, NLAR, NFAR, NLAN, NFAL, NREV,
2      NTHB, NRLT, NWL, IcMM, IcKK, IcNC, IcPH, IcCH,
3      IcNT, IcNU, IcNK, IcNS, IcNR, IcLT, IcRL, IcRV,
4      IcWL, IcFL, IcFO, IcKF, IcTB, IcKN, IcKT, NcAW,
5      NcWT, NcTT, NcAA, NcCO, NcRV, NcLT, NcRL, NcFL,
6      NcKT, NcWL, NcRU, NcRC, NcPA, NcKF, NcKR, NcK1,
7      NcK2, NcK3, NcK4, NcI1, NcI2, NcI3, NcI4
C
      CALL CKCPML (T, ICKWRK, RCKWRK, RCKWRK(NcK1))
C
      CPBML = 0.0
      DO 100 K = 1, NKK
          CPBML = CPBML + X(K)*RCKWRK(NcK1 + K - 1)
100 CONTINUE
C
C      Convert unit from ergs/(mole*K) to J/(K mole*K)
C
      CPBML = CPBML * 1.0D-4
      RETURN
      END
C
C-----C
C
      SUBROUTINE CK_HML (T, ICKWRK, RCKWRK, HML)
C
C      START PROLOGUE
C
C      SUBROUTINE CKHML (T, ICKWRK, RCKWRK, HML)
C      Returns the enthalpies in molar units
C
C      INPUT

```

```

C  T  - Temperature.
C      cgs units - K
C      Data type - real scalar
C  ICKWRK - Array of integer workspace.
C      Data type - integer array
C      Dimension ICKWRK(*) at least LENIWK.
C  RCKWRK - Array of real work space.
C      Data type - real array
C      Dimension RCKWRK(*) at least LENRWK.
C
C OUTPUT
C  HML  - Enthalpies in molar units for the species.
C      units - J/Kmole, which is converted from
C      cgs units - ergs/mole
C      Data type - real array
C      Dimension HML(*) at least KK, the total number of
C      species.
C
C END PROLOGUE
C
C*****double precision
      IMPLICIT DOUBLE PRECISION (A-H, O-Z), INTEGER (I-N)
C*****END double precision
C*****single precision
C      IMPLICIT REAL (A-H, O-Z), INTEGER (I-N)
C*****END single precision
C
      DIMENSION ICKWRK(*), RCKWRK(*), HML(*), TN(10)
      COMMON /CKSTRT/ NMM , NKK , NII , MXSP, MXTB, MXTP, NCP , NCP1,
1      NCP2, NCP2T, NPAR, NLAR, NFAR, NLAN, NFAL, NREV,
2      NTHB, NRLT, NWL,  IcMM, IcKK, IcNC, IcPH, IcCH,
3      IcNT, IcNU, IcNK, IcNS, IcNR, IcLT, IcRL, IcRV,
4      IcWL, IcFL, IcFO, IcKF, IcTB, IcKN, IcKT, NcAW,
5      NcWT, NcTT, NcAA, NcCO, NcRV, NcLT, NcRL, NcFL,
6      NcKT, NcWL, NcRU, NcRC, NcPA, NcKF, NcKR, NcK1,
7      NcK2, NcK3, NcK4, NcI1, NcI2, NcI3, NcI4
C
      RUT = T*RCKWRK(NcRU)
      TN(1) = 1.0
      DO 150 N = 2, NCP
          TN(N) = T**(N-1)/N
150 CONTINUE
C
      DO 250 K = 1, NKK
          L = 1
          DO 220 N = 2, ICKWRK(IcNT + K - 1)-1
              TEMP = RCKWRK(NcTT + (K-1)*MXTP + N - 1)
              IF (T .GT. TEMP) L = L+1
220 CONTINUE
C
          NA1 = NcAA + (L-1)*NCP2 + (K-1)*NCP2T
          SUM = 0.0
          DO 225 N = 1, NCP
              SUM = SUM + TN(N)*RCKWRK(NA1 + N - 1)
225 CONTINUE

```

```

      HML(K) = RUT * (SUM + RCKWRK(NA1 + NCP1 - 1)/T)
C
C Convert units from ergs/mole to J/Kmole
C
      HML(K) = HML(K) * 1.0D-4
250 CONTINUE
      RETURN
      END
C
C-----C
C
      SUBROUTINE CK_REACT_HEAT (PR, HML, RCKWRK, RH)
C
C START PROLOGUE
C
C SUBROUTINE CK_REACT_HEAT (PR, HML, RH)
C Returns the rate of the reaction heat
C
C INPUT
C PR - Production rate of species
C      units - Kg/(m^3*s)
C      Dimension PR(*) at least KK, the total number of
C      species
C HML - Enthalpies in molar units for the species.
C      mks units - J/Kmole
C      Data type - real array
C      Dimension HML(*) at least KK, the total number of
C      species.
C
C OUTPUT
C RH - Rate of the heat of reaction
C      units - J/(m^3*s)
C      Data type - real scalar
C
C END PROLOGUE
C
C*****double precision
      IMPLICIT DOUBLE PRECISION (A-H, O-Z), INTEGER (I-N)
C*****END double precision
C*****single precision
      IMPLICIT REAL (A-H, O-Z), INTEGER (I-N)
C*****END single precision
C
      DIMENSION PR(*), HML(*), RCKWRK(*)
      COMMON /CKSTRT/ NMM , NKK , NII , MXSP, MXTB, MXTP, NCP , NCP1,
1      NCP2, NCP2T,NPAR, NLAR, NFAR, NLAN, NFAL, NREV,
2      NTHB, NRLT, NWL, IcMM, IcKK, IcNC, IcPH, IcCH,
3      IcNT, IcNU, IcNK, IcNS, IcNR, IcLT, IcRL, IcRV,
4      IcWL, IcFL, IcFO, IcKF, IcTB, IcKN, IcKT, NcAW,
5      NcWT, NcTT, NcAA, NcCO, NcRV, NcLT, NcRL, NcFL,
6      NcKT, NcWL, NcRU, NcRC, NcPA, NcKF, NcKR, NcK1,
7      NcK2, NcK3, NcK4, NcI1, NcI2, NcI3, NcI4
C
      RH = 0.0
      DO 150 N = 1, NKK

```

```

      RH = RH + PR(N)*HML(N)/RCKWRK(NcWT + N - 1)
150 CONTINUE
      RETURN
      END
C
C-----C
C
      SUBROUTINE CK_MMWX (X, ICKWRK, RCKWRK, WTM)
C
C START PROLOGUE
C
C SUBROUTINE CKMMWX (X, ICKWRK, RCKWRK, WTM)
C Returns the mean molecular weight of the gas mixture given the
C mole fractions; see Eq. (4).
C
C INPUT
C X - Mole fractions of the species.
C cgs units - none
C Data type - real array
C Dimension X(*) at least KK, the total number of
C species.
C ICKWRK - Array of integer workspace.
C Data type - integer array
C Dimension ICKWRK(*) at least LENIWK.
C RCKWRK - Array of real work space.
C Data type - real array
C Dimension RCKWRK(*) at least LENRWK.
C
C OUTPUT
C WTM - mean molecular weight of the species mixture.
C MKS units - kgm/kmol
C Data type - real scalar
C
C END PROLOGUE
C
C*****double precision
      IMPLICIT DOUBLE PRECISION (A-H, O-Z), INTEGER (I-N)
C*****END double precision
C*****single precision
      IMPLICIT REAL (A-H, O-Z), INTEGER (I-N)
C*****END single precision
C
      DIMENSION X(*), ICKWRK(*), RCKWRK(*)
      COMMON /CKSTRT/ NMM , NKK , NII , MXSP, MXTB, MXTP, NCP , NCP1,
1      NCP2, NCP2T,NPAR, NLAR, NFAR, NLAN, NFAL, NREV,
2      NTHB, NRLT, NWL, IcMM, IcKK, IcNC, IcPH, IcCH,
3      IcNT, IcNU, IcNK, IcNS, IcNR, IcLT, IcRL, IcRV,
4      IcWL, IcFL, IcFO, IcKF, IcTB, IcKN, IcKT, NcAW,
5      NcWT, NcTT, NcAA, NcCO, NcRV, NcLT, NcRL, NcFL,
6      NcKT, NcWL, NcRU, NcRC, NcPA, NcKF, NcKR, NcK1,
7      NcK2, NcK3, NcK4, NcI1, NcI2, NcI3, NcI4
C
      WTM = 0.0
      DO 100 K = 1, NKK
          WTM = WTM + X(K)*RCKWRK(NcWT + K - 1)

```

```

100 CONTINUE
  RETURN
  END
C
C-----C
C-----C
C
  SUBROUTINE CK_MMWY (Y, ICKWRK, RCKWRK, WTM)
C
C START PROLOGUE
C
C SUBROUTINE CKMMWY (Y, ICKWRK, RCKWRK, WTM)
C Returns the mean molecular weight of the gas mixture given the
C mass fractions; see Eq. (3).
C
C INPUT
C Y - Mass fractions of the species.
C cgs units - none
C Data type - real array
C Dimension Y(*) at least KK, the total number of
C species.
C ICKWRK - Array of integer workspace.
C Data type - integer array
C Dimension ICKWRK(*) at least LENIWK.
C RCKWRK - Array of real work space.
C Data type - real array
C Dimension RCKWRK(*) at least LENRWK.
C
C OUTPUT
C WTM - mean molecular weight of the species mixture.
C MKS units - kgm/Kmole
C Data type - real scalar
C
C END PROLOGUE
C
C*****double precision
  IMPLICIT DOUBLE PRECISION (A-H, O-Z), INTEGER (I-N)
C*****END double precision
C*****single precision
  IMPLICIT REAL (A-H, O-Z), INTEGER (I-N)
C*****END single precision
C
  DIMENSION Y(*), ICKWRK(*), RCKWRK(*)
  COMMON /CKSTRT/ NMM , NKK , NII , MXSP, MXTB, MXTP, NCP , NCP1,
  1 NCP2, NCP2T, NPAR, NLAR, NFAR, NLAN, NFAL, NREV,
  2 NTHB, NRLT, NWL, IcMM, IcKK, IcNC, IcPH, IcCH,
  3 IcNT, IcNU, IcNK, IcNS, IcNR, IcLT, IcRL, IcRV,
  4 IcWL, IcFL, IcFO, IcKF, IcTB, IcKN, IcKT, NcAW,
  5 NcWT, NcTT, NcAA, NcCO, NcRV, NcLT, NcRL, NcFL,
  6 NcKT, NcWL, NcRU, NcRC, NcPA, NcKF, NcKR, NcK1,
  7 NcK2, NcK3, NcK4, NcI1, NcI2, NcI3, NcI4
C
  WTM = 0.0
  DO 100 K = 1, NKK
    WTM = WTM + Y(K)/RCKWRK(NcWT + K - 1)

```

100 CONTINUE

WTM = 1.0/WTM

RETURN

END

C

C-----C

C

SUBROUTINE CK_SPECIES_SOURCE (P, T, Y, ICKWRK, RCKWRK, WDOT)

C

C START PROLOGUE

C

C SUBROUTINE CK_SPECIES_SOURCE (P, T, Y, ICKWRK, RCKWRK, WDOT)

C

Returns the mass production rates of the species given the
pressure, temperature and mass fractions; see Eq. (49).

C

C INPUT

C

P - Pressure.

C

mks units - N/m² will be converted into

C

cgs units - dynes/cm² for CHEMKIN LIBRARY

C

1 N/m² = 10 dyne/cm²

C

Data type - real scalar

C

T - Temperature.

C

units - K

C

Data type - real scalar

C

Y - Mass fractions of the species.

C

cgs units - none

C

Data type - real array

C

Dimension Y(*) at least KK, the total number of
species.

C

ICKWRK - Array of integer workspace.

C

Data type - integer array

C

Dimension ICKWRK(*) at least LENIWK.

C

RCKWRK - Array of real work space.

C

Data type - real array

C

Dimension RCKWRK(*) at least LENRWK.

C

C OUTPUT

C

WDOT - Chemical mass production rates of the species.

C

mks units - Kg/(m³*sec)

C

Data type - real array

C

Dimension WDOT(*) at least KK, the total number of
species.

C

C

C

C

C

C

C

C

C

C

C

C

C

C

C

C

C

DIMENSION ICKWRK(*), RCKWRK(*), Y(*), WDOT(*)

```

COMMON /CKSTRT/ NMM , NKK , NII , MXSP, MXTB, MXTP, NCP , NCP1,
1      NCP2, NCP2T,NPAR, NLAR, NFAR, NLAN, NFAL, NREV,
2      NTHB, NRLT, NWL, IcMM, IcKK, IcNC, IcPH, IcCH,
3      IcNT, IcNU, IcNK, IcNS, IcNR, IcLT, IcRL, IcRV,
4      IcWL, IcFL, IcFO, IcKF, IcTB, IcKN, IcKT, NcAW,
5      NcWT, NcTT, NcAA, NcCO, NcRV, NcLT, NcRL, NcFL,
6      NcKT, NcWL, NcRU, NcRC, NcPA, NcKF, NcKR, NcK1,
7      NcK2, NcK3, NcK4, NcI1, NcI2, NcI3, NcI4

dimension km(3000),im(3000),num(3000),nok(100)
common /ckknui/ km,im,num,nok,norderk
C
CALL CKRATT (RCKWRK, ICKWRK, NII, MXSP, RCKWRK(NcRU),
1      RCKWRK(NcPA), T, ICKWRK(IcNS), ICKWRK(IcNU),
2      ICKWRK(IcNK), NPAR+1, RCKWRK(NcCO), NREV,
3      ICKWRK(IcRV), RCKWRK(NcRV), NLAN, NLAR, ICKWRK(IcLT),
4      RCKWRK(NcLT), NRLT, ICKWRK(IcRL), RCKWRK(NcRL),
5      RCKWRK(NcK1), RCKWRK(NcKF), RCKWRK(NcKR),
6      RCKWRK(NcI1))
C
P = P * 10.0 /* Convert into dyne/cm^2 */

CALL CKYTCP (P, T, Y, ICKWRK, RCKWRK, RCKWRK(NcK1))
C
C for some reason, if molar fraction is less than zero, the concentration would
C be assigned to zero
C
C do i = 1 , NKK
C   if(RCKWRK(Nck1+i-1) .LT. 0.0d0) RCKWRK(Nck1+i-1) = 0.0d0
C   enddo

CALL CKRATX (NII, NKK, MXSP, MXTB, T, RCKWRK(NcK1), ICKWRK(IcNS),
1      ICKWRK(IcNU), ICKWRK(IcNK), NFAL, ICKWRK(IcFL),
2      ICKWRK(IcFO), ICKWRK(IcKF), NFAR, RCKWRK(NcFL),
3      NTHB, ICKWRK(IcTB), ICKWRK(IcKN), RCKWRK(NcKT),
4      ICKWRK(IcKT), RCKWRK(NcKF), RCKWRK(NcKR),
5      RCKWRK(NcI1), RCKWRK(NcI2), RCKWRK(NcI3))
C
DO 50 K = 1, NKK
  WDOT(K) = 0.0
50 CONTINUE

ncount = 0
DO 110 KK = 1 , norderk
  Do 120 N = 1 , nok(KK)
    ncount = ncount + 1
    I = im(ncount)
    K = km(ncount)
    WDOT(K) = WDOT(K)+(RCKWRK(NcI1+I-1)-RCKWRK(NcI2+I-1))*num(ncount)
120 CONTINUE
110 CONTINUE
C
C convert from moles/cm^3*s into Kg/m^3*s

```

```

C
DO 150 K = 1, NKK
  WDOT(K) = WDOT(K)*RCKWRK(NcWT+K-1)*1.0d3
150 CONTINUE

P = P * 1.0D-1 /* Convert into N/M^2 */
RETURN
END

C
C-----C
C
C SUBROUTINE CK_FLUX (P, T, Y, NOS, CREAT, ICKWRK, cckwrk, rckwrk)
C
C START PROLOGUE
C
C INPUT
C P - Pressure.
C     mks units - N/m^2 will be converted into
C     cgs units - dynes/cm^2 for CHEMKIN LIBRARY
C     1 N/m**2 = 10 dyne/cm^2
C     Data type - real scalar
C T - Temperature.
C     units - K
C     Data type - real scalar
C Y - Mass fractions of the species.
C     cgs units - none
C     Data type - real array
C     Dimension Y(*) at least KK, the total number of
C     species.
C ICKWRK - Array of integer workspace.
C     Data type - integer array
C     Dimension ICKWRK(*) at least LENIWK.
C RCKWRK - Array of real work space.
C     Data type - real array
C     Dimension RCKWRK(*) at least LENRWK.
C
C
C END PROLOGUE
C
C*****precision > double
  IMPLICIT DOUBLE PRECISION (A-H, O-Z), INTEGER (I-N)
C*****END precision > double
C*****precision > single
  IMPLICIT REAL (A-H, O-Z), INTEGER (I-N)
C*****END precision > single
C
  DIMENSION ICKWRK(*), RCKWRK(*), Y(*)
  COMMON /CKSTRT/ NMM , NKK , NII , MXSP, MXTB, MXTP, NCP , NCP1,
1     NCP2, NCP2T,NPAR, NLAR, NFAR, NLAN, NFAL, NREV,
2     NTHB, NRLT, NWL, IcMM, IcKK, IcNC, IcPH, IcCH,
3     IcNT, IcNU, IcNK, IcNS, IcNR, IcLT, IcRL, IcRV,
4     IcWL, IcFL, IcFO, IcKF, IcTB, IcKN, IcKT, NcAW,
5     NcWT, NcTT, NcAA, NcCO, NcRV, NcLT, NcRL, NcFL,
6     NcKT, NcWL, NcRU, NcRC, NcPA, NcKF, NcKR, NcK1,

```



```

7      NcK2, NcK3, NcK4, NcI1, NcI2, NcI3, NcI4
CHARACTER CCKWRK(*)*(*),CREACT(*)*(*)
logical found
dimension ir(300),Q(300)
dimension km(3000),im(3000),num(3000),nok(100)
common /ckknui/ km,im,num,nok,norderk

```

C

```

CALL CKRATT (RCKWRK, ICKWRK, NII, MXSP, RCKWRK(NcRU),
1      RCKWRK(NcPA), T, ICKWRK(IcNS), ICKWRK(IcNU),
2      ICKWRK(IcNK), NPAR+1, RCKWRK(NcCO), NREV,
3      ICKWRK(IcRV), RCKWRK(NcRV), NLAN, NLAR, ICKWRK(IcLT),
4      RCKWRK(NcLT), NRLT, ICKWRK(IcRL), RCKWRK(NcRL),
5      RCKWRK(NcK1), RCKWRK(NcKF), RCKWRK(NcKR),
6      RCKWRK(NcI1))

```

C

```

P = P * 10.0 /* Convert into dyne/cm^2 */

```

```

CALL CKYTCP (P, T, Y, ICKWRK, RCKWRK, RCKWRK(NcK1))

```

```

CALL CKRATX (NII, NKK, MXSP, MXTB, T, RCKWRK(NcK1), ICKWRK(IcNS),
1      ICKWRK(IcNU), ICKWRK(IcNK), NFAL, ICKWRK(IcFL),
2      ICKWRK(IcFO), ICKWRK(IcKF), NFAR, RCKWRK(NcFL),
3      NTHB, ICKWRK(IcTB), ICKWRK(IcKN), RCKWRK(NcKT),
4      ICKWRK(IcKT), RCKWRK(NcKF), RCKWRK(NcKR),
5      RCKWRK(NcI1), RCKWRK(NcI2), RCKWRK(NcI3))

```

C

```

do i = 1 , 100
  Q(i) = 0.0d0
  ir(i) = 0
enddo

```

C

C Locate the reactions which are related to the species of interest

C

```

found = .false.
ncount = 0
nc = 1
DO 110 KK = 1 , norderk
  Do 120 N = 1 , nok(KK)
    ncount = ncount + 1
    I = im(ncount)
    K = km(ncount)
    if(K .eq. NOS) then
      found = .true.
      Q(nc) = (RCKWRK(NcI1+I-1)-RCKWRK(NcI2+I-1))*num(ncount)*1.0d3
      ir(nc) = I
      nc = nc + 1
    endif
120 CONTINUE
110 CONTINUE

```

```

if(.not. found) stop 'there is no reaction related to this species found'
nc = nc - 1

```

C

C Sort out the reactions by the absolute values and rank them
C

```
Do 130 i = 2 , nc
  do 140 j = i , 2 , -1
    if(ABS(Q(j)) .GT. ABS(Q(j-1))) then
      buffer = Q(j)
      Q(j) = Q(j-1)
      Q(j-1) = buffer
      ibuffer = ir(j)
      ir(j) = ir(j-1)
      ir(j-1) = ibuffer
    else
      goto 130
    endif
  140 continue
130 continue
```

C
C Print out the ranking also provide the information about the percentage with
C regard to the maximum reaction rate
C

```
write(6,'(A,A,A//)' '----- Rank of reactions associated to ',
& cckwrk(IcKK+NOS-1),'-----')
write(6,*) 'No.      Reaction      Reaction rate  %'
write(6,*) '          (K mole/m^3*s)  '
write(6,*) '-----'
```

```
Do i = 1 , nc
  k = ir(i)
  write(6,'(I3,A35,1PE12.4,3X,1PE10.2)') i,creact(k)(1:35),Q(i),
& Q(i)/Q(1)*100
enddo
```

P = P * 1.0D-1 /* Convert into N/M^2 */

RETURN
END

C

C-----C

C

SUBROUTINE CK_MOLE_PRODUCTION (P, T, Y, ICKWRK, RCKWRK, WDOT)

C

C START PROLOGUE

C

C SUBROUTINE CK_MOLE_PRODUCTION (P, T, Y, ICKWRK, RCKWRK, WDOT)

C Returns the mole fraction production rates of the species given the

C pressure, temperature and mass fractions; see Eq. (49).

C

C INPUT

C P - Pressure.

C mks units - N/m^2 will be converted into

C cgs units - dynes/cm^2 for CHEMKIN LIBRARY

C 1 N/m**2 = 10 dyne/cm^2

C Data type - real scalar

```

C  T  - Temperature.
C      units - K
C      Data type - real scalar
C  Y  - Mass fractions of the species.
C      cgs units - none
C      Data type - real array
C      Dimension Y(*) at least KK, the total number of
C      species.
C  ICKWRK - Array of integer workspace.
C      Data type - integer array
C      Dimension ICKWRK(*) at least LENIWK.
C  RCKWRK - Array of real work space.
C      Data type - real array
C      Dimension RCKWRK(*) at least LENRWK.
C
C  OUTPUT
C  WDOT - Chemical mole fraction production rates of the species.
C      mks units - Kmole/(m^3*sec)
C      Data type - real array
C      Dimension WDOT(*) at least KK, the total number of
C      species.
C
C  END PROLOGUE
C
C*****precision > double
C      IMPLICIT DOUBLE PRECISION (A-H, O-Z), INTEGER (I-N)
C*****END precision > double
C*****precision > single
C      IMPLICIT REAL (A-H, O-Z), INTEGER (I-N)
C*****END precision > single
C
C      DIMENSION ICKWRK(*), RCKWRK(*), Y(*), WDOT(*)
C      COMMON /CKSTRT/ NMM , NKK , NII , MXSP, MXTB, MXTP , NCP1,
1      NCP2, NCP2T,NPAR, NLAR, NFAR, NLAN, NFAL, NREV,
2      NTHB, NRLT, NWL,  IcMM, IcKK, IcNC, IcPH, IcCH,
3      IcNT, IcNU, IcNK, IcNS, IcNR, IcLT, IcRL, IcRV,
4      IcWL, IcFL, IcFO, IcKF, IcTB, IcKN, IcKT, NcAW,
5      NcWT, NcTT, NcAA, NcCO, NcRV, NcLT, NcRL, NcFL,
6      NcKT, NcWL, NcRU, NcRC, NcPA, NcKF, NcKR, NcK1,
7      NcK2, NcK3, NcK4, NcI1, NcI2, NcI3, NcI4
C
C      CALL CKRATT (RCKWRK, ICKWRK, NII, MXSP, RCKWRK(NcRU),
1      RCKWRK(NcPA), T, ICKWRK(IcNS), ICKWRK(IcNU),
2      ICKWRK(IcNK), NPAR+1, RCKWRK(NcCO), NREV,
3      ICKWRK(IcRV), RCKWRK(NcRV), NLAN, NLAR, ICKWRK(IcLT),
4      RCKWRK(NcLT), NRLT, ICKWRK(IcRL), RCKWRK(NcRL),
5      RCKWRK(NcK1), RCKWRK(NcKF), RCKWRK(NcKR),
6      RCKWRK(NcI1))
C
C      P = P * 10.0 /* Convert into dyne/cm^2 */
C
C      CALL CKYTCP (P, T, Y, ICKWRK, RCKWRK, RCKWRK(NcK1))
C
C for some reason, if molar fraction is less than zero, the concentration would
C be assigned to zero

```

C

```
CALL CKRATX (NII, NKK, MXSP, MXTB, T, RCKWRK(NcK1), ICKWRK(IcNS),
1   ICKWRK(IcNU), ICKWRK(IcNK), NFAL, ICKWRK(IcFL),
2   ICKWRK(IcFO), ICKWRK(IcKF), NFAR, RCKWRK(NcFL),
3   NTHB, ICKWRK(IcTB), ICKWRK(IcKN), RCKWRK(NcKT),
4   ICKWRK(IcKT), RCKWRK(NcKF), RCKWRK(NcKR),
5   RCKWRK(NcI1), RCKWRK(NcI2), RCKWRK(NcI3))
```

C

```
DO 50 K = 1, NKK
  WDOT(K) = 0.0
50 CONTINUE
```

```
DO 100 N = 1, MXSP
  DO 100 I = 1, NII
    K = ICKWRK(IcNK + (I-1)*MXSP + N - 1)
    NU = ICKWRK(IcNU + (I-1)*MXSP + N - 1)
    IF (K .NE. 0)
      1   WDOT(K) = WDOT(K) + (RCKWRK(NcI1+I-1) - RCKWRK(NcI2+I-1)) * NU
100 CONTINUE
```

C

C convert from moles/cm³*s into Kmole/m³*s

C

```
DO 150 K = 1, NKK
  WDOT(K) = WDOT(K) * 1.0d3
150 CONTINUE
```

```
P = P * 1.0D-1 /* Convert into N/M2 */
RETURN
END
```

C

C-----C

C

```
SUBROUTINE CK_Y2X (Y, ICKWRK, RCKWRK, X)
```

C

C START PROLOGUE

C

```
C SUBROUTINE CK_Y2X (Y, ICKWRK, RCKWRK, X)
```

C Convert molar fractions of the species to mass fractions of the
C the species.

C

C INPUT

C Y - Mass fractions of the species.

C mks units - none

C Data type - real array

C Dimension X(*) at least KK, the total number of
C species.

C ICKWRK - Array of integer workspace.

C Data type - integer array

C Dimension ICKWRK(*) at least LENIWK.

C RCKWRK - Array of real work space.

C Data type - real array

C Dimension RCKWRK(*) at least LENRWK.

```

C
C OUTPUT
C X - Array of mole fractions of the species.
C
C Dimension X(*) at least KK, the total number of
C species.
C
C END PROLOGUE
C
C*****double precision
IMPLICIT DOUBLE PRECISION (A-H, O-Z), INTEGER (I-N)
C*****END double precision
C*****single precision
C IMPLICIT REAL (A-H, O-Z), INTEGER (I-N)
C*****END single precision
C
DIMENSION Y(*), ICKWRK(*), RCKWRK(*), X(*)
COMMON /CKSTRT/ NMM , NKK , NII , MXSP, MXTB, MXTP, NCP , NCP1,
1 NCP2, NCP2T,NPAR, NLAR, NFAR, NLAN, NFAL, NREV,
2 NTHB, NRLT, NWL, IcMM, IcKK, IcNC, IcPH, IcCH,
3 IcNT, IcNU, IcNK, IcNS, IcNR, IcLT, IcRL, IcRV,
4 IcWL, IcFL, IcFO, IcKF, IcTB, IcKN, IcKT, NcAW,
5 NcWT, NcTT, NcAA, NcCO, NcRV, NcLT, NcRL, NcFL,
6 NcKT, NcWL, NcRU, NcRC, NcPA, NcKF, NcKR, NcK1,
7 NcK2, NcK3, NcK4, NcI1, NcI2, NcI3, NcI4
C
WTM = 0.0
DO 100 K = 1, NKK
WTM = WTM + Y(K)/RCKWRK(NcWT + K - 1)
100 CONTINUE
WTM = 1 / WTM

DO 200 I = 1, NKK
X(I) = Y(I)* WTM / RCKWRK(NcWT + I - 1)
200 CONTINUE

RETURN
END
C
-----C
C
SUBROUTINE CK_X2Y (X, ICKWRK, RCKWRK, Y)
C
C START PROLOGUE
C
C SUBROUTINE CK_X2Y (X, ICKWRK, RCKWRK, Y)
C Convert molar fractions of the species to mass fractions of the
C the species.
C
C INPUT
C X - Molar fractions of the species.
C mks units - none
C Data type - real array
C Dimension X(*) at least KK, the total number of
C species.

```

```

C  ICKWRK - Array of integer workspace.
C      Data type - integer array
C      Dimension ICKWRK(*) at least LENIWK.
C  RCKWRK - Array of real work space.
C      Data type - real array
C      Dimension RCKWRK(*) at least LENRWK.
C
C OUTPUT
C  Y  - Array of mass fractions of the species.
C
C      Dimension X(*) at least KK, the total number of
C      species.
C
C END PROLOGUE
C
C*****double precision
C      IMPLICIT DOUBLE PRECISION (A-H, O-Z), INTEGER (I-N)
C*****END double precision
C*****single precision
C      IMPLICIT REAL (A-H, O-Z), INTEGER (I-N)
C*****END single precision
C
C      DIMENSION Y(*), ICKWRK(*), RCKWRK(*), X(*)
C      COMMON /CKSTRT/ NMM , NKK , NII , MXSP, MXTB, MXTP, NCP , NCP1,
1      NCP2, NCP2T, NPAR, NLAR, NFAR, NLAN, NFAL, NREV,
2      NTHB, NRLT, NWL,  IcMM, IcKK, IcNC, IcPH, IcCH,
3      IcNT, IcNU, IcNK, IcNS, IcNR, IcLT, IcRL, IcRV,
4      IcWL, IcFL, IcFO, IcKF, IcTB, IcKN, IcKT, NcAW,
5      NcWT, NcTT, NcAA, NcCO, NcRV, NcLT, NcRL, NcFL,
6      NcKT, NcWL, NcRU, NcRC, NcPA, NcKF, NcKR, NcK1,
7      NcK2, NcK3, NcK4, NcI1, NcI2, NcI3, NcI4
C
C      WTM = 0.0
C      DO 100 K = 1, NKK
C          WTM = WTM + X(K)*RCKWRK(NcWT + K - 1)
100 CONTINUE
C
C      DO 200 I = 1, NKK
C          Y(I) = X(I)* RCKWRK(NcWT + I - 1) / WTM
200 CONTINUE
C
C      RETURN
C      END
C-----C
C
C      SUBROUTINE CK_INITIAL_KNUI(ICKWRK)
C
C START PROLOGUE
C
C      INITIALIZATION SUBROUTINE
C
C INPUT
C  ICKWRK - ARRAY OF INTEGER WORKSPACE.
C      DATA TYPE - INTEGER ARRAY

```

```

C          DIMENSION ICKWRK(*) AT LEAST LENIWK.
C
C OUTPUT
C
C END PROLOGUE
C
C*****precision > double
C  IMPLICIT DOUBLE PRECISION (A-H, O-Z), INTEGER (I-N)
C*****END precision > double
C*****precision > single
C  IMPLICIT REAL (A-H, O-Z), INTEGER (I-N)
C*****END precision > single
C
  DIMENSION ICKWRK(*)
  COMMON /CKSTRT/ NMM , NKK , NII , MXSP, MXTB, MXTP, NCP , NCP1,
1      NCP2, NCP2T,NPAR, NLAR, NFAR, NLAN, NFAL, NREV,
2      NTHB, NRLT, NWL, IcMM, IcKK, IcNC, IcPH, IcCH,
3      IcNT, IcNU, IcNK, IcNS, IcNR, IcLT, IcRL, IcRV,
4      IcWL, IcFL, IcFO, IcKF, IcTB, IcKN, IcKT, NcAW,
5      NcWT, NcTT, NcAA, NcCO, NcRV, NcLT, NcRL, NcFL,
6      NcKT, NcWL, NcRU, NcRC, NcPA, NcKF, NcKR, NcK1,
7      NcK2, NcK3, NcK4, NcI1, NcI2, NcI3, NcI4

  DIMENSION KM(3000),IM(3000),NUM(3000),NOK(100)
  COMMON /CKKNUI/ KM,IM,NUM,NOK,NORDERK
C
C DEMYSTERIFY THE MEANINGS OF VARIABLES :
C K : SPECIES
C I : REACTION
C NU : STOICHIOMETRIC COEFFICIENT ASSOCIATED WITH REACTION I FOR SPECIES K
C
  NCOUNT = 0
  DO 100 N = 1, MXSP
    DO 100 I = 1, NII
      K = ICKWRK(IcNK + (I-1)*MXSP + N - 1)
      NU= ICKWRK(IcNU + (I-1)*MXSP + N - 1)
      IF (K .NE. 0) THEN
        NCOUNT = NCOUNT + 1
        KM(NCOUNT) = K
        IM(NCOUNT) = I
        NUM(NCOUNT) = NU
      endif
    100 CONTINUE
C
C SORT OUT THE MATRIES ACCORDING TO THE ORDER OF K

  DO 150 I = 2 , NCOUNT
    DO 200 N = I,2,-1
      IF(KM(N-1) .GT. KM(N)) THEN
        KBUFFER = KM(N-1)
        KM(N-1) = KM(N)
        KM(N) =KBUFFER
        IBUFFER = IM(N-1)
        IM(N-1) = IM(N)
        IM(N) =IBUFFER

```

```

    NBUFFER = NUM(N-1)
    NUM(N-1) = NUM(N)
    NUM(N) = NBUFFER
  ENDIF

```

```

200 CONTINUE
150 CONTINUE

```

C COUNT HOW MANY ELEMENTS ARE OCCUPIED BY EACH K

```

  NKCOUNT = 1
  NORDERK = 1
  DO I = 2, NCOUNT
    IF (KM(I-1) .EQ. KM(I)) THEN
      NKCOUNT = NKCOUNT+1
    ELSE
      NOK(NORDERK) = NKCOUNT
      NKCOUNT = 1
      NORDERK = NORDERK + 1
    ENDIF
  ENDDO

```

C CHECK THE LAST ELEMENT

```

  IF(NKCOUNT .NE. 1) NOK(NORDERK) = NKCOUNT

```

```

  RETURN
  END

```

C

C-----C

C

```

  SUBROUTINE CK_REACTION_I (P,T,Y,ICKWRK,RCKWRK,NOS,NOR,IR,RM)

```

C

C START PROLOGUE

C

C RETURNS THE MOLE FRACTION PRODUCTION RATES OF THE SPECIES GIVEN THE
 C PRESSURE, TEMPERATURE AND MASS FRACTIONS; SEE EQ. (49) IN CHEMKIN MEMU.

C

C INPUT

C P - PRESSURE.

C MKS UNITS - N/M^2 WILL BE CONVERTED INTO

C CGS UNITS - DYNES/CM^2 FOR CHEMKIN LIBRARY

C 1 N/M**2 = 10 DYNE/CM^2

C DATA TYPE - REAL SCALAR

C T - TEMPERATURE.

C UNITS - K

C DATA TYPE - REAL SCALAR

C Y - MASS FRACTIONS OF THE SPECIES.

C CGS UNITS - NONE

C DATA TYPE - REAL ARRAY

C DIMENSION Y(*) AT LEAST KK, THE TOTAL NUMBER OF

C SPECIES.

C ICKWRK - ARRAY OF INTEGER WORKSPACE.

C DATA TYPE - INTEGER ARRAY

C DIMENSION ICKWRK(*) AT LEAST LENIWK.


```

C RCKWRK - ARRAY OF REAL WORK SPACE.
C DATA TYPE - REAL ARRAY
C DIMENSION RCKWRK(*) AT LEAST LENRWK.
C NOR - NUMBER OF REACTION OF INTEREST
C IR - ARRAY OF REACTIONS OF INTEREST
C DATA TYPE - INTEGER ARRAY DIMENSION
C IR(*) AT LEAST NOR
C
C OUTPUT
C RM - ARRAY OF REACTIONS RATE OF INTEREST
C DATA TYPE - DOUBLE PRECISION ARRAY
C MKS UNITS - KMOLE/(M^3*SEC)
C
C END PROLOGUE
C
C*****precision > double
C IMPLICIT DOUBLE PRECISION (A-H, O-Z), INTEGER (I-N)
C*****END precision > double
C*****precision > single
C IMPLICIT REAL (A-H, O-Z), INTEGER (I-N)
C*****END precision > single
C
C DIMENSION ICKWRK(*), RCKWRK(*), Y(*), RM(*),IR(*)

COMMON /CKSTRT/ NMM , NKK , NII , MXSP, MXTB, MXTP, NCP , NCP1,
1 NCP2, NCP2T,NPAR, NLAR, NFAR, NLAN, NFAL, NREV,
2 NTHB, NRLT, NWL, IcMM, IcKK, IcNC, IcPH, IcCH,
3 IcNT, IcNU, IcNK, IcNS, IcNR, IcLT, IcRL, IcRV,
4 IcWL, IcFL, IcFO, IcKF, IcTB, IcKN, IcKT, NcAW,
5 NcWT, NcTT, NcAA, NcCO, NcRV, NcLT, NcRL, NcFL,
6 NcKT, NcWL, NcRU, NcRC, NcPA, NcKF, NcKR, NcK1,
7 NcK2, NcK3, NcK4, NcI1, NcI2, NcI3, NcI4
C
CALL CKRATT (RCKWRK, ICKWRK, NII, MXSP, RCKWRK(NcRU),
1 RCKWRK(NcPA), T, ICKWRK(IcNS), ICKWRK(IcNU),
2 ICKWRK(IcNK), NPAR+1, RCKWRK(NcCO), NREV,
3 ICKWRK(IcRV), RCKWRK(NcRV), NLAN, NLAR, ICKWRK(IcLT),
4 RCKWRK(NcLT), NRLT, ICKWRK(IcRL), RCKWRK(NcRL),
5 RCKWRK(NcK1), RCKWRK(NcKF), RCKWRK(NcKR),
6 RCKWRK(NcI1))
C
P = P * 10.0 /* Convert into dyne/cm^2 */

CALL CKYTCP (P, T, Y, ICKWRK, RCKWRK, RCKWRK(NcK1))

CALL CKRATX (NII, NKK, MXSP, MXTB, T, RCKWRK(NcK1), ICKWRK(IcNS),
1 ICKWRK(IcNU), ICKWRK(IcNK), NFAL, ICKWRK(IcFL),
2 ICKWRK(IcFO), ICKWRK(IcKF), NFAR, RCKWRK(NcFL),
3 NTHB, ICKWRK(IcTB), ICKWRK(IcKN), RCKWRK(NcKT),
4 ICKWRK(IcKT), RCKWRK(NcKF), RCKWRK(NcKR),
5 RCKWRK(NcI1), RCKWRK(NcI2), RCKWRK(NcI3))

DO 50 K = 1, NOR
RM(K) = 0.0
50 CONTINUE

```

```

DO 100 II = 1, NOR
DO 100 N = 1, MXSP
I = IR(II)
K = ICKWRK(IcNK + (I-1)*MXSP + N - 1)
NU= ICKWRK(IcNU + (I-1)*MXSP + N - 1)
IF (K .EQ. NOS)
1   RM(II) = RM(II)+(RCKWRK(NcI1+I-1)-RCKWRK(NcI2+I-1))*NU*1.0d3
100 CONTINUE

P = P * 1.0D-1 /* Convert into N/M^2 */
RETURN
END

```

(d) tran_1d

```

C
C-----
C
C   SUBROUTINE MC_ACON (T, X, RMCWRK, CONMIX)
C
C*****double precision
C   IMPLICIT DOUBLE PRECISION (A-H, O-Z), INTEGER (I-N)
C*****END double precision
C
C*****single precision
C   IMPLICIT REAL (A-H, O-Z), INTEGER (I-N)
C*****END single precision
C
CCCCCCCCCCCCCCCCCCCCCCCCCCCCCCCCCCCCCCCCCCCCCCCCCCCCCCCCCCCCCCCC
CCC
C
C SUBROUTINE MCACON (T, X, RMCWRK, CONMIX)
C
C THIS SUBROUTINE COMPUTES THE MIXTURE THERMAL CONDUCTIVITY, GIVEN
C THE TEMPERATURE AND THE SPECIES MOLE FRACTIONS.
C
C INPUT-
C T   - TEMPERATURE
C     CGS UNITS - K.
C X   - ARRAY OF MOLE FRACTIONS OF THE MIXTURE.
C     DIMENSION X(*) AT LEAST KK.
C
C WORK-
C RMCWRK - ARRAY OF FLOATING POINT STORAGE AND WORK SPACE. THE
C STARTING ADDRESSES FOR THE RMCWRK SPACE ARE STORED IN
C COMMON /MCMCMC/.
C     DIMENSION RMCWRK(*) AT LEAST LENRMC.
C
C OUTPUT-
C CONMIX - MIXTURE THERMAL CONDUCTIVITY

```

```

C      UNITS - J/M*K*S, which is converted from cgs unit,
C      used in CHEMKIN library (ERG/CM*K*S).
C
CCCCCCCCCCCCCCCCCCCCCCCCCCCCCCCCCCCCCCCCCCCCCCCCCCCCCCCCCCCCCCCC
CCCC
C
C      DIMENSION X(*), RMCWRK(*)
C
COMMON /MCMCMC/ RU, PATMOS, SMALL, NKK, NO, NLITE, INLIN, IKTDIF,
1      IPVT, NWT, NEPS, NSIG, NDIP, NPOL, NZROT, NLAM,
2      NETA, NDIF, NTDIF, NXX, NVIS, NXI, NCP, NCROT,
3      NCINT, NPARK, NBIND, NEOK, NSGM, NAST, NBST,
4      NCST, NXL, NR, NWRK, K3
C
C
C      IN THE FOLLOWING CALL:
C      THE PURE SPECIES CONDUCTIVITIES ARE IN RMCWRK(NXI)
C
      ALOGT = LOG(T)
      CALL MCEVAL (ALOGT, NKK, NO, RMCWRK(NLAM), RMCWRK(NXI))
      DO 25 K = 1, NKK
          RMCWRK(NXI+K-1) = EXP(RMCWRK(NXI+K-1))
25 CONTINUE
C
      SUM = 0.0E0
      SUMR = 0.0E0
      DO 100 K = 1, NKK
          SUM = SUM + X(K)*RMCWRK(NXI+K-1)
          SUMR = SUMR + X(K)/RMCWRK(NXI+K-1)
100 CONTINUE
C
      CONMIX = 0.5E0 * (SUM + 1.0E0/SUMR)
C
      Change unit from ERG/CM*K*S to J/M*K*S

      CONMIX = CONMIX * 1.0E-5
C
      RETURN
      END
C
C-----
C
SUBROUTINE MC_ADIF (P, T, X, RMCWRK, D)
C
C*****double precision
      IMPLICIT DOUBLE PRECISION (A-H, O-Z), INTEGER (I-N)
C*****END double precision
C
C*****single precision
      IMPLICIT REAL (A-H, O-Z), INTEGER (I-N)
C*****END single precision
C
CCCCCCCCCCCCCCCCCCCCCCCCCCCCCCCCCCCCCCCCCCCCCCCCCCCCCCCCCCCCCCCC
CCC
C

```

```

C SUBROUTINE MCADIF (P, T, X, RMCWRK, D)
C
C THIS SUBROUTINE COMPUTES MIXTURE-AVERAGED DIFFUSION COEFFICIENTS
C GIVEN THE PRESSURE, TEMPERATURE, AND SPECIES MASS FRACTIONS.
C
C INPUT-
C P - PRESSURE
C     UNITS - PA, WHICH IS USED IN 1-D CODE, WILL BE CONVERTED INTO
C     CGS UNITS - DYNES/CM**2.
C T - TEMPERATURE
C     CGS UNITS - K.
C X - ARRAY OF MOLE FRACTIONS OF THE MIXTURE.
C     DIMENSION X(*) AT LEAST KK.
C
C WORK-
C RMCWRK - ARRAY OF FLOATING POINT STORAGE AND WORK SPACE. THE
C     STARTING ADDRESSES FOR THE RMCWRK SPACE ARE STORED IN
C     COMMON /MCMCMC/.
C     DIMENSION RMCWRK(*) AT LEAST LENRMC.
C
C OUTPUT-
C D - ARRAY OF MIXTURE DIFFUSION COEFFICIENTS
C     UNITS - M**2/S, which is converted from CGS unit,
C     used in CHEMKIN library.
C     DIMENSION D(*) AT LEAST KK.
C
CCCCCCCCCCCCCCCCCCCCCCCCCCCCCCCCCCCCCCCCCCCCCCCCCCCCCCCCCCCC
CCCC
C
C     DIMENSION X(*), D(*), RMCWRK(*)
C
COMMON /MCMCMC/ RU, PATMOS, SMALL, NKK, NO, NLITE, INLIN, IKTDIF,
1     IPVT, NWT, NEPS, NSIG, NDIP, NPOL, NZROT, NLAM,
2     NETA, NDIF, NTDIF, NXX, NVIS, NXI, NCP, NCROT,
3     NCINT, NPARK, NBIND, NEOK, NSGM, NAST, NBST,
4     NCST, NXL, NR, NWRK, K3
C
CALL MCEDIF (T, NO, NKK, X, RMCWRK(NDIF), RMCWRK(NWT), SMALL,
1     RMCWRK(NXX), RMCWRK(NBIND), D)
C
DO 100 K = 1, NKK

D(K) = D(K) * PATMOS/(P*1.0D1)
C Change unit from CM**2/S to M**2/S

D(K) = D(K) * 1.0E-4

100 CONTINUE
C
RETURN
END
C
SUBROUTINE MCINIT (LINKMC, LOUT, LENIMC, LENRMC, IMCWRK, RMCWRK)
C
C*****precision > double

```

```

      IMPLICIT DOUBLE PRECISION (A-H, O-Z), INTEGER (I-N)
C*****END precision > double
C
C*****precision > single
C  IMPLICIT REAL (A-H, O-Z), INTEGER (I-N)
C*****END precision > single
C
CCCCCCCCCCCCCCCCCCCCCCCCCCCCCCCCCCCCCCCCCCCCCCCCCCCCCCCCCCCC
CCC
C
C SUBROUTINE MCINIT (LINKMC, LOU, LENIMC, LENRMC, IMCWRK, RMCWRK)
C
C THIS SUBROUTINE SERVES TO READ THE LINKING FILE FROM THE FITTING
C CODE AND TO CREATE THE INTERNAL STORAGE AND WORK ARRAYS, IMCWRK(*)
C AND RMCWRK(*). MCINIT MUST BE CALLED BEFORE ANY OTHER TRANSPORT
C SUBROUTINE IS CALLED. IT MUST BE CALLED AFTER THE CHEMKIN PACKAGE
C IS INITIALIZED.
C
C INPUT-
C LINKMC - LOGICAL UNIT NUMBER OF THE LINKING FILE.
C          FITTING CODE WRITE TO DEFAULT UNIT 35
C LOU     - LOGICAL UNIT NUMBER FOR PRINTED OUTPUT.
C LENIMC  - ACTUAL DIMENSION OF THE INTEGER STORAGE AND WORKING
C          SPACE, ARRAY IMCWRK(*). LENIMC MUST BE AT LEAST:
C          LENIMC = 4*KK + NLITE
C          WHERE, KK  = NUMBER OF SPECIES.
C          NLITE = NUMBER OF SPECIES WITH MOLECULAR WEIGHT
C          LESS THAN 5.
C LENRMC  - ACTUAL DIMENSION OF THE FLOATING POINT STORAGE AND
C          WORKING SPACE, ARRAY RMCWRK(*). LENRMC MUST BE AT LEAST:
C          LENRMC = KK*(19 + 2*NO + NO*NLITE) + (NO+15)*KK**2
C          WHERE, KK  = NUMBER OF SPECIES.
C          NO   = ORDER OF THE POLYNOMIAL FITS,
C          DEFAULT, NO=4.
C          NLITE = NUMBER OF SPECIES WITH MOLECULAR WEIGHT
C          LESS THAN 5.
C
C WORK-
C IMCWRK  - ARRAY OF INTEGER STORAGE AND WORK SPACE. THE STARTING
C          ADDRESSES FOR THE IMCWRK SPACE ARE STORED IN
C          COMMON /MCMCMC/.
C          DIMENSION IMCWRK(*) AT LEAST LENIMC.
C RMCWRK  - ARRAY OF FLOATING POINT STORAGE AND WORK SPACE. THE
C          STARTING ADDRESSES FOR THE RMCWRK SPACE ARE STORED IN
C          COMMON /MCMCMC/.
C          DIMENSION RMCWRK(*) AT LEAST LENRMC.
C
CCCCCCCCCCCCCCCCCCCCCCCCCCCCCCCCCCCCCCCCCCCCCCCCCCCCCCCCCCCC
CCCCCCC
C
      DIMENSION IMCWRK(*), RMCWRK(*)
      CHARACTER*16 VERS, PREC
      LOGICAL IOK, ROK, KERR
      COMMON /MCCONS/ VERS, PREC, KERR, LENI, LENR
C

```

```

COMMON /MCMCMC/ RU, PATMOS, SMALL, NKK, NO, NLITE, INLIN, IKTDIF,
1      IPVT, NWT, NEPS, NSIG, NDIP, NPOL, NZROT, NLAM,
2      NETA, NDIF, NTDIF, NXX, NVIS, NXI, NCP,
3      NCROT, NCINT, NPARK, NBIND, NEOK, NSGM,
4      NAST, NBST, NCST, NXL, NR, NWRK, K3
C
C
C      THE FOLLOWING NUMBER SMALL IS USED IN THE MIXTURE DIFFUSION
C      COEFFICIENT CALCULATION. ITS USE ALLOWS A SMOOTH AND WELL
C      DEFINED DIFFUSION COEFFICIENT AS THE MIXTURE APPROACHES A
C      PURE SPECIES, EVEN THOUGH STRICTLY SPEAKING THERE DOES NOT
C      EXIST A DIFFUSION COEFFICIENT IN THIS CASE. THE VALUE OF
C      "SMALL" SHOULD BE SMALL RELATIVE TO ANY SPECIES MOLE FRACTION
C      OF IMPORTANCE, BUT LARGE ENOUGH TO BE REPRESENTED ON THE
C      COMPUTER.
C
SMALL = 1.0E-20
RU   = 8.314E+07
PATMOS= 1.01325E+06
C
CCCCCCCCCCCCCCCCCCCCCCCCCCCCCCCCCCCCCCCCCCCCCCCCCCCCCCCCCCCC
CCCCCC
C
C      WRITE VERSION NUMBER
C
WRITE (LOUT, 15)
15 FORMAT(
1' TRANLIB: Multicomponent transport library,',
2'   CHEMKIN-II Version 1.7, October 1992',
C*****precision > double
3'   DOUBLE PRECISION')
C*****END precision > double
C*****precision > single
C 3'   SINGLE PRECISION')
C*****END precision > single
C
CCCCCCCCCCCCCCCCCCCCCCCCCCCCCCCCCCCCCCCCCCCCCCCCCCCCCCCCCCCC
CCCCCCC
C
C      READ THE PROBLEM SIZE
C
CALL MCLEN (LINKMC, LOUT, LI, LR)
IOK = (LENIMC .GE. LI)
ROK = (LENRMC .GE. LR)
write(6,*) LENRMC, LR
C
IF (.NOT.IOK .OR. .NOT.ROK) THEN
  IF (.NOT. IOK) WRITE (LOUT, 300) LI
  IF (.NOT. ROK) WRITE (LOUT, 350) LR
  STOP
ENDIF
C
REWIND LINKMC
READ (LINKMC, ERR=999) VERS, PREC, KERR
READ (LINKMC, ERR=999) LI, LR, NO, NKK, NLITE

```

C
NK = NO*NKK
NK2 = NO*NKK*NKK
K2 = NKK*NKK
K3 = 3*NKK
K32 = K3*K3
NKT = NO*NKK*NLITE

C
C APPORTION THE REAL WORK SPACE
C THE POINTERS HAVE THE FOLLOWING MEANINGS:
C NWT - THE SPECIES MOLECULAR WEIGHTS.
C NEPS - THE EPSILON/K WELL DEPTH FOR THE SPECIES.
C NSIG - THE COLLISION DIAMETER FOR THE SPECIES.
C NDIP - THE DIPOLE MOMENTS FOR THE SPECIES.
C NPOL - THE POLARIZABILITIES FOR THE SPECIES.
C NZROT - THE ROTATIONAL RELAXATION COLLISION NUMBERS.
C NLAM - THE COEFFICIENTS FOR THE CONDUCTIVITY FITS.
C NETA - THE COEFFICIENTS FOR THE VISCOSITY FITS.
C NTDIF - THE COEFFICIENTS FOR THE THERMAL DIFFUSION
C RATIO FITS.
C NXX - THE MOLE FRACTIONS.
C NVIS - THE SPECIES VISCOSITIES.
C NXI - THE ROTATIONAL RELAXATION COLLISION NUMBERS BEFORE
C THE PARKER COFFECTION.
C NCP - THE SPECIES SPECIFIC HEATS.
C NCROT - THE ROTATIONAL PARTS OF THE SPECIFIC HEATS.
C NCINT - THE INTERNAL PARTS OF THE SPECIFIC HEATS.
C NPARK - THE ROTATIONAL RELAXATION COLLISION NUMBERS AFTER
C THE PARKER CORRECTION.
C NBIND - THE BINARY DIFFUSION COEFFICIENTS.
C NEOK - THE MATRIX OF REDUCED WELL DEPTHS.
C NSGM - THE MATRIX OF REDUCED COLLISION DIAMETERS.
C NAST - THE MATRIX OF A* COLLISION INTEGRALS FOR EACH
C SPECIES PAIR.
C NBST - THE MATRIX OF B* COLLISION INTEGRALS FOR EACH
C SPECIES PAIR.
C NCST - THE MATRIX OF C* COLLISION INTEGRALS FOR EACH
C SPECIES PAIR.
C NXL - THE "L" MATRIX.
C NR - THE RIGHT HAND SIDES OF THE LINEAR SYSTEM
C INVOLVING THE "L" MATRIX.
C NWRK - THE WORK SPACE NEEDED BY LINPACK TO SOLVE THE
C "L" MATRIX LINEAR SYSTEM.
C

NWT = 1
NEPS = NWT + NKK
NSIG = NEPS + NKK
NDIP = NSIG + NKK
NPOL = NDIP + NKK
NZROT = NPOL + NKK
C
NLAM = NZROT + NKK
NETA = NLAM + NK
NDIF = NETA + NK
NTDIF = NDIF + NK2

```

C
NXX = NTDIF + NO*NKK*NLITE
NVIS = NXX + NKK
NXI = NVIS + NKK
NCP = NXI + NKK
NCROT= NCP + NKK
NCINT= NCROT + NKK
NPARK= NCINT + NKK
C
NBIND= NPARK + NKK
NEOK = NBIND + K2
NSGM = NEOK + K2
NAST = NSGM + K2
NBST = NAST + K2
NCST = NBST + K2
C
NXL = NCST + K2
C
NR = NXL + K32
NWRK = NR + K3
NTOT = NWRK + K3 - 1
C
C   APPORTION THE INTEGER WORK SPACE
C   THE POINTERS HAVE THE FOLLOWING MEANING:
C
C   INLIN - THE INDICATORS FOR THE MOLECULE LINEARITY.
C   IKTDIF- THE SPECIES INDICIES FOR THE "LIGHT" SPECIES.
C   IPVT - THE PIVOT INDICIES FOR LINPACK CALLS.
C
INLIN = 1
IKTDIF= INLIN + NKK
IPVT = IKTDIF + NLITE
ITOT = IPVT + K3 - 1
C
C   READ THE DATA FROM THE LINK FILE
C
READ (LINKMC, ERR=999) PATMOS, (RMCWRK(NWT+N-1),
1 RMCWRK(NEPS+N-1), RMCWRK(NSIG+N-1),
2 RMCWRK(NDIP+N-1), RMCWRK(NPOL+N-1), RMCWRK(NZROT+N-1),
3 IMCWRK(INLIN+N-1), N=1,NKK),
4 (RMCWRK(NLAM+N-1), N=1,NK), (RMCWRK(NETA+N-1), N=1,NK),
5 (RMCWRK(NDIF+N-1), N=1,NK2),
6 (IMCWRK(IKTDIF+N-1), N=1,NLITE), (RMCWRK(NTDIF+N-1), N=1,NKT)
C
C   SET EPS/K AND SIG FOR ALL I,J PAIRS
C
CALL MCEPSG (NKK, RMCWRK(NEPS), RMCWRK(NSIG), RMCWRK(NDIP),
1 RMCWRK(NPOL), RMCWRK(NEOK), RMCWRK(NSGM) )
C
300 FORMAT (10X,'IMCWRK MUST BE DIMENSIONED AT LEAST ', I5)
350 FORMAT (10X,'RMCWRK MUST BE DIMENSIONED AT LEAST ', I5)
RETURN
999 WRITE (LOUT, *) ' Error reading Transport linking file...'

```



```

STOP
END
C
C-----
C
SUBROUTINE MCLen (LINKMC, LOUT, LI, LR)
C
C*****precision > double
IMPLICIT DOUBLE PRECISION (A-H, O-Z), INTEGER (I-N)
C*****END precision > double
C
C*****precision > single
C IMPLICIT REAL (A-H, O-Z), INTEGER (I-N)
C*****END precision > single
C
PARAMETER (NLIST = 3)
LOGICAL KERR, IERR, VOK, POK
CHARACTER*16 LIST(NLIST), VERS, PREC, V, P
COMMON /MCCONS/ VERS, PREC, KERR, LENI, LENR
DATA LIST/'1.7','1.8','1.9'/
C
VERS = ''
PREC = ''
LENI = 0
LENR = 0
LI = LENI
LR = LENR
KERR = .FALSE.
IERR = KERR
C
REWIND (LINKMC)
READ (LINKMC, ERR=999) VERS, PREC, KERR
C
VOK = .FALSE.
DO 5 N = 1, NLIST
IF (VERS .EQ. LIST(N)) VOK = .TRUE.
5 CONTINUE
C
POK = .FALSE.
C*****precision > double
IF (INDEX(PREC, 'DOUB') .GT. 0) POK = .TRUE.
C*****END precision > double
C*****precision > single
C IF (INDEX(PREC, 'SING') .GT. 0) POK = .TRUE.
C*****END precision > single
C
IF (KERR .OR. (.NOT.POK) .OR. (.NOT.VOK)) THEN
IF (KERR) THEN
WRITE (LOUT, '(A,A)')
1 ' There is an error in the transport linking file...',
2 ' Check TRANFIT output for error conditions.'
ENDIF
IF (.NOT. VOK) THEN
WRITE (LOUT, '(A,A)')
1 ' Transport Linking File is incompatible with Transport',

```

```

2  'Library Version 1.7'
  ENDIF
  IF (.NOT. POK) THEN
    WRITE (LOUT, '/A,A')
1  ' Precision of Transport Linking File does not agree with',
2  ' precision of Transport Library'
  ENDIF
  STOP
ENDIF
C
  READ (LINKMC, ERR=999) LENIMC, LENRMC, NO, NKK, NLITE
  REWIND (LINKMC)
  LENI = LENIMC
  LENR = LENRMC
  LI = LENI
  LR = LENR
  RETURN
C
999 CONTINUE
C
  WRITE (LOUT, 50)
50 FORMAT
  1 (' Error reading Multi-component Transport linking file.')
  STOP
  END
C-----
C
  SUBROUTINE MCEPSG (KK, EPS, SIG, DIP, POL, EOK, SGM)
C
C*****precision > double
  IMPLICIT DOUBLE PRECISION (A-H, O-Z), INTEGER (I-N)
C*****END precision > double
C
C*****precision > single
  IMPLICIT REAL (A-H, O-Z), INTEGER (I-N)
C*****END precision > single
C
CCCCCCCCCCCCCCCCCCCCCCCCCCCCCCCCCCCCCCCCCCCCCCCCCCCCCCCCCCCC
CCCCCC
C
C SUBROUTINE MCEPSG (KK, EPS, SIG, DIP, POL, EOK, SGM)
C
C THIS SUBROUTINE COMPUTES THE REDUCED WELL DEPTH EOK(I,J) AND
C COLLISION DIAMETER SGM(I,J) FOR EACH I,J SPECIES PAIR. THE
C ROUTINE IS CALLED ONLY ONCE BY THE INITIALIZATION SUBROUTINE MCINT
C THIS ROUTINE IS NORMALLY NOT CALLED BY THE USER.
C
C INPUT-
C KK   - NUMBER OF SPECIES
C EPS  - ARRAY OF LENNARD-JONES POTENTIAL WELL DEPTHS.
C       CGS UNITS - K.
C       DIMENSION EPS(*) AT LEAST KK
C SIG  - ARRAY OF LENNARD-JONES COLLISION DIAMETERS.
C       UNITS - ANGSTROMS.
C       DIMENSION SIG(*) AT LEAST KK

```

```

C DIP - ARRAY OF DIPOLE MOMENTS
C     UNITS - DEBYE
C     DIMENSION DIP(*) AT LEAST KK
C POL - ARRAY OF POLARIZABILITIES.
C     UNITS - ANGSTROMS**3.
C     DIMENSION POL(*) AT LEAST KK
C
C OUTPUT-
C EOK - MATRIX OF REDUCED WELL DEPTHS FOR EACH SPECIES PAIR.
C     UNITS - K
C     DIMENSION EOK(KDIM,*) EXACTLY KDIM FOR THE FIRST
C     DIMENSION, AND AT LEAST KK FOR THE SECOND.
C SGM - MATRIX OF REDUCED COLLISION DIAMETERS FOR EACH SPECIES
C     PAIR.
C     UNITS - ANGSTROMS.
C     DIMENSION SGM(KDIM,*) EXACTLY KDIM FOR THE FIRST
C     DIMENSION, AND AT LEAST KK FOR THE SECOND.
C
CCCCCCCCCCCCCCCCCCCCCCCCCCCCCCCCCCCCCCCCCCCCCCCCCCCCCCCCCCCC
CCCCC
C
C     DIMENSION EPS(*), SIG(*), DIP(*), POL(*), EOK(KK,*), SGM(KK,*)
C
C     DATA PI/3.1415926535/, FDT CGS/1.0E-18/, FATCM/1.0E8/,
1     DIPMIN/1.0E-20/, BOLTZ/1.38056E-16/
C
C     COMPUTE AND STORE EPS/K AND SIGMA FOR ALL PAIRS
C
C     DO 1000 J = 1, KK
C
C     DO 1000 K = 1, J
C
C     IF((DIP(J).LT.DIPMIN .AND. DIP(K).GT.DIPMIN)) THEN
C
C     K IS POLAR, J IS NONPOLAR
C
C     XI = 1.0E0 + 0.25E0*(POL(J)/SIG(J)**3) *
1     (FDT CGS**2*FATCM**3/BOLTZ) *
2     (DIP(K)**2/(EPS(K)*SIG(K)**3)) *
3     SQRT(EPS(K)/EPS(J))
C     SGM(K,J) = 0.5E0 * (SIG(J)+SIG(K)) * XI**(-1.0E0/6.0E0)
C     SGM(J,K) = SGM(K,J)
C     EOK(K,J) = SQRT(EPS(J)*EPS(K)) * XI**2
C     EOK(J,K) = EOK(K,J)
C
C     ELSE IF((DIP(J).GT.DIPMIN .AND. DIP(K).LT.DIPMIN)) THEN
C
C     J IS POLAR, K IS NONPOLAR
C
C     XI = 1.0E0 + 0.25E0*(POL(K)/SIG(K)**3) *
1     (FDT CGS**2*FATCM**3/BOLTZ) *
2     (DIP(J)**2/(EPS(J)*SIG(J)**3)) *
3     SQRT(EPS(J)/EPS(K))
C     SGM(K,J) = 0.5E0 * (SIG(J)+SIG(K)) * XI**(-1.0E0/6.0E0)
C     SGM(J,K) = SGM(K,J)

```

```

EOK(K,J) = SQRT(EPS(J)*EPS(K)) * XI**2
EOK(J,K) = EOK(K,J)
C
  ELSE
C
  NORMAL CASE, EITHER BOTH POLAR OR BOTH NONPOLAR
C
  SGM(K,J) = 0.5E0 * (SIG(J) + SIG(K))
  SGM(J,K) = SGM(K,J)
  EOK(K,J) = SQRT(EPS(J)*EPS(K))
  EOK(J,K) = EOK(K,J)
C
  ENDIF
1000 CONTINUE
C
  RETURN
  END
C
C-----
C
  SUBROUTINE MCEVAL (TF, KK, NO, COF, VAL)
C
C*****precision > double
  IMPLICIT DOUBLE PRECISION (A-H, O-Z), INTEGER (I-N)
C*****END precision > double
C
C*****precision > single
  IMPLICIT REAL (A-H, O-Z), INTEGER (I-N)
C*****END precision > single
C
CCCCCCCCCCCCCCCCCCCCCCCCCCCCCCCCCCCCCCCCCCCCCCCCCCCCCCCCCCCC
C
C SUBROUTINE MCEVAL (TF, KK, NO, COF, VAL)
C
C THIS SUBROUTINE USES HORNERS ALGORITHM TO EVALUATE A POLYNOMIAL
C FIT. THIS ROUTINE IS NOT NORMALLY CALLED BY THE PACKAGE USER.
C
C INPUT-
C TF - INDEPENDENT VARIABLE OF FIT. EITHER TEMPERATURE
C OR LOG TEMPERATURE.
C KK - NUMBER OF SPECIES.
C NO - ORDER OF FIT.
C COF - MATRIX OF FIT COEFFICIENTS. COF(N,K) IS THE NTH
C COEFFICIENT OF A FIT FOR KTH SPECIES PROPERTY.
C DIMENSION COF(NO,*) EXACTLY NO FOR THE FIRST
C DIMENSION AND AT LEAST KK FOR THE SECOND.
C
C OUTPUT-
C VAL - ARRAY OF VALUES, EVALUATED FROM THE FIT AT TF.
C DIMENSION VAL(*) AT KEAST KK.
C
CCCCCCCCCCCCCCCCCCCCCCCCCCCCCCCCCCCCCCCCCCCCCCCCCCCCCCCCCCCC
C
  DIMENSION COF(NO,*), VAL(*)
C

```

```

NOM1 = NO-1
C
DO 200 K = 1, KK
  B = COF(NO,K)
  DO 100 I = 1, NOM1
    B = COF(NO-I,K) + B*TF
  100 CONTINUE
  VAL(K) = B
  200 CONTINUE
C
  RETURN
  END
C
C-----
C
SUBROUTINE MCEDIF(T, NO, KK, X, COFD, WT, SMALL, XX, DJK, D)
C
C*****precision > double
  IMPLICIT DOUBLE PRECISION (A-H, O-Z), INTEGER (I-N)
C*****END precision > double
C
C*****precision > single
  IMPLICIT REAL (A-H, O-Z), INTEGER (I-N)
C*****END precision > single
C
CCCCCCCCCCCCCCCCCCCCCCCCCCCCCCCCCCCCCCCCCCCCCCCCCCCCCCCCCCCC
CCC
C
C SUBROUTINE MCEDIF(T, NO, KK, X, COFD, WT, SMALL, XX, DJK, D)
C
C THIS SUBROUTINE IS USED INTERNALLY TO COMPUTE THE MIXTURE
C DIFFUSION COEFFICIENTS. NORMALLY NOT CALLED BY THE PACKAGE USER.
C
C INPUT-
C T - TEMPERATURE
C CGS UNITS - K.
C NO - ORDER OF FIT.
C KK - NUMBER OF SPECIES.
C X - ARRAY OF MOLE FRACTIONS OF THE MIXTURE.
C DIMENSION X(*) AT LEAST KK.
C COFD - COEFFICIENTS OF THE FITS FOR THE BINARY DIFFUSION
C COEFFICIENTS.
C DIMENSION COFD(NO, KK, *) EXACTLY NO FOR
C FIRST DIMENSION, KK FOR THE SECOND, AND AT
C LEAST KK FOR THE THIRD.
C WT - ARRAY OF SPECIES MOLECULAR WEIGHTS.
C DIMENSION WT(*) AT LEAST KK.
C SMALL - A SMALL NUMBER ADDED TO ALL MOLE FRACTIONS BEFORE
C COMPUTING THE MIXTURE DIFFUSION COEFFICIENTS.
C THIS PROCESS AVOIDS AN UNDEFINED SITUATION WHEN
C A PURE SPECIES CONDITION IS APPROACHED.
C XX - ARRAY OF MOLE FRACTIONS PLUS "SMALL," TO AVOID THE
C PROBLEM OF A PURE SPECIES.
C DIMENSION XX(*) AT LEAST KK.
C

```

```

C WORK-
C RMCWRK - ARRAY OF FLOATING POINT STORAGE AND WORK SPACE. THE
C STARTING ADDRESSES FOR THE RMCWRK SPACE ARE STORED IN
C COMMON /MCMCMC/.
C DIMENSION RMCWRK(*) AT LEAST LENRMC.
C
C OUTPUT-
C D - ARRAY OF MIXTURE DIFFUSION COEFFICIENTS
C CGS UNITS - CM**2/S.
C DIMENSION D(*) AT LEAST KK.
C DJK - MATRIX OF BINARY DIFFUSION COEFFICIENTS. DJK(J,K) IS
C DIFFUSION COEFFICIENT OF SPECIES J IN SPECIES K.
C CGS UNITS - CM**2/S
C DIMENSION DJK(KDIM,*) EXACTLY KDIM FOR THE FIRST
C DIMENSION AND AT LEAST KK FOR THE SECOND.
C
CCCCCCCCCCCCCCCCCCCCCCCCCCCCCCCCCCCCCCCCCCCCCCCCCCCCCCCCCCCC
CCCC
C
DIMENSION X(*), COFD(NO, KK, *), WT(*), XX(*), DJK(KK, *), D(*)
C
ALOGT = LOG(T)
DO 100 K = 1, KK
CALL MCEVAL (ALOGT, KK, NO, COFD(1,1,K), DJK(1,K) )
100 CONTINUE
C
DO 150 K = 1, KK
DO 150 J = 1, KK
DJK(J,K) = EXP(DJK(J,K))
150 CONTINUE
C
WTM = 0.
DO 175 K = 1, KK
WTM = WTM + WT(K)*X(K)
XX(K) = X(K) + SMALL
175 CONTINUE
C
DO 300 K = 1, KK
C
SUMXW = 0.0E0
SUMXOD = 0.0E0
C
DO 200 J = 1, KK
IF (J .NE. K) THEN
SUMXW = SUMXW + XX(J)*WT(J)
SUMXOD = SUMXOD + XX(J)/DJK(J,K)
ENDIF
200 CONTINUE
C
D(K) = SUMXW/(WTM*SUMXOD)
C
300 CONTINUE
C
RETURN
END

```

Appendix 3.2 Post-processing codes

(a) post.f

PROGRAM POST

```
*=====
* Convert the numerical results (in binary format) from one dimensional program into the format
* which would be taken as input files for MATLAB M-files for graphic processing.
*=====
```

IMPLICIT NONE

```
integer      npts,npde,npdemx,nptsmx,nstep,LDATA,LINKCK,LINKMC,LOUT,
:            HEAT,NOC,i,ii,j,k,leniwk, lenrwk, lencwk
parameter    (npdemx = 80, nptsmx =205, nstep = 100, LDATA=18, LINKCK=25,
:            LINKMC=35, LOUT=6, leniwk = 7500, lenrwk = 90000, lencwk = 500
:            ,HEAT=12, NOC= 15)
```

```
integer      ickwrk(leniwk), imcwrk(leniwk), numofc(npdemx)
double precision  rckwrk(lenrwk), rmcwrk(lenrwk)
character      cckwrk(lencwk)*(16)
character      namet*11
double precision  time(nstep),x(nstep, nptsmx),temp(nptsmx),
:            molar(nptsmx,npdemx), thc(nptsmx),
:            u(nstep,npdemx*nptsmx),pressure(nstep),y(npdemx),
:            mf(npdemx), conmix, heatflux
```

logical finish

```
integer      NMM , NKK , NII , MXSP, MXTB, MXTP, NCP , NCP1,
1            NCP2, NCP2T,NPAR, NLAR, NFAR, NLAN, NFAL, NREV,
2            NTHB, NRLT, NWL, IcMM, IcKK, IcNC, IcPH, IcCH,
3            IcNT, IcNU, IcNK, IcNS, IcNR, IcLT, IcRL, IcRV,
4            IcWL, IcFL, IcFO, IcKF, IcTB, IcKN, IcKT, NcAW,
5            NcWT, NcTT, NcAA, NcCO, NcRV, NcLT, NcRL, NcFL,
6            NcKT, NcWL, NcRU, NcRC, NcPA, NcKF, NcKR, NcK1,
7            NcK2, NcK3, NcK4, NcI1, NcI2, NcI3, NcI4
```

```
COMMON /CKSTRT/ NMM , NKK , NII , MXSP, MXTB, MXTP, NCP , NCP1,
1            NCP2, NCP2T,NPAR, NLAR, NFAR, NLAN, NFAL, NREV,
2            NTHB, NRLT, NWL, IcMM, IcKK, IcNC, IcPH, IcCH,
3            IcNT, IcNU, IcNK, IcNS, IcNR, IcLT, IcRL, IcRV,
4            IcWL, IcFL, IcFO, IcKF, IcTB, IcKN, IcKT, NcAW,
5            NcWT, NcTT, NcAA, NcCO, NcRV, NcLT, NcRL, NcFL,
6            NcKT, NcWL, NcRU, NcRC, NcPA, NcKF, NcKR, NcK1,
7            NcK2, NcK3, NcK4, NcI1, NcI2, NcI3, NcI4
```

```
open(UNIT=LDATA, status='old', file='rawdata', form='unformatted')
open(UNIT=LINKCK, status='old', file='cklink', form='unformatted')
open(UNIT=LINKMC, status='old', file='tplink', form='unformatted')
open(UNIT=10, status='new', file='test.dat', form='unformatted')
open(UNIT=11, status='new', file='name.dat', form='formatted')
open(UNIT=HEAT, status='new', file='heat.dat', form='formatted')
```

```

open(UNIT=NOC, status='old', file='noc_list', form='formatted')

call ckinit(leniwk, lenrwk, lencwk, LINKCK, LOUT, ickwrk, rckwrk, cckwrk)
call mcinit(LINKMC, LOUT, leniwk, lenrwk, imcwrk, rmcwrk)

read(LDATA) npts,npde

do i = 1,npde-1
  read(NOC,'(I1)') numofc(i)
enddo

k = 1
finish = .false.

do while (.not. finish)
  read(LDATA,end=1000) time(k)
  read(LDATA) (x(k,i), i = 1 , npts)
  read(LDATA) (u(k,i), i = 1 , npde*npts)
  read(LDATA) pressure(k)
  k = k + 1
enddo

1000 continue
k = k - 1

write(10) npts,npde,k
*
* Convert mass fraction to molar fraction
*
do j = 1 , k
  do i = 1 , npts
    temp(i) = u(j,npde*(i-1)+npde)
    do ii = 1 , npde-1
      y(ii) = u(j,npde*(i-1)+ii)
    enddo
    call ck_y2x(y,ickwrk,rckwrk,mf)
    thc(i) = 0.0d0
    do ii = 1 , npde-1
      molar(i,ii) = mf(ii)
      thc(i) = thc(i) + molar(i,ii)*numofc(ii)
    enddo
    if (i .eq. 1) call mc_acon(temp(1), mf, rmcwrk, conmix)

  enddo
  write(10) (x(j,i), i=1,npts),(temp(i),i=1,npts),
:          ((molar(i,ii),i=1,npts),ii=1,npde-1),(thc(i),i=1,npts)
*
* Produce the list of species name according to the order in cklink file
*
namet = 'Temperature'
write(11,9010) namet
do i = 1 , NKK
  write(11,9020) CCKWRK(IcKK+i-1)
enddo

```



```

9005 format(7(1x,1PE11.4))
9010 format(A11)
9020 format('Species name : ',A11)
    end

```

(b) post.m (MATLAB M-file)

% post-processor for one-dimensional in-cylinder hydrocarbon oxidation simulation code

```

fid = fopen('test.dat','r');
fseek(fid,4,'bof');
parameter = fread(fid,3,'int');

npts = parameter(1);
npde = parameter(2);
timestep = parameter(3);

nspecies = npde-1;

fseek(fid,24,'bof');
test = fread(fid,timestep*npts*(npde+2)+(timestep-1),'double');
fida = fopen('noc_list','r');

for i = 1:1:nspecies
aa = fgets(fida);
noclist(i) = str2num(aa);
end

load int1d.dat
time = int1d(:,1);
not = size(time,1);
rpm = input('Enter the engine speed (for example : 1500) :');

for k = 1:1:timestep
    for i = 1:1:npts
        index = i+((npde+2)*npts+1)*(k-1);
        x(i,k) = test(index);
        indext = npts + i + ((npde+2)*npts+1)*(k-1);
        t(i,k) = test(indext);
        cad(i,k) = time(k)*6*rpm;
    end
end

% declare the size of the matrix of total
total = 1:not;
total = rot90(total);
total = total*0;
temp = 1:not;
temp = rot90(temp);
temp = temp*0;

```

```

x = x * 1000.00;

range = 0;

while 1

    choice = menu('Enter your choice', 'Molar fraction vs x plot', 'Temperature vs x plot', 'Molar fraction vs x
plot (multi-species)', 'Fuel/Nonfuel/CO plot', 'Molar fraction vs T plot', 'Molar fraction vs T plot(multi-
species)', 'Exit');

    if choice == 1
        [sn,y] = sort_yy(1,nspecies,timestep,npts,npde,test);
        name = view_spa(sn,x,y,cad,'x (mm)', 'Molar Fraction', 'CAD',range,nspecies);

        rescale = 0;

        while 1
            choice1 = menu('Now you want to', 'see next species', 'see specific one', 'see details about this
species', 'use matlab command', 'print', 'rescale x axis', 'select part of total time steps', 'go to upper menu');
            if choice1 == 1
                sn = sn + 1;
                for k = 1:1:timestep
                    for i = 1:1:npts
                        index = ((sn+1)*npts)+ i + ((npde+2)*npts+1)*(k-1);
                        y(i,k) = test(index);
                    end
                end
                name = view_spa(sn,x,y,cad,'x (mm)', 'Molar fraction', 'CAD',range,nspecies);
                if rescale == 1
                    set(gca,'XLim',[0,xmax]);
                end
            elseif choice1 == 2
                [sn,y] = sort_yy(1,nspecies,timestep,npts,npde,test);
                name = view_spa(sn,x,y,cad,'x (mm)', 'Molar Fraction', 'CAD',range,nspecies);

                if rescale == 1
                    set(gca,'XLim',[0,xmax]);
                end
            elseif choice1 == 3
                choice2 = menu('So you want to :', 'see one step at a time', 'plot it');

                if choice2 == 1
                    dum = onestep(timestep,time,name,x,y);
                else
                    dum = plotit(timestep,time,name,'x (mm)', 'ppmC1',x,y);
                end

            elseif choice1 == 4
                keyboard;
            elseif choice1 == 5
                print -dps;
            elseif choice1 == 6
                xmax = input('Input the maximum value of x :');
                set(gca,'XLim',[0,xmax]);
            end
        end
    end
end

```

```

    rescale = 1;
elseif choice1 == 7
    range = input('How many timesteps do you want to include ?');
    name = view_spa(sn,x,y,cad,'x (mm)','Molar fraction','CAD',range,nspecies);
else
    range = 0;
    break;
end
end

elseif choice == 2

    name = view_spa(0,x,t,cad,'x (mm)','Temperature (K)','CAD',range,nspecies);

    while 1
        choice3 = menu('Now you want to', 'see details about this species','use matlab command','print','rescale x
scale','select a part of total timesteps','go to upper menu');
        if choice3 == 1
            choice4 = menu('So you want to :','see one step at a time','plot it');

            if choice4 == 1
                dum = onestep(timestep,time,name,x,t);
            else
                dum = plotit(timestep,time,name,'x (mm)','Temperature (K)',x,t);
            end
        elseif choice3 == 2
            keyboard;
        elseif choice3 == 3
            print -dps;
        elseif choice3 == 4
            xmax = input('Input the maximum value of x :');
            set(gca,'XLim',[0,xmax]);
            rescale = 1;
        elseif choice3 == 5
            range = input('How many timesteps do you want to include ?');
            name = view_spa(sn,x,t,cad,'x (mm)','Temperature (K)','CAD',range,nspecies);
        else
            range = 0;
            break;
        end
    end

elseif choice == 3

    nsp = input('How many species do you want to show on the plot ? :');
    [sn,yy] = sort_yy(nsp,nspecies,timestep,npts,npde,test);
    dum = view_muls(nsp,npts,time,timestep,'x (mm)','Molar fraction',x,yy);

elseif choice == 4

    disp('Please tell me the number of fuel according to following list. ');
    [snf,fuel] = sort_yy(1,nspecies,timestep,npts,npde,test);
    noc = input('Please enter the number of the carbon atoms this fuel molecule has:');
    fuel = fuel * noc * 1000000;

```

```

disp('Please tell me the number of CO according to following list. ');
[snco,CO] = sort_yy(1,nspecies,timestep,npts,npde,test);

CO = CO * 1000000;

disp('Please enter the number of "total hydrocarbon" according to following list. ');
[snthc,thc] = sort_yy(1,nspecies,timestep,npts,npde,test);

thc = thc * 1000000;
nonfuel = thc-fuel;

while 1
choices = menu('Enter your choice :','Fuel','NonFuel','CO','Total Hydrocarbons',' All together','Matlab
command','Return to upper menu');

if choices == 1
y = fuel;
sn = snf;
elseif choices == 2
y = nonfuel;
sn = snthc+1;
elseif choices == 3
y = CO;
sn = snco;
elseif choices == 4
y = thc;
sn = snthc;
elseif choices == 5

for k = 1:timestep
for i = 1:npts
yy(i,k) = fuel(i,k);
yy(i+npts,k) = nonfuel(i,k);
yy(i+2*npts,k) = CO(i,k);
yy(i+3*npts,k) = thc(i,k);
end
end
extra = input('How many extra species do you want to add on the same plot ? ');

if extra ~= 0
[extsn,extyy] = sort_yy(extra,nspecies,timestep,npts,npde,test);
for e = 1:extra
for k = 1:timestep
for i = 1:npts
yy(i+(3+e)*npts,k) = extyy(i+(e-1)*npts,k)*1000000;
end
end
end
end

nsp =4+extra;
dum = view_muls(nsp,npts,time,timestep,'x (mm)','ppmC1',x,yy);
y_n = input('Would you like to plot the same plot against temperature as well?(1: yes, anykey : no)');
if y_n == 1
dum = view_muls(nsp,npts,time,timestep,'temperature (K)','ppmC1',t,yy);

```

```

end
elseif choices == 6
    keyboard;
else
    break;
end

if ( choices ~= 5 & choices ~= 6 )
    name = view_sp(sn,x,y,'x (mm)', 'ppmC1',range,nspecies);
    choices1 = menu('So you want to :','see one step at a time','plot it');

    if choices1 == 1
        dum = onestep(timestep,time,name,x,y);
    else
        dum = plotit(timestep,time,name,'x (mm)', 'ppmC1',x,y);
    end
end
end

elseif choice == 5
    [sn,y] = sort_yy(1,nspecies,timestep,npts,npde,test);
    name = view_sp(sn,t,y,'Temperature (k)', 'Molar Fraction',range,nspecies);
    while 1
        choice5 = menu('Now you want to', 'see next species','see specific one','see details about this
species','use matlab prompt','print','go to upper menu');
        if choice5 == 1
            sn = sn + 1;
            for k = 1:1:timestep
                for i = 1:1:npts
                    index = ((sn+1)*npts)+ i + ((npde+2)*npts+1)*(k-1);
                    y(i,k) = test(index);
                end
            end
            name = view_spa(sn,t,y,cad,'Temperature (k)', 'Molar Fraction','CAD',range,nspecies);
        elseif choice5 == 2
            [sn,y] = sort_yy(1,nspecies,timestep,npts,npde,test);
            name = view_spa(sn,t,y,cad,'Temperature (K)', 'Molar Fraction','CAD',range,nspecies);
        elseif choice5 == 3
            choice6 = menu('So you want to :','see one step at a time','plot it');

            if choice6 == 1
                dum = onestep(timestep,time,name,t,y);
            else
                dum = plotit(timestep,time,name,'Temperature (K)', 'Molar Fraction',t,y);
            end
        elseif choice5 == 4
            keyboard;
        elseif choice5 == 5
            print -dps;
        else
            break;
        end
    end
end
elseif choice == 6
    nsp = input('How many species do you want to show on the plot ? :');

```

```

[sn,yy] = sort_yy(nsp,nspecies,timestep,npts,npde,test);
dum = view_muls(nsp,npts,time,timestep,'Temperature (K)','Molar fraction',t,yy);
else
break;
end
end
end
%-----
function h = plotit(timestep,time,name,x_label,y_label,t,s)

style = ['g-' ;'m-' ;'c-' ;'b-' ;'r-' ;'g--' ;'m--' ;'c--' ;'b--' ;'r--' ;'g-.' ;'m-.' ;'c-.' ;'b-.' ;'r-.'];

for i = 1:timestep
% the crank angle degree is converted from time based on 1500 rpm speed
cad(i) = round(time(i)/0.00011);
string = [num2str(i),'. ',num2str(cad(i)),'CAD ',num2str(time(i))];
disp(string);
end

counter = 1;
h = figure;

while 1
cho_t = input('Please input the choice of time (input number) :');
if (cho_t > timestep | cho_t <= 0)
disp('What you enter is out of the range !');
else
plot(t(:,cho_t),s(:,cho_t),style(counter));
string = [num2str(cad(cho_t))];
gtext(string);
counter = counter + 1;
while 1
choice = menu('What is your choice ?','Continue plotting','Matlab command','Rescale maximum x
value','Return to upper menu');
if choice == 1
break;
elseif choice == 2
keyboard;
elseif choice == 3
xmax = input('Enter the value of maximum x you want to plot :');
set(gca,'XLim',[0,xmax]);
elseif choice == 4
hold off;
title(name);
xlabel(x_label);
ylabel(y_label);
figure;
return;
else
end
end
hold on;
end
end
end
%-----

```

```

function d = onestep(timestep,time,name,t,s)

% plotting spatial temperature or species concentration profile at the specific time

for i = 1:timestep
% the crank angle degree is converted from time based on 1500 rpm speed
    cad(i) = round(time(i)/0.00011);
    string = [num2str(i),'. ',num2str(cad(i)),'CAD ',num2str(time(i))];
end

ncolumn = size(t,2);
plot(t(:,1),s(:,1));
title([name,num2str(cad(1)),'CAD ']);

rescale = 0;

for n = 2:ncolumn
    choice4 = menu(' You want...','Continue next step','Rescale X axis','Matlab prompt','Go back upper menu');
    if choice4 == 1
        plot(t(:,n),s(:,n));
        title([name,num2str(cad(n)),'CAD ']);
        if rescale == 1
            set(gca,'XLim',[0,xmax]);
        end
    elseif choice4 == 2
        xmax = input('Input the maximum value of x :');
        set(gca,'XLim',[0,xmax]);
        rescale = 1;
    elseif choice4 == 3
        keyboard;
    else
        hold off;
        return
    end
end
check = ishold;
if check == 1
    hold off;
end

%-----
function dum = view_muls(nsp,npts,time,timestep,xlab,ylab,x,yy)

style = ['g- ','m- ','c- ','b- ','r- ','g--','m--','c--','b--','r--','g-'];

disp(' The crank angle degree is converted from time based on 1500 rpm engine speed. If it is not the case
please modify view_muls ');

% the crank angle degree is converted from time based on 1500 rpm speed
for i = 1:timestep
    cad(i) = round(time(i)/0.00011);
    string = [num2str(i),'. ',num2str(cad(i)),'CAD ',num2str(time(i))];
    disp(string);
end

```

```

cho_t = input('Input the initial step you would like to see :');

for j = 1:1:nsp
    max = 0.0
    for i = 1:1:npts
        if (abs(yy(i+(j-1)*npts,cho_t)) > max)
            max = abs(yy(i+(j-1)*npts,cho_t));
        end
    end

    string = ['The maximum value of the species is',num2str(max)];
    disp(string);
    factor(j) = input('Multiply by factor :');
end

for j = 1:1:nsp
    plot(x(:,cho_t),yy(((j-1)*npts+1):(j*npts),cho_t)*factor(j),style(j));
    hold on
end
string = [num2str(cad(cho_t)), 'CAD '];
title(string);
xlabel(xlab);
ylabel(ylab);
hold off
rescale = 0;
while 1
    choice = menu('Input your chooses:', 'See next step', 'See specified step', 'Readjust the factor', 'Rescale x
axis', 'Matlab command', 'Return to upper menu');

    if choice == 1
        cho_t = cho_t+1;
        if(cho_t > timestep)
            break
        end
        for j = 1:1:nsp
            plot(x(:,cho_t),yy(((j-1)*npts+1):(j*npts),cho_t)*factor(j),style(j));
            hold on
        end
        string = [num2str(cad(cho_t)), 'CAD '];
        title(string);
        xlabel(xlab);
        ylabel(ylab);
        if rescale == 1
            set(gca, 'XLim', [0,xmax]);
        end
        hold off

    elseif choice == 2
        for i = 1:1:timestep
            cad(i) = round(time(i)/0.00011);
            string = [num2str(i), ' ', num2str(cad(i)), 'CAD ', num2str(time(i))];
            disp(string);
        end

        cho_t = input('Input the step you would like to see :');

```



```

for j = 1:1:nsp
    plot(x(:,cho_t),yy(((j-1)*npts+1):(j*npts),cho_t)*factor(j),style(j));
    hold on
end
if rescale == 1
    set(gca,'XLim',[0,xmax]);
end
hold off
elseif choice == 3
    for j = 1:1:nsp
        max = 0.0
        for i = 1:1:npts
            if(abs(yy(i+(j-1)*npts,cho_t)) > max)
                max = abs(yy(i+(j-1)*npts,cho_t));
            end
        end
        string = ['The maximum value of the species is',num2str(max)];
        disp(string);
        factor(j) = input('Multiply by factor :');
    end
    for j = 1:1:nsp
        plot(x(:,cho_t),yy(((j-1)*npts+1):(j*npts),cho_t)*factor(j),style(j));
        hold on
    end
    if rescale == 1
        set(gca,'XLim',[0,xmax]);
    end
    hold off
elseif choice == 4
    xmax = input('Enter the maximum value of x axis:');
    set(gca,'XLim',[0,xmax]);
    rescale = 1;
elseif choice == 5
    keyboard;
else
    figure;
    return
end
end
end

```

```

function [sn,yy] = sort_yy(nsp,nspecies,timestep,npts,npde,test)

```

```

% return an array of molar fractions as functions of space and time for species

```

```

for j = 1:1:nsp
    sn = choose_sp(nspecies);
    for k = 1:1:timestep
        for i = 1:1:npts
            index = ((sn+1)*npts)+ i + ((npde+2)*npts+1)*(k-1);
            yy(i+(j-1)*npts,k) = test(index);
        end
    end
end
end

```

```

%-----
function name = view_sp(sn,t,s,xll,yll,range,nspecies)

% plotting time-evolving temperature or species concentration profiles (in 2D or 3D)

fida = fopen('name.dat','r');
name = fgets(fida);

if sn == 0
    name = 'Temperature Histories';
elseif sn == nspecies + 1
    name = 'Total hydrocarbon';
elseif sn == nspecies + 2
    name = 'Nonfuel species';
else
    for i = 1:1:sn
        name = fgets(fida);
    end
end

if range == 0
    plot(t,s);
else
    plot(t(:,1:range),s(:,1:range));
end

title(name);
xlabel(xll);
ylabel(yll);
return;

%-----
function name = view_spa(sn,t,s,cad,xll,yll,zll,range,nspecies)

% plotting time-evolving temperature or species concentration profiles (in 2D or 3D)

fida = fopen('name.dat','r');
name = fgets(fida);

if sn == 0
    name = 'Temperature Histories';
elseif sn == nspecies + 1
    name = 'Total hydrocarbon';
elseif sn == nspecies + 2
    name = 'Nonfuel species';
else
    for i = 1:1:sn
        name = fgets(fida);
    end
end

choice = menu('Do you want to view the result in','3D','2D');
if choice == 1
    surf(cad,t,s);
    colorbar;
end

```

```
    ylabel(yll);
    xlabel(zll);
    ylabel(xll);
else
    if range == 0
        plot(t,s);
    else
        plot(t(:,1:range),s(:,1:range));
    end
    xlabel(xll);
    ylabel(zll);
end
title(name);
return;
```